Micropollutant biodegradation at the sediment water interface, coupled biomolecular and biogeochemical approaches

Adrien Borreca

Ecole Doctorale des Sciences de la Terre et de l'Environnement (ED 413)
Institut Terre et Environnement de Strasbourg (ITES)

UMR 7063/ ENGEES/ CNRS/Université de Strasbourg

***Thèse présentée par* :**

Adrien Borreca

Soutenance prévue le **12 juin 2024**

Pour obtenir le grade de : Docteur de l'Université de Strasbourg

Discipline Sciences de la Terre et de l'Univers

Spécialité Géochimie

Biodégradation des micropolluants à l'interface sédiment-eau, approche biomoléculaire et géochimique

---

Thèse dirigée par :

M. IMFELD Gwenaël	Directeur de recherche CNRS, ITES, UMR 7063 CNRS, Université de Strasbourg/CNRS/ENGEES
M. VUILLEUMIER Stéphane	Professeur des Universités, GMGM, UMR 7156 CNRS, Université de Strasbourg

Rapporteurs :

Mme CÉBRON Aurélie	Directrice de recherche CNRS, LIEC, UMR7360, Université de Lorraine
M. PESCE Stéphane	Directeur de recherches, INRAE, UR RiverLy, Villeurbanne

Examinateurs :

Mme HELLAL Jennifer	Ingénieure-Chercheuse, BRGM, UR Geomicrobiology and Environmental Monitoring, Orléans
Mme MULLER Emilie	Chargée de recherche CNRS, GMGM, UMR 7156 CNRS, Université de Strasbourg

Acknowledgments

This research and the fellowship of this thesis were funded by the CNRS 80|Prime program (2020-2023) and by the EU within the European Regional Development Fund (ERDF), support measure INTERREG VI in the Upper Rhine as part of the Reactive City project (Towards a Reactive City without Biocides).

I would like to express my sincere gratitude to my supervisors, Gwenaël Imfeld and Stéphane Vuilleumier, for their support throughout this journey. Their stimulating discussions, insightful feedback, and invaluable advice were instrumental (and significant!) in shaping this thesis. I particularly appreciate their guidance and the trust they placed in me in approaching this research from a holistic perspective. I am also deeply grateful for the opportunity to have matured as a scientist under their mentorship.

I would like to express my particular gratitude to the members of the jury, Aurélie Cébron, Stéphane Pesce, Jennifer Hellal, and Emilie Muller, for accepting the evaluation of this thesis.

Without the guidance and friendship of Tetyana Gilevska, this thesis would not be the same. I especially cherish the memories of cooking delicious Pelmeni and other dumplings with you – a tradition I hope we can continue.

I am also incredibly grateful to all the wonderful people who have supported me throughout my journey. This includes the original crew: Lulu, Tobi, Dani, Roch, Carmen, and Sara. I also extend my gratitude to the newer members who have bravely endured my jokes: Jakob (thanks for the cookies), Lucille, Enrico, Domitille, Louis-François, Agata, Oscar, Lou, Felix, Christophe, Aline, and Xiao.

To the office crew, Nicolas and Céline, your constant supply of food, laughter, and emotional support has been a lifesaver. To Véronique, "Il n'y a que les montagnes qui ne se recroisent jamais".

I would like to thank the members of the BISE and AIME teams for their invaluable help with my projects, both big and small. My sincere thanks go to Benoit, Sylvain, Emilie, Jeremy, and Thierry. Arii, my wonderful intern – possibly the best ever! – I'm so glad you're back in your paradise, and I'm incredibly grateful for your invaluable work.

Finally, to my family – thank you for your support throughout this journey. I know you're all longing for my return, and I can't wait to be back with you soon.

Résumé

L'utilisation croissante de pesticides, de médicaments et de produits de soins personnels dans les activités agricoles et urbaines pose un défi environnemental majeur. Ces substances, communément appelées microppolluants en raison de leur présence à des concentrations infimes (de quelques nanogrammes à quelques microgrammes par litre), contaminent fréquemment les plans d'eau via les eaux usées mal traitées ou le lessivage. L'interface eau-sédiment, zone de transition complexe et dynamique, joue un rôle crucial dans le devenir de ces microppolluants dans les écosystèmes aquatiques.

Cette zone constitue un véritable hotspot biogéochimique, où se concentrent et interagissent de nombreux processus physiques, chimiques et biologiques qui influencent la distribution et la persistance des contaminants. Malgré la diversité et l'abondance des micro-organismes présents à cette interface, les mécanismes qui régissent la dégradation des microppolluants et leur impact sur les communautés microbiennes restent largement méconnus. La co-occurrence de multiples microppolluants et la présence de facteurs environnementaux variables, comme la disponibilité en oxygène, complexifient davantage la compréhension de leur dissipation dans les écosystèmes aquatiques.

Cette thèse vise à approfondir notre compréhension des dynamiques et des mécanismes régissant la dissipation des microppolluants à l'interface eau-sédiment, en mettant l'accent sur les mécanismes de biodégradation et les communautés microbiennes associées. Un cadre conceptuel complet a été élaboré pour évaluer le comportement des produits pharmaceutiques, des biocides agricoles et urbains, en tenant compte des voies de dissipation biotiques et abiotiques. Ce cadre intègre des facteurs tels que les scénarios de multi-contamination, les contaminations consécutives, l'alternance de la disponibilité en oxygène et leur impact collectif sur les communautés procaryotiques.

L'identification des micro-organismes responsables de la dégradation des microppolluants constitue un autre objectif majeur de cette thèse. Ce travail contribuera à enrichir notre compréhension des dynamiques complexes impliquées dans le devenir de ces substances dans divers contextes environnementaux.

Les résultats de cette recherche fourniront des informations précieuses pour la gestion durable des ressources en eau et la protection des écosystèmes aquatiques. Une meilleure compréhension des processus de biodégradation des microppolluants permettra de développer des stratégies d'assainissement plus efficaces et de réduire l'impact environnemental de ces contaminants. De plus, l'identification des micro-organismes impliqués dans la dégradation pourrait ouvrir la voie à de nouvelles applications biotechnologiques pour la dépollution des sites contaminés.

Pour ces travaux, la metformine, le métolachlore et le terbutryn ont été choisis comme micropolluants modèles en raison de leurs propriétés physico-chimiques distinctes, de leur occurrence généralisée et de la forte probabilité de co-occurrence dans les eaux de surface. S'attaquant à des lacunes critiques dans les connaissances actuelles, cette thèse examine des questions de recherche cruciales concernant l'interface eau-sédiment des écosystèmes aquatiques :

- Quel est l'impact des micropolluants, qu'ils soient introduits individuellement ou en mélange, sur leur dynamique de dissipation et la réponse des communautés procaryotiques associées ?

- Comment les conditions de disponibilité de l'oxygène affectent-elles la dissipation de contaminants et la composition des communautés procaryotiques associées ?

- Quels micro-organismes jouent un rôle dans la biodégradation de la metformine, en l'utilisant comme source de carbone ?

Trois études expérimentales utilisant des microcosmes simulant l'interface eau-sédiment, ont été conduites dans le cadre de cette thèse pour élucider les mécanismes de la contamination par les micropolluants et répondre à ces trois grandes questions de recherches.

Etude I :

Effets combinés des micropolluants sur leur dissipation et sur les communautés procaryotiques à l'interface eau-sédiment.

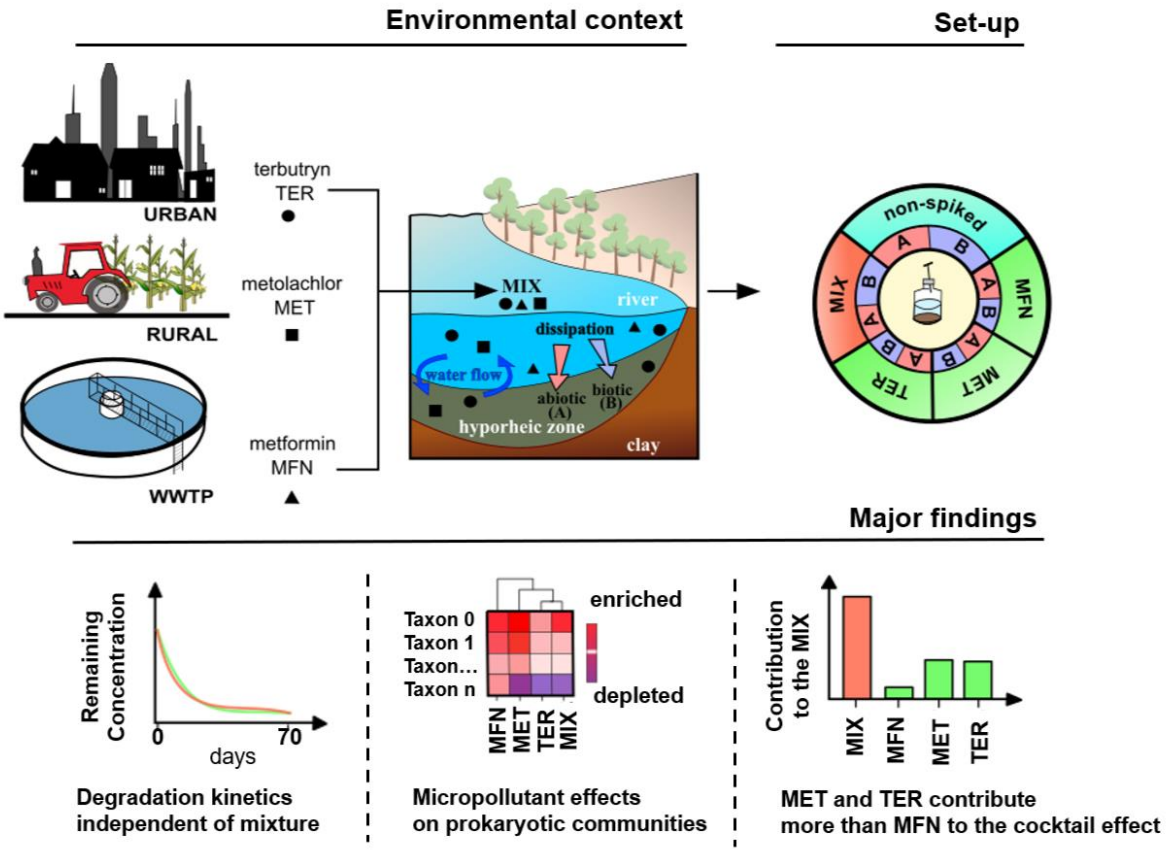

Notre première étude s'intéresse à la dissipation et à l'impact d'un mélange de micropolluants à l'interface eau-sédiment, dans l'objectif de comprendre leur transformation et leurs effets sur les communautés microbiennes.

Les écosystèmes aquatiques sont exposés en permanence à des cocktails complexes de pesticides et de produits pharmaceutiques. La dissipation et l'impact de ces micropolluants sur les sédiments et les eaux de surface sont régis par une multitude de processus. Ces contaminants, souvent persistants, peuvent impacter les micro-organismes même à de faibles concentrations. Notre étude s'est intéressée à la dissipation et aux effets sur les communautés procaryotiques de la metformine (médicament antidiabétique), du métolachlore (herbicide agricole) et du terbutryn (herbicide présent dans les matériaux de construction). Ces contaminants ont été introduits individuellement ou en mélange (à une concentration de 17,6 µM par micropollutant) dans des microcosmes de laboratoire reproduisant l'interface eau-sédiment.

La metformine et le métolachlore se sont entièrement dissipés en 70 jours, tandis que le terbutryn a persisté dans l'environnement simulé. Fait intéressant, la présence d'un mélange n'a pas affecté le taux de dissipation individuel des micropollutants. Cela suggère que les mécanismes de dégradation de ces substances opèrent indépendamment les uns des autres.

L'analyse de séquences d'amplicons du gène d'ARNr 16S a révélé des réponses distinctes des communautés procaryotiques, présentes à la fois dans les sédiments et dans l'eau. Les variations observées au sein de ces communautés étaient principalement liées à la composition de la matrice (eau ou sédiment) et à la durée d'incubation. L'exposition aux micropolluants a joué un rôle secondaire mais néanmoins important, avec des effets prononcés du métolachlore et du terbutryn, plus persistants au sein du mélange.

L'étude a mis en évidence des effets non additifs, à la fois antagonistes et synergiques, sur des taxons spécifiques à différents niveaux taxonomiques, en réponse au mélange de micropolluants. Ces résultats indiquent que certains micro-organismes peuvent être favorisés ou défavorisés par la présence conjointe de plusieurs contaminants.

Cette étude souligne l'importance de considérer la diversité des interactions entre les micropollutants, les communautés procaryotiques et leurs environnements respectifs. L'analyse des interfaces eau-sédiment contaminées par des mélanges de contaminants nécessite une approche holistique qui tient compte de ces interactions complexes.

Etude II :

Dynamique de la dissipation de la metformine en fonction de la disponibilité en oxygène à l'interface eau-sédiment et ses effets sur les communautés procaryotiques.

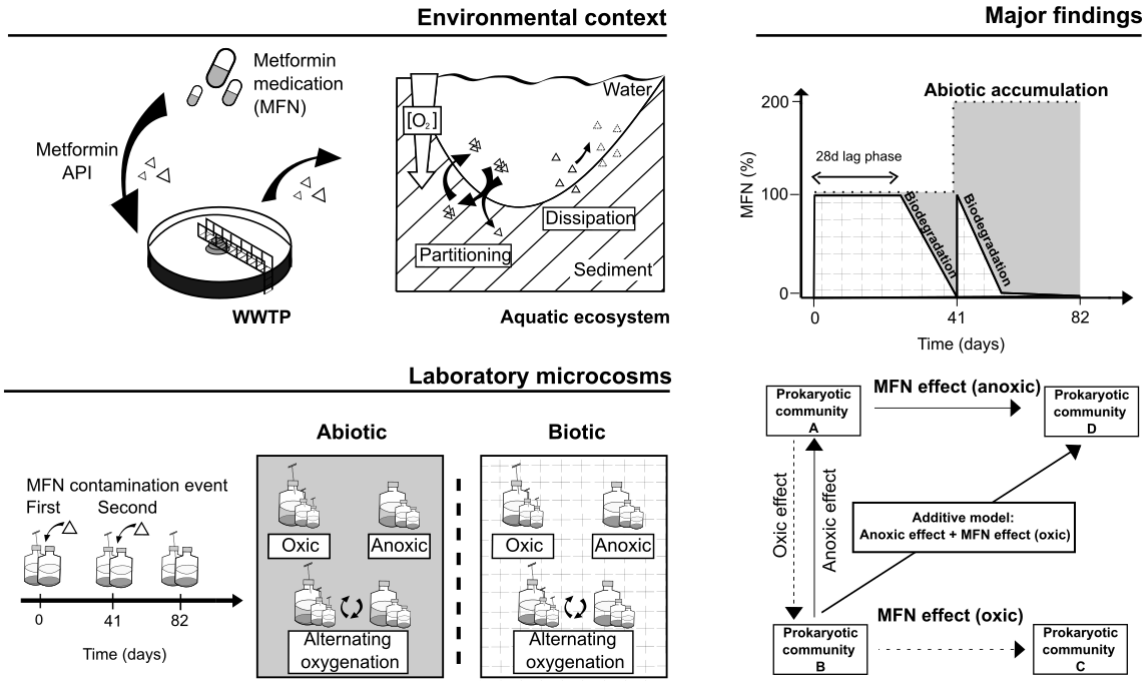

L'objectif de la deuxième étude est de combler les lacunes sur la dissipation de la metformine en conditions oxiques, anoxiques ou alternant ces deux dernières, ainsi que comprendre sa transformation et ses effets sur les communautés procaryotiques. L'étude s'intéresse aussi à l'impact d'une contamination répétée sur sa propre dissipation et les communautés procaryotiques.

La metformine, principal médicament antidiabétique, est fréquemment détectée dans les milieux aquatiques en raison de la contamination anthropique par la metformine non métabolisée et de son élimination partielle par les stations d'épuration. Cette étude examine la dégradation et l'impact de la metformine (17,6 µM) sur les communautés procaryotes dans des microcosmes de laboratoire simulant l'interface sédiment-eau sous différentes conditions d'oxygénation, y compris l'alternance entre des conditions oxiques et anoxiques.

Des expériences abiotiques, indépendamment de la présence d'oxygène, ont révélé une disparition lente de la metformine et une formation limitée de produits de transformation.

En revanche, l'oxygénation et la durée d'incubation ont significativement affecté la composition des communautés procaryotes dans des conditions biotiques. L'effet de la metformine s'est accru lors d'expositions répétées.

La dégradation de la metformine s'est achevée en moins de 13 jours après un délai initial pouvant atteindre 28 jours. La guanylurée a été détectée de manière transitoire comme unique produit de transformation. Ceci suggère une dégradation de la metformine via des voies impliquant l'hydrolase de la metformine, produisant de la guanylurée et de la diméthylamine comme source potentielle de carbone pour la croissance microbienne.

Les changements dans les communautés procaryotes indiquent que les effets combinés de l'exposition à la metformine et des niveaux d'oxygène étaient principalement additifs. Cependant, des effets synergiques ou antagonistes ont également été observés pour certains taxons, permettant l'identification de bioindicateurs potentiels de l'exposition à la metformine dans des conditions d'oxygénation changeantes.

Dans l'ensemble, cette étude souligne l'importance de prendre en compte les facteurs environnementaux, les communautés procaryotes et leur interaction lors de l'évaluation de la contamination par les produits pharmaceutiques et de ses effets à l'interface eau-sédiment.

Etude III :

Impact des micropolluants sur l'activité microbienne et identification des acteurs de la biodégradation.

Notre dernière étude se concentre sur l'utilisation du marquage isotopique stable (SIP) pour identifier les procaryotes qui utilisent la metformine comme source de carbone et d'énergie. Le SIP présente un défi notable en raison du besoin d'un composé marqué, ce qui peut s'avérer coûteux.

Bien que nous ayons réussi à obtenir de la metformine marquée, nous avons initialement choisi une approche plus économique en utilisant du glucose marqué pour calibrer nos expériences. Dans une troisième étude en microcosme, nous avons examiné l'impact de micropolluants pharmaceutiques et biocides individuels ou mélangés (metformine, (S)-métolachlore, terbutryn) sur des procaryotes assimilateurs de glucose (GAP). Notre hypothèse suggère que la toxicité aiguë induite par les micropolluants peut sélectionner certains GAP tout en favorisant d'autres bénéficiant de l'élimination des concurrents (procaryotes compétitifs), ceux actifs uniquement en présence de micropolluants (dégradeurs potentiels), ou ceux résistants aux polluants.

Cette étude vise à délimiter la réponse communautaire des GAPs par SIP dans des conditions de contamination simple et double à l'interface eau-sédiment servant de référence technique pour le marquage isotopique stable avant d'identifier éventuellement les procaryotes assimilateurs de diméthylamine à partir de metformine (DAP). Cette étude suggère que les micropolluants impactent soit la sélection des GAPs ou leurs capacités à se servir du glucose comme source de carbone. En élargissant les bases techniques établies précédemment, nous avons conçu une quatrième étude en microcosmes pour explorer l'implication des procaryotes dans l'assimilation de la metformine, en utilisant de la metformine marquée au niveau de ses deux groupes N-méthyl.

La distinction des procaryotes dégradant la metformine et assimilant la diméthylamine libérée par hydrolyse de la metformine de ceux assimilant uniquement la diméthylamine ne peut être faite à ce stade. Néanmoins, cette étude marque une étape initiale et significative dans l'identification des acteurs procaryotes. Des recherches futures utilisant des approches plus informatives, telles que la métagénomique, pourraient apporter davantage d’informations, notamment sur les gènes et les fonctions potentiels impliqués dans la biodégradation de la metformine.

En résumé cette thèse s'attaque à des questions cruciales liées à la pollution de l'eau par les micropolluants, en se concentrant sur l'interface eau-sédiment, un environnement complexe où se jouent des processus de biodégradation essentiels. La recherche explore trois aspects clés :

Effets cocktails : L'impact de l'exposition simultanée à plusieurs micropolluants, un scénario fréquent dans l'environnement, est étudié. Les effets combinatoires sur les communautés microbiennes et les processus de biodégradation sont évalués.

Expositions successives : L'influence de conditions environnementales variables, telles que la teneur en oxygène, sur la biodégradation des micropolluants est examinée. La résilience et l'adaptabilité des communautés microbiennes face à ces changements sont explorées.

Identification des acteurs de la biodégradation : Les micro-organismes responsables de la dégradation de la metformine, un micropolluant d'intérêt, sont identifiés pour la première fois. Cette avancée permet de mieux comprendre les mécanismes de dépollution naturelle à l'interface eau-sédiment.

La thèse apporte des contributions importantes à la compréhension de la dissipation des micropolluants dans l'environnement, notamment grâce à la création d’un modèle mathématiques. Un modèle innovant permettant de simuler pour la première fois l'effet combinatoire de multiples facteurs (contaminants entre eux ou avec des variables environnementales) sur les communautés microbiennes. Ces outils précieux permettent d'évaluer l'impact cumulé de la pollution sur les écosystèmes aquatiques. Cette thèse a permis pour la première fois l’identification des acteurs de la biodégradation de la metformine, grâce à la technique du SIP (Stable Isotope Probing). Cette découverte fondamentale ouvre la voie à une meilleure compréhension des processus de biodégradation de ce micropolluant et de molécules similaires.

Cette thèse pose les bases pour des recherches futures sur la contamination par les micropolluants à l'interface eau-sédiment. Des études expérimentales intégrant le transport et la biodégradation des micropolluants dans des conditions environnementales réalistes sont nécessaires pour affiner les modèles et mieux prédire la dissémination des contaminants. L'application des modèles développés à divers types de contamination et de régimes environnementaux permettra d'évaluer l'impact de la pollution sur une large gamme d'écosystèmes aquatiques.

En s'attaquant à des questions fondamentales liées à la biodégradation des micropolluants à l'interface eau-sédiment, cette thèse fournit des connaissances précieuses pour la gestion durable des ressources en eau et la protection de l'environnement. Les résultats obtenus ouvrent la voie à de nouvelles recherches et au développement d'outils de modélisation plus précis pour mieux comprendre et prédire la dissémination des contaminants dans les milieux aquatiques.

Agencement de la thèse, objectifs et hypothèses

L'objectif de ma thèse de doctorat était d'améliorer notre compréhension du comportement et des mécanismes régissant la dissipation des micropolluants à l'interface eau-sédiment (IES), en mettant l'accent sur les processus de biodégradation et les micro-organismes associés. Un cadre complet a été développé pour évaluer le comportement des produits pharmaceutiques et des biocides agricoles et urbains, en tenant compte des processus biotiques et abiotiques de dissipation des biocides. Cela comprenait une grande diversité de variables telles que la contamination multiple, la contamination répétée, la fluctuation d'oxygène et la réponse des communautés procaryotes. Un objectif secondaire était d'identifier les dégradeurs de micropolluants afin d'avoir une compréhension plus holistique de la dynamique complexe impliquée dans le devenir de ces produits chimiques dans l'environnement.

La metformine, le métolachlore et le terbutryn ont été choisis comme micropolluants modèles pour l'étude, en raison de leurs propriétés physico-chimiques contrastées, de leur omniprésence et de leur forte probabilité de co-occurrence dans les eaux de surface.

Pour combler les lacunes identifiées dans les connaissances actuelles, ma thèse de doctorat a cherché à explorer les questions de recherche clés suivantes à l'interface eau-sédiment des écosystèmes aquatiques :

- Quel est l'impact des micropolluants, qu'ils soient introduits individuellement ou en mélange, sur leur dynamique de dissipation et la réponse des communautés procaryotiques associées ?

- Comment les conditions de disponibilité de l'oxygène affectent-elles la dissipation de contaminants et la composition des communautés procaryotiques associées ?

- Quels micro-organismes jouent un rôle dans la biodégradation de la metformine, en l'utilisant comme source de carbone ?

Trois séries différentes d'expérimentations en microcosmes de laboratoire ont été choisies pour étudier ces questions, et elles sont présentées aux chapitres 4 à 6. Les approches expérimentales et les méthodes d'analyse utilisées dans ce travail sont présentées au chapitre 3.

J'ai d'abord conçu une étude en microcosme de laboratoire (Chapitre 4) avec des sédiments de rivière pour explorer la dynamique de dissipation des trois micropolluants d'importance environnementale étudiés dans ma thèse. Ces micropolluants, choisis pour leurs propriétés physico-chimiques et leurs usages distincts, ont été examinés individuellement et en mélange afin d'évaluer leur devenir et leur impact sur le compartiment biotique à l'interface eau-sédiment (IES). Mon hypothèse était que la dissipation de ces micropolluants à l'IES est influencée par leurs caractéristiques physico-chimiques distinctives ainsi que par leur toxicité.

J'ai également choisi de développer une étude en microcosme de laboratoire pour simuler l'interface eau-sédiment et étudier spécifiquement les effets d'une contamination répétée par la metformine dans différentes conditions d'oxygénation (Chapitre 5). La conception expérimentale comprenait le fonctionnement à long terme (41 jours) de microcosmes parallèles en conditions oxiques ou anoxiques, suivi d'un deuxième événement de contamination avec des conditions d'oxygénation maintenues ou inversées. Cette conception est basée sur l'hypothèse que la dissipation de la metformine dépend des conditions d'oxygénation, et visait à étudier les réponses des communautés procaryotes aux changements d'oxygénation et à l'exposition à la metformine en utilisant des méthodes basées sur l'ADN et en suivant la cinétique de dissipation de la metformine et de la formation de ses produits de transformation (TPs).

Par ailleurs, j'avais également pour objectif d'identifier les micro-organismes procaryotes actifs impliqués dans la dégradation des micropolluants en conditions d'exposition à ces contaminants (Chapitre 6). Pour atteindre cet objectif, des études exploratoires en microcosmes de laboratoire ont été menées sur des sédiments de rivière afin d'étudier l'impact individuel ou combiné des trois micropolluants sélectionnés pour cette étude, en utilisant la technique du marquage isotopique stable (SIP).

Dans un premier temps, j'ai introduit une approche originale utilisant du glucose marqué au 13C disponible dans le commerce pour étudier la toxicité des micropolluants. Mon hypothèse de travail concernant les effets des micropolluants était double : la toxicité aiguë résultant de l'exposition aux micropolluants pouvait affecter négativement les taxons associés à l'assimilation du glucose, et inversement, la présence de micropolluants pouvait favoriser l'augmentation de l'abondance relative de certains taxons.

Afin d'explorer plus en avant le potentiel de l'approche SIP, j'ai également appliqué de la metformine marquée au $^{13}C_2$ pour identifier les taxons associés à l'assimilation de la metformine dans des conditions de microcosmes de laboratoire oxiques.

Enfin, le chapitre 7, intitulé "Conclusions générales et perspectives", propose une synthèse et une discussion complète des principaux résultats de la thèse, ainsi que leurs implications pour les perspectives de recherche.

Mots clefs : Interface eau-sédiment, micropolluants, biodégradation, effets cocktail, écotoxicologie microbienne, marquage isotopique stable

Abstract

The intensive use of pesticides, pharmaceuticals, and personal care products in agriculture and urban areas raises major environmental concerns. These substances, known as micropollutants due to their presence at concentrations ranging from nanograms to micrograms per litre frequently reach water bodies through inefficient wastewater treatment or leaching. The water-sediment interface, a complex and dynamic transition zone, plays a crucial role in the fate of micropollutants in aquatic ecosystems. This zone is a veritable biogeochemical hotspot, where numerous physical, chemical, and biological processes that impact the distribution and persistence of contaminants are concentrated and interact. Despite the diversity and abundance of microorganisms present at the water-sediment interface, the mechanisms governing micropollutant degradation and their impact on microbial communities remain largely unknown. The co-occurrence of multiple micropollutants and the presence of variable environmental factors, such as oxygen availability, complicate the understanding of their dissipation in aquatic ecosystems. This thesis aims to deepen our understanding of the dynamics and mechanisms governing micropollutant dissipation at the water-sediment interface, with a primary focus on biodegradation mechanisms and associated microbial communities. A comprehensive framework has been developed to assess the behaviour of pharmaceuticals, agricultural, and urban biocides, considering both biotic and abiotic dissipation pathways. This framework integrates factors such as multi-contamination scenarios, consecutive contaminations, variable oxygen availability, and their collective impact on prokaryotic communities. Identifying the microorganisms responsible for micropollutant degradation is another major objective of this thesis, enriching our understanding of the complex dynamics involved in the fate of these substances in various environmental contexts.

Metformin, metolachlor, and terbutryn were chosen as model micropollutants due to their distinct physicochemical properties, widespread occurrence, and high probability of co-occurrence in surface waters. Addressing critical gaps in current knowledge, this thesis examines crucial research questions concerning the water-sediment interface of aquatic ecosystems:

o What is the impact of micropollutants, introduced individually or in mixtures, on their dissipation dynamics and the response of associated prokaryotic communities?

o How do conditions of oxygen availability affect the dissipation of consecutively introduced contaminants and the composition of associated prokaryotic communities?

o Which microorganisms play a role in the biodegradation of metformin, by utilizing it as a carbon source?

Our first study focuses on the dissipation and impact of a mixture of micropollutants at the water-sediment interface. We aim to understand how these pollutants transform and affect microbial communities. We explore the interactions between micropollutants and prokaryotic communities by examining metformin, metolachlor, and terbutryn individually or in combination within laboratory microcosms replicating the water-sediment interface. Analysed basing on a mathematical model developed to evaluate the additive impact of micropollutants on prokaryotic communities, the results indicate that mixtures of these pollutants can affect these communities in an additive, synergistic, or antagonistic manner. However, the dissipation of

the micropollutants themselves remains unaffected by the presence of a mixture. This systematic investigation, involving 125 microcosms distributed across five parallel experiments, provides valuable insights into micropollutant dynamics and their impact on prokaryotic communities at the water-sediment interface. This knowledge offers valuable perspectives for ecotoxicological risk assessment.

Our final study focuses on utilizing stable isotope probing (SIP) to identify prokaryotes that utilize metformin as a carbon and energy source. SIP presents a notable challenge due to the requirement for a labelled compound, which can be costly. While we successfully obtained labelled metformin, we initially opted for a more economical approach using labelled glucose to calibrate our experiments. In a third microcosm experiment, we examined the impact of individual or mixed pharmaceutical and biocide micropollutants (metformin, (S)-metolachlor, terbutryn) on glucose-assimilating prokaryotes (GAPs). Our hypothesis suggests that acute toxicity induced by micropollutants may select certain GAPs while favouring others that benefit from the elimination of competitors (competitive prokaryotes), those active only in the presence of micropollutants (potential degraders), or those resistant to pollutants. This study aims to delineate the community response of GAPs by SIP under single and double contamination conditions at the water-sediment interface, serving as a technical reference for stable isotope labelling before potentially identifying metformin dimethylamine (DAP)-assimilating prokaryotes. This study suggests that micropollutants impact either the selection of GAPs or their ability to use glucose as a carbon source. By extending the technical bases established previously, we designed a fourth microcosm experiment to explore the involvement of prokaryotes in the uptake of metformin uptake, using metformin labelled at the level of its two N-methyl groups. The distinction between prokaryotes degrading metformin and assimilating the dimethylamine released by hydrolysis of metformin from those assimilating only dimethylamine cannot be made at this stage. Nevertheless, this study marks a significant initial step in the identification of the relevant prokaryotic players. Future research using more informative approaches, such as metagenomics, will provide further information, particularly on the potential genes and functions involved in the biodegradation of metformin.

In summary, this thesis has addressed key questions concerning cocktail effects, successive exposures under varying environmental conditions such as oxygen availability, and the identification of players involved in biodegradation processes. This research lays the foundation for future studies on micropollutants at the water-sediment interface, which could include reactive transport experiments and modelling under different environmental factors and contamination types. This thesis provides valuable insights into the dissipation of micropollutants at the water-sediment interface. The proposed mathematical models allow for the first time to address the combinatorial effect of factors (contaminant-contaminant or contaminant-variable) on prokaryotic communities. Identifying putative metformin biodegraders using SIP for the first time in the literature posed a significant challenge. Its successful implementation for a micropollutant represents a notable advance.

Keywords: water-sediment interface, micropollutants, biodegradation, cocktail effects, microbial ecotoxicology, stable isotope probing

List of abbreviations

Abbreviation	Full name
AIMT	4-amino-2-imino-1-methyl-1,2-dihydro-1,3,5-triazine
AMT	2-amino-4-methylamino-1,3,5-triazine
APIs	Active pharmaceutical ingredients
b.d.l	Below detection limits
DAPS	Dimethylamine assimilator prokaryotes
DAT	2,4-diamino-1,3,5-triazine
DMbG	dimethylbiguanide
DMG	dimethylguanidine
DNA	desoxyribonucleic acid
DU	dimethylurea
ESA	metolachlor ethanesulfonic acid
GAPS	Glucose assimilator prokaryotes
GUA	guanylurea
LEfSe	Linear discriminant analysis effect size
MET	metolachlor
METd11	metolachlor-d11
MFN	metformin
MFNd6	metformin-d6
NOA	metolachlor N-oxa-ethanosulfonic acid
NPMANOVA	Non-parametric multivariate analysis of variance
OXA	metolachlor oxanilic acid
PAHs	polycyclic aromatic hydrocarbon
PPCPs	Pharmaceuticals and personal care products
SIP	Stable isotope probing
SWI	Sediment-water interface
TER	terbutryn

Abbreviation	Full name
TerDesE	desethyl-terbutryn
TerDesEOH	desethyl-2-hydroxy-terbutryn
TerOH	terbutryn-2-hydroxy
TPs	Transformation products
U	urea

List of Tables

Chapter 1.

Chapter 3.

Chapter 4.

List of Figures

Chapter 1.

Chapter 3.

Chapter 4.

Chapter 5.

Chapter 6.

Table of contents

Chapter 1.
General introduction

1.1. Micropollutants in aquatic ecosystems
1.1.1. Worldwide use and transport of micropollutants
1.1.1.1. Pesticides

In the last two decades, there has been a notable escalation in global pesticide utilization, with quantities employed ranging from 100,000 to 1,000,000 tons per continent. Europe currently sees a marginal reduction (-0.2%) in pesticide application. Taken together, Northern Hemisphere continents witness a relatively modest rise (less than 10%), in contrast to other continents. Specifically, South America witnessed an important increase (+119.4%), Africa experienced a notable surge (+67.8%), and Oceania observed a substantial and concerning escalation (+88.4%) in pesticide usage[1] (Fig. 1.1).

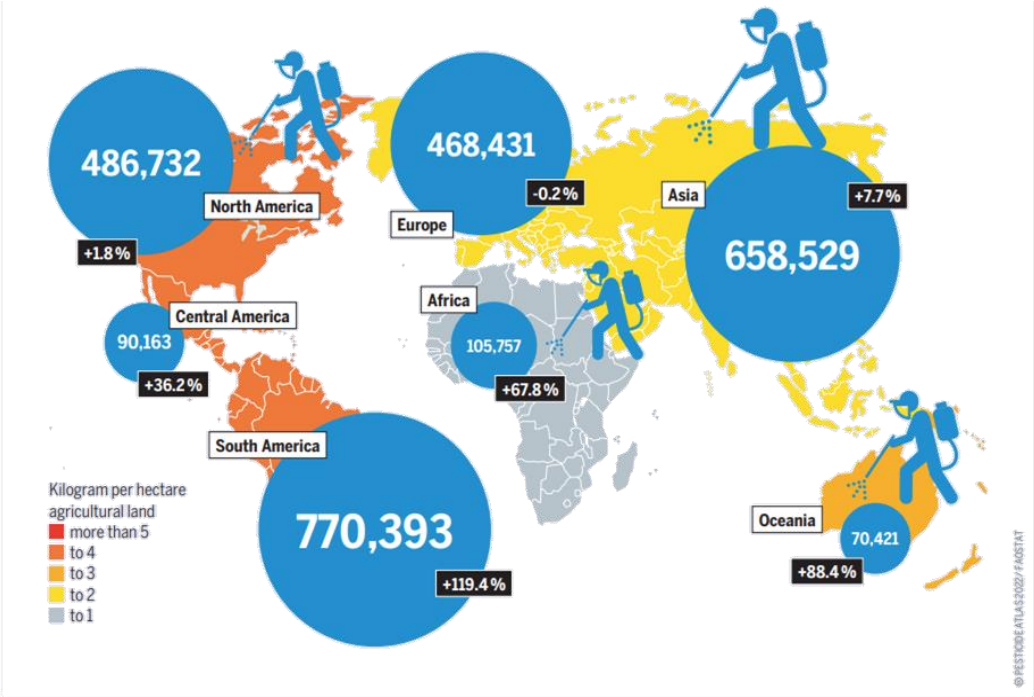

***Figure 1.1**. Pesticide use in tons by continent in 2020 (blue circle) and change since 1999 (stack box). Adapted from [1].*

The dynamics of pesticide usage and trade are global and involve widespread import and export activities. In the year 2021, China emerged as the largest global exporter, and Brazil claimed the leading position as the first importer. Notably, various countries such as the United States, France, India, Spain, and Italy actively participate in both import and export processes. France in particular secured the third rank among countries exporting pesticides, registering a value of 4.57 billion U.S. dollars. At the same time, it reached second position among importing nations, with a value of 2.04 billion U.S. dollars[2] (Fig. 1.2).

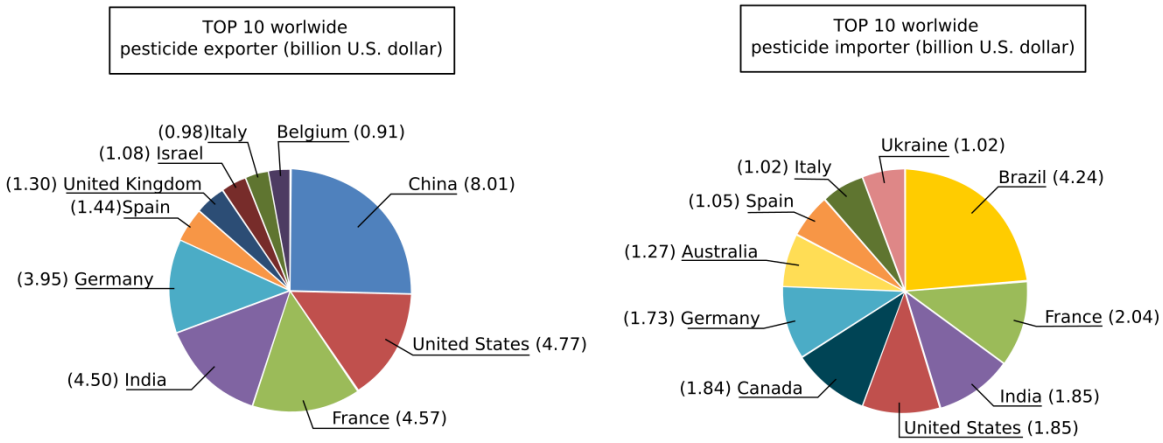

***Figure 1.2**. Top 10 pesticide importer and exporter countries and their worth in billions of U.S. dollars (2021). Adapted from [2].*

Certain pesticides, notably neonicotinoids, remain partly unauthorized for use in Europe because of concerns regarding their environmental impact, particularly on pollinators and biodiversity. This regulatory restriction reflects the European Union's commitment to preserving pollination processes and ecosystem health, prompted by evidence indicating potential harm to bees and other non-target organisms[3]. Despite their interdiction in Europe, such pesticides continue to be produced and sold to Southern continents and non-European nations. For example, the pesticide company NuFarm notified in late 2020 the export of 42 tons of insecticides containing the banned neonicotinoid imidacloprid from the UK, even though relevant EU laws on plant protection products were retained in Great Britain after Brexit. The destinations for these exports included countries such as Ukraine, Belarus, Russia, Tunisia, and Sudan[3].

Beyond ethical concerns, exporting unauthorized pesticides has wider repercussions, creating a “boomerang” effect when residues of these micropollutants are detected in food products imported by destination countries[1]. A positive development in addressing such practices has occurred in France, where the EGALIM law was enacted in January 2022. This legislation prohibits the manufacture, storage, and export of pesticides banned by the EU. This step represents a significant move towards aligning national regulations with EU standards[4].

1.1.1.2. Pharmaceuticals

On a global scale, the pharmaceutical market shows a pronounced dominance by the United States, followed by Europe, Southeast Asia, and East Asia. Prominent pharmaceutical companies enjoy worldwide distribution of their products. In the case of Pfizer for example, the company disseminates its products across 125 countries, achieving pharmaceutical sales totalling 45.3 billion U.S. dollars in 2018[5].

The contemporary pharmaceutical landscape features a vast array of more than 3000 currently utilized pharmaceuticals[6]. The escalation of global human longevity and industrialization has contributed to a notable increase in the worldwide consumption of pharmaceuticals, particularly for chronic and age-related affections, especially in regions with facilitated access to pharmaceuticals[5] (Fig. 1.3). This upward trajectory is discernible in increased utilization of various pharmaceutical categories, comprising, e.g., oncological,

cholesterol-lowering, antidepressant, antihypertensive, and antidiabetic drugs[5]. For instance, the consumption of cholesterol-lowering drugs showed a nearly quadruple increase over two decades, escalating from 26 to 95 doses per 1000 people per day in OECD member countries. Similarly, the utilization of antidepressants and antihypertensive drugs doubled over the same period[5].

In countries situated in the Northern Hemisphere, the predominant drug categories consumed are those addressing the cardiovascular system, nervous system, alimentary tract, and metabolism. This trend is closely correlated with the prevalence of non-communicable diseases representing health conditions not caused by infectious agents and not transmissible between individuals. As of 2019, these non-communicable diseases accounted for 74% of global deaths[5,7].

Considering the global and annual consumption of pesticides and pharmaceuticals in terms of mass, and the observed sustained upward trend driven by ongoing population growth and aging, it becomes imperative to assess the behaviour of these substances in the environment. Such an evaluation should also comprehensively address their transformation and potential impact on ecosystems diversity and functioning.

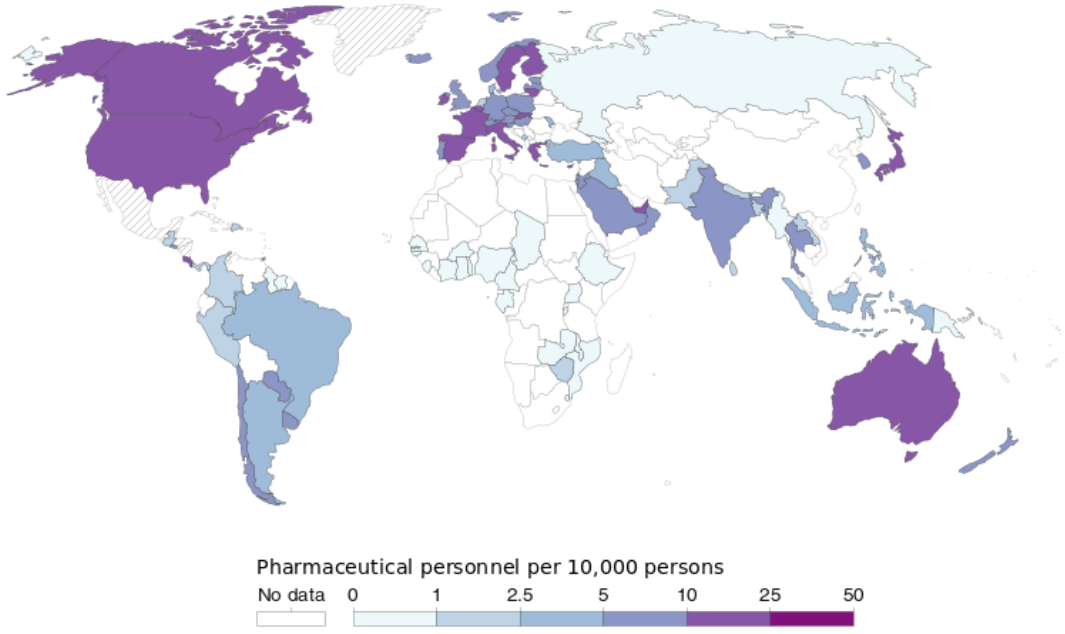

***Figure 1.3**. Pharmaceutical personnel per 10,000 persons (2021). Data from multiple sources compiled by the UN – processed by "Our World in Data" [8].*

1.1.1.3. Micropollutant-associated risks to aquatic ecosystems

The ecosystem concept was historically defined by A. G. Tansley in 1935 as that entity resulting from the interaction of all living organisms with each other and with the physical and chemical factors of their non-living environment[9]. Building on this, the term 'aquatic ecosystem' refers to the ecosystem of water bodies, and includes such diverse biotopes as lakes, ponds, rivers, oceans, estuaries, and wetlands. Aquatic biodiversity within these ecosystems spans phytoplankton, zooplankton, aquatic plants, insects, fishes, birds, and mammals[10]. Notably,

procaryotes and in particular bacteria as well as fungi play crucial roles in aquatic ecosystems, and contribute to nutrient cycling, decomposition, and ecosystem functioning[11].

Bacteria play essential roles in aquatic ecosystems by participating in crucial processes such as the nitrogen cycle, the decomposition of organic matter, and by supporting the growth of various organisms[12]. Similarly, fungi found in aquatic and terrestrial environments contribute significantly to fundamental processes such as decomposition, nutrient cycling, and the establishment of symbiotic relationships with plants (e.g., *Laccaria* and *Glomus*)[13]. In aquatic settings, these microorganisms make substantial contributions to the biodiversity and functioning of the ecosystem[14], underscoring the intricate interdependence and dynamics among various life forms within aquatic ecosystems but also with nearby terrestrial ecosystems, thereby forming a meta-ecosystem[15].

In aquatic ecosystems, trace concentrations of pesticides, pharmaceuticals, and personal care products (PCPs) are commonly detected in water bodies, typically ranging between ng L^{-1} and µg L^{-1} [16–18]. These anthropogenic trace compounds (ATCs), also known as micropollutants, show diverse chemical properties including variations in half-life (DT_{50}), octanol-water partitioning (log K_{ow}), and organic carbon partitioning (K_{oc}). The degradation of micropollutants leads to the production of transformation products including metabolites and products from abiotic transformation processes, each possessing its unique set of physicochemical properties, varying in hydrophobicity (K_{ow}), mobility (K_{oc}), and recalcitrance (DT_{50}) (Table 1.1).

Table 1.1. *Environmental characteristics of micropollutants from different sources. Average prediction values for soil absorption coefficient K_{oc} (*) were obtained from the EPA CompTox database. Log K_{ow} were obtained from the PubChem database (**).*

Source	Compound	K_{oc}*	Log K_{ow}**	Hydrophobicity	Half-life DT_{50} (days) in river waters	DT_{50} references
Pesticides	glyphosate	1004	-3.40	−	[14 -301]	[17]
	terbutryn	657	3.74	+	[177-644]	[18]
	metolachlor	262	3.13	+	[50 – (>200)]	[19]
	atrazine	174	2.61	+	>200	[20]
Personal Care Products	nicotine	102	1.17	+	~3	[21]
	caffein	62	-0.07	+/−	[2 - 240]	[22,23]
Pharmaceuticals	paracetamol	48	0.46	+/−	[4-12]	[24]
	metformin	10	-2.64	−	[5-10]	[25]

Aquatic ecosystems and organisms living therein are particularly sensitive to chemical effects, including contamination by micropollutants. An illustrative example is the feminization of fish observed in the presence of metformin at a concentration of 40 µg L^{-1} in wastewater treatment plant effluents[26]. The dynamic nature of water bodies also raises concerns about potential groundwater contamination by micropollutants and their implications for public and environmental health. This concern is particularly pertinent in light of the escalating global water scarcity issue[27], marked by a six-fold increase in global freshwater use over the past century and a consistent growth of approximately 1% per year since the 1980s[28].

The decline in water quality is also an alarming issue, with 80% of diseases and 50% of child deaths worldwide attributed to poor water quality[29]. Water bodies not only face the potential impact of micropollutants but also of others contaminants such as arsenic, chromium, and nitrate as an additional source of concern[29]. Consequently, special attention to the behaviour and transformation of these micropollutants in aquatic ecosystems is now imperative considering their impact on biodiversity and the associated risks to public health.

1.1.2. Micropollutants entry into aquatic ecosystems

Pesticides constitute a wide class of micropollutants. The products commonly grouped under the term 'pesticides' are defined based on their uses according to two distinct European regulations: i) phytopharmaceuticals (Regulation (EC) Nº 1107/2009); ii) biocides (Regulation (EC) Nº 528/2012)[30]. Phytopharmaceutical products are either used to prevent or refrain undesired plant growth (herbicide such as *(S)*-metolachlor), or to protect from detrimental organisms (insecticides, nematicides, rodenticides, etc.). Similarly to manure, they can enter aquatic ecosystems by leaching[31]. Biocides are also used to protect human-produced structures and objects, such as terbutryn in facade coatings which is then leached into urban wastewaters[31]. Biocides are also used in personal care products (PCPs). For example, the antiseptic hexamidine applied as a preservative in cosmetics can also be found in sewage[32]. Veterinary or human antiparasitics may, on occasion, be encompassed within the category of biocides. The ANSES has proposed a clarification to aid in determining whether such "borderline" formulations would be classified as pharmaceuticals or biocides under European legislation[33]. At least 450 synthetic pesticides in more than 1700 product formulations are applied in conventional agriculture[1] (Fig. 1.4).

Most orally administered pharmaceuticals are used in excessive 'external doses' to account for incomplete absorption and to achieve the desired effective 'internal dose'[34]. Consequently, a fraction of such medications is eliminated via perspiration, urination, and defecation, and subsequently channelled through WWTPs, where treatment efficacy is frequently insufficient for complete micropollutant removal[35], leading to the release of contaminants in aquatic ecosystems (Fig. 1.4). Human pharmaceuticals primarily originate from urban wastewater discharge, with additional contributions from secondary sources such as industrial manufacturing and hospitals[36]. In contrast, veterinary pharmaceuticals (mainly antibiotics and antiparasitics)[37] enter aquatic ecosystems through different pathways. Just as human waste, manure of treated animals contains residues of these pharmaceuticals. Since manure is often used as fertilizer, this results in further risk of leaching to aquatic ecosystems[38]. For personal care products (PCPs), another potential source is direct contamination of waters, as exemplified by the introduction of galaxolide from sunscreens in recreational swimming[39] (Fig. 1.4).

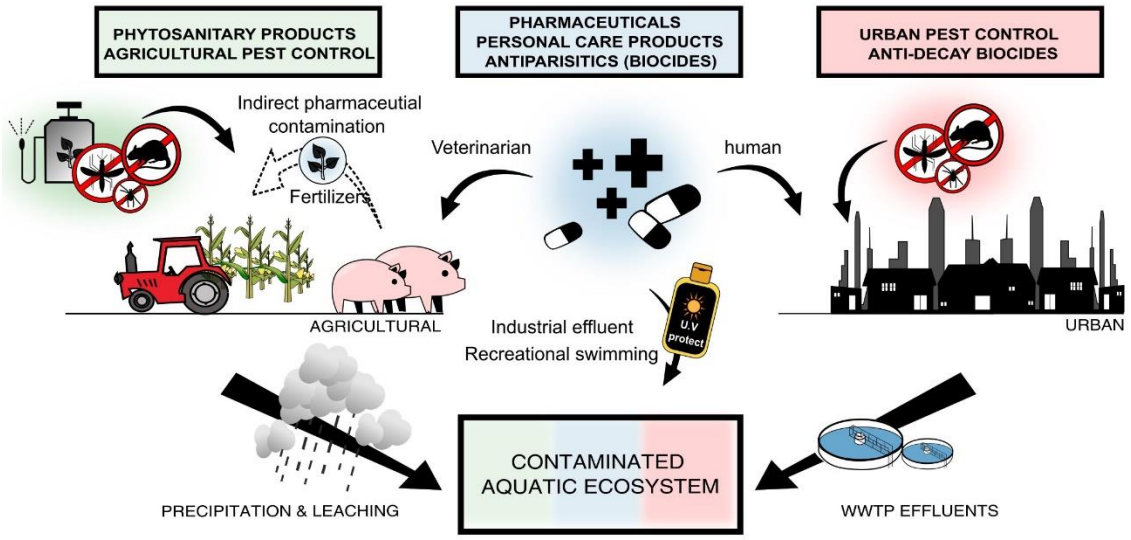

***Figure 1.4**. Main sources and transport pathways of micropollutants reaching aquatic ecosystems.*

The entry of micropollutants into aquatic ecosystems raises questions about their fate, transport, and their effect on organisms and trophic chains in aquatic ecosystems. Many studies address the impact of micropollutants on crustaceans[40], macroinvertebrates[41] and amphibians[42], yet, comparatively, the microbial compartment remains poorly explored. With regard to fate and transport, computational methods prove useful, determining the transport and fate in aquifers[43] and rivers[44], including the urban scale[45]. Notably, these modelling approaches often require in situ data for calibration and validation. In other words, models must be calibrated and validated using actual data collected from the studied environment. This process ensures that the computational models accurately represent the real-world conditions and behaviour of micropollutants in the environment. Hence, the combination of computational modelling and real in situ data is crucial to develop reliable predictions and understand the complex dynamics of micropollutant transport and fate in aquatic systems.

Another already mentioned aspect to consider regarding the entry of micropollutants in aquatic ecosystems is that existing wastewater treatment plants (WWTPs) do not systematically remove micropollutants and especially pharmaceuticals from wastewater[46]. The improvement of treatment methods has gained recent attention, with ongoing testing of processes for improved cleanup of WWTP effluent[47–49]. Nevertheless, even if certain processes demonstrate effectiveness in small-scale trials, the feasibility of scaling up these methods for application in full-scale WWTPs remains a significant challenge. Together with limiting source emissions, achieving practical and efficient large-scale implementation of treatment measures is a critical consideration in efforts to improve the capacity of WWTPs to manage and mitigate micropollutant contamination in water systems.

1.1.3. Micropollutants transport and transformation in aquatic ecosystems

Once in the aquatic ecosystem, micropollutants are subject to transport and transformation. Micropollutant transport processes are summarized in Figure 1.5. Transport

mainly depends on the partitioning of the micropollutant between the water and solid phases, which itself depends on the physicochemical properties of the considered molecule[50]. For instance, pharmaceuticals such as paracetamol, metronidazole, and metformin are polar molecules with a strong affinity for the water phase, as reflected by their low octanol-water partition coefficients (log K_{ow}) of 0.46, −0.02, and −2.64, respectively. Additionally, their organic carbon partition coefficients (K_{oc}) of 21, 23, 19 L Kg^{-1} indicates a very low potential for sediment sorption. In contrast, urban biocides such as terbutryn, commonly found in paints and renders, display low water affinity (log K_{ow} = 3.74) and high sorption potential (K_{oc} ranging from 42 to 366 L Kg^{-1}). Widely used herbicides such as metolachlor also present a low partitioning to water, with a log K_{ow} at 3.13 and a strong potential for sorption onto soil and sediment, with a K_{oc} ranging from 22 to 2320 L Kg^{-1} [51]. Micropollutants are also subject to sorption/desorption processes and they are also transported longitudinally through the water body. As an example, antibiotics such as sulfamethoxazole, sulfadiazine, and sulfamethazine were still detected 13 km downstream WWTP effluent[52]. Micropollutants are also transported to the underground water, leaching being the highest for weakly sorbed and persistent chemicals. Micropollutant transport into groundwater will be facilitated in climates with high precipitation and low temperatures, and soils with low organic matter and sandy texture[53].

Micropollutants are not only transported through different compartments of aquatic ecosystems, they can also be transformed, partially degraded and even mineralized[54]. Micropollutants are subject to degradation into various transformation products by either biotic or abiotic mechanisms. These transformation products can be further transformed until complete mineralization[54] or they can be more persistent and toxic than the parent molecules[55]. Transformation products can thus be used as markers of degradative processes and transformation pathways in environmental ecology. In certain instances, micropollutants characterized by high sorption potential and low transformation rates may persist in the solid matrix and remain detectable even decades later[55]. For example, atrazine was detected in 20% of the monitoring stations in Germany in 2016 despite being banned in 1991 due to groundwater pollution[1]. Conversely, chemicals such as caffeine show high mobility and can undergo transformation within a short period[56].

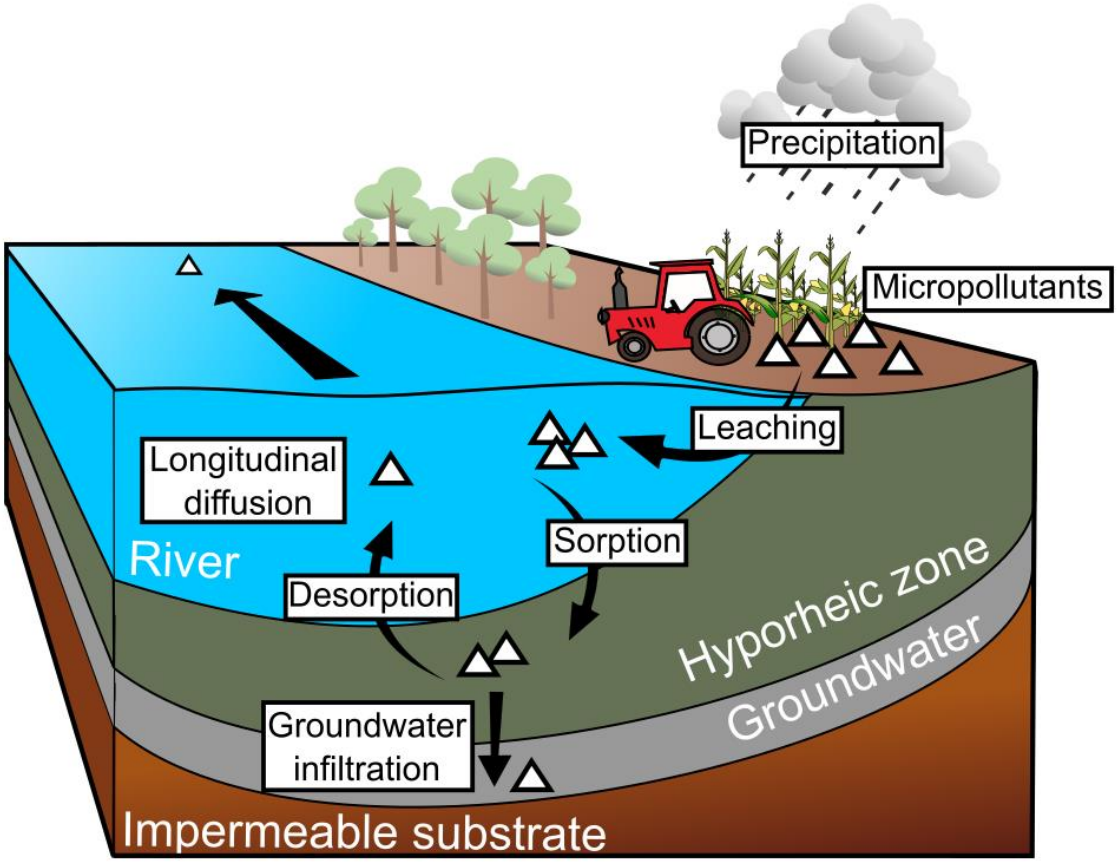

Figure 1.5. *Transport of micropollutants in aquatic ecosystem compartments.*

Different issues arise from processes related to the transport and transformation of micropollutants in aquatic ecosystems. The detection and quantification of these pollutants and their transformation products often present analytical challenges, particularly when dealing with contaminant concentrations ranging from ng to µg L^{-1}. Notably, the absence of detection or a decrease in the concentration of a contaminant does not necessarily indicate a positive outcome for the aquatic ecosystem mainly due to sampling heterogeneities, sample volumes and extraction methods. In addition, a significant volume of water must be preconcentrated to enable effective detection, quantification, and contribution assessment[16]. However, this preconcentration step introduces a 'matrix effect,' with other elements also concentrated adding a background effect. Another issue is the requirement for standards of transformation products, which need to be custom-synthesized if they are not commercially available, to validate their detection and identification[57]. Indeed, the parent molecules are in some cases less harmful than some of their transformation products, and these could also be more recalcitrant in the environment[58].

1.1.4. Ubiquitous occurrence of micropollutants in aquatic ecosystems

1.1.4.1. Pesticides

Rivers receive 0.73 Gg of pesticide contaminants from their drainage at a rate of 10 to more than 100 kg yr^{-1} km^{-1} globally and are thus ubiquitous[59]. As an example, a peer-reviewed study conducted at over 2,500 sites in 73 countries showed that 68.5% of these sites present

concentrations of insecticides in surface water or sediment surpassing regulatory threshold level[35]. Ubiquity of micropollutant can also be monitored at lower scales. For instance, in the Alsace region of France, the occurrence of herbicide *(S)*-metolachlor and its main transformation product ESA-metolachlor, primarily employed for beetroot and corn cultivation, have raised concerns. These substances were consistently detected in groundwater at levels exceeding potability thresholds, as reported by the Regional Agency for the Environment and Work Protection (APRONA)[60]. This contamination might arise from agricultural leaching into surface waters, then reaching groundwaters[60]. Another case involves the biocide terbutryn, extensively employed as an additive in urban construction materials, particularly in facade coatings as an anti-decay agent. This usage has resulted in a persistent source of contamination associated with precipitation, at the urban scale[61].

1.1.4.2. Pharmaceuticals and personal care products

The excreted dose in urine and stools going through WWTPs reflects the use of these chemicals. Hence the most common marketed pharmaceuticals (APIs) and PCPs such as acetaminophen, metformin, caffeine, and nicotine are the most detected and concentrated worldwide[46]. These compounds were detected in over 50% of sampling sites in a large-scale worldwide campaign[46]. However, their concentration in rivers varies in the range of ng to µg (Fig. 1.6).

A major concern associated with APIs is the potential increase in discharge into aquatic ecosystems, particularly given the aging populations and the rise in non-communicable diseases. As an example, metformin is prescribed worldwide for the management of type II diabetes. However, it also demonstrates promising results as a meta-drug, playing a role in treatments for conditions such as cognitive impairments and cancer[62]. Currently, metformin is the second most frequently detected pharmaceutical and the third most concentrated pharmaceutical worldwide[46].

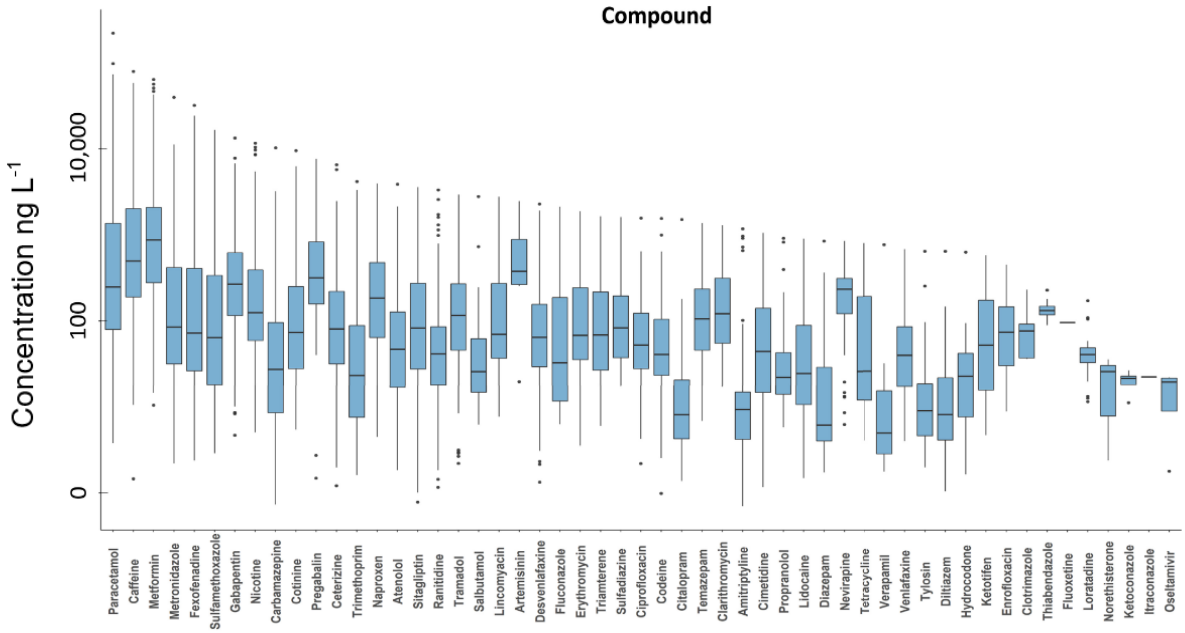

Figure 1.6. *Global concentrations (ng L-1) of individual APIs showing mean, minimum, maximum, and upper and lower quartile concentrations. Adapted from [46].*

1.1.5. Global trends

At the global scale, API contamination is largest for countries presenting 'Lower-middle income', also referred to as 'emerging economies. Corresponding so-called developing countries have now gained access to pharmaceuticals, yet they still lack proper and efficient infrastructures for water treatment[46] (Fig. 1.7).

Similar to APIs, pesticides are widespread in rivers globally, ranging from ng to µg L^{-1} concentrations. Their presence correlates closely with usage patterns, and their transport in the environment is not as heavily influenced by the efficiency of WWTPs. Consequently, the contamination of rivers by pesticides worldwide is more diffuse when compared to that by APIs[59] (Fig. 1.8). Notably, global studies on this matter depend on the selection of sampling sites and the specific compounds considered. Pesticide concentrations also show dependence on seasons, and measurement outcomes can vary across different seasons[1].

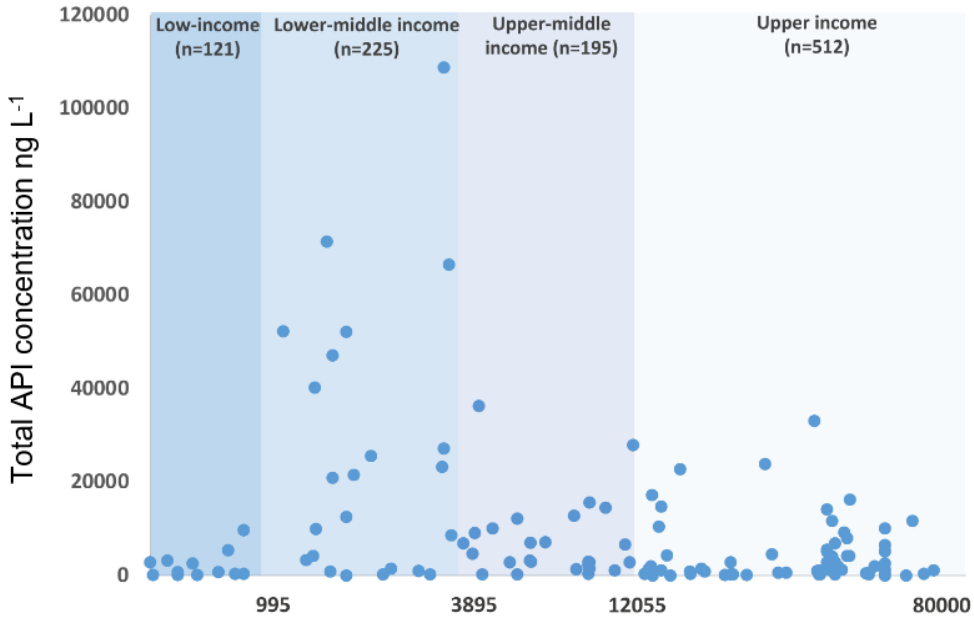

Figure 1.7. *Cumulative concentrations of APIs observed across respective river catchments (blue dots; n, number of sampling sites), organized by World Bank GNI per capita. Adapted from [46].*

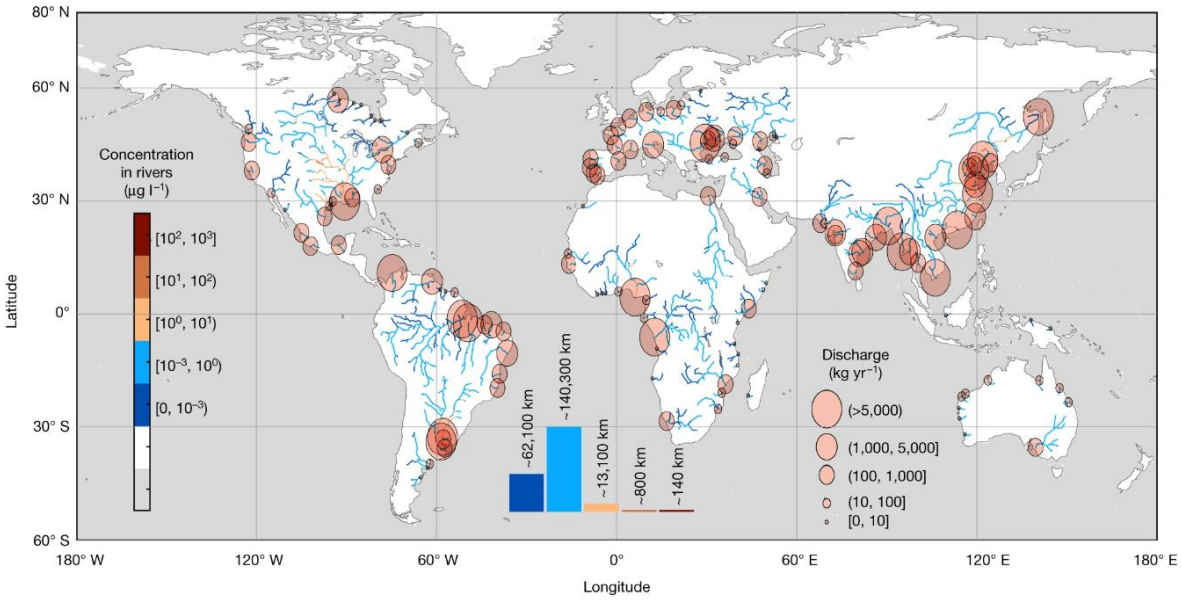

***Figure 1.8**. Average total pesticide active substances (PAS) concentrations in river reaches and annual average PAS discharge to oceans. Histograms quantify the cumulative length of river reaches receiving PAS at specific concentrations. Adapted from [59].*

1.1.6. Co-occurrence of different micropollutants

Even if individual APIs and pesticides occur in world river waters in the range of the ng to µg, their cumulative concentration skyrockets when they are summed up. Highest cumulative concentration events in a worldwide study of 22 selected APIs in rivers[46] was detected in Lahore, Pakistan (70.8 µg L^{-1}), followed by La Paz, Bolivia (68.9 µg L^{-1}), and Addis Ababa, Ethiopia (51.3 µg L^{-1}). Interestingly, the mean concentration for La Paz, Bolivia was about 10 ± 35 µg L^{-1}. The important standard deviation observed highlights the variability in term of concentration of APIs (from supplementary data[46]).

For pesticides, the global concentration predictions by Maggi et al. (2023)[59] and its European Union (EU) counterpart by Pistocchi et al. (2023)[63] were based on a combination of monitoring data, emissions, and modeling. These studies, which emerged as a response to the insufficient data on concentration levels, highlighted limitations in monitoring pesticides, and emphasize the co-occurrence of pesticides in river bodies. In particular, the challenge of detection limits was emphasized, with micropollutants present at biologically active levels yet at concentrations too low for detection. Globally, it was estimated that 62,100 km of rivers showed average cumulative pesticide concentrations below detection limits of 10^{-3} µg L^{-1}, 140,300 km presented concentrations up to 1 µg L^{-1}, and over 13,000 km exceeded 1 µg L^{-1} [59]. Pesticides in river waters worldwide were estimated to comprise 52.6% herbicides, 35.6% multipurpose pesticides, 11.2% fungicides and 0.6% insecticides[59].

Inevitably, micropollutants co-occur within aquatic ecosystems. In addition, understanding their behaviour in aquatic ecosystems requires specific consideration of the sediment-water interface (SWI) as a hotspot of biogeochemical processes. This transition zone, which can be

qualified as an ecotone, is still poorly understood and is presented and discussed in the next section.

1.2. The sediment-water interface and biogeochemical processes

In aquatic ecosystems such as rivers, streams and lakes, water is in dynamic flux between the liquid phase and interstitial water within the porous sediment phase. This sediment phase is a complex matrix comprising particles that can itself originate directly from aquatic ecosystems (autochthonous particles) or from outside water ecosystems (allochthonous particles), or from the atmosphere[64]. Most mineral sediment arises from erosion and weathering, whereas organic sediment is typically composed of detritus and decomposing material[65].

1.2.1. Sediment matrix composition

Sediment results from the deposition of organo-mineral particles at the bottom of water bodies. Its composition can vary based on the nature of the water body, seasons, and years. In rivers and streams, autochthonous particles are formed in part through the growth of algae, aquatic vascular plants, mosses, bacteria, and animals within the aquatic ecosystem. A portion of these particles is organic and carbon-rich, comprising approximately 50% carbon[64,66]. Inorganic compounds can also originate from dead organisms. For example, diatoms, a type of unicellular algae, possess a silica skeleton that contributes to sediment. Photosynthesis often also results in the formation of calcium carbonate, specifically the mineral calcite ($CaCO_3$), by corresponding organisms such as foraminifera[64,66].

Particulate material of allochthonous origin primarily comes from bedrock and soils dominated by minerals. Chemical and physical weathering processes convert large rock masses into a spectrum of smaller rocks or particles. Some of these particles may be transported by flowing water, and inorganic weathering products stored in soils where they may undergo changes in size or chemical composition over geological time scales. Weathering products contribute to the formation of clay, silt, sand, gravel, cobble, and boulders in drainage networks[64,66].

Additionally, streams and rivers receive significant amounts of particulate organic matter, including leaf litter, organic particles from soils, and faecal material from animals. Large organic particles such as leaves or wood are known as coarse particulate organic matter (CPOM). while smaller particles are referred to as fine particulate organic matter (FPOM).

Small particles often contain hybrid forms of organic and inorganic matter with organic chemicals often adsorbed to particle surfaces. Small particles are subject to electrostatic forces due to their high surface area-to-volume ratio, leading to particle aggregation in the aquatic environment. Solids and solutes entering aquatic ecosystems are subjected to phenomena such as dispersion, dilution, and direct degradation.

1.2.2. Sediment mixing

Sediment mixing in aquatic environments involves natural physical processes. In streams and rivers, particles of different grain sizes may be eroded from material bed, transported by wind, and sediment when winds subside (Fig. 1.9a)[67]. In lakes, such processes also depend on the depth of the water column (Fig. 1.9b)[67].

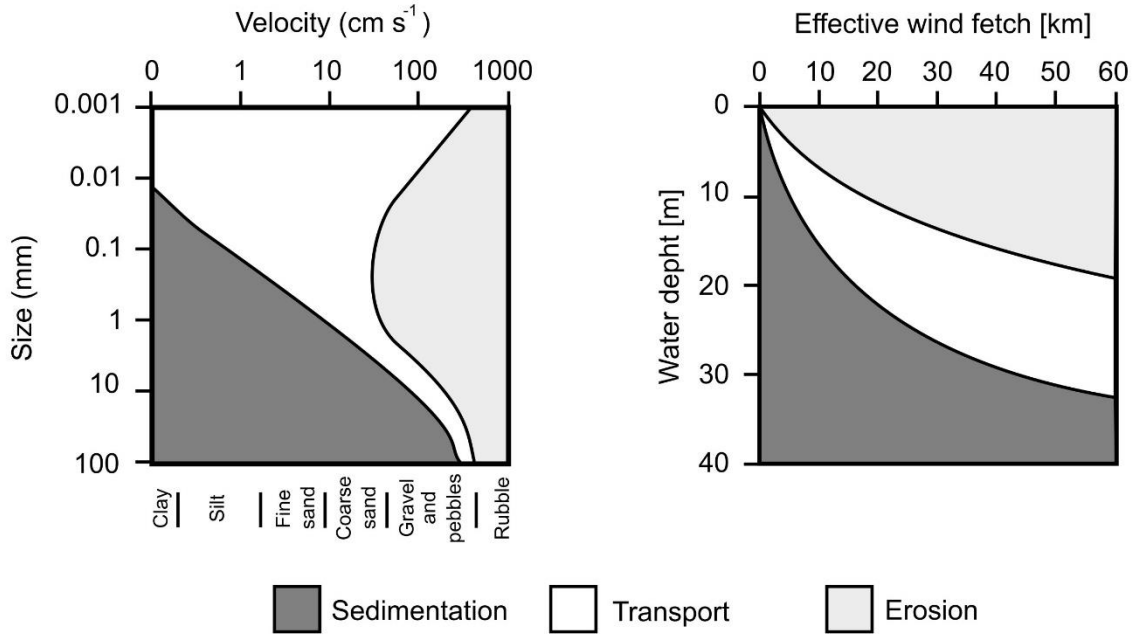

Figure 1.9. *Relationship between sedimentation, transport and erosion to the grain size and current velocity for streams and rivers: Hjulström diagram (a) or wind fetch and water depth (b). Adapted from [67].*

Macroinvertebrates play a crucial role in the dynamics of sediment mixing. The resuspension of particles from the sediment to the water phase can occur through the ejection by organisms, a process known as bioturbation. This bioturbation process is primarily driven by macroinvertebrates, including burrowing worms, insects, amphipods, clams but also vertebrates such as fish, and other animals. These organisms resuspend particles and organic matter into the water phase[65].

Additionally, particles may resuspend in water by hydrodynamic forces, particularly in the water layer immediately above sediments. This diffusive layer is referred to as the benthic boundary. Consequently, sediments originate from multiple sources and undergo continuous mixing from various processes[65] (Fig. 1.10).

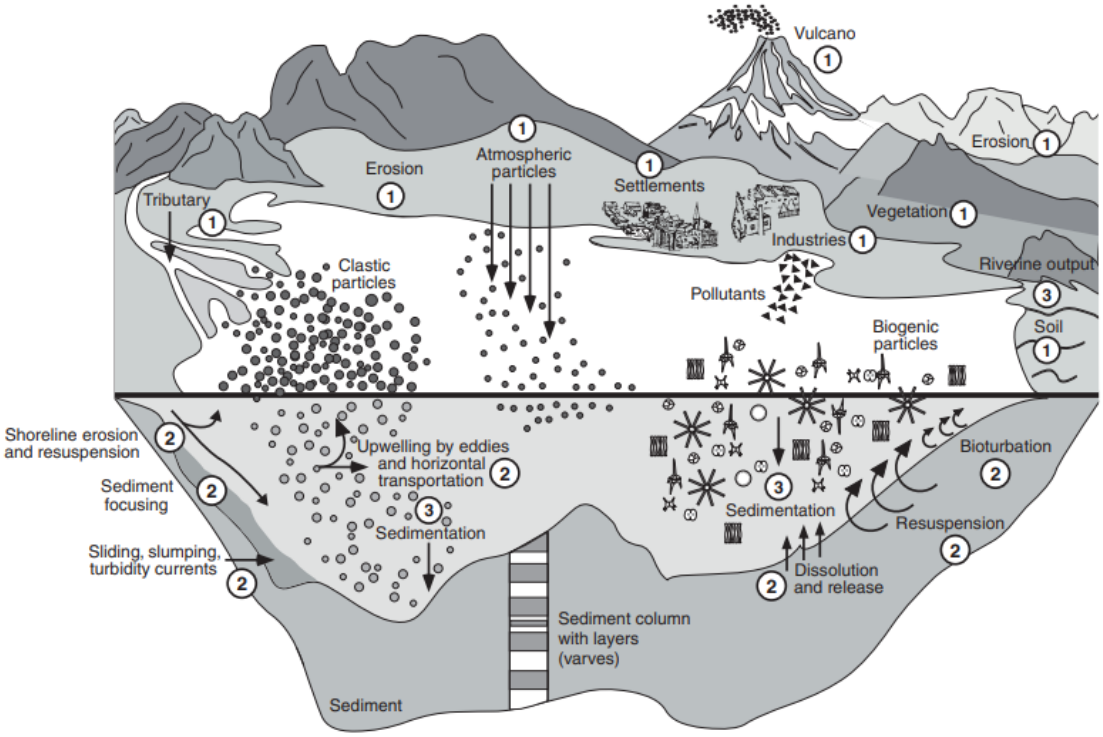

Figure 1.10. *Effect of external and internal environmental factors on suspended sediments, sedimentation, and sediment formation in a lake basin. 1: sources of suspended particulate matter (SPM); 2: transport and transformation of SPM; 3: removal of SPM. Clastic particles have a grain size of > 2mm. Turbidity currents originate from slope slides on steep shores. Biogenic particles and varves (sediment layers) refer to particles produced by combined chemical and biological processes. Taken from* [66].

1.2.3. Hyporheic zone, benthic boundary layer, and conceptualization of the sediment-water interface

1.2.3.1. Hyporheic zone

The hyporheic zone (HZ) is an ecotone between the stream and subsurface, a dynamic area of mixing between surface water and groundwater[68]. Peter et al. (2019)[69] defined the hyporheic zone as a natural bioreactor that is capable of "attenuating" chemical pollutants. The HZ consists of sediment saturated with water from the water column. Worthy of note, not all continental water bodies feature this hyporheic zone. The HZ may be formed by different processes. In certain instances, water may directly rest on an impermeable stratum (Fig. 1.11A). However, in the presence of permeable sediment, channel water can form an HZ by advection, i.e., lateral flow (Fig. 1.11B), or infiltration, i.e., vertical flow till the groundwater zone (Fig. 1.11C) or not (Fig. 11D). In some cases, a continuum will be created between channel water, HZ, and groundwater due to advection processes in both phases (Fig. 1.11E)[70].

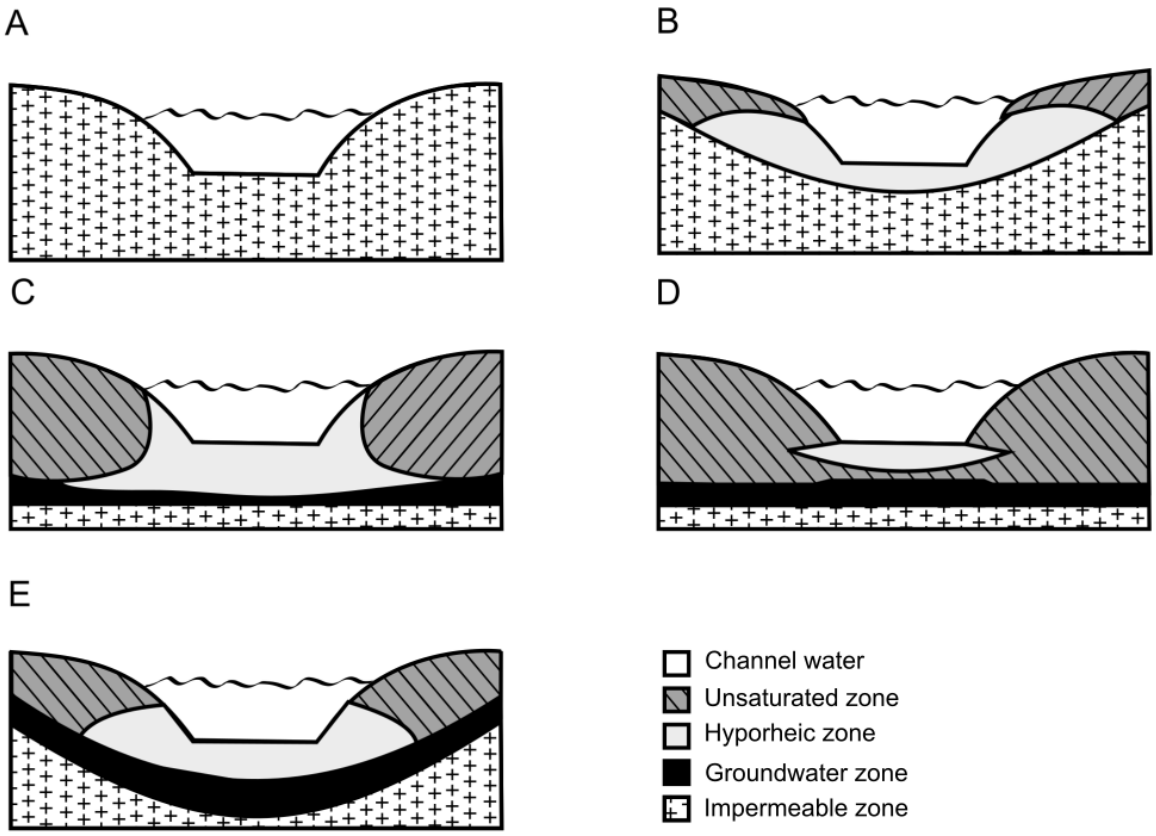

***Figure 1.11**. Conceptual cross-sectional models of surface channels and beds showing relationships of channel water to hyporheic, groundwater, and impermeable zones. A, no hyporheic zone; B, hyporheic zone created only by advected channel water; C, hyporheic zone formed only by infiltration of channel water beneath the stream bed; D, perched hyporheic zone formed only by infiltration of channel water beneath the stream bed; E, hyporheic zone formed by advection from both channel and ground water. Adapted from [70].*

1.2.3.2. Benthic boundary layer

The benthic boundary layer (BBL) in lakes, reservoirs, and rivers refers to the portion of the water column directly affected by the presence of the sediment-water interface[71]. The vertically structured BBL is affected by the physical processes governing the vertical transport of momentum and solutes. The first sublayer in contact with sediment is called 'diffusive sublayer', in which the exchange of heat, dissolved solids, and gases is regulated between the sediment and water column[71]. This layer, in which ions, nutrients, and organic materials move through molecular diffusion, is approximatively 1 mm thick[71]. The second 'viscous' sublayer above the first one, approximately 1 cm thick, is the place where vertical transport of momentum is governed by molecular viscosity (i.e., result of the interaction between the different molecules in a fluid). The last 'logarithmic' sublayer can be up to several meters above the sediment surface. Here, transport is governed by turbulent eddies, leading to high mixing rates[71].

1.2.3.3. Sediment-water interface concept

As mentioned above, the hyporheic zone is an ecotone between the stream and subsurface: a dynamic area of mixing between surface water and groundwater at the sediment-water interface, and a natural bioreactor capable of "attenuating" chemical pollutants[69,70]. This definition may be particularly relevant to the top layer of the hyporheic zone. The SWI is defined as this upper part of sediment[65], on a scale of millimeters[65] to centimeters[72] (Fig. 1.12), however some authors also include in it the first sub-layer of the benthic boundary layers, also called diffusive layer[65]. Considering that SWI is a biogeochemical hotspot involving dissipation of organic chemicals and transport of solutes from sediment to water, both the top layer of sediment and the diffusive sublayer of the benthic boundary layer (Fig. 1.12) can be included in the definition of the SWI.

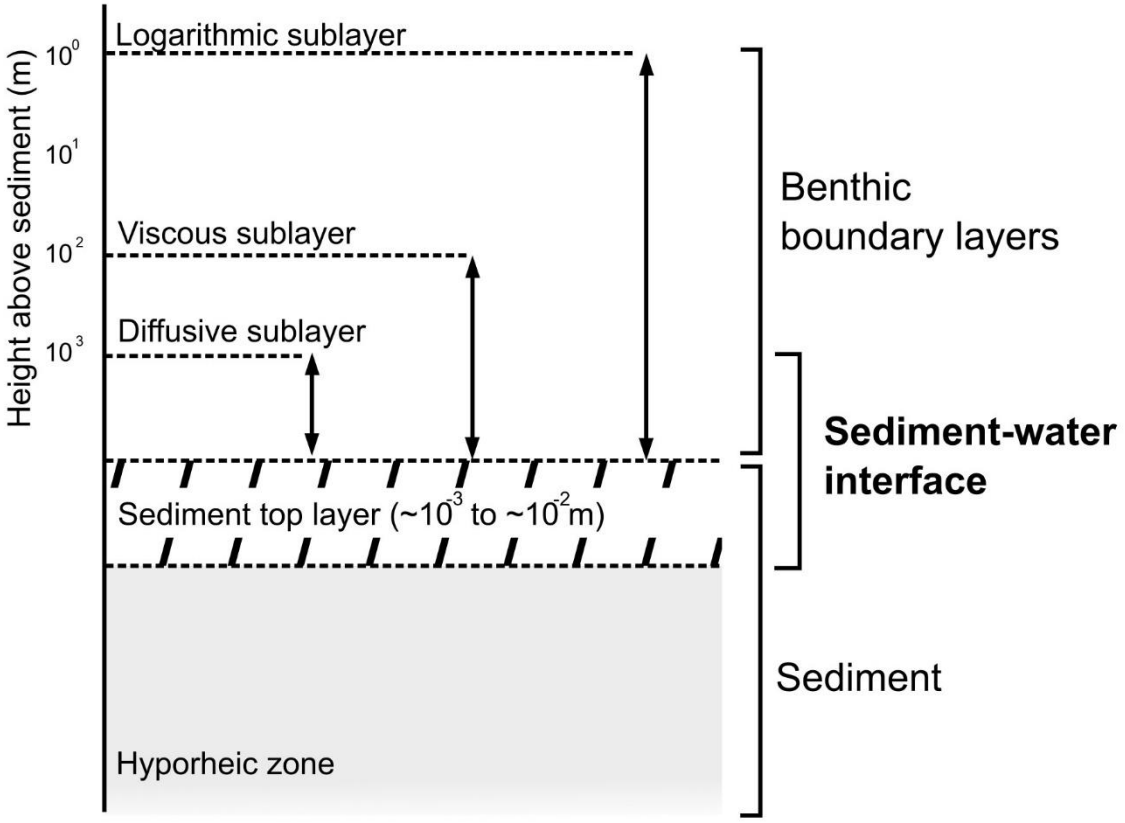

***Figure 1.12**. Conceptualization of the sediment-water interface. Adapted from [71].*

Concerning micropollutants, the SWI plays a pivotal dual role both as a sink and a transformation hotspot[73,74]. The sediment component of the SWI comprises inorganic materials such as clay, silt, and sand alongside organic matter. Micropollutants may be sorbed onto this sediment, and may then desorb under certain conditions, sediment particles thereby acting successively sink and a source of micropollutants[75,76]. For specific pesticides, the sorption process is affected by clay content, sorption with increasing clay content and to a lesser extent with organic matter[77,78]. The presence of $CaCO_3$ also significantly affects the sorption of micropollutants. $CaCO_3$ coating on sediment or soil particles can limit the sorption of chemicals with low water solubility or conversely, enhance the sorption for chemicals with higher water solubility[79]. These sorption-desorption processes are in equilibrium, meaning that sediment receiving a large amount of contaminants will continuously supply the water column with smaller amounts of this contaminant, thereby partitioning them between the sediment and the water column[76]. The partitioning of contaminants largely depends on their physical-chemical properties, especially their hydrophobicity (log K_{ow})[80]. Additionally, a portion of the contaminant may remain unsorbed in pore water of the sediment[80]. Conversely, some of the contaminant may be sorbed to dissolved organic matter in the water column[81]. Hydrophobic pesticides (log $K_{ow} > 3$) sorb onto suspended particles, particularly on finer particles. For example, Passeport *et al.* (2011)[82] experimentally demonstrated that the sorption of various pesticides with low K_d values is similar to desorption for silty clay loam at pH 6.5 to 8.5. In contrast, desorption of pesticides with intermediate or higher K_d values may be neglected, as sorption is much faster than desorption[83].

At the SWI, micropollutant dissipation results from both conservative, non-degradative mechanisms involving sorption, volatilization, and dilution[84], and from degradation processes[85] that comprise the transformation of parent molecules into various products. The degradative mechanisms of micropollutants include chemical or photolytic hydrolysis and can also arise from biotic processes, with microorganisms utilizing contaminants as sources of carbon and energy, or cometabolically, with microorganisms using non-specific enzymes to degrade environmental pollutants that do not support microbial growth. However, contaminant transformation can lead either to the complete dissipation of the parent contaminant and its transformation products (e.g., metformin) or to the formation of an even more recalcitrant product (e.g., *(S)*-metolachlor and terbutryn).

Partitioning of micropollutants also affects their transformation through altered exposure of the microbial compartment of the SWI. Primarily dominated by bacteria[86], it may also include other types of organisms also potentially involved in micropollutant degradation.

Worthy of note, water exchange between the sediment and the liquid phase may also promote biological transformation of recalcitrant and typically poorly water-soluble micropollutants[83] in the aqueous phase. In short, the SWI represents a potential hotspot for micropollutant dissipation.

1.3. Micropollutant dissipation at the sediment-water interface

Within the aquatic ecosystem, transformation products (TPs) at the SWI can arise not only from metabolic or cometabolic processes of living organisms, but also from reactions driven by physical and chemical factors of the abiotic components of the ecosystem.

1.3.1. Photodegradation

At the surface of water column of aquatic ecosystems, photodegradation of micropollutants can occur due to exposure to sunlight irradiance. This process can occur through direct exposure to sunlight when the target molecule shows UV-visible absorption at wavelengths greater than 290 nm. Upon reaching the energy activation threshold (*hv*), catalysis initiates the breaking down of C-H bonds[87]. Photodegradation can also occur indirectly through the generation of reactive oxygen species in the presence of dissolved organic matter and NO_3^- [87]. The most reactive oxygen species is ·OH, which attacks C-H bonds in a relatively non-selective manner at diffusion-controlled rates, and it likely participates in the photodegradation of pesticides[87]. However, the formation and dissipation of radical species in aquatic ecosystems are complex processes that involve other reactive species such as CO_3^{2-}, $^1O_2$, and $HO_2^{\cdot}$ (Fig. 1.13).

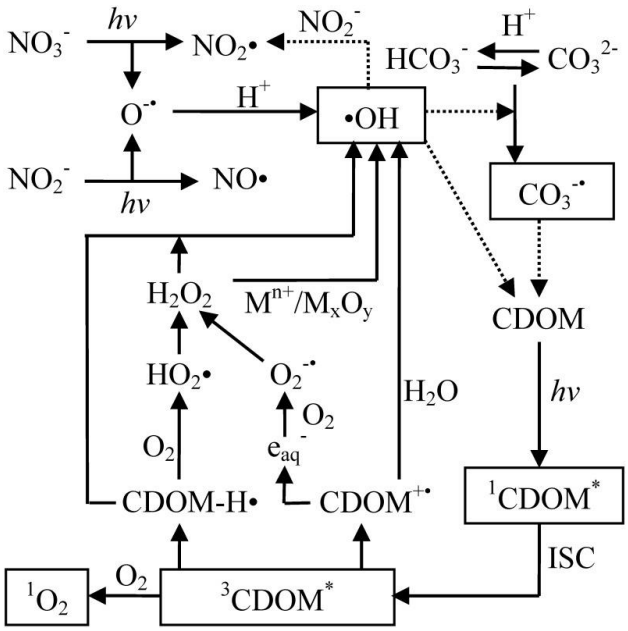

Figure 1.13. *Reactive species involved in indirect photolysis of pesticide in the aquatic environment. Formation (solid lines) and dissipation (dotted lines). ISC, inter-system crossing; CDOM, coloured (>290 nm absorption) dissolved organic matter with superscripts 1* and 3* indicate singlet and triplet excited species, respectively; Mn+, metal cation; MxOy, metal oxides. Taken from [87].*

An illustrative example is terbutryn, primarily utilized as a building material additive in construction materials for aesthetic and anti-decay purposes on facades. Due to exposure to sunlight and rain events, terbutryn may leach from buildings and be phototransformed into diverse TPs, such as terbutryn-sulfoxide, 2-hydroxyterbutryn or desethyl-terbutryn, and further into desethyl-2-hydroxyterbutryn[61] (Fig. 1.14). Contribution of direct and indirect photodegradation of terbutryn in water was investigated by Junginger et al. (2022)[61] at ITES (UMR7063) and proved significant at the top of the water column (Fig. 1.14).

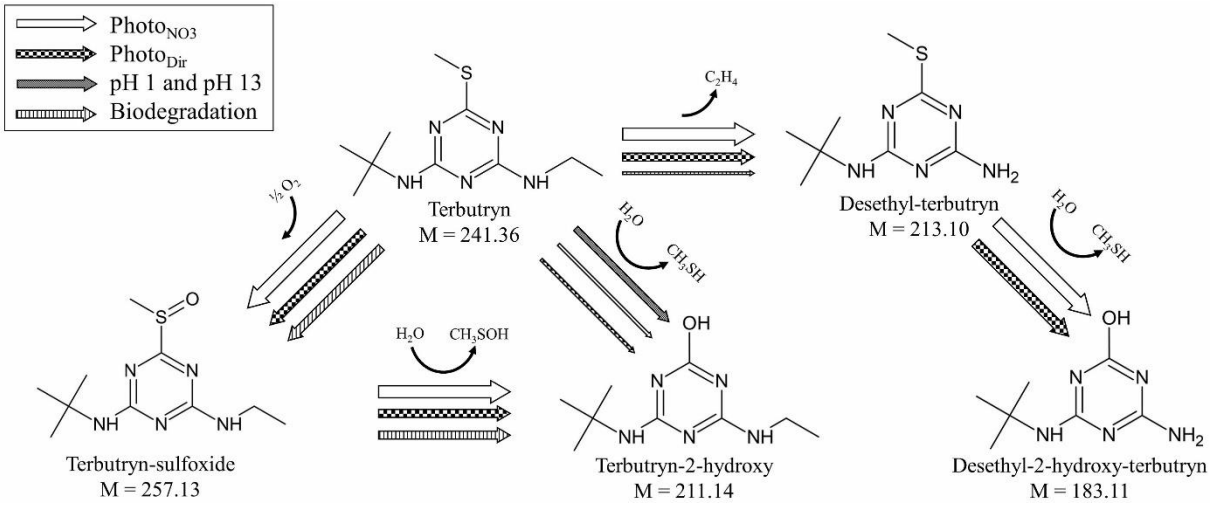

Figure 1.14*. Putative degradation pathways of terbutryn in the environment. Arrow thickness indicates the contribution of each process to overall transformation. Taken from [61].*

The significance of photolysis at the SWI may be limited due to lower penetration of sunlight with increasing depth. Direct photolysis primarily occurs in the first centimeters of the water column[82]. The presence of vegetation creating shaded zones may constrain and decelerate the contribution of photolytic activity in aquatic ecosystems[88]. Photodegradation likely plays a role in surface waters and sun-exposed areas such as soil and facades. Its contribution at the sediment-water interface, however, remains uncertain.

1.3.2. Abiotic hydrolysis

Abiotic hydrolysis of contaminants refers to the chemical hydrolytic degradation of pollutants without intervention of living organisms. In this process, contaminants interact with water molecules, causing the breaking of chemical bonds within the pollutant molecule. This interaction may involve catalysis by protons, hydroxide ions, and sometimes inorganic ions such as phosphate ions. Abiotic hydrolysis is particularly influenced by pH, along with factors such as temperature and the presence of dissolved organic matter[89].

Masbou et al. (2018)[89] conducted a comprehensive study on the hydrolysis of pesticides such as atrazine under diverse conditions over a 200-day period. The experiments were performed at two different temperatures (20 and 30°C) and included scenarios with or without added dissolved organic matter. The obtained results indicated that atrazine underwent hydrolysis exclusively under conditions characterized by either acidity (pH ≤ 4) or high alkalinity (pH = 12). Chloroacetanilides, specifically (S)-metolachlor, were degraded solely under alkaline conditions and at 30°C, and remained negligible at 20°C. Also, no significant hydrolysis was observed at neutral pH[89]. In the case of the triazine terbutryn, hydrolysis was limited even under extreme acidic and alkaline pH levels (1 and 13)[61].

However, a modelling study predicted that formation of hydrolysis products of organic chemicals under neutral pH conditions are still possible, with the half-life of the reaction depending on the type of reaction and the molecular structure of the contaminants involved[90]. For instance, a molecule containing an amide functional group at a neutral pH (pH = 7) is predicted to have a median half-life exceeding one year. In contrast, a molecule containing a carbamate group is predicted to show a median half-life for hydrolysis between 7 and 60 days at pH = 7 [90]. Considering that surface water bodies such as freshwater lakes, ponds, and streams, typically maintain a pH range of 6 to 8 [91], hydrolysis may thus occur to a limited extent but will be strongly dependent on the structure of the contaminant (Fig. 1.14).

1.3.3. Biodegradation

The SWI is colonized by microorganisms which may form heterotrophic biofilms and play a significant role in the biochemical transformation of pollutants[83]. Biodegradation is a process facilitated by microorganisms that utilize contaminants as a source of energy and carbon or can degrade them to resist their toxicity. In this context, biotic degradation of pollutants is typically catalysed by enzymes that accelerate corresponding chemical reactions. Today, the enzymatic systems and the microorganisms associated with pesticide biodegradation and the SWI are largely unknown, and thus remain unidentified i*n situ*[83]. Therefore, isolating strains involved in the biodegradation of micropollutants may prove useful for a better understanding of these processes. For example, work from our laboratory showed that metformin is used as a carbon and nitrogen source by *Aminobacter* strain MD1, which employs metformin hydrolase to break down metformin into guanylurea (TP) and dimethylamine (carbon source)[92] (Fig.

1.15a). Alternatively, enzymatically-mediated hydrolysis could occur on the imine/guanidine function (Fig. 1.15b), leading to the formation of dimethylurea and guanidine, which could be further mineralized into two CO_2 molecules. Another hydrolysis pathway involves the second imine/guanidine, leading to the liberation of urea and dimethylguanidine (Fig. 1.15c). Demethylation is also a plausible process that could result in the formation of biguanide after release of formaldehyde (Fig. 1.15).

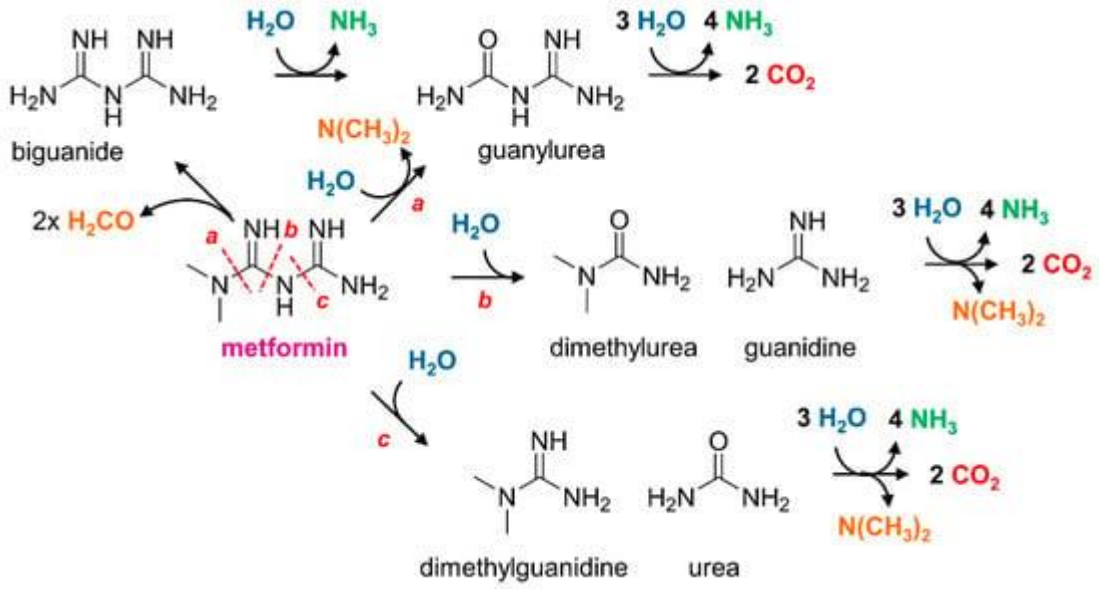

***Figure 1.15**. Potential biodegradation pathways of metformin. Bacteria may use metformin as the sole carbon source for bacterial growth. Energy for growth from carbon is only available from the oxidation of the two methyl groups of dimethylamine (orange). Monooxygenases acting on these N-methyl groups will produce formaldehyde (left), which may then be oxidized to CO_2, generating reducing equivalents for growth. Alternatively, hydrolysis of the two guanidine groups by carbon-nitrogen hydrolases (alternative pathways* a–c*) will release dimethylamine either directly (*a*) or at later stages of metformin degradation (*b,c*), with concomitant production of different intermediates with guanidine and/or amide functional groups, including but not limited to those shown. Energy for growth may also be derived from oxidation of ammonia (green) released by hydrolysis reactions. Taken from [92].*

Altogether, biodegradation emerges as the most promising and effective process for micropollutant removal at the SWI when compared to photodegradation and hydrolysis, as indicated in Table 1.2. Among the three representative compounds examined in this study, namely terbutryn, (S)-metolachlor, and metformin, abiotic hydrolysis demonstrates the least efficiency in degradation. While biodegradation may dominate as the primary degradation mechanism, the microbial entities participating in this process remain inadequately characterised both taxonomically and functionally. Consequently, pathways of dissipation often remain ambiguous, and understanding of the impacts of micropollutants on non-target organisms and microbial communities within the SWI remains limited.

Table 1.2. *Half-lives (DT_{50}) of urban pesticide terbutryn, agricultural pesticide (S)-metolachlor, and active pharmaceutical ingredient (API) metformin in hydrolysis, photolysis, and biodegradation processes. (n.s) non-significant degradation.*

	Hydrolysis		**Photolysis**	**Biodegradation in aquatic ecosystem**
	pH	DT_{50} range (days)	DT_{50} range (days)	DT_{50} range (days)
Terbutryn[61]	13	[12-26]	[2-12]	[2-5]
	7	n.s		
	1	[1-3]		
(S)-metolachlor[89,93,94]	12 (at 30°C)	[99-139]	[2-3]	[8-33]
	12	n.s		
	4	n.s		
Metformin[95]	9	n.s	~28	[7-55]
	7	n.s		
	5	n.s		

1.4. Effects of micropollutants on organisms at the sediment water interface

1.4.1. Assessment of individual and combined effects

1.4.1.1. Toxic unit model

Laboratory studies usually investigate the effects of chemicals individually to avoid confounding factors associated with cocktail effects. For example, OECD guidelines 201, 203, 210, 211, and 222 include tests of individual chemicals on various model organisms (algae, fish, crustaceans, worms) to assess the toxicity of a compound in the environment. One approach for Environmental Risk Assessment (ERA) of individual compounds involves using the PEC/PNEC ratio (Predicted Environmental Concentration/ Predicted No Effect Concentration) also known as 'toxic unit' (TU) ratio. A TU ratio greater than 1 for a given chemical indicates an environmental risk[96]. However, relying solely on the PEC/PNEC ratio for individual micropollutants and focusing on model organisms has relatively limited predictive value. Indeed, this approach offers only a fragmented perspective on the environmental reality, and lacks consideration of potentially intricate and complex interactions between different contaminants.

Thus, an increasing number of more integrative studies are now emerging[97–99] which take the ubiquity, diversity and coexistence of micropollutants into account. Conceptual models have been developed to address the disparity between the effects of individual pharmaceuticals and those of their mixtures. One proposed approach involves the use of a hazard quotient (HQ) score[28]. Another strategy relies on the well-established concentration addition (CA) model[100]. These methods still rely on the PNEC/PEC ratio and a limited database

of aquatic organisms. Nevertheless, when coupled with a modelling approach that incorporates various toxicity scenarios of micropollutant interactions, the CA model could prove particularly relevant in that it also takes the limitations in detection and quantification into consideration[101].

For example, the multi-scenario risk assessment strategy applied to mixtures of chemicals of emerging concern from Inostroza et al. (2023)[101] proposes to handle non-detects and missing concentration values as follows:

i) Exposure-scenario 1: Non-detects are set to zero, representing the scenario with the lowest risk that is still compatible with the analytical data.

ii) Exposure-scenario 2: Non-detects are set to their method detection limits (MDLs), representing the scenario with the highest risk that is still compatible with the analytical data.

iii) Exposure-Scenario 3: Missing concentration values are estimated using Kaplan-Meier modelling, providing the most accurate basis for the risk assessment although not allowing the identification of individual risk drivers.

To illustrate these modelling approaches, Pistocchi et al (2023)[63] predicted the cumulative toxicity of a mixture of pesticides at the European scale, with individual pesticides present mainly at TU below 0.1. Cumulative toxicity present TU exceeding 0.1 for more than 27% of the EU stream network and exceeding 1 TU for more than 4% of the stream network (Fig. 1.16)[63].

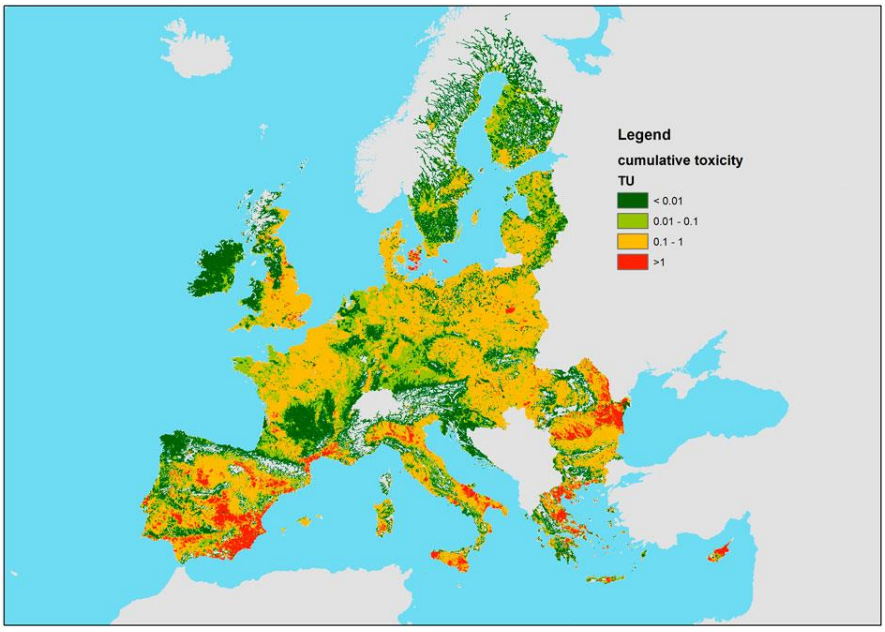

***Figure 1.16**. Map of cumulative water toxicity due to pesticides. Taken from [63].*

Addressing contamination mixtures also highlights the challenges posed by transformation products. A single contaminant can generate multiple TPs, effectively increasing the number and potential toxicity of the contaminants present[102]. Chemical synthesis of transformation products for biological tests on aquatic organisms is often complex, time-consuming and costly, making the inclusion of transformation products in PNEC/PEC a challenge[57]. In this context, emerging *in silico* tools, such as the "EPI Suite Tool" based on Simplified Molecular Input Line Entry Specification (SMILE)[57] provide a promising approach for predictions of toxicity

in fish, daphnia, and green algae. This was applied to neonicotinoid insecticides and their potential transformation products and revealed that some transformation products could cause serious damage to aquatic ecosystems[57]. *In silico* models thus represent a promising approach to address the diversity of parent molecules and their transformation products. Nevertheless, modelling approaches depend on experimental or in situ data that for the larger part, remain to be tested and validated[103].

1.4.1.2. Additive, synergistic, and antagonistic effects of contaminant mixtures

Mixture-based laboratory approaches provide a more realistic representation of real-world situations, where organisms and ecosystems encounter complex combinations of pollutants. Simultaneous exposure to multiple contaminants can lead to different types of effects: i) additive effects, when the sum of individual effects represents the mixture effect; ii) synergistic effects, when the mixture effect is greater than the additive effect; and iii) antagonistic effects, when the sum of individual effects is less than the mixture effect[104].

As an example of antagonism, the combined application of atrazine and bentazone was observed to slow down their degradation, increasing the lag phase necessary before the onset of this degradation and making these micropollutants more recalcitrant when applied in a cocktail on agricultural soil at a concentration 5.03 g kg^{-1} of soil[105].

As for synergistic effects, they are especially observed at medium and higher dose when the target of the different contaminants is the same and a certain threshold concentration is exceeded, or when the effects of contaminants with different targets interact and/or potentiate each other[104]. For example, dissipation kinetics of mesotrione combined with metolachlor applied on agricultural soil at concentrations of 0.45 mg kg^{-1} of soil[97] differed compared to those in experiments with individual micropollutants with a clear synergistic effect on the structure of microbial communities in that the same effect was observed for these contaminants applied together than when applied alone at a 10 times higher dose[97].

While investigations of binary combinations of contaminants remain manageable, considering more than two contaminants is more complex and renders the understanding of the contribution of each contaminant more uncertain. This clearly represents a challenge for risk assessment when one considers that aquatic ecosystems are often contaminated with hundreds of different chemicals[106]. Hence, mixture-based approaches provide a more realistic perspective although they are not without their limitations at present.

The non-food Scientific Committees of the European Commission have identified two main gaps in this context. Given the almost infinite number of potential combinations of chemicals to which humans and other living organisms are exposed, there is a need for an initial filter to focus on mixtures of potential concern, and several criteria have been provided[104]. However, there is still a significant knowledge gap due to the lack of information on the effects of exposure and the limited number of chemicals for which there is sufficient information on their mode of action on organisms. There is currently no agreed inventory of modes of actions of chemicals, nor a defined set of criteria on how to characterize or predict the mode of action for chemicals for which little data are yet available.

1.4.2. Effects on biogeochemical functioning and services

The sediment-water interface is the location where gradients in physical, chemical, and biological properties are most pronounced in natural waters[65]. Chemical and microbiological transformation processes contribute to the cycling of elements between water and sediments. Biogeochemical cycles involve transformative processes for essential nutrients, including carbon, nitrogen, sulphur, oxygen, and various other elements, with microorganisms playing a crucial role in these cycles[65]. Micropollutants such as pesticides can have unintended effects on microorganisms, potentially inducing dysbiosis and posing a threat to the biosphere by disrupting biogeochemical cycles.

For instance, the extensive use of fertilizers contributes to nitrogen input into aquatic ecosystems. This imbalance in nitrogen cycling, coupled with the application of antifungal pesticides adversely affecting natural cyanobacteria parasites, may result in the excessive growth of harmful algal blooms[107]. This phenomenon cascades and depletes oxygen levels through excessive respiration[107], along with the production of toxins affecting fish, birds, mammals, benthic epi- and in-fauna, and submerged aquatic vegetation. Outbreaks of algal blooms (algal eutrophication) and the rapid growth of aquatic grasses (grass eutrophication) may in turn lead to the accumulation and subsequent decay of large amounts of algae and aquatic grass debris, intensifying the carbon cycle of lakes and significantly impacting aquatic environments and ecosystems[108].

1.4.2.1. C-cycling

Carbon cycling involves the storage and dynamic fluxes of carbon among its primary reservoirs, namely the atmosphere, terrestrial biosphere, oceans, and sediments[109]. Within these exchanges, various transformative processes of organic matter occur. Organic matter comprising material derived from organisms at all trophic levels as a result of excretion, secretion, death, or lysis[65,110] cycles through sediment and the water phase. As a result, organic matter and particles are continuously deposited at the sediment-water interface and buried at rates ranging from millimetres to centimetres per year, depending on the water body[65].

Conversely, the combined effect of all biological activities on particle and pore water dynamics at the sediment-water interface, such as bioturbation primarily involving macroinvertebrates, leads to the resuspension of particles and organic matter in the water phase[65]. As the sediment-water interface is heavily colonized by microorganisms, reaching up to 10^{10} microorganisms per cm^3 [65], a portion of these microorganisms will utilize dissolved organic matter (DOM) as an energy substrate[111]. Microbial growth and activity depend on the availability of DOM as an energy substrate. As oxygen depletes with depth from the water column to sediment[65], dissolved organic matter (DOM) undergoes various fates. In the oxic sub-layer, microorganisms use this organic matter as a central substrate for respiration, leading to CO_2 production (mineralization). Deeper down, organic matter undergoes hydrolysis, acidogenesis, acetogenesis, and methanogenesis, resulting in the release of carbon dioxide (CO_2) and methane (CH_4). A portion of the carbon contributes to biomass production (Fig. 1.17). These two crucial pathways have shown potential alterations due to micropollutants such as pesticides. Simazine and $CuSO_4$ have been reported to decrease methanogenesis in pond sediments[112], and N-methyl-carbamate pesticides have been found to stimulate methanogenesis in salt marsh sediment[113].

In aquatic ecosystems, insecticides have consistently been shown to stimulate respiratory CO_2 production. Herbicides, in contrast, lower respiration by altering the composition of phytoplankton or by decreasing the abundance of phytoplankton[114]. Moreover, specific contaminants such as chlorpyrifos, phosalone, dimethoate, l-cyhalothrin, and kresoxim-methyl have demonstrated inhibitory effects on both basal and substrate-induced microbial respiration[115]. Of note, the impact of contaminants such as pesticides on carbon cycling has primarily been described for agricultural soils[116], and the overall impact of micropollutants including pharmaceuticals on carbon cycling, especially at the SWI, remains poorly characterized. Fáberová et al. (2019)[117] concluded that acute exposure to non-antibiotic pharmaceuticals is likely to stimulate methanogenesis, while chronic exposure would inhibit it[118].

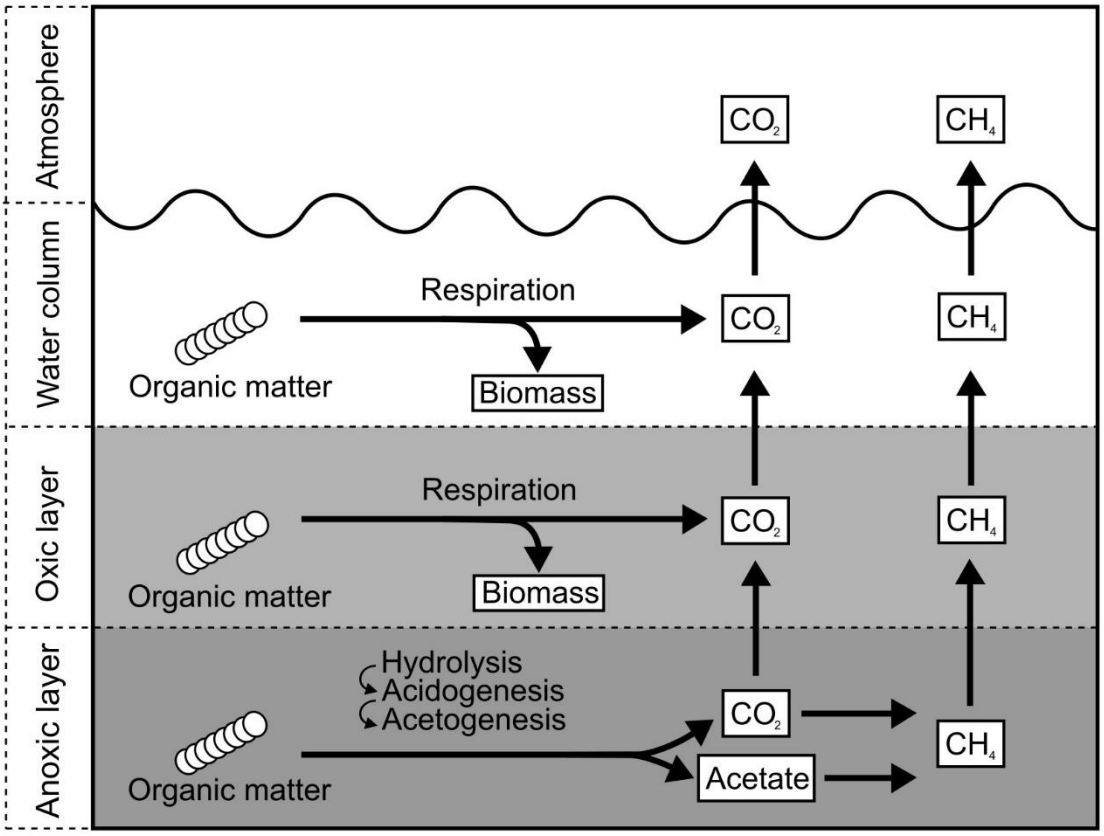

Figure 1.17. *C-cycling of organic matter near the sediment-water interface with (a) anoxic oxidation of methane, and (b) oxic oxidation of methane.*

1.4.2.2. N-cycling

Microorganisms involved in nitrogen fixation, nitrification, and denitrification play a crucial role in converting nitrogen from its inert dinitrogen form in the atmosphere into nitrogen sources assimilable by plants or microorganisms, ultimately leading to the release of N_2 back into the atmosphere[119]. The nitrogen cycle in water is driven by complex biogeochemical transformations mediated by microorganisms, including nitrogen fixation, denitrification, assimilation, and anaerobic ammonia oxidation[120] (Fig. 1.18). This N-cycling was conceptualized for the SWI by *Wankel et al.* (2009)[121] (Fig. 1.19).

Many studies provide examples of how micropollutants may[121–124] or may not[125] affect nitrogen cycle functioning at the SWI. For example, chlorothalonil fungicides were shown to inhibit the denitrification process in riparian sediment by impacting organic matter metabolism (electron production), the electron respiration chain (electron transport), and the activities of denitrifying enzymes (electron utilization). This effect is more pronounced than any alterations to denitrifier communities or denitrifying gene abundances[123]. Pesticides with non-specific modes of action such as metolachlor and chlorothalonil are more likely to significantly affect the nutrient dynamics of sediment microbes because they may disrupt microbial respiration[124].

Similarly, insecticides (potassium oil, malathion, pyrethrin) and herbicides (dichlorprop-P, glyphosate, nonane Acid) were demonstrated to negatively affect the nitrification process at high concentrations in sediment[125]. Other compounds such as metolachlor decreased ammonium and phosphate uptake, while chlorothalonil decreased nitrate remineralization and phosphate uptake in sediment[124].

A few studies have also investigated the direct effects of pharmaceuticals on the nitrogen cycle in water and soil. Some pharmaceuticals have no observable effect on the nitrogen cycle in water and soil, while others appear to inhibit or stimulate it. Among these, amoxicillin, chlortetracycline, ciprofloxacin, clarithromycin, enrofloxacin, erythromycin, narasin, norfloxacin, and sulfamethazine had the most significant effects on nitrogen cycle processes[120]. Underlying mechanisms are not yet elucidated, and are likely due to the stimulation or the inhibition of microbial metabolism through potential impacts on specific enzymes or as competitive substrates for example[120].

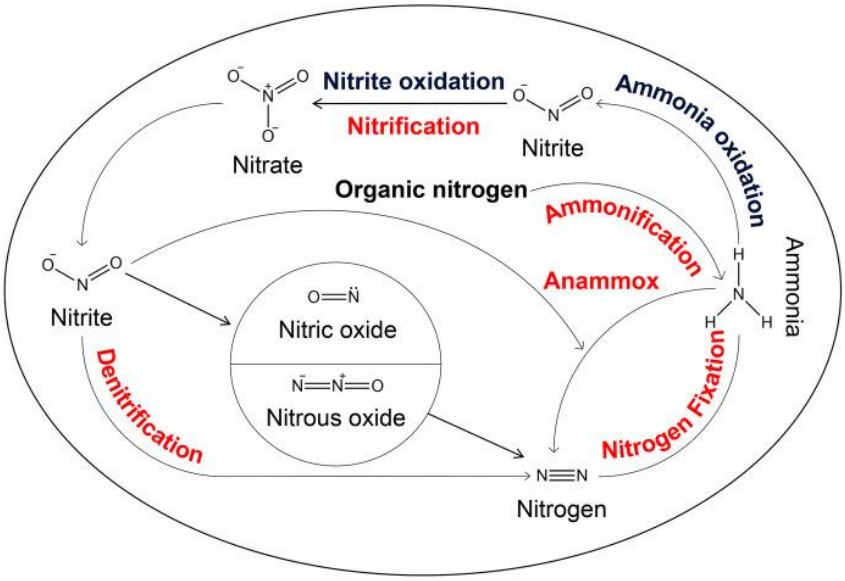

Figure 1.18. *The nitrogen cycle. Taken from [120].*

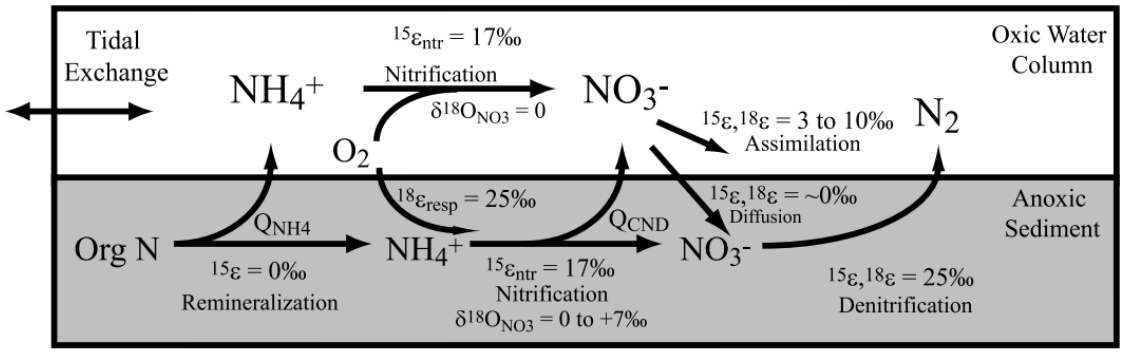

Figure 1.19. *Sediment-water nitrogen cycling represented in steady state box model. Q_{NH4} refers to the amount of NH_4^+ diffusing upward out of the sediment that escapes oxidation at the sediment surface or in the water column. Taken from [121].*

Clearly, the overall effect of micropollutants on biogeochemical cycles at the SWI remains to be understood in more detail. Much of the existing literature primarily focuses on agricultural soil and WWTP sludge. However, the limited information available at present indicates that micropollutants may indeed affect biogeochemical cycles. This represents an important area for future study and will require investigations of micropollutant effects on all types of living organisms, both individually and within ecosystems.

1.4.3. Response of the microbial compartment to micropollutant exposure

1.4.3.1. Prokaryotes as models of choice

Research on the response of the biological compartment to micropollutants may be conducted at the level of higher organisms such as fish and crustaceans as well as at the microbial level, targeting bacteria, archaea, and fungi. The SWI is predominantly colonized by bacteria and archaea[86,126]. Due to their small size and high surface-to-volume ratio, procaryotes feature extensive contact interfaces with their surrounding environment[127–129], and this makes them prime candidates as bioindicators of micropollutant exposure. Other characteristics such as their short generation time and functional role in biogeochemical cycles, combined with recent advances in molecular techniques, such as metagenomics and metatranscriptomics, make them increasingly worthy of consideration to evaluate the effect of various stressors and dissipation processes in aquatic environments[130]. Moreover, microorganisms in aquatic settings often develop as biofilms, which play a significant role in the transformation of pollutants[83]. As major players of SWI bioreactivity, microorganisms thus represent key objects of choice for in-depth studies of micropollutant dissipation at the SWI.

1.4.3.2. Individual organisms

The effects of contaminants may be studied at various ecosystem levels ranging from individual organisms to complex biological communities. Unicellular organisms, including many well-investigated bacteria can be cultivated in the laboratory and represent a valuable resource for reproducible experiments delving into mechanistic details[92,131]. Such microorganisms may provide insights into pollutant toxicity and shed light on degradation pathways for contaminants of interest. For instance, pollutant-degrading strains were isolated for the micropollutant

atrazine, such as *Bacillus licheniformis* and *Bacillus megaterium*[132] or *Ensifer* sp.[133]. Such strains are highly valuable as they allow to identify pathways and genes involved in catabolic processes of contaminants of interest. For instance, the *Ensifer* sp. pathway for atrazine degradation was shown to involve 6 genes (*AtzABCDEF*)[133]. However, other atrazine-degrading strains showed different genes such as *trzD* and *trzN*, and different major combinations of genes such as *trzN–atzBC*, *atzABC–trzD* and *atzABCDEF*[133]. Several studies have also suggested that transposition and plasmid-mediated horizontal gene transfer may contribute to the dissemination of atrazine-degrading genes[134], highlighting the fact that identification of functional genes may be more informative than strain identification in studies aiming at using bacterial indicators of contamination and/or remediation. By identifying the functional genes responsible for contaminant degradation, we gain a more comprehensive understanding that transcends specific bacterial strains. This approach offers greater information content, as the same genes may be found in a variety of microbial communities, enabling broader applicability of the knowledge. Furthermore, identifying gene functions enhances our predictive capabilities. Approaches based on cultivation remain key sources of knowledge for deciphering biodegradation pathway. However, it is often estimated that some 99% of environmental bacteria are uncultivable[135]. Hence, molecular approaches based on omics at the community level are useful in investigating the effects on prokaryotic communities of contaminants and associated physicochemical conditions[136,137], especially at the community level.

1.4.3.3. Community studies and ecotoxicological approaches

Working with microbial communities may introduce more variability[138], but it can provide molecular-level information on interactions and microbial dynamics relatively easily[139]. In this context, an approach termed microbial ecotoxicology was recently introduced[140]. Ecotoxicology is defined by Chapman, J (2002)[137] as a modern scientific discipline derived from ecology and toxicology, and a subdiscipline of environmental toxicology. Its focus lies on the toxicological impacts of contaminants on wildlife, differentiating it from human, domesticated animal, and crop toxicology. Ideally, ecotoxicology strives to seamlessly combine the disciplines of ecology and toxicology. Subsequently, the microbial ecotoxicology was defined by Ghiglione F., Martin-Laurent F. and Pesce S. (2016)[141] as a branch of science that studies both (i) the ecological impacts of chemical (synthetic or natural origin) or biological (toxic species) pollution at the microbial scale and on the various functions that they ensure in the ecosystems and (ii) the role of microbial communities in the ecodynamic of the pollutants (source, transfer, degradation, transformation). It is a multidisciplinary scientific endeavour at the crossroad between microbial ecology, microbial toxicology, physics, and chemistry.

The response of prokaryotic communities may be examined at different levels. These include direct analysis using DNA metabarcoding, which enables the inventory and diversity analysis of prokaryotic taxa present in a given sample at a time and under conditions of interest. Changes in this diversity may reflect the impact of a contaminant on resistance and resilience over time. Moreover, this may serve as a diagnostic tool, particularly in identifying prokaryotic units, i.e. taxa, which are representative of the contaminated environment, and can then be referred to as biomarkers. A complementary approach involves monitoring the abundance of functional genes of interest by qPCR or shotgun metagenome sequencing, as employed for example in the study of nitrogen cycling[142]. This allows to predict biogeochemical changes (e.g., decreased abundance of nitrification genes and increased abundance in genes

for nitrogen fixation). Such approaches may be facilitated by techniques such as DNA-stable isotope probing which may help to identify strains involved in assimilative metabolism of pollutants[129].

Given the complexity of ecosystems in the field, laboratory microcosms that effectively mimic the SWI of environmental aquatic ecosystems allows variables such as temperature, homogeneity, and eco-exposome conditions to be controlled, facilitating experimental reproducibility. The major advantage of such setups is that they enable a high degree of experimental control and replication which would be virtually impossible to achieve in field studies[139]. Additionally, microcosms facilitate the work with highly toxic substances[143]. Concerns are sometimes expressed that laboratory microcosm studies may be too small spatially and temporally to fully replicate natural processes. However, the goal of such experiments is not to precisely reproduce complex ecosystems but to simplify them sufficiently to capture essential dynamics[129] and help elucidate the mechanistic details of processes of interest[143]. Field studies, in contrast, may often only provide correlative evidence of certain phenomena.

Worthy of note in this context, a significant knowledge gap exists regarding the aquatic environment in terms of microcosm studies. Indeed, the effects of micropollutants, and particularly pesticides, have been extensively studied mainly for aquatic organisms including crustaceans[40], macroinvertebrates[41] and amphibians[42], and mainly at the aquatic surface. Moreover, the effects of micropollutants on microbial composition have primarily been investigated for agricultural soil[97,105,142] and activated sludge[54,144–146] , and only occasionally in aquifers[41,43]. In contrast, studies exploring the impacts of micropollutants on microbial communities at the SWI have been notably scarce, with only a handful of exceptions[147–150]. However, these exceptions have predominantly concentrated on the sediment itself, rather than examining the broader SWI context.

1.5. Summary and gaps of knowledge

Micropollutants including pharmaceuticals, personal care products and pesticides enter aquatic ecosystems through various channels. They are then often found as complex mixtures of chemicals with highly diverse physicochemical properties. Micropollutant transformation, often initiated at the SWI, leads to the exposure of non-target organisms and in particular bacteria to such compounds as well as to their transformation products. Thus, understanding the response of aquatic ecosystems to micropollutant contamination requires consideration of a complex eco-exposome. Research has begun to investigate the fate of individual micropollutants at the SWI through laboratory experiments[94,151], but knowledge on the transformation of micropollutants mixtures compared to individual compounds and the effects of simultaneous exposure of microbial communities to different contaminants remains limited. Clearly, research is now needed to assess the combined effects of different contaminants at the SWI, including potential synergistic or antagonistic interactions. Investigating the interactions between micropollutants and microbial communities at the sediment-water interface, as potential sinks and sources of micropollutants, is crucial for assessing the fate of these compounds and their potential impacts on the biological compartment of aquatic ecosystems.

In addition, the overview of the scientific literature has highlighted that the role of sediment microorganisms in the transformation, degradation, or stabilization of micropollutants is not fully understood at present. Accessing such information has great importance for effective sediment and water risk management and remediation, particularly in the context of the implementation of bioremediation strategies. Again, the SWI plays a pivotal role as a biodegradation hotspot, but it is also characterized by complex physical-chemical variations such as oxygenation[65,152]. Prokaryotic communities respond and may adapt to variations in environmental conditions[153], including exposure to contaminants. However, there is currently limited understanding regarding the potential interactions between environmental stress and xenobiotic stress in the acclimation of prokaryotic communities at the SWI. Understanding the activity and diversity of prokaryotes at the SWI may offer valuable insights into biodegradation pathways. Such knowledge will be essential in developing and refining models that consider the microbial compartment at the SWI, working towards increasing accuracy of risk assessment.

In summary, contaminants, physicochemical parameters, and prokaryotic communities represent three interconnected components within the SWI, as depicted in Figure 1.20. There is still limited research on how variations in temperature, precipitation patterns, and hydrological cycles influence the fate and transport of micropollutants at the sediment-water interface. My major hypothesis is that a better understanding of the dynamic interplay among these SWI components is essential for understanding the dynamics of aquatic environments and their responses to global changes.

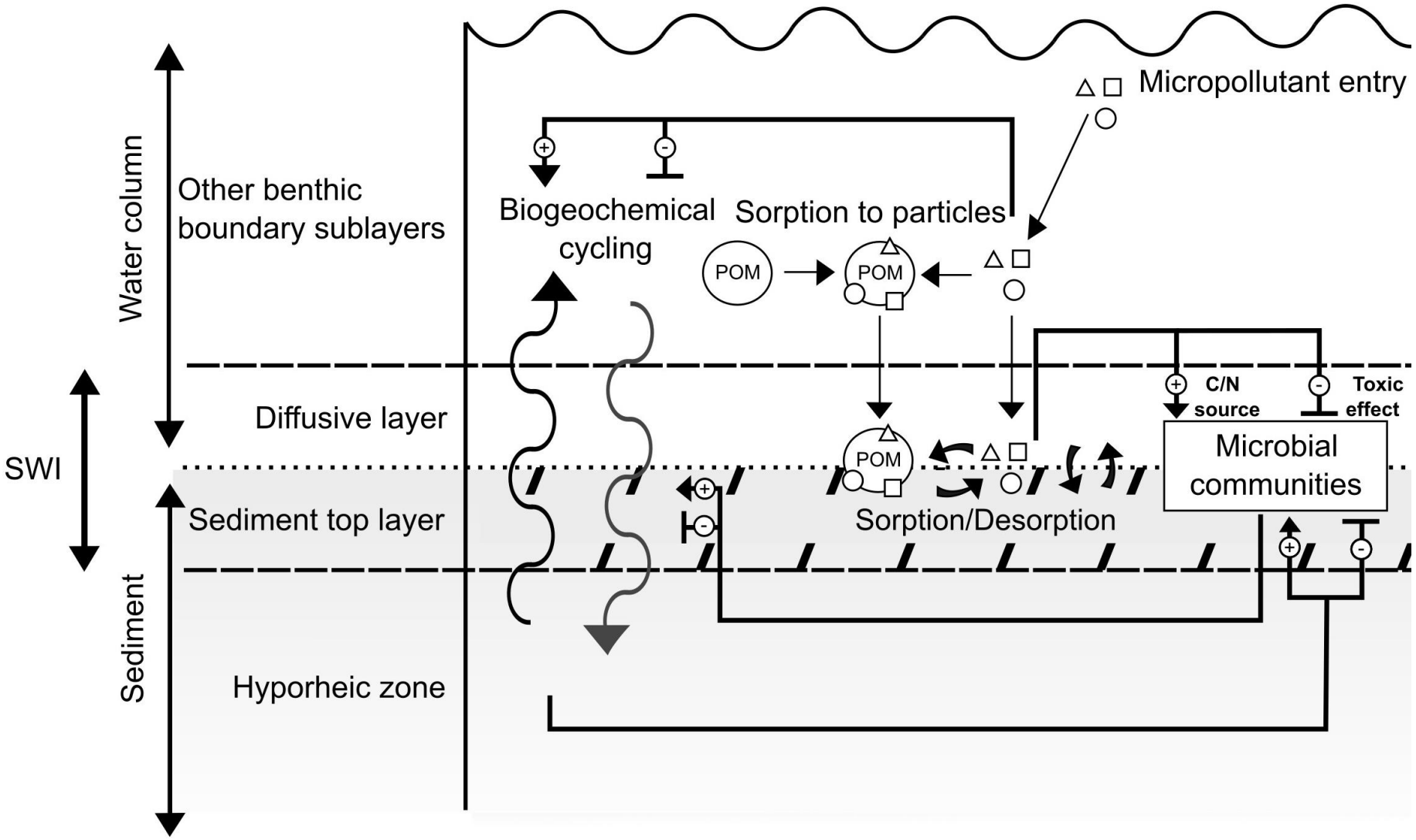

Figure 1.20: *Process interplay at the sediment-water interface (SWI). Processes may be either inhibited (-) or promoted (+).*

Chapter 2.
Aims, research questions and general approach of the thesis

The objective of my PhD thesis was to increase our understanding of the behaviour and mechanisms governing dissipation of micropollutants at the sediment-water interface (SWI), with a particular focus on biodegradation processes and associated microorganisms. A comprehensive framework was developed to evaluate the behaviour of pharmaceuticals and agricultural and urban biocides, taking both biotic and abiotic processes of biocide dissipation into account. This involved a large diversity of variables such as multiple contamination, repeated contamination, oxygen fluctuation, and response of prokaryotic communities. A secondary aim was to identify micropollutant degraders to provide a more holistic understanding of the intricate dynamics involved in the fate of such chemicals in the environment (Figure 1.4). Metformin (an antidiabetic drug), metolachlor (a pesticide widely used in agriculture), and terbutryn (an antifungal agent utilized as a construction material additive) were selected as model micropollutants for study, based on their contrasted physicochemical properties (see Table 1.1), ubiquity, and the high likelihood of their co-occurrence in surface waters.

To address identified gaps in current knowledge, my PhD thesis sought to explore the following key research questions at the sediment-water interface of aquatic ecosystems:

- What is the impact of micropollutants, individually or as a mixture, on their dissipation and the response of prokaryotic communities?
- How do variations in oxygen concentration affect the dissipation of repeated metformin contamination and prokaryotic community composition?
- Which prokaryotic taxa are associated with utilization of metformin as a source of carbon for growth?

Three different series of laboratory microcosm experiments were chosen to investigate these questions, and they are presented in Chapters 4-6. The experimental approaches and analysis methods that were used in this work are first presented in Chapter 3.

I first designed a laboratory microcosm investigation (Chapter 4) with river sediment to explore the dissipation dynamics of the three environmentally significant micropollutants investigated my work. These micropollutants, chosen for their distinct physicochemical properties and usage, were examined individually and as a mixture to assess their fate and impact on the biotic compartment at the sediment-water interface (SWI). My hypothesis posited that dissipation of these micropollutants at the SWI is influenced by their distinctive physicochemical characteristics as well as by their toxicity.

I also chose to develop a laboratory microcosm study to simulate the sediment-water interface and specifically investigate the effects of repeated metformin contamination under different oxygenation conditions (Chapter 5). Experimental design involved long-term (41 days) operation of parallel microcosms under either oxic or anoxic conditions, followed by a second

contamination event with oxygenation conditions either maintained or reversed. This design based on the premise that metformin dissipation depends on oxygenation conditions, and aimed at investigating the responses of prokaryotic communities to both oxygenation shifts and metformin exposure using DNA-based methods and following kinetics of metformin dissipation and formation of its transformation products (TPs).

I also aimed to identify the active prokaryotic microorganisms associated with micropollutant degradation in the context of exposure to such contaminants (Chapter 6). To achieve this, exploratory laboratory microcosm studies were conducted on river sediment to investigate the individual or combined impact of the three micropollutants selected for this study by stable isotope probing (SIP). First, I introduced an original approach using commercially available ^{13}C-labelled glucose to investigate the toxicity of micropollutants. My working hypothesis about micropollutant effects was twofold: acute toxicity resulting from micropollutant exposure could negatively affect taxa associated with glucose assimilation, and conversely, micropollutant presence could promote the increase in relative abundance of some taxa. To further explore the potential of the SIP approach, I also applied $^{13}C_2$-labelled metformin to identify taxa associated with metformin assimilation under oxic laboratory microcosm conditions.

Finally, Chapter 7, titled "General Conclusions and Perspectives," provides a synthesis and a comprehensive discussion of the principal findings of the thesis, along with their implications for research perspectives.

Chapter 3.
General materials and methods

3.1. Souffel sediment

Sediment (top 10 cm) was collected from 10 randomly selected spots within a 10 m² vegetated area of the Avenheimerbach riverbed in Alsace, France (48°39'58.08" N, 07°35'36.92" E) on November 12, 2020 (Fig. 3.1). The chosen area was adjacent to agricultural plots growing maize and beetroot, where metolachlor is typically used in spring[154]. Previous research[155,156] indicated that sediment from this location shows biodegradation potential for metolachlor. However, no metformin, metolachlor, or terbutryn was detected in the river sediment. Subsamples of the sediment were combined, thoroughly mixed by stirring, wet-sieved at 2 mm to remove pebbles, rocks, and branches, then homogenized again before being stored at 4°C. Storage at 4°C is not expected to affect significantly the potential for micropollutant degradation[157]. However, storage may alter the initial environmental microbiota[158] since microbial communities within sediment can undergo changes when stored at 4°C. In this doctoral thesis, our objective was to utilize Souffel sediment as an initial and standard matrix for investigating micropollutant degradation at the SWI. Consequently, microbial communities were initially characterized, and then monitored throughout the experiment to evaluate the temporal changes of microbial populations under varying conditions.

Figure 3.1. *Avenheimerbach riverbed (France, 48°39'58.08" N, 07°35'36.92" E), sampling area.*

3.2. Sediment-water ratios for microcosms setup

According to OECD guideline No. 309, a river microcosm should consist of two phases: sediment and water and should show a total suspended solids (TSS) concentration ranging

from 0.01 to 1 g L^{-1}, similar to that found in continental surface water[159]. TSS obtained from setups with different sediment-water ratios was quantified to assess their representativeness in terms of partitioning of ions, nutrients, and particles, and select the appropriate ratio for further experiments. Microcosms were established in 6×2 cm (20 mL) vials with a headspace, each in triplicate with sediment-water ratios of 1:3, 1:6, 1:10, or 1:20 (Table 3.1). These microcosms were then incubated at 30°C in the dark and subjected to continuous orbital agitation at a rate of 120 rpm to ensure homogeneity. An initial one-week pre-incubation phase was conducted to achieve stable partitioning of ions, nutrients, and particles within the microcosms[160,161]. After a week, we filtered the maximum volume of water that could be collected without disturbing the sediment phase through nitrocellulose membranes (47 mm diameter, 0.22 µm porosity, GVS filter technology). The TSS mass was determined by measuring the weight difference between dry filters (before and after filtration, dried at 60°C for 2 days) and normalized by the filtered volume. Among the tested ratios, those ranging from 1:6 to 1:20 met the criteria outlined by OECD, with TSS concentrations ranging from 0.13 ± 0.02 to 0.44 ± 0.01 (Table 3.1). Based on these results, additional microcosms were established within this range of ratios to ensure the representativeness of the experimental setup.

Table 3.1. *Microcosms sediment-water ratios from 1:3 to 1:20 and associated total suspended solids (TSS) concentration.*

Sediment: water ratio	Total sediment (g)	Dry sediment (g)	Interstitial water (mL)	Water added (mL)	Total water (mL)	TSS concentration (g L^{-1})	OCDE criteria met
1:3	1	0.5	0.5	1	1.5	12.38 ± 11.44	no
1:6	1	0.5	0.5	2.5	3	0.44 ± 0.01	yes
1:10	1	0.5	0.5	4.5	5	0.17 ± 0.02	yes
1:20	1	0.5	0.5	9.5	10	0.13 ± 0.02	yes

3.3. Sediment physicochemical characteristics

Sediment texture analysis was conducted by laser diffraction particle size analysis using LS 13 320 Laser Diffraction Particle Size Analyzer (Beckman Coulter). The sediment pH was determined by adding deionized water to sediment and get measured when equilibrium was reached. Carbon and nitrogen content were obtained using elemental analyzer FLASH 2000 NC (Thermo Fisher Scientific). The measurement of carbonate content was conducted by measuring the volume of water displaced by the CO_2 released during their destruction through attack with concentrated hydrochloric acid, under controlled atmosphere. The organic matter proportion was determined using ignition loss. Initially, samples were dehydrated at 60°C for 5 hours. Subsequently, they were placed in a furnace overnight at 375°C. The organic matter percentage was estimated from the difference between the weight of the dry sediment and the weight of the dry sediment after combustion.

Analyses were conducted on both the pristine river sediment and the sediment subjected to three successive autoclaving cycles (with 24-hour intervals between each) to evaluate changes in physicochemical properties induced by autoclaving. The sediment, classified as silt loam, showed a composition comprising 69 ± 4% silt, 13 ± 1% clay, and 18 ± 6% sand (Table

3.2 and Fig. 3.2). The recorded parameters include the C/N ratio, sediment pH, organic matter content, and carbonate levels, all of which are delineated in Table 3.2.

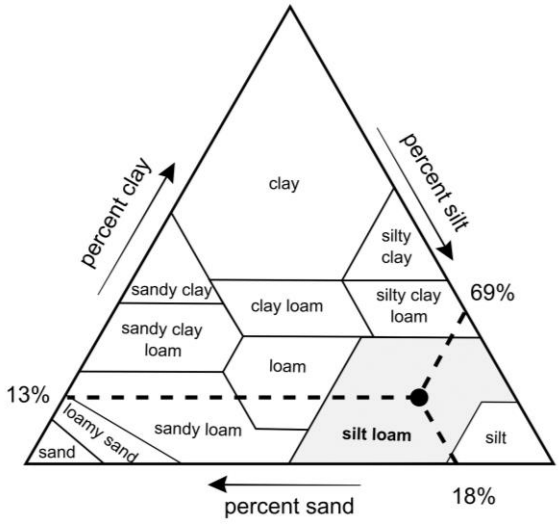

Figure 3.2. *Soil textural triangle and characterization of Souffel sediment as silt loam.*

Table 3.2. *Sediment properties and texture*

Parameters	Control	Autoclaved	Mean
C/N ratio	16.5	17	16.8 ± 0.3
pH	7.8	7.8	7.8 ± 0
% Organic matter	4	4	4 ± 0
% Carbonates	15	15	15 ± 0
% Clay	14	12	13 ± 1
% Sand	14	22	18 ± 6
% Silt	72	66	69 ± 4

3.4. Microcosm set-up

Microcosms offer significant advantages in controlling experimental variables such as temperature, homogeneity, and eco-exposome, while also providing an accessible means to generate reproducible data and capture essential dynamics. The thesis predominantly used microcosm experiments, with over 500 microcosms set up throughout the different studies.

3.4.1. General set-up for Oxic and Anoxic microcosms

Microcosms were set up in 9×3 cm vials with a headspace for a total volume of 50 mL. Vials were filled with a 1:6 sediment-water mixture containing sediment equivalent to 8 g dry weight combined with a total volume of 40 mL of water. This resulted in a concentration of total suspended solids (TSS) of 0.44 g L^{-1}, in the typical range observed in river environments[1].

Oxic microcosms were fitted with PTFE caps pierced by a needle mounted with a filter (⌀ 0.22 µm) to allow gas exchanges while preventing water loss and contamination[159] (Fig. 3.3). The atmosphere within anoxic microcosms was evacuated and refilled with nitrogen (N_2) in three successive cycles, following an established in-lab procedure. In total, 404 microcosms were set up following this process for experiments depicted in detail in chapters 4 and 5. Microcosms were spiked with individual and mixtures of micropollutants according to the experiment (see Chapters 4 and 5 for additional details). Microcosms were incubated at 30°C in the dark and subject to continuous orbital agitation at a rate of 120 rpm for homogeneity.

Figure 3.3. *Anoxic (left) and oxic (right) microcosms.*

3.4.2. Set-up of microcosms for stable isotope probing (SIP)

To mitigate the requirements and costs linked to labelled metformin for stable isotope probing experiments (SIP, Chapter 6), adjustments were made to the microcosm volume. The microcosms were set up in 5×3.5 cm vials with headspace for a total volume of 30 mL. These vials were filled with a sediment-water mixture at a ratio of 1:20, with 0.5 g dry weight combined with a total volume of 10 mL of water. This configuration resulted in a total suspended solids (TSS) concentration of 0.1 g L^{-1}, falling within the typical range observed in river environments[6]. Oxic microcosms were equipped with blue butyl rubber caps fitted with needles mounted with a filter (⌀ 0.22 µm) to facilitate gas exchange while preventing water loss and contamination[7].

3.4.2.1. Microcosms for the labelled glucose experiment

A total of 42 microcosms were established, each representing various contamination regimes under biotic conditions. The experiment was conducted in triplicate. The microcosms were incubated at 30°C in darkness and subjected to continuous orbital agitation at 120 rpm to ensure homogeneity. An initial pre-incubation phase of one week was implemented to achieve stable partitioning of ions, nutrients, and particles within the microcosms [160,161] (Fig. 3.5(I)). Additionally, microcosms were spiked with 5 µmol g^{-1} of $^{12}C_6$-glucose (12C-glucose) as a trigger for prokaryotic activity (except for pristine microcosms, free of any glucose and micropollutant, Fig. 3.5(II)).

We chose a concentration of glucose that aligns with typical levels used in other SIP experiments involving glucose[162]. This chosen concentration falls within the acceptable ranges established for labelled carbon in SIP experiments based on previous research[163,164]. Concentration of labelled carbon should range from 5 to 500 µmol g^{-1} of sediment or 1 to 100 µM in water. As our set-up encompass both sediment and water phase, we aim for a balanced concentration using 5 µmol g^{-1} of uniformly labelled $^{13}C_6$-glucose (13C-GLUCOSE) results in 2 µmol g^{-1} and 105 µM of labelled carbon.

Following the pre-incubation period, metformin (MFN) and terbutryn (TER) were spiked at a concentration of 17.6 µM each into the water phase, consistent with previous experiments. Microcosms were spiked with either a single micropollutant (MFN or TER) or a combination of both micropollutants (DUO), as illustrated in Fig. 3.5(III). The MFN stock solution (5 g L^{-1} in sterile milliQ water) was directly added to the microcosms. Stock solutions of TER were prepared in acetonitrile (ACN) at a concentration of 1 g L^{-1}. Aliquots (0.4 mL) of ACN solutions were initially mixed with 30 mL water, and the resulting solutions were stirred until complete evaporation of ACN. Microcosms were then spiked with the resulting aqueous micropollutant solutions as appropriate. Upon complete dissipation of glucose (approximately 2 days), microcosms were either spiked with $^{12}C_6$-glucose or $^{13}C_6$-glucose or left pristine. Concurrently, a setup using $^{12}C_6$-glucose only (‘Pristine’) was established to monitor glucose dissipation and associated microbial activity (Fig. 3.1, C).

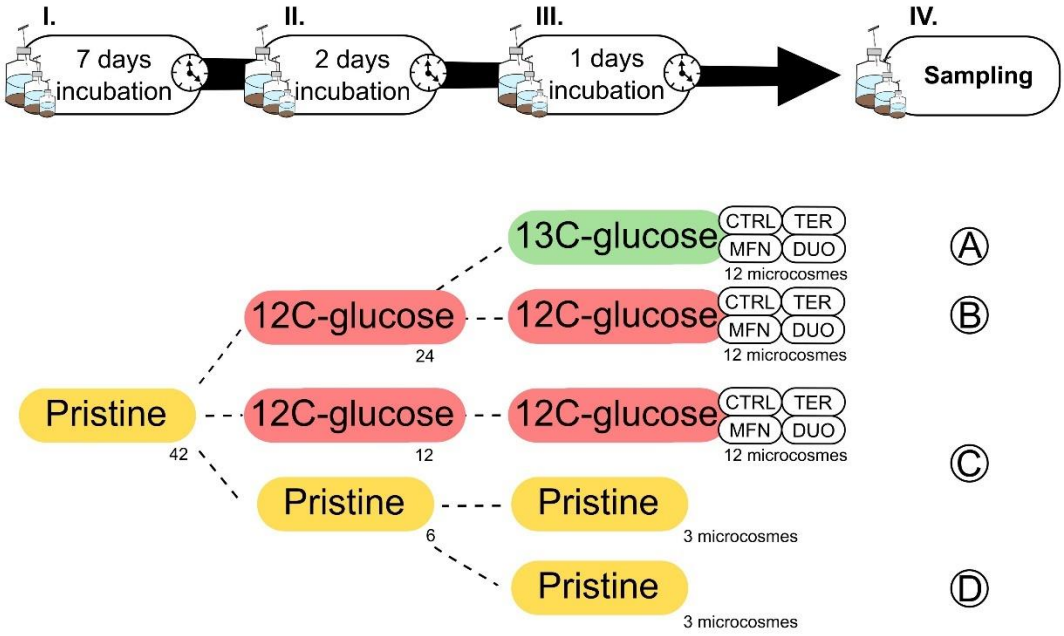

Figure 3.4. *Set-up for the SIP glucose experiment. I. Pre-incubation for water-sediment equilibrium; II. pre-incubation with non-labelled 12C-glucose; III. Incubation with 12C-glucose (or labelled 13C-glucose) and micropollutants; IV. Sampling time. A. Set-up with 13C-glucose and contaminant (CTRL, MFN, TER, DUO) for the SIP; B. Set-up with 12C-glucose and contaminant (CTRL, MFN, TER, DUO) for the SIP; C. Control (Pristine) set-up with 12C-glucose for monitoring pH, glucose concentration, FDA, and ATP; D. Set-up for DNA analysis from pristine samples. Number of microcosms are displayed for each condition.*

3.4.2.2. Microcosms for the labelled metformin experiment

The labelled $^{13}C_2$-metformin (labelled on its dimethylamine functional group) was obtained, through collaboration with Eliot Starck and Prof. Jean-Marc Weibel from the Laboratory of Synthesis, Organic Reactivity, and Catalysis (UMR 7177 CNRS - Institut de Chimie)

In total, 15 microcosms were established with conditions set in triplicates. Microcosms were incubated at 30°C in the dark and subject to continuous orbital agitation at 120 rpm for homogeneity (Fig 3.5). An initial one-week pre-incubation phase ensured stable partitioning of ions, nutrients, and particles in the microcosms (Fig. 3.6(I)). After the initial pre-incubation, 12 microcosms were spiked with 5 µmol g^{-1} of $^{12}C_6$-metformin (12C-metformin) to trigger prokaryotic activity, except for pristine microcosms (Fig. 3.6(II)). The three leftovers were not spiked with metformin and were considered 'pristine' control microcosms. Among the 12 microcosms spiked with 12C-metformin, 6 microcosms were dedicated to analytical monitoring (FDA, ATP, concentration), three were biotic microcosms and 3 were abiotic controls. Water and sediment phases in abiotic microcosms were sterilized independently by autoclaving three times at 24 h intervals. By comparing dissipation rates in abiotic and biotic microcosms, the extent of biodegradation can be estimated. Once the concentration of 12C-metformin dropped below 10% of its initial concentration after 2 weeks, microcosms were then spiked with either

12C- metformin or $^{13}C_2$-metformin (referred further as 13C-metformin) (Fig. 3.6(III)). The concentration of metformin used in this set-up correspond to 33 mg L^{-1}, i.e., ~100 µM or 5 µmol g^{-1}. This is far from representative from environmental contamination level (from 0.1 to 40 µg L^{-1})[26] but necessary to achieve the recommended threshold for SIP in both water and sediment [1-100µM and 5-500 µmol g^{-1}].

Figure 3.5*. Oxic microcosms for stable isotope probing experiments.*

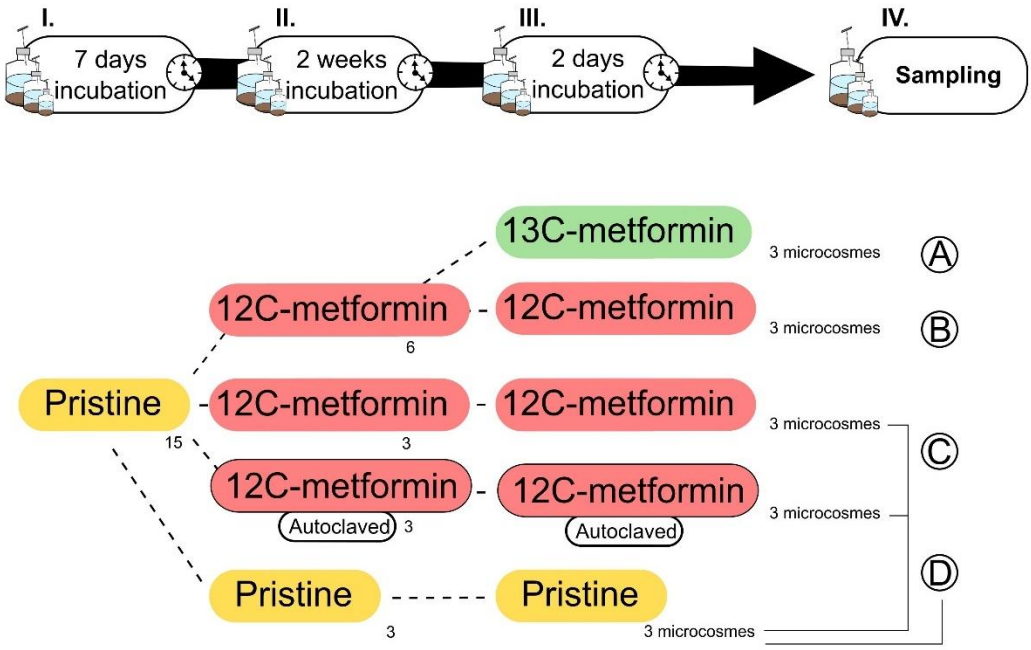

Figure 3.6. *Set-up for the SIP metformin experiment. I. Pre-incubation for water-sediment equilibrium; II. pre-incubation with 12C-metformin; III. incubation with 12C-metformin (or 13C-metformin); IV. Sampling time. A. Set-up including 13C-metformin for the SIP; B. Set-up including 12C-metformin for the SIP; C. Parallel set-up in 12C-metformin autoclaved or not, and pristine for monitoring pH, glucose concentration, FDA, and ATP; D. Set-up to obtain DNA from pristine samples. Number of microcosms are displayed for each condition.*

3.5. Micropollutant extraction, detection, and quantification

3.5.1. Extractions

3.5.1.1. Micropollutant extraction from sediment (QueChERS-MUSE method)

Micropollutants and their transformation products were extracted from sediment using Quick, Easy, Cheap, Effective, Rugged and Safe procedure (QuEChERS) modified by ultrasonic-assisted extraction (MUSE)[165]. Five grams of river sediment (dry weight) were placed in an amber glass centrifuge tube. Sediment samples were all extracted keeping 100% of water content. 1 mL of DCM:pentane (3:1) per gram of sample was then added and vortexed for 5 s, followed by 5 min in an ultrasonic bath (Branson 5510, 40 kHz) for homogenization. The sample was vortexed for 1 min, followed by centrifugation (2400 rpm) for 20 min. The supernatant was transferred to an amber glass vial, and the extraction method was repeated two more times. The supernatants were pooled and concentrated at room temperature under a gentle nitrogen stream to the last drop before resuspension into ACN to a volume of 1 mL by vortexing (5 s) and ultrasonication (5 min) to collect pesticide residues. Then 75 mg of anhydrous magnesium sulfate ($MgSO_4$) was added to remove residual water and 13 mg of primary-secondary amine (PSA bonded silica, Supelco P/N 52738) as a clean-up agent. The vial was vortexed for 30 s, centrifuged at 2400 rpm for 5 min, and the supernatant was transferred to a clean amber glass. Ultimately extract was transfer into 1.5 mL screw vials (Advion Interchim Scientific) vial and stored at −20°C for further analysis.

3.5.1.2. Extractions in water (SPE method and direct sampling)

Solid phase extraction (SPE) of pesticides was carried out using SolEx C18 cartridges (1 g, Dionex) and an AutroTrace 280 SPE system (Dionex), following an in-house method[155]. SPE cartridges were sequentially rinsed with 10 mL of deionized water. Filtered liquid samples (47 mm diameter, 0.22 µm porosity, GVS filter technology) were then loaded at 10 mL min^{-1} and cartridges were dried afterwards under nitrogen flux for 10 min. Then a sequential elution with 5 mL of EtOAc and ACN allowed pesticide elution before pre-concentration up to the last droplet under nitrogen flux and resuspension in 1 mL of ACN. Ultimately extract was transfer into 1.5 mL screw vials (Advion Interchim Scientific) vial and stored at −20°C for further analysis. Hydrophilic character of metformin allowed for direct quantification without extraction, samples were filtered (47 mm diameter, 0.22 µm porosity, GVS filter technology), transferred into 1.5 mL screw vials (Advion Interchim Scientific) vial and stored at −20°C for further analysis.

3.5.1.3. Micropollutant extraction recovery rates

Extraction recovery yields of the sediment using QueChERS-MUSE and the water phase using the SPE method were assessed through control extractions. Sediment and water samples were spiked with two different known concentrations: 8 and 20 µg g^{-1} of dry sediment or 1 and 2.5 mg L^{-1}. For sediment, 15 g of sediment were spiked in a 50 mL amber glass container. Sediment samples were homogenized for 3 minutes using a vortex mixer, then placed under a rotational agitator at a speed of 60 rpm for 24 hours. Micropollutants were subsequently extracted following the QueChERS-MUSE method described above. For the water phase, 100 mL of autoclaved and deionized water were spiked and vortexed for 3 minutes, after which micropollutants were extracted using the SPE method. Quantification of

micropollutants was performed using the appropriate procedures described below. Average micropollutant extraction yields are provided in Table 3.3.

Table 3.3. *Recovery rates for metformin, metolachlor, and terbutryn for QueChERS-MUSE and SPE extractions methods from river sediment. Uncertainty denotes standard deviation from triplicate experiments.*

Extraction methods	Metformin	Metolachlor	Terbutryn
QueChERS-MUSE	non-significant (<10%)	74 ± 4%	67 ± 7%
SPE	-	115 ± 23 %	86 ± 17%

3.5.2. Micropollutant quantification

3.5.2.1. Detection and quantification of metolachlor and terbutryn

Metolachlor and terbutryn were quantified with a gas chromatograph (GC, Trace 1300, ThermoFisher Scientific) coupled to a mass spectrometer (MS, ISQ™, ThermoFisher Scientific). The chromatographic separation was performed with a TG-5MS column (30 m × 0.25 mm ID, 0.25 µm film thickness)[166]. Samples were injected at a temperature of 280°C in split less mode with a carrier flow of 1.500 mL/min. Column was heated at a temperature of 50°C for 2 min and then heat up to 150°C at a rate of 30°C/min. Temperature increased to 180°C at a rate of 2°C/min, then 280°C at a rate of 15°C/min held for 1 min. Finally, temperature was increased to 330°C at a rate of 30°C/min and was held at 330°C for 1 min.

3.5.2.2. Detection and quantification of metformin and transformation products

Metformin and its transformation products (TPs) were quantified using an Ultra High Performance Liquid Chromatography (UHPLC, Ultimate 3000, Thermo Fisher Scientific) coupled with a triple quadrupole mass spectrometer (MS/MS, TSQ Quantiva, Thermo Fisher Scientific) equipped with a Accucore aQ C18 column (100 x 2.1 mm, 2.6 µm granulometry, Thermo Fischer Scientific). The column and autosampler temperatures were 20°C and 9°C, respectively. The sample (10 µL) containing metformin-d6 (at 200 µg L^{-1}) as an internal standard was injected with an ACC-3000 autosampler (Ultimate 3000, Thermo Fisher Scientific). LC-grade water and acetonitrile acidified with 0.1% and 0.05% formic acid respectively were used as eluents for the chromatographic gradient at a flow rate of 0.3 mL/min (10% to 40% acetonitrile in 1 min, 40 to 90% acetonitrile in 20 s, isocratic elution at 90% acetonitrile for 40s, 90% to 10% ACN in 15 s, and reconditioning in 10% acetonitrile for 30 s). The MS/MS was operated at an ionization voltage of 1500V (in positive mode) and 2000 V (in negative mode), CID gas at 1.5 mTorr and vaporizing temperature of 300 °C. Precursors and fragments ions were acquired in multi reaction mode (MRM).

The same method was adapted for metolachlor and terbutryn. For metolachlor, LC-grade water and acetonitrile, both acidified with 0.1% and 0.05% formic acid respectively, were utilized as eluents for the chromatographic gradient, running at a flow rate of 0.3 mL/min. The gradient program consisted of a transition from 10% to 90% acetonitrile over 8 minutes, followed by isocratic elution at 90% for 1 minute, then returning to 10% acetonitrile over 1 minute, and finally reconditioning with 10% acetonitrile for 3 minutes. As for terbutryn, LC-

grade water and methanol, both acidified with 0.1% and 0.05% formic acid respectively, served as eluents for the chromatographic gradient, operating at a flow rate of 0.4 mL/min. The gradient program initiated with a transition from 10% to 90% acetonitrile over 8 minutes, followed by an isocratic elution phase at 90% for 5 minutes, then returning to 10% acetonitrile over 1 minute, and finally reconditioning with 10% acetonitrile for 3 minutes. In this instance, the MS/MS was operated at an ionization voltage of 1800 V in positive mode, with collision-induced dissociation (CID) gas at 1.5 mTorr and a vaporizing temperature of 300°C.

3.5.2.3. Limits of detection, quantification, and relative errors

Before initiating any measurements involving a new compound, it was imperative to establish the limits of detection (LoD) and quantification (LoQ), along with assessing the associated relative error (RE) to gauge the level of uncertainty surrounding measurements. This was achieved through a calibration curve using >6 concentration points, typically ranging from 1 to 40 µg L^{-1} or higher depending on the compound. Analyses were performed in triplicate or more. LoD and LoQ parameters were determined from the standard deviation of the lowest measured and detected value across the calibration curve. Specifically, the standard deviation was multiplied by 3.3 for LoD and by 10 for LoQ[167,168]. Limits of detection and quantification of MFN, MET, and TER and their transformation products are provided in Table 3.4.

Table 3.4. *Analytical parameters with limits of detection (LoD) and limits of quantification (LoQ) for LC/MS-MS and GC/MS measurements.*

	Compound	Instruments	LoD (µg L^{-1})	LoQ (µg L^{-1})	Relative measurement error (%) at 95% confidence interval	Precursor (polarity mode)	Fragment
Parent molecule	MFN	LC/MS-MS	0.064	0.195	2.4	130 (+)	126/60
	MET	GC/MS	5.772	17.490	10.1	-	162/238
	TER	GC/MS	15.793	47.859	11.2	-	185/226
MFN_TPs	GUA	LC/MS-MS	0.031	0.925	4.2	103 (+)	60/86
	U	LC/MS-MS	0.194	0.587	5.9	61 (+)	44/-
	DU	LC/MS-MS	2.955	8.954	11.9	89 (+)	72/46
	MAM	LC/MS-MS	33.574	101.7385	31.4	127 (+)	85/68
	DAT	LC/MS-MS	16.922	512.794	55.1	112 (+)	70/68
	DMbG	LC/MS-MS	6.209	18.816	8.8	88 (+)	71/46
MET_TPs	ESA	LC/MS-MS	2.121	6.427	3.5	328 (−)	121/134
	OXA	LC/MS-MS	2.639	7.998	2.9	278 (−)	174/205
	NOA	LC/MS-MS	1.738	5.268	3.7	328 (−)	256/284
TER_TPs	TerOH	LC/MS-MS	7.315	22.168	11.7	212 (+)	86/156
	TerDesE	LC/MS-MS	2.728	8.266	10.1	214 (+)	158/210
	TerDesEOH	LC/MS-MS	2.800	8.485	6.1	184 (+)	184/86

3.6. Biomolecular approaches

3.6.1. Nucleic acid extraction and quantification

Environmental DNA was extracted from different matrices such as sediment, water, or homogenized mixed of sediment and water, using the DNeasy PowerSoil Pro Kit (QIAGEN) according to the manufacturer's instructions. DNA concentrations were determined by fluorometry using Qubit dsDNA HS and BR kits (Thermofisher Scientific). DNA extracts were stored at −20°C. Extraction procedures were conducted either directly on the sediment matrix or on a filter (47 mm diameter filter with 0.22 µm porosity, GVS filter technology) for water samples and homogenized mixtures of sediment and water. In the case of the latter, where a mixture of sediment and water was homogenized, the filter was halved and extracted separately before being pooled together.

3.6.2. Stable isotope probing

Samples from the stable isotope probing experiment described in Chapter 6 were also subjected to fractionation on an isopycnic gradient. For each sample, a gradient was prepared as follows: up to 5 µg of the target DNA and Gradient Buffer (GB) were combined in a 15 mL Falcon tube. The GB composition per 100 mL included 0.5 mL EDTA 0.2 M pH 8.0, 10 mL Tris-HCl 1 M pH 8.0, and 10 mL KCl 1M. Subsequently, 4.8 mL of CsCl (1.85 mg mL^{-1} prepared in GB) was added. The resulting solution was then transferred into ultracentrifugation tubes (5.1 mL, Quick-Seal Round-Top Polypropylene Tube 13 x 51 mm -50 Pk; Beckman Coulter) using sterile needles (0.8 mm, Fine-Ject) and syringes. The weight of the tubes was adjusted in pairs (± 0.01 g), followed by thermo-sealing (Beckman Coulter). The tubes were then placed in an ultracentrifuge (Optima XPN-100-IVD) and centrifuged at 177,000 g for 40 hours at 20°C.

Following ultracentrifugation and the formation of CsCl gradients, each tube was fractionated from the bottom using a sterile needle (0.8 mm) connected to a peristaltic pump (Schenchen YZ515x) with PharMed BPT tubing (1.6 mm inner diameter x 4.8 mm outer diameter x 1.6 mm wall thickness). The pump operated at a rate of 0.45 mL/min and injected a solution of bromophenol blue (0.02%) from the top to aid elution. A total of 12 fractions, each containing 450 µL, were eluted and stored in 1.5 mL Eppendorf tubes. Density measurements were performed using 50 µL of each fraction with a calibrated Reichert AR200 Digital Handheld Refractometer.

Subsequently, nucleic acids were precipitated by adding 2 volumes of a 30% polyethylene glycol (PEG) solution and 20 µg of glycogen overnight at room temperature. The mixture was then centrifuged at 18,000 x g for 30 minutes at 20°C, and the supernatant was discarded. The resulting pellets were washed with 150 µL of ice-cold 70% ethanol, followed by another spin for 5 minutes at 18,000 x g at 20°C. After discarding the supernatant, the pellets were air-dried for 5 minutes and then resuspended in 30 µL of diethyl pyrocarbonate (DEPC)-treated water. The fractions were stored at 4°C, and the DNA concentrations of each fraction were determined using fluorometry with the Qubit dsDNA High Sensitivity (HS) and Broad Range (BR) kits from Thermo Fisher Scientific. Concentrations are presented in Table 3.5 for glucose and Table 3.6 for metformin.

Table 3.5. *DNA concentrations (ng μL^{-1}) for each of the 12 fractions extracted during the GLU-SIP experiment (density np-dc). Please note that despite the experiment being conducted in triplicates, DNA precipitation was not yet optimized for this experiment. Consequently, only one sample was obtained for each contamination type (CTRL, MFN, TER, DUO) for both ^{12}C-metformin and 13C-metformin. Light fractions were defined from fractions 1.4023 to 1.4034, intermediate from 1.4036 to 1.4036, and heavy from 1.4037 to 1.4041. Below detection limit (b.d.l)*

		12C-metformin				13C-metformin			
Fractions	**Buoyant density**	**CTRL**	**MFN**	**TER**	**DUO**	**CTRL**	**MFN**	**TER**	**DUO**
	1.4045	-	-	-	b.d.l	-	b.d.l	-	-
	1.4044	-	-	-	-	-	-	-	-
	1.4043	-	b.d.l	-	-	b.d.l	-	-	b.d.l
	1.4042	-	-	b.d.l	-	b.d.l	-	b.d.l	b.d.l
	1.4041	-	b.d.l	b.d.l	-	b.d.l	b.d.l	0.1	0.2
	1.4040	b.d.l		b.d.l	b.d.l	4.4	b.d.l	0.1	b.d.l
Heavy	1.4039	b.d.l	b.d.l	b.d.l	b.d.l	11.2	b.d.l		
	1.4038	-	b.d.l	-	b.d.l	-	0.1	b.d.l	b.d.l
	1.4037	b.d.l		0.6	b.d.l	7.8		2.3	0.2
Intermediate	1.4036	b.d.l	b.d.l	-	b.d.l	0.3	3.8	20.8	-
	1.4035	-	2.8	3.6	-	-	11.2	-	0.5
	1.4034	0.15	11.0	19.7	5.4	91.3	-	61.7	14.8
	1.4033	7.32	22.6	35.1	16.5	77.8	14.4	-	11
	1.4032	13.7	20.0	8.5	31.1	b.d.l	36.5	0.6	0.2
	1.4031	21.6	17.7	38.0	35.3	-	27.1	9.0	-
	1.4030	-	-	-	-	1.0	b.d.l	37.0	9.1
Light	1.4029	-	0.2	-	-	-		-	-
	1.4028	16.7	2.8	19.7	22.3	9.9	1.8	-	5.4
	1.4027	-	-	-	11.5	-	-	-	-
	1.4026	9.3	-	-	-	-	-	-	-
	1.4025	1.3	-	b.d.l	9.6	-	9.5	-	-
	1.4024	0.3	-	-	-	-	-	1.3	-
	1.4023	-	-	-	-	-	-	-	-

Table 3.6. *The DNA concentrations (ng µL^{-1}) in each fraction extracted during the MFN-SIP (density np-dc) were determined. Fractions were obtained from triplicates labelled as a, b, and c, for both 12C- and 13C-metformin experiment. Light fractions were defined from fractions 1.4022 to 1.4036, intermediate from 1.403 to 1.4038, and heavy from 1.4039 to 1.4043. Below detection limit (b.d.l).*

		Replicates of 12C-metformin			Replicates of 13C-metformin		
Fractions	**Buoyant density**	**a**	**b**	**c**	**a**	**b**	**c**
	1.4044	-	b.d.l	-	-	-	b.d.l
	1.4043	-	b.d.l	-	-	-	0.1
	1.4042	-	-	b.d.l	-	0.1	-
Heavy	1.4041	b.d.l	b.d.l	-	-	-	0.1
	1.404	b.d.l	b.d.l	b.d.l	0.5	0.2	0.2
	1.4039	-	-	b.d.l	-	0.2	-
Intermediate	1.4038	b.d.l	0.63	0.5	0.5	0.3	0.6
	1.4037	0.1	-	0.6	0.3	-	-
	1.4036	-	3.9	8.9	-	1.9	4.0
	1.4035	-	-	-	1.4	-	-
	1.4034	0.8	13.6	-	-	10.4	7.2
	1.4033	7.7	-	7.9	7.5	-	-
	1.4032	-	16.6	-	-	23.6	15.0
	1.4031	7.8	-	5.1	15.7	-	-
	1.403	-	11.5	4.8	-	-	13.1
Light	1.4029	14.5	-	-	26.8	26.6	-
	1.4028	7.5	4.4	2.3	11.8	-	5.4
	1.4027	-	-	2.4	5.7	10.4	-
	1.4026	5.8	1.9	-	2.4	-	2.3
	1.4025	-	-	-	-	5.4	-
	1.4024	1.0	-	-	-	-	-
	1.4023	-	-	-	0.1	4.1	-
	1.4022	-	-	-	-	-	-

3.6.3. Fractions and pooling

A threshold was established to categorize samples into two groups: isotopically light and heavy fractions. This threshold was chosen based on a significant increase in ^{13}C-DNA abundance, coinciding with a consistently low level of ^{12}C-DNA. Refer to Tables 3.5 and 3.6 for details.

3.6.3.1. Fractions and pooling principle for the glucose stable isotope probing experiment

The light fractions, consistent across all samples and ranging from 1.4020 to 1.4034 nt-dc (density), were aggregated within each replicate and then combined once more across replicates to generate an “average” sample for 12C-glucose and 13C-glucose. Pooling samples enabled the acquisition of a representative sample across replicates and could serve as a contingency plan in the event of sequencing failure for a specific replicate. Fractions 1.4035 and 1.4036, observed in both 12C-glucose and 13C-glucose samples, may contain a

mixture of labelled and unlabelled DNA, forming a hybrid fraction. Following the methodology used for the light fraction, these fractions were combined as previously described and termed intermediate fractions. Additionally, individual fractions were also submitted for analysis. The heavy fractions, ranging from 1.4037 to 1.4041, predominantly contained DNA from the 13C-metformin samples. Similar to the approach used for the light fraction, the heavy fractions were pooled accordingly.

3.6.3.2. Fractions and pooling principles for the metformin SIP experiment

The light fractions, with consistent densities ranging from 1.4020 to 1.4037 nt-dc, were aggregated within each replicate and subsequently combined across replicates to create an averaged sample for both 12C-metformin and 13C-metformin. Pooling samples facilitates the acquisition of a representative sample across replicates and allow to compensate cases of sequencing failure. Fractions with densities of 1.4038 and 1.4037, observed in both 12C-glucose and 13C-glucose, may contain a mixture of labelled and unlabelled DNA, forming a hybrid fraction. These fractions were pooled as described earlier and designated as “intermediate fractions”. Additionally, individual fractions were also subjected to analysis. The heavy fractions, ranging from 1.4039 to 1.4043, predominantly comprised DNA from 13C-metformin samples. Following a similar approach to that used for the light fraction, the heavy fractions were pooled accordingly.

3.6.4. Amplicon sequencing

The hypervariable V3−V4 region of the 16S rRNA gene was PCR amplified with the Pro341f/Pro806r primer pair targeting both bacteria and archaea[169]. Barcoded amplicon sequencing (paired-end 250 bases) was performed with the NovaSeq PE250 sequencing platform (Novogene. Cambridge. United-Kingdom). Raw data were trimmed. filtered and denoised using the DADA2 pipeline[170]. Obtained sequences were clustered at 100% identity to obtain Amplicon Sequence Variants (ASVs). Each ASV was annotated by applying the QIIME2’s classify-sklearn algorithm and the Silva database (version 138. December 2019).

3.7. Microbial activity and other monitoring

3.7.1. Fluorescein diacetate (FDA) assay to evaluate total microbial activity

The protocol for measuring microbial activity was adapted from Adam and Duncan (2001)[171]. This test is based on the cleavage of fluorescein diacetate (FDA) by esterases into fluorescein, which absorbs light at 490 nm. Esterases are enzymes present in all living organisms, including bacteria and fungi, and are only active in living cells. Therefore, the cleavage reaction from FDA into fluorescein enables the monitoring of changes in the total microbial activity of a given sample.

In a 15 mL polypropylene centrifuge tube, 0.2 g of sediment sample was mixed with 3.75 mL of phosphate buffer solution (PBS) and 50 µL of a reagent solution containing FDA at a concentration of 1 mg mL^{-1} in acetone. The samples were vigorously vortexed until homogeneous and then subjected to agitation on a rack at 500 rpm (IKA-VIBRAX. VXR) for 45 min. Following this, 3.75 mL of a stopper solution composed of chloroform/methanol (2:1, v:v) was introduced into the tubes, and they were agitated on the rack at 500 rpm for 20 min to stop

the esterification process of FDA. Subsequently, the tubes underwent centrifugation for 3 min at 2000 rpm. Following centrifugation, triplicate samples of 200 µL were carefully transferred from the aqueous phase (top layer) into the wells of a 96-well plate with a clear bottom, ensuring no contamination from organic phases (bottom layer) or particulate matter. The absorbance at λ=490 nm was then measured using a TECAN spectrophotometer (M Nano+, Infinite).

3.7.2. Measurement of microbial activity with ATP-metry

In the stable isotope probing experiment, quantification of adenosine triphosphate (ATP) served as an additional indicator of microbial activity. This approach shows a robust correlation with 16S gene copies while augmenting prokaryotic abundance data.[172] ATP quantification was conducted through ATP-metry using Dendridiag® SW ATP tests designed for drinking water analysis (GL BIOCONTROL), in accordance with the manufacturer's instructions, and adapted for a sample volume of 1 mL.

3.7.3. Oxygen, pH and major ions monitoring

Dissolved dioxygen concentration was monitored *in situ* in all experiments with non-invasive sensor spots (PreSens Unisense). Total organic carbon (TOC) and dissolved organic carbon (DOC) were analyzed using a TOC analyzer (TOC-V-CPH Shimadzu. NF EN 1484). Major ions (NH_4^+, Na^+, K^+, Mg^{2+}, Ca^{2+}, Cl^-, NO_3^-, SO_4^{2-}, PO_4^{3-}) were quantified by ion chromatography (Dionex ICS-5000. Thermo Scientific). Aqueous solution pH was also monitored routinely using pH paper.

3.7.4. Glucose quantification

In Chapter 6, pertaining to the stable isotope probing experiment, microcosms were enriched with glucose. The dissipation of glucose was tracked utilizing the Glucose Colorimetric/Fluorometric Assay Kit (Sigma, catalog MAK263), with measurements taken in a 96-well plate format. Monitoring occurred at specific time intervals, including Day 0, Day 2 (following the initial enrichment), as well as subsequent time points of Day 0, +4 hours, +9 hours, and +20 hours thereafter.

3.8. Data processing

3.8.1. Evaluating micropollutant dissipation

The contribution of biotic degradation ($\boldsymbol{B.t}$ %) to overall micropollutant dissipation at time *t* (Eq.1) was determined as described previously[7] from the relative dissipation *D.t* (100 - remaining percentage) in biotic and abiotic microcosms.

$$\boldsymbol{B.t}\ \% = (\boldsymbol{D_{biotic}.t}\ \%) - (\boldsymbol{D_{abiotic}.t}\ \%) \qquad \text{Eq. 1}$$

Dissipation rate *k* and half-lives (DT_{50}) were determined from first-order kinetics (Eq. 2) with C_t the remaining concentration at time *t* and C_0 the initial concentration. Confidence intervals (95%) were calculated with a Z-score of 1.96 to compare *k* values across conditions and corrected by sample size $\sqrt{\boldsymbol{n}}$ (Eq. 3).

$$\boldsymbol{C_t} = \boldsymbol{C_0}.\boldsymbol{e^{-kt}} \qquad \text{Eq. 2}$$

$$IC = \pm \frac{Z_{score} * \sigma}{\sqrt{n}}$$ Eq. 3

Partitioning of the micropollutants ***(P)*** between the sediment and water phase was estimated C_t the remaining concentration at time ***t*** and $C_{t.\ sed}$ the remaining concentration at time with ***t*** in the sediment (Eq. 4). As $C_{t.\ sed}$ is the counterpart of $C_{t.\ wat}$ (Eq. 5) standard deviation (SD) was estimated based on the error propagation of $C_{t.\ sed}$. and $C_{t.\ wat}$ (Eq. 6).

$$P = \frac{C_{t.\ sed}}{C_t}$$ Eq. 4

$$C_t = C_{t.\ sed} + C_{t.\ wat}$$ Eq. 5

$$\mathbf{SD} = \sqrt{(\mathrm{SD}(C_{t.\ sed})^2 + \mathrm{SD}(C_{t.\ wat})^2)}$$ Eq. 6

3.8.2. Evaluation of prokaryotic community changes

After sequencing the 16S rRNA gene and generating amplicon sequence variants (ASVs), a 'phyloseq object' was assembled. A 'phyloseq object' is a structured data format designed to streamline the analysis of microbiome data. This object comprised three essential components:

- A table detailing the abundance of reads for each Amplicon Sequence Variant (ASV) in every sample, serving as an inventory.
- A taxonomic affiliation table, offering the taxonomic classification of each ASV according to the Silva's database, spanning taxonomic levels from Kingdom to Species.
- A metadata table linking each sample to its corresponding experimental group.

Initially, abundance data underwent filtering to remove background noise. ASVs absent in at least two replicates within a sample triplicate were deemed absent in that triplicate. Subsequently, abundance data were either rarified to the lowest read count present across all samples for subsequent alpha-diversity analyses or normalized to acquire relative abundance datasets for other analyses. Taxonomic assignments were less accurate at finer taxonomic levels when utilizing the Silva's database. For instance, in Chapter 4, 1.1% of taxa remained unassigned at the Kingdom level, followed by 1.6%, 4.1%, 9.8%, 31.2%, and 92.8% at the Class, Order, Family, Genus, and Species levels, respectively. Unassigned ASVs were categorized based on their affiliation with the most precise taxonomic level available.

The rarefied data facilitated the computation of alpha diversity indices, including Chao1, ACE, Observed, Shannon, Simpson, Simpson's evenness, Carmargo's evenness, and Pielou's evenness. These diversity indices were compared across experimental groups as specified in the metadata. Utilizing relative abundance aided in the construction of a phyloseq object and allowed to detect discrepancies in the prokaryotic composition of experimental groups. Employing a non-rarefied dataset for evaluating changes in prokaryotic composition helped mitigate bias where ASVs initially present were eliminated due to rarefaction. This approach prevented potential underestimation of overall prokaryotic community diversity and mitigated the risk of diminished statistical power[173].

When comparing two or more variables in ecological data analysis, non-parametric approaches are often more suitable due to the nature of the data[174]. Therefore, Wilcoxon and Kruskal-Wallis tests were applied when necessary. Post-hoc analysis such as Dunn test were performed with a corrective to control the false discovery rate proposed by Benjamini and Hochberg[175], *i.e.,* the type I error inflation when accounting for multiple tests at the same time[176].

A Bray-Curtis dissimilarity matrix was employed to analyse prokaryotic communities. This matrix considers both the presence and absence of ASVs in a sample, along with differences in their abundance. For each pair of samples U and V, the Bray-Curtis index (BC_{UV}) is computed based on Eq. 7. Compared to the Jaccard and Sørensen indices, the Bray-Curtis index is more comprehensive as it considers not only the presence or absence of taxa but also their relative abundances. In Eq. 7, for each ASV $x_{U\cdot}$ and $x_{V\cdot}$ represent the abundance of ASV at site U and V. The Bray-Curtis distance measures the ratio between the absolute sum of the differences between the abundances for each ASV and the total abundance of each ASV[177].

$$BC_{UV} = \frac{\sum_{j=1}^{ASV} |x_{Uj} - x_{Vj}|}{\sum_{j=1}^{ASV} (x_{Uj} + x_{Vj})} \quad \text{Eq. 7}$$

Utilizing this dissimilarity matrix, multivariate analyses can be conducted to assess whether an experimental parameter influences prokaryotic communities. To this end, a non-parametric multivariate analysis of variance (NPMANOVA) was utilized. This model computes a pseudo F-ratio by contrasting the total sum of squared dissimilarities among various groups with that of objects within the same group (Eq. 8). The pseudo F-value incorporates the sum of square within (SSW) and between groups (SSB), while considering the number of groups (a) and the total number of objects (N)[178].

$$pseudo\ F = \frac{\left(\frac{SS_B}{a-1}\right)}{\left(\frac{SS_W}{N-a}\right)} \quad \text{Eq. 8}$$

Following this, samples are shuffled between groups to estimate the likelihood of obtaining a lower or equal pseudo F score with a randomized dataset (Fig. 3.7). Thus, this probability, represented as *p*, is determined by the frequency of occurrences where a pseudo F score lower or equal to the original pseudo F score is observed, divided by the total number of permutations.

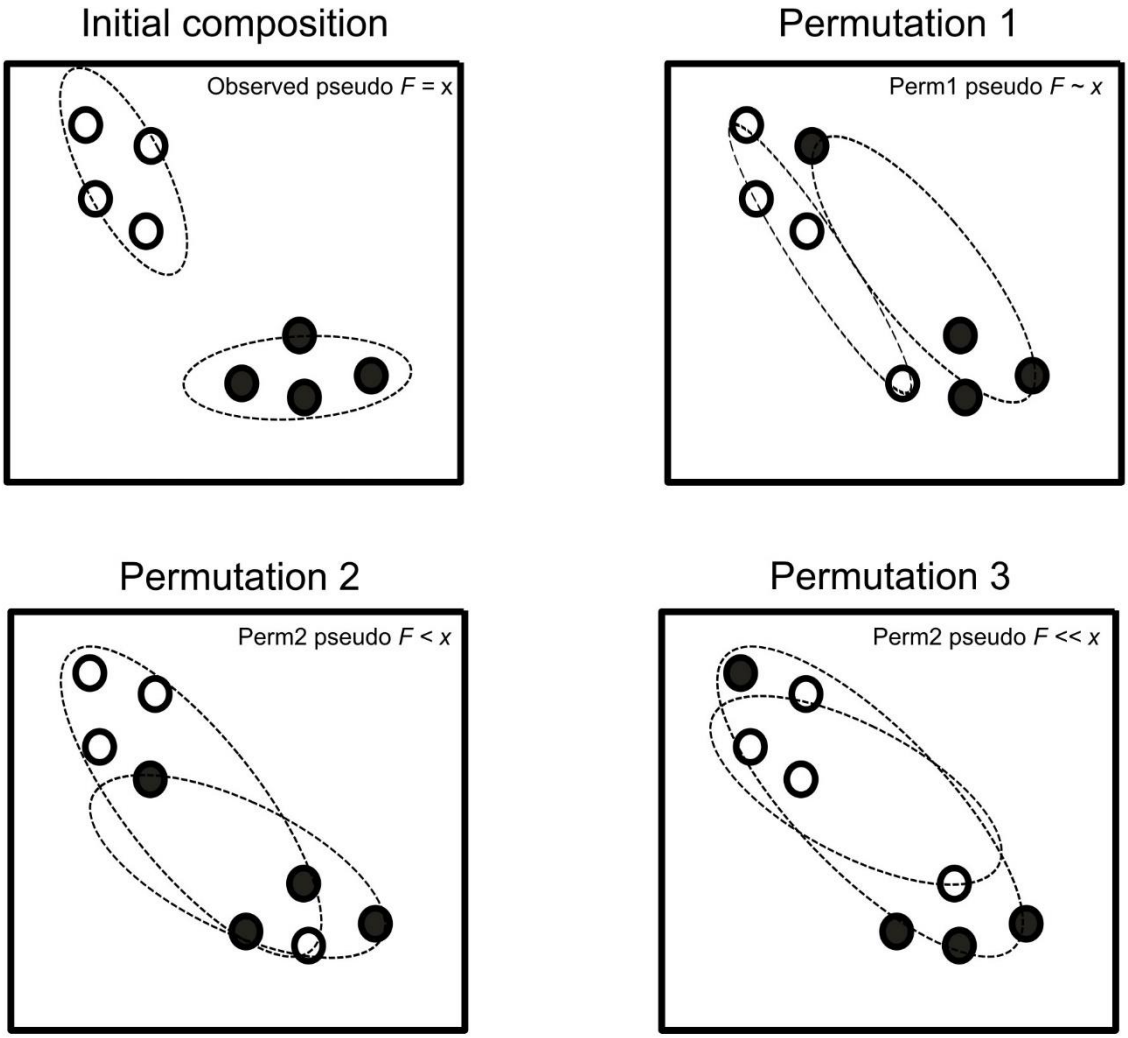

Figure 3.7. *During permutations, starting from the initial composition of objects, a sample from one group (black or white) is exchanged with a sample from another group. Subsequently, pseudo F scores are compared between the original composition and the permutations. For instance, in permutation 1, the pseudo F score closely resembles the observed one. In permutations 2 and 3, the pseudo F scores are lower than the observed score.*

To pinpoint specific taxa enriched in one group compared to another, conventional non-parametric methods like the Wilcoxon and Kruskal-Wallis tests may be enhanced with linear discriminant analysis (LDA). A heightened LDA score indicates successful integration of group differentiation into the linear discriminant model. Consequently, a high LDA score, coupled with non-parametric tests, aids in identifying enriched taxa within a particular group. This dual-step methodology, known as linear discriminant analysis effect size (LEfSe), can also be extended to other analyses involving gene abundance or functional abundance[179].

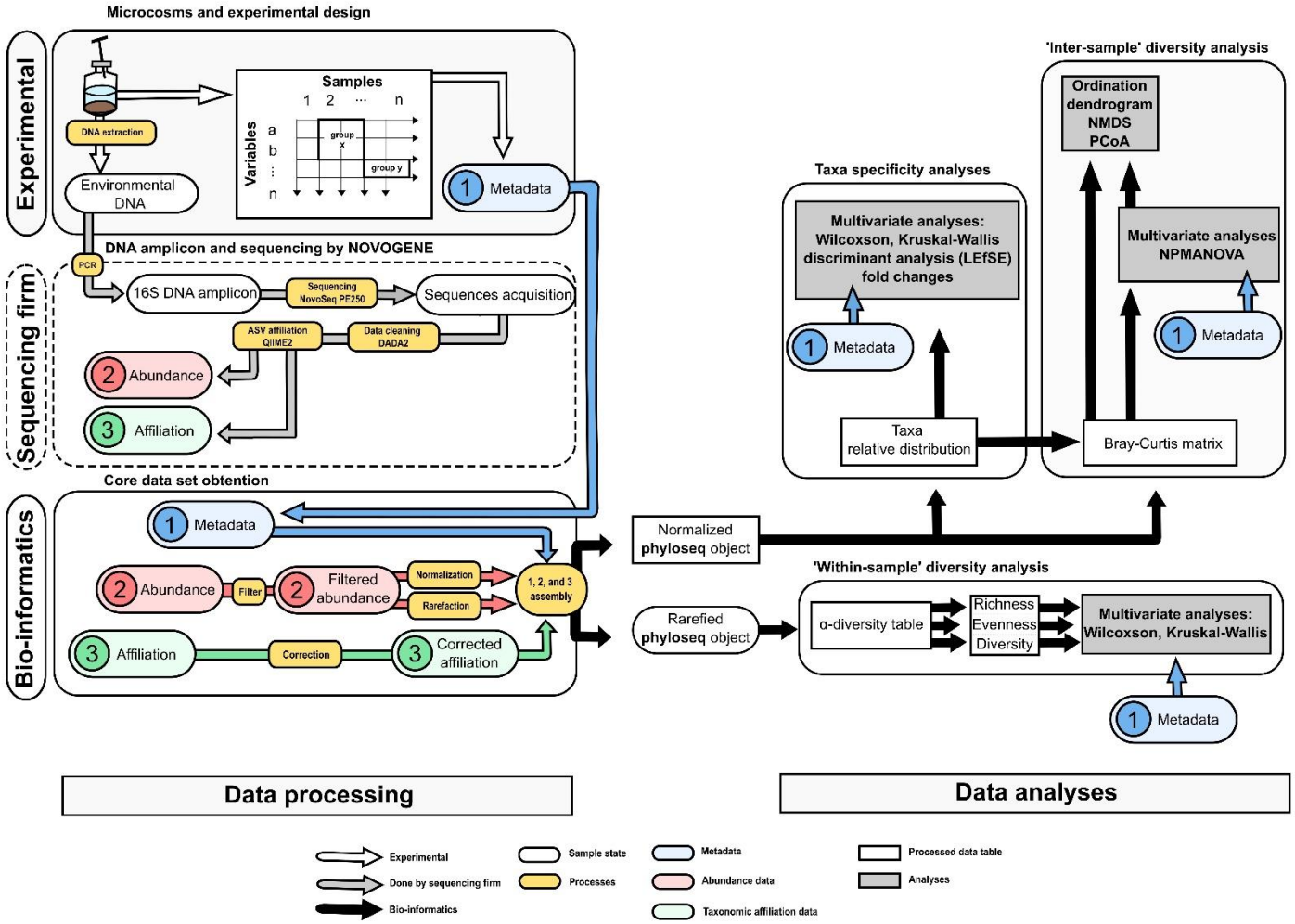

Figure 3.8. *illustrates the analysis pipeline, spanning from the microcosms to amplicon variant sequencing, and further to prokaryotic community and diversity analysis.*

3.8.3. Identification of ^{13}C-labelled prokaryotes in stable isotope probing experiments

3.8.3.1. Comparison of two screening methods, toward a hybrid method

Stable isotope probing (SIP) stands as a robust technique in microbiology for discerning microbes actively utilizing specific compounds. After data acquisition, a means is requisite to discriminate between microbes that assimilated the 13C (indicating utilization of the compound and its incorporation into their DNA) and those that did not. This paragraph outlines three distinct analytical methods (A, B, and C) deployed to differentiate these active microbes based on their DNA sequences derived from the SIP experiment. Method A was adapted from Thomas et al. (2019)[180], while method B was adapted from Farhan Ul Haque et al. (2022)[181].

- Method A: This approach aims to encompass a wider spectrum of potentially active microbes. It requires a minimal abundance of ASV in the sample (0.05%) and an escalation in proportion in the labelled experiment relative to the non-labelled counterpart.
- Method B: This method is geared towards ensuring high-confidence identification of active microbes. It employs a more stringent threshold for minimal ASV abundance (1%) and mandates an augmentation in the labelled fraction in contrast to the light fraction within the labelled experiment. Additionally, it verifies for a more pronounced enrichment of the isotope in the labelled experiment compared to the non-labelled one.
- Method C (Hybrid): This proprietary method amalgamates features from both A and B. It retains the low abundance threshold from A to encompass a broader array of microbes but adopts the rigorous criteria from B concerning enrichment within the labelled experiment and isotopic disparity between labelled and non-labelled experiments.

In Chapter 6, using these methods, we explored the possibility of analysing intermediate fractions obtained during the SIP process, where microbes might be partially utilizing the labelled compound.

3.8.3.2. Screening adaption method for the glucose SIP experiment

Chapter 6 delves into a thorough analysis of the SIP results from the glucose experiment. However, not all amplicon sequencing for the glucose experiment could be obtained, resulting in an insufficient number of successfully sequenced samples. Consequently, the previously established methods A, B, and C, tailored for a larger dataset, could not be applied. To overcome this hurdle and analyse the limited glucose dataset, we devised an additional method, method D. This novel approach amalgamates criteria from both methods A and B. Employing a minimal abundance threshold of 0.05% (Method A), ASVs must show a minimum relative abundance of 0.05% to be considered. Furthermore, ASVs must demonstrate a heightened relative abundance in the heavy fraction (H13) of the labelled experiment compared to the light fraction (L13) (Method B). By adapting these criteria, method D enabled to analyse data from glucose SIP experiment despite the constraints encountered during sequencing

Chapter 4.
Combined effects of micropollutants and their degradation on prokaryotic communities at the sediment-water interface

This study tackles the understudied issue of micropollutant mixtures at the sediment-water interface and the associated response of prokaryotic communities. Investigations into the fate of micropollutants at the SWI have already been reported[97,146,151]. Prokaryotic communities colonize the SWI[83], playing a vital role in its biogeochemical functioning and services[65,111,121]. Micropollutants have been shown to disrupt these very biogeochemical cycles[114,115,118,120,124,125]. Significant knowledge gaps remain regarding the transformation of micropollutant mixtures compared to that of individual compounds and associated effects on prokaryotic communities, in particular for aquatic ecosystems. Previous research indeed suggests that non-target organisms and particularly prokaryotic communities (bacteria and archaea) are susceptible to micropollutant mixtures[97,104,105], with potential cascading effects throughout entire ecosystems. Acquiring specific additional information on such topics is critical for future effective management of the risks associated with sediment and water contamination, including for implementation of bioremediation strategies.

Current risk assessment approaches usually focus on estimating the toxicity of individual pollutants using tools like Toxic Unit (TU)[96], in general with specific individual organisms. Here, we specifically assessed potential cocktail effects of multiple contamination that would be greater than the sum of the effects of individual compounds. For this, laboratory microcosms mimicking natural environments provide a valuable approach for controlled experimental investigations in a realistic context. We designed a study to investigate the effects of the three common micropollutants metformin (a pharmaceutical), metolachlor and terbutryn (both herbicides) on prokaryotic communities. These substances were introduced individually and as a mixture to laboratory microcosms replicating the crucial sediment-water interface. A detailed analysis of micropollutant mixture dissipation was performed that included high-throughput sequencing of 16S rRNA gene amplicons to examine the taxonomic composition of prokaryotic communities. A novel approach is introduced to analyse the obtained data and address ecotoxicological effects on prokaryotic communities. It allows to estimate whether the cumulative impact of mixtures of micropollutants is I) additive (the combined effect is equal to the sum of individual impacts), II) antagonistic (the combined effect is less than the sum of individual impacts) or III) synergistic (the combined effect is greater than the sum of individual impacts).

No significant difference in dissipation rates between individual micropollutants and their mixture were observed. However, sequence analysis revealed distinct responses in sediment and water communities upon micropollutant exposure, which emerged as the second most impacting factor shaping prokaryotic communities after matrix type (sediment or water phase). Our results indeed identified non-additive interactions between micropollutants for the response of some microbial taxa, highlighting a potential underestimation of micropollutant

effects when only individual pollutants are investigated. The analytical framework developed in this study may help future studies to prioritize and assess microbial responses to specific compounds within complex micropollutant mixtures.

This is an edited version of a manuscript currently under peer review at the journal Scientific Reports (Authors: Borreca, A., Vuilleumier, S., Imfeld, G.) and entitled "Combined effects of micropollutants and their degradation on prokaryotic communities at the sediment-water interface."

Abstract

Pesticides and pharmaceuticals enter aquatic ecosystems as complex mixtures. Various processes govern their dissipation and impact on the sediment and surface waters. These micropollutants often show persistence and adverse effects on microorganisms even at low concentrations. We investigated the dissipation and effects on prokaryotic communities of metformin (antidiabetic drug), metolachlor (agricultural herbicide), and terbutryn (herbicide in building materials) added individually or as a mixture (17.6 µM per micropollutant) to laboratory microcosms mimicking the sediment-water interface. Complete dissipation of metformin and metolachlor occurred within 70 days, while terbutryn persisted. Dissipation did not differ when micropollutants were present individually or as part of a mixture. Sequence analysis of 16S rRNA gene amplicons evidenced distinct responses of prokaryotic communities in sediment and water. Micropollutant exposure was the second factor contributing to the observed variations in prokaryotic communities, with a pronounced effect of metolachlor and recalcitrant terbutryn on the overall effect of the micropollutant mixture. Non-additive antagonistic and synergistic effects of micropollutants were detected for specific taxa across taxonomic levels. Our study highlights the importance of considering the diversity of potential interactions between micropollutants, prokaryotic communities, and their respective environments in investigations of multi-contaminated sediment-water interfaces.

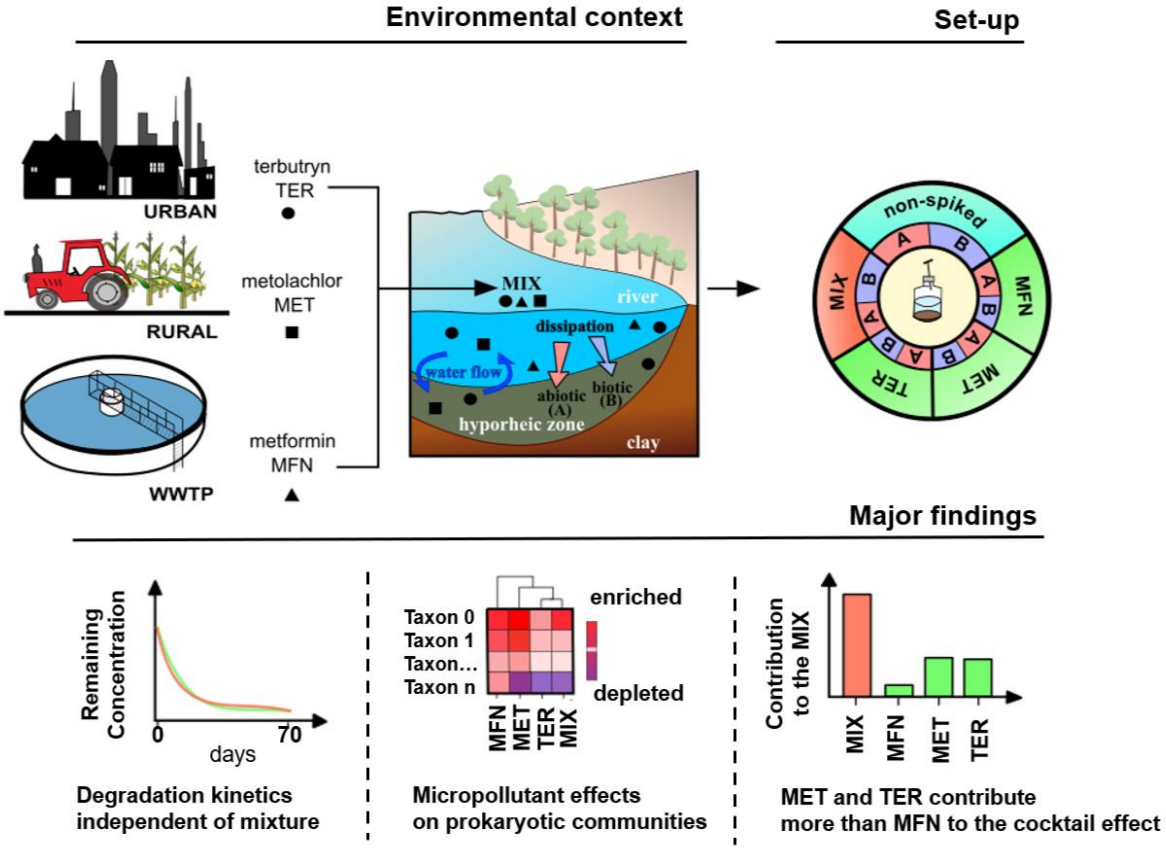

Keywords: micropollutants, sediment-water interface, cocktail effect, microcosms, prokaryotic communities

4.1. Introduction

Over 350,000 chemicals are officially registered for production and application[182]. Among these, biocides, additives, and pharmaceuticals, despite their typically low environmental concentrations, are increasingly recognized as micropollutants and potential threats to biodiversity, ecosystem functionality, and human health[183]. Aquatic ecosystems are particularly relevant in this context since micropollutants infiltrate surface and groundwater systems as complex mixtures through a variety of entry points. Pharmaceuticals and personal care products are released to surface waters via wastewater treatment facilities where their transformation is frequently incomplete[184]. Herbicides employed in agriculture[166] and building materials[61] may also reach aquatic ecosystems directly.

The fate of micropollutant mixtures in aquatic ecosystems is primarily determined by their compartments and the biogeochemical processes involved. The sediment-water interface (SWI) plays a pivotal, dual role as a sink and as a hotspot for transformative processes[74,185]. Micropollutants first partition between the aqueous phase and the sediment as a function of their physicochemical properties. This partitioning and potential associated accumulation of micropollutants define variations in exposure of the biological compartment at the SWI[97,186] and in particular of prokaryotic communities, typically dominated by bacteria[86] that may also be associated with micropollutant degradation. Continuous exchange of water between sediment and water may enhance biodegradation in the aqueous phase, particularly for recalcitrant and often poorly water-soluble micropollutants. These different processes may lead to significant changes in prokaryotic communities[84] which so far have not often been examined through the lens of underlying biogeochemical processes.

The fate of micropollutants at the SWI has begun to be addressed in laboratory experiments[97,146,151]. However, little is yet known about the transformation of micropollutant mixtures as compared to that of individual compounds, and the effects on prokaryotic communities of simultaneous exposure to micropollutants of different sources. Gathering such information appears crucial for effective management of the risks associated with sediment and water contamination, particularly with respect to implementation of bioremediation approaches.

Here, we designed a laboratory microcosm study with river sediment to examine the dissipation of three major micropollutants characterized by markedly different chemical structures and applications: metformin, an antidiabetic drug, and the herbicides metolachlor, widely used in agriculture, and terbutryn, mainly used as a building material additive in construction materials. These three micropollutants were studied individually and as a mixture, and the response of associated prokaryotic communities was examined at the SWI. We hypothesized that dissipation of micropollutants at the SWI depend on their contrasting physicochemical and biological properties. We also asked whether their occurrence as part of a micropollutant mixture elicits effects on prokaryotic communities distinct from those of the individual compounds. This was investigated by evaluation of micropollutant dissipation kinetics and formation of transformation products (TPs), and comprehensive analysis of prokaryotic community composition in water and sediment.

4.2. Materials and methods

4.2.1. Chemicals

Micropollutants, standards and their sources are listed in the Supporting Information (Appendix, Table A4.1). HPLC grade (purity: >99.9%) dichloromethane (DCM), acetonitrile (ACN), ethyl acetate (EtOAc), methanol (MeOH), and anhydrous magnesium sulphate (reagent grade: >97%) were purchased from Sigma–Aldrich. Primary-secondary amine-bonded silica (PSA) was purchased from Supelco.

4.2.2. Experimental sediments and laboratory microcosms

To assess the impact on microbial communities, microcosms were established employing the Souffel sediment (Chapter 3, Section 4.1). The establishment of microcosms adhered to the protocols detailed in Chapter 3, Section 1.

In total, 125 microcosms were established as five parallel experiments involving different contamination regimes under either biotic or abiotic conditions. Biotic experiments were conducted in triplicate and abiotic experiments in duplicate. Water and sediment phases in abiotic microcosms were sterilized independently by autoclaving three times at 24 h intervals. Microcosms were incubated at 30°C in the dark and subject to continuous orbital agitation at 120 rpm to ensure homogeneity. An initial one-week pre-incubation ensured stable partitioning of ions, nutrients, and particles in the microcosms[160,161,187].

Metformin (MFN), metolachlor (MET) and terbutryn (TER) were spiked at a concentration of 17.6 µM each in the water phase to allow quantification of transformation products despite the small volume of collected samples. Microcosms were spiked with a single micropollutant (‘ONE experiments’) or a combination of the three micropollutants (‘MIX experiment’). The MFN stock solution (5 g L^{-1} in sterile milliQ water) was added directly into the microcosms. Stock solutions of MET and TER were prepared in ACN (5 g L^{-1}). Aliquots (3 mL) of ACN solutions were initially mixed with 750 mL water and the obtained solutions stirred until complete ACN evaporation. Microcosms were then amended with the resulting aqueous micropollutant solutions as appropriate. Two sets of abiotic and biotic control microcosms (CTRL) were left unspiked. Sampling was carried out on days 0, 15, 30, 50, and 70 by a sacrificial approach (Fig. 4.1)

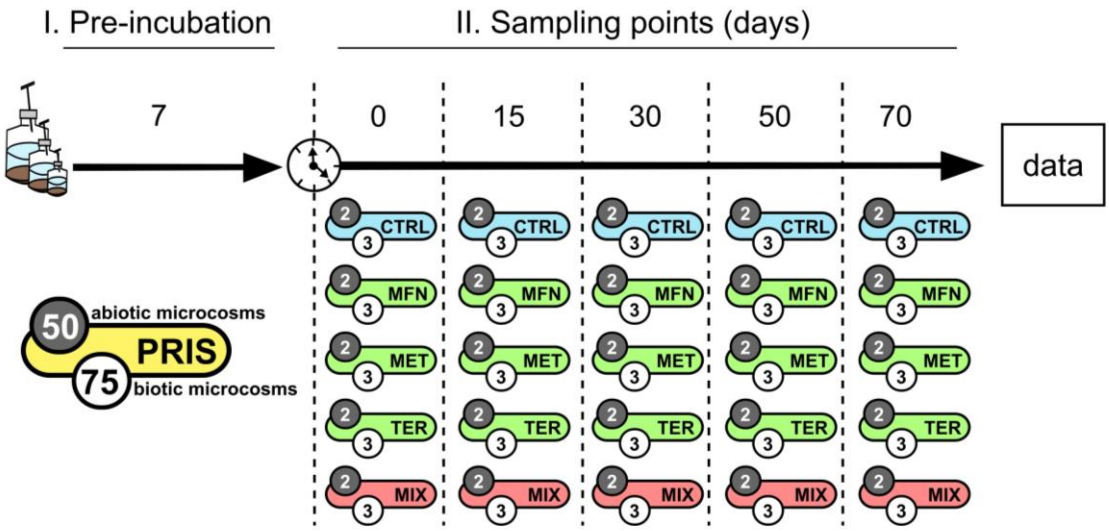

Figure 4.1. *Overview of the microcosm set-up and sacrificial work-plan. I. Pre-incubation for achieving water-sediment equilibrium with pristine microcosms (PRIS). II. Sampling points at days 0, 15, 30, 50, and 70 for microcosms containing either no micropollutant (CTRL), metformin (MFN), metolachlor (MET), terbutryn (TER), or a mixture of the three (MIX). Abiotic microcosms are represented by dark circles, and biotic microcosms by white circles.*

4.2.3. Chemical analysis

4.2.3.1. Biogeochemistry

Dissolved dioxygen concentration was monitored *in situ* with non-invasive sensor spots (PreSens, Unisense) in all experiments. Total organic carbon (TOC) and dissolved organic carbon (DOC) were analyzed using a TOC analyzer (TOC-V-CPH Shimadzu, NF EN 1484). Major ions (NH_4^+, Na^+, K^+, Mg^{2+}, Ca^{2+}, Cl^-, NO_3^-, SO_4^{2-}, PO_4^{3-}) were quantified by ion chromatography (Dionex ICS-5000, Thermo Scientific). Water pH was also monitored routinely.

4.2.3.2. Extraction and quantification of micropollutants

Micropollutants and their transformation products (TPs, Table 3.4) were extracted from water and sediment and analyzed as described previously in Chapter 3, part 5. Quantification methods and limits of detection and quantification are provided in Chapter 3, part 5.2 and Table 3.4. Evaluation of micropollutant dissipation is conducted following procedures described in Chapter 3, part 8.1.

4.2.4. Prokaryotic composition analysis

4.2.4.1. DNA extraction

Environmental DNA was extracted from sediment and water at day 0 and day 70 for each condition using the DNeasy PowerSoil Pro Kit (QIAGEN) according to the manufacturer's instructions. DNA concentrations (average 92 ng μL^{-1}, maximum 248 ng μL^{-1}) were determined by fluorometry using Qubit dsDNA HS and BR kits (Thermofisher Scientific). DNA preparations were stored at −20°C.

4.2.4.2. Amplicon sequencing and processing

Amplicon sequencing follow procedures described in Chapter 3, part 6.1. Obtained sequences were clustered at 100% identity, yielding a total of 26,354 Amplicon Sequence Variants (ASVs). Each ASV was annotated by applying QIIME2's classify-sklearn algorithm on the Silva database (version 138, December 2019). Good's coverage values indicated that sequencing depth exceeded 97.7% (average 99.2 ± 0.4 %). ASVs present in only one of the triplicate samples of a given condition were discarded and data analysis was carried out based on the two other replicates, yielding 3,146 ASVs for taxonomic analysis. Taxonomic assignment decreased at finer taxonomic levels, with 1.1% of taxa remaining unassigned at the Kingdom level, followed by 1.6%, 4.1%, 9.8%, 31.2%, and 92.8% at the class, order, family, genus, and species levels, respectively. Unassigned ASVs were grouped by affiliation to the most precise taxonomic level available. Rarefaction curves for Chao1, Simpson, Pielou's evenness, and Shannon indices (Fig. 4.2 and 4.3) indicated sufficient depth sequencing for all samples.

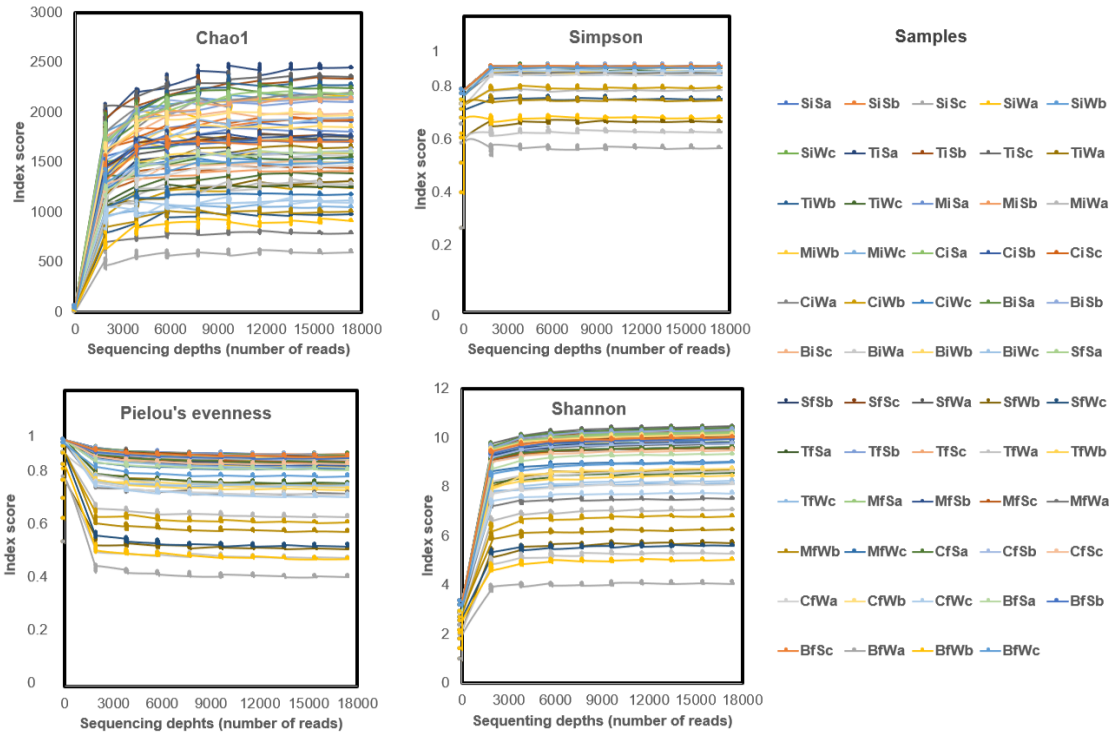

***Figure 4.2**. Sample rarefaction curves for Chao1, Simpson, Pielou's evenness, and Shannon indices. Indices were obtained at 10, 1946, 3883, 5820, 7756, 9693, 11630, 13566, 15503, and 17440 reads, replicated 5 times.*

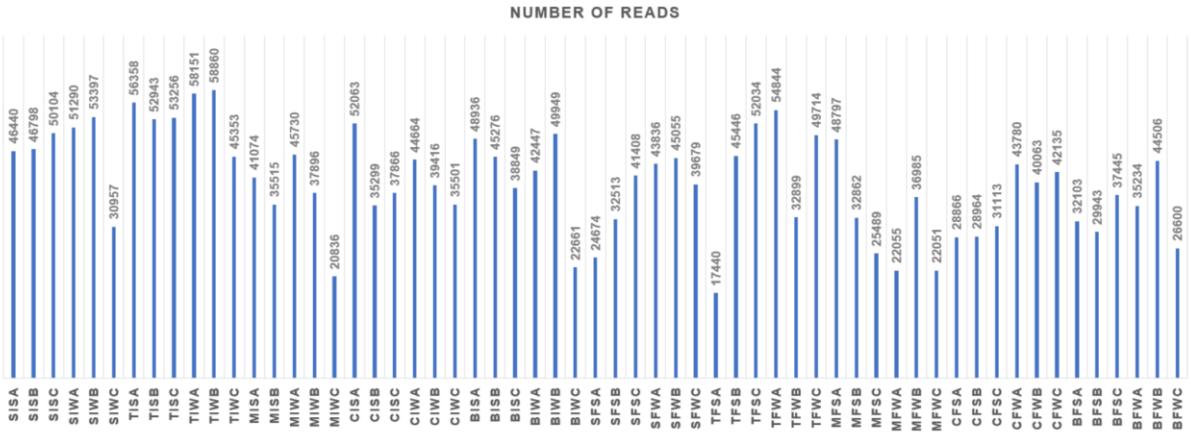

Figure 4.3. *Number of reads for each water and sediment sample.*

4.2.4.3. Data analysis

ASV sequences were analysed in R (version 4.3.1). Richness metrics (observed, Chao1, ACE), evenness indices (Camargo, Pielou, Simpson), and diversity measures (Shannon and Simpson) were computed (Table A4.2). Bray-Curtis matrices and dendrograms were generated employing the 'phyloseq' package. Analyses of similarities (NPMANOVA) were conducted with the 'adonis2' package.

Taxon-level mean fold change (FC) in relative abundance were calculated for each sample relative to its corresponding control (CTRL), i.e., the non-spiked sample for the same matrix and timepoint as the sample of interest at all taxonomic levels according to equation 1 (Eq. 1). In cases where a sample had one null abundance measurement among the three replicates, it was treated as a duplicate. A correction was applied, involving the addition of 0.001 to both the numerator (n) and denominator (d) (Eq. 1), to prevent division by zero and avoid undefined or infinite results.

$$FC_{taxon,sample} = \left(\frac{mean_{(taxon,sample)}+0.001}{mean_{(taxon,control)}+0.001}\right) = \frac{n}{d} \; ; n = d * FC_{taxon,sample} \qquad \text{Eq. 1}$$

A positive FC indicates an increase in relative abundance of a particular taxon when compared to the control condition. Log_{10} FC heatmaps were obtained after logarithmic transformation of FC values using “dplyr”, “tidyr”, “phyloseq”, “tibble”, and “heatmapply” packages.

The effects of individual micropollutants MFN, MET or TER (‘ONE experiments’) were compared with those of the micropollutant mixture (‘MIX experiment’) to investigate the occurrence of different types of interactions between micropollutants: additivity, antagonism, and synergism. Fold Change (FC) values were converted according to equation 2 (Eq. 2) into interaction coefficient (IC) values to assess the change in relative abundance of a taxon from the control to the sample of interest:

$$IC_{taxon,sample} = \left(\frac{n-d}{d}\right) = \left(\frac{d*FC_{taxon,sample}-d}{d}\right) = FC_{taxon,sample} - 1 \qquad \text{Eq. 2}$$

To evaluate the sum of micropollutant effects, the sum of IC values obtained for individual ‘ONE experiments’ with MFN, MET and TER was defined as $IC_{taxon,ADD}$ (equation 3, Eq. 3):

$$For\ sample_k, i.e., MFN, MET, and\ TER: \; IC_{taxon,ADD} = \sum_{k=1}^{3}(IC_{taxon,sample_k}) \qquad \text{Eq. 3}$$

$IC_{taxon,ADD}$ values were constrained to a minimum value of −1, which implies the absence of the considered taxon in all ‘ONE experiments’.

$IC_{taxon,ADD}$ values were then compared for each taxon with IC values of the corresponding MIX experiment (IC_{MIX}). A conservative uncertainty of ±64% was associated with IC values basing on the third quartile (Q3) of ASV relative abundances from replicate experiments. Thus, when IC_{MIX} ± 64% for a given taxon overlapped with IC_{ADD} ± 64%, the interaction of micropollutant effects was considered to be additive. However, when IC_{MIX} ± 64% exceeded IC_{ADD} ± 64%, interaction of micropollutants was considered synergistic. Conversely, when IC_{MIX}

± 64% was smaller than IC_{ADD} ± 64%, interaction of micropollutants was classified as antagonistic. Within the antagonistic category, two cases were identified without individual quantification: i) "repressing" when $IC_{MIX} < IC_{ADD}$, and ii) "opposing" when IC_{MIX} and IC_{ADD} were of opposite sign, i.e., positive in IC_{ADD} and negative in IC_{MIX}, or the reverse.

The contribution of individual micropollutants to the additive model at the Phylum and ASV levels was evaluated based on the proportion of taxa exhibiting the least difference between the observed FC scores of individual contaminants (MFN, MET, TER) and the mixture (MIX). In cases where two micropollutants ranked equally, they were defined as a 'binary combination' (i.e., MFN_MET, MFN_TER, and MET_TER).

Statistical tests for significance ($p \leq 0.05$), including NPMANOVA, Wilcoxon, Dunn with Benjamini-Hochberg adjustment, Kruskal-Wallis, and the computation of confidence intervals, were conducted as required. For multiple comparisons, clusters were defined as replicate samples (n = 3) sharing a specific set of variables.

4.3. Results and discussion

Laboratory microcosms mimicking the sediment-water interface of river surface waters allowed to investigate the dissipation of metformin (MFN), S-metolachlor (MET) and terbutryn (TER), spiked individually or as a mixture, and associated effects on prokaryotic communities. Unlike sediment-water interfaces in natural rivers, microcosms were not replenished in nutrients and were thus exposed to gradual accumulation of transformation products. Nevertheless, overall biological activity did not change significantly over time, as assessed by fluorescein diacetate transformation[171] (data not shown).

Microcosms were monitored in terms of chemical parameters throughout the experiment, and prokaryotic composition was analysed at initial and final (day 70) timepoints. All microcosms displayed stable physicochemical parameters, with oxic conditions (dissolved oxygen concentrations >8 ppm) maintained throughout. Values of pH, electric conductivity, and concentrations of the major elements (NH_4^+; Na^+; K^+; Mg^{2+}; Ca^{2+}; Cl^-; NO_3^-; SO_4^{2-}; PO_4^2) did not change significantly across all conditions (Table 4.1). Biotic microcosms showed similar TOC levels as the original river water (5 ± 7 ppm), but with lower phosphate concentrations (0.01 ± 0.01 *vs* 2.94 mmol) and conductivities (Table 4.1).). TOC was lower in biotic microcosms than in abiotic (autoclaved) microcosms (141 ± 123 ppm), suggesting DOC release to the water phase upon autoclaving as previously observed[188].

Table 4.1. *Hydrochemistry of river water and microcosm water phase at days 0 and 70 in biotic and abiotic microcosm experiments.*

	d0		d70		
	Abiotic	**Biotic**	**Abiotic**	**Biotic**	**River**
NH_4^+ (mmol L^{-1})	0.21	0.02	3.54	0.11	b.d.l
Na^+ (mmol L^{-1})	0.31	0.26	0.34	0.23	0.49
K^+ (mmol L^{-1})	0.18	0.03	0.25	0.14	0.14
Mg^{2+} (mmol L^{-1})	0.76	0.22	1.08	1.14	1.71
Ca^{2+} (mmol L^{-1})	2.29	0.19	1.89	1.76	3.95
Cl^- (mmol L^{-1})	0.18	1.38	0.29	0.21	1.33
NO_3^- (mmol L^{-1})	0.01	0.21	0.02	0.04	0.80
SO_4^{2-} (mmol L^{-1})	1.14	1.48	0.27	0.81	1.98
PO_4^{3-} (mmol L^{-1})	b.d.l	0.22	0.01	b.d.l	2.89
TOC (ppm)	228	< 1	54	10	3
Conductivity (S m^{-1})	59	61	70	48	81
pH (-)	~8	~8	~8	~8	~8
Dissolved oxygen concentration (mg L^{-1})	>8.00	>8.00	>8.00	>8.00	>8.00

4.3.1. Dissipation and transformation of micropollutants at the sediment-water interface

MFN, MET and TER showed distinct partitioning in line with their physicochemical properties between the sediment and the water phase (Fig. 4.4). The highly hydrophilic MFN was primarily found in water, and the more hydrophobic TER predominantly partitioned to the sediment, with MET showing intermediate behaviour (Fig. 4.4 and Table 4.2 and 4.3). This affected micropollutant dissipation dynamics, half-lives (DT_{50}) (Table 4.3) and formation of transformation products (TPs) (Fig. 4.4 and Table 3.4). Micropollutant dissipation was similar when spiked individually (ONE experiments) or as part of a mixture (MIX experiment) for all three investigated micropollutants (Table 4.2).

MFN is a highly hydrophilic compound with a low octanol-water partitioning constant ($\log P < -2.48$)[189] and soil adsorption coefficient (K_{oc} < 20 L g^{-1})[190]. Unlike what was observed in a previous report[189], metformin was only detected in the water phase of microcosms (Fig. 4.4 and Table 4.3). Absence of significant sorption to the sediment does not preclude passive water exchange between the water column and interstitial sediment water, allowing transformation of MFN in both water and sediment depending on the prevailing conditions and microbial activity in each compartment. MFN was unique among the three investigated micropollutants in showing significantly different dissipation between biotic and abiotic conditions (Table 4.3 and Fig. 4.5). MFN dissipation rates were significantly higher under biotic conditions ($CI_{95\%}$ $k_{abiotic}$ = [0.009 to 0.017] day^{-1}; $CI_{95\%}$ k_{biotic} = [0.054 to 0.066] day^{-1}; Table 4.3) and unaffected by the two other micropollutants (Fig. 4.2, Table 4.5). Evidence for microbial

biodegradation of MFN has been abundantly documented, and bacteria growing with this compound as carbon and/or nitrogen source were reported recently[92,152,191,192].

Guanylurea, the major transformation product of MFN, appeared transiently at days 15 and 30 in ONE experiments, and at day 50 in the MIX experiment (Fig. 4.5). Guanylurea is utilised for growth by some bacteria with guanylurea hydrolase[25]. The delayed and transient detection of guanylurea in the MIX experiment compared to microcosms spiked exclusively with MFN is of particular interest. Organisms involved in the degradation of MFN and guanylurea may have been adversely impacted by co-occurrence of MET and/or TER, resulting in transient guanylurea accumulation in MIX experiment. In addition to guanylurea, minor transformation products 2-amino-4-methylamino-1,3,5-triazine (AMT) and 4-amino-2-imino-1methyl-1,2-dihydro-1,3,5-triazine (AIMT)[193] were identified in ONE experiments but remained undetected in the MIX experiment (Fig. 4.5). Other potential MFN transformation products dimethylguanidine, dimethylbiguanide, 2,4-diamino-1,3,5-triazine, dimethylurea or urea were not detected, suggesting that they were not produced or rapidly metabolised.

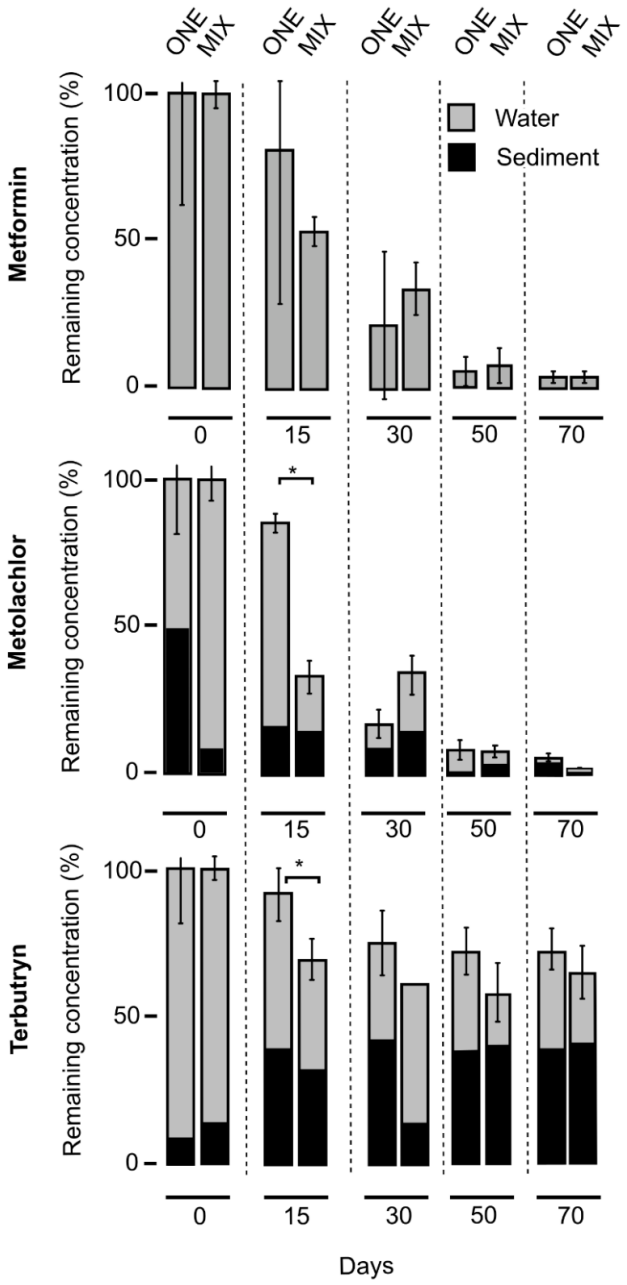

***Figure 4.4**. Distribution and dissipation of metformin, metolachlor and terbutryn in water and sediment phases in single (ONE) and multi-contamination (MIX) biotic experiments. Error bars represent SD (n=3).*

Table 4.2. *Partitioning of MFN, MET and TER between sediment and water phases in individual (ONE) and multi-contaminated (MIX) experiments under biotic and abiotic conditions.*

Contaminant	Contamination type	Time (days)	$P_{sediment, abiotic}$ Contaminant in sediment fraction (%) ± SD	$P_{sediment, biotic}$ Contaminant in sediment fraction (%) ± SD	$\Delta(P_{sediment, abiotic} - P_{sediment, biotic})$ (%) ± SD	Δ(Psediment, abiotic, ONE - Psediment, abiotic, MIX) (%) ± SD	Δ(Psediment, biotic, ONE - Psediment, biotic, MIX) (%) ± SD
MFN	ONE	0	0 ± 0	0 ± 0		-	
		15	0 ± 0	0 ± 0			
		30	0 ± 0	0 ± 0			
		50	0 ± 0	0 ± 0			
		70	0 ± 0	0 ± 0			
	MIX	0	0 ± 0	0 ± 0			
		15	0 ± 0	0 ± 0			
		30	0 ± 0	0 ± 0			
		50	0 ± 0	0 ± 0			
		70	0 ± 0	0 ± 0			
MET	ONE	0	18 ± 1	31 ± 21	13 ± 21	-	-
		15	31 ± 5	25 ± 5	6 ± 7		
		30	60 ± 15	48 ± 11	12 ± 18		
		50	44 ± 1	27 ± 6	**16 ± 6**		
		70	58 ± 14	65 ± 3	6 ± 14		
	MIX	0	32 ± 20	9 ± 5	**24 ± 20**	14 ± 20	22 ± 22
		15	52 ± 12	32 ± 18	20 ± 22	**21 ± 13**	7 ± 19
		30	41 ± 1	46 ± 5	5 ± 5	**19 ± 15**	2 ± 12
		50	44 ± 5	52 ± 16	8 ± 17	0 ± 5	**25 ± 17**
		70	66 ± 4	53 ± 7	**13 ± 8**	8 ± 15	**12 ± 8**
TER	ONE	0	18 ± 3	9 ± 6	**9 ± 7**	-	-
		15	48 ± 7	42 ± 1	6 ± 7		
		30	60 ± 7	59 ± 3	1 ± 7		
		50	58 ± 3	56 ± 6	2 ± 7		
		70	57 ± 6	52 ± 5	5 ± 8		
	MIX	0	37 ± 17	21 ± 13	**26 ± 21**	19 ± 17	12 ± 15
		15	54 ± 15	47 ± 4	7 ± 17	6 ± 17	5 ± 8
		30	61 ± 0	44 ± 18	17± 18	1 ± 7	15 ± 19
		50	73 ± 0	71 ± 7	2 ± 7	15 ± 3	**15 ± 10**
		70	78 ± 4	63 ± 6	**15 ± 7**	**21 ± 7**	**11 ± 10**

$P_{sediment,t}$*:** micropollutant concentration at time t in the sediment compartment (sediment fraction). ***$P_{water\ t}$*:** micropollutant concentration at time t in the water compartment (dissolved fraction)4 ***SD: standard deviation was estimated based on the equation $SD(C) = \sqrt{(\mathrm{SD(A)}^2 + \mathrm{SD(B)}^2)}$

$\Delta(P)_{biot}$: difference in partitioning of biotic and abiotic experiments

$\Delta(P)_{mix}$: difference in partitioning of SIN and MIX experiments under biotic (***Δ(P)mix, biotic)*** and a biotic (***Δ(P)mix, abiotic***) conditions

Table 4.3. *Dissipation constants for MFN, MET, and TER in single (ONE) and multi-contamination (MIX) experiments under biotic and abiotic conditions.*

Contaminant	Contamination type	Time (days)	$D_{abiotic,t,\ system}$ (%) ± SD	$D_{biotic,t,\ system}$ (%) ± SD	$B_{compound,t,\ system}$ (%) ± SD	$K_{abiotic}$ ± SE (day^{-1})	Estimated $DT50_{abiotic}$ range (days)	K_{biotic} ± SE (day^{-1})	Estimated $DT50_{biotic}$ range (days)	$CI_{95\%}$ $K_{abiotic}$	$CI_{95\%}$ K_{biotic}
MFN	ONE	0	0 ± 24	0 ± 38	0 ± 45	0.019 ± 0.004 (n=10)	[30 : 46]	0.060 ± 0.011 (n=13)	[10 : 14]	[0.017 : 0.021]	[0.054 : 0.066]
		15	33 ± 26	19 ± 53	-14 ± 59						
		30	40 ± 1	79 ± 24	39 ± 25						
		50	50 ± 29	95 ± 5	45 ± 29						
		70	77 ± 8	97 ± 2	20 ± 8						
	MIX	0	0 ± 0	0 ± 5	0 ± 5	0.013 ± 0.006 (n=9)	[36 : 99]	0.059 ± 0.008 (n=15)	[10 : 14]	[0.009 : 0.017]	[0.055 : 0.063]
		15	43 ± 42	47 ± 8	4 ± 43						
		30	60 ± 53	67 ± 15	6 ± 55						
		50	57 ± 4	93 ± 10	36 ± 10						
		70	71 ± 5	97 ± 4	27 ± 6						
MET	ONE	0	0 ± 2	0 ± 13	0 ± 13	0.060 ± 0.010 (n=10)	[10 : 14]	0.045 ± 0.004 (n=15)	[14 : 17]	[0.054 : 0.066]	[0.043 : 0.047]
		15	9 ± 9	14 ± 3	5 ± 9						
		30	68 ± 26	83 ± 5	15 ± 26						
		50	96 ± 1	91 ± 3	-5 ± 3						
		70	99 ± 0	94 ± 1	-5 ± 1						
	MIX	0	0 ± 7	0 ± 8	0 ± 11	0.072 ± 0.008 (n=10)	[9 : 11]	0.054 ± 0.003 (n=15)	[12 : 14]	[0.067 : 0.077]	[0.052 : 0.056]
		15	36 ± 4	67 ± 6	31 ± 7						
		30	46 ± 2	66 ± 7	20 ± 7						
		50	96 ± 0	93 ± 2	3 ± 2						
		70	99 ± 1	98 ± 0	1 ± 1						
TER	ONE	0	-	0 ± 10	-	0.006 ± 0.001 (n=8)	[99 : 139]	0.005 ± 0.001 (n=14)	[116 : 173]	[0.005 : 0.007]	[0.004 : 0.006]
		15	0 ± 9	8 ± 9	-1 ± 8						
		30	-2 ± 5	25 ± 8	27 ± 9						
		50	19 ± 8	28 ± 4	9 ± 9						
		70	23 ± 7	27 ± 3	4 ± 8						
	MIX	0	-	0 ± 4	-	0.009 ± 0.004 (n=6)	[53 : 139]	0.005 ± 0.002 (n=12)	[99 : 231]	[0.006 : 0.012]	[0.004 : 0.006]
		15	0 ± 1	31 ± 5	31 ± 5						
		30	-	39 ± 0	-						
		50	3 ± 19	43 ± 10	40 ± 21						
		70	40 ± 16	35 ± 7	-5 ± 17						

***B*:** Biodegradation fraction; SD: error was estimated based on error propagation based on 1 σ.

k: Dissipation rate estimated by the linear form of the first-order kinetic model $\mathbf{ln\ Ct = ln\ C0 - {}^{kt}}$; SE: standard error obtained from regression analysis of the first-order kinetic model

DT50: estimated half-life of the compound

$\mathbf{CI_{95\%}}$ confidence interval of **k** calculated with a Z-score of 1.96

Unlike MFN, MET partitioned equally between water and sediment (Table 4.2), in line with its higher octanol-water and soil adsorption constants (LogP = 2.9; K_{oc} = 33 ± 9 L g^{-1})[151]. In the environment, MET undergoes photolysis[94], hydrolysis[89], and biodegradation[97], with formation of potentially toxic transformation products (TPs). Also in contrast to MFN, dissipation rates of MET (Fig. 4.4) remained similar under biotic and abiotic conditions (Table 4.3). Patterns of detected TPs (Fig. 4.5) were similar under biotic and abiotic conditions suggesting that abiotic transformation processes were prominent (Table 4.3). Different pathways are known for MET degradation that involve abiotic and biotic transformations and the same TPs[85]. For example, formation of MET N-oxaethanesulfonic acid (NOA) from MET ethanesulfonic acid (ESA) was reported in soil[105]. Here, only NOA was detected, while ESA or the other major oxanilic acid derivative of metolachlor (OXA) were not identified (Fig. 4.5). Half-lives for MET displayed a slight yet statistically significant increase in ONE experiments containing MET alone (14-17 days) as compared to the MIX experiment (12-14 days) (Table 4.5). This contrasts with previous reports of slower dissipation of a given micropollutant in the presence of other contaminants[97,105,194].

TER was the most recalcitrant micropollutant in our experiments (Fig. 4.4 and Fig. 4.5), again in line with octanol-water partitioning and soil adsorption constants (LogP = 3.4; K_{oc} = 560 ± 240 L g^{-1})[195,196]. TER partitioned predominantly to the sediment and its concentration did not change significantly over time (Fig. 4.4, Table 4.2). Estimated half-lives for TER (53-231 days, Table 4.3) are in agreement with previously reported values for aerobic river sediment (180 days)[197] and groundwater (193-644 days)[198]. Dissipation rates and transformation patterns were not affected by the other two micropollutants investigated (Fig. 4.4, Fig. 4.5, Table 4.3). Transformation products[199] 2-hydroxy-terbutryn (TerOH), desethyl-tebutryn (TerDesE), and desethyl-2-hydroxyterbutryn (TerDesEOH) were detected in all TER and MIX microcosms (Fig. 4.5 and Table 3.4). Together with the similar dissipation rates observed in biotic and abiotic experiments (Table 4.3), this suggests that transformation of TER in biotic microcosms mainly occurred by abiotic processes.

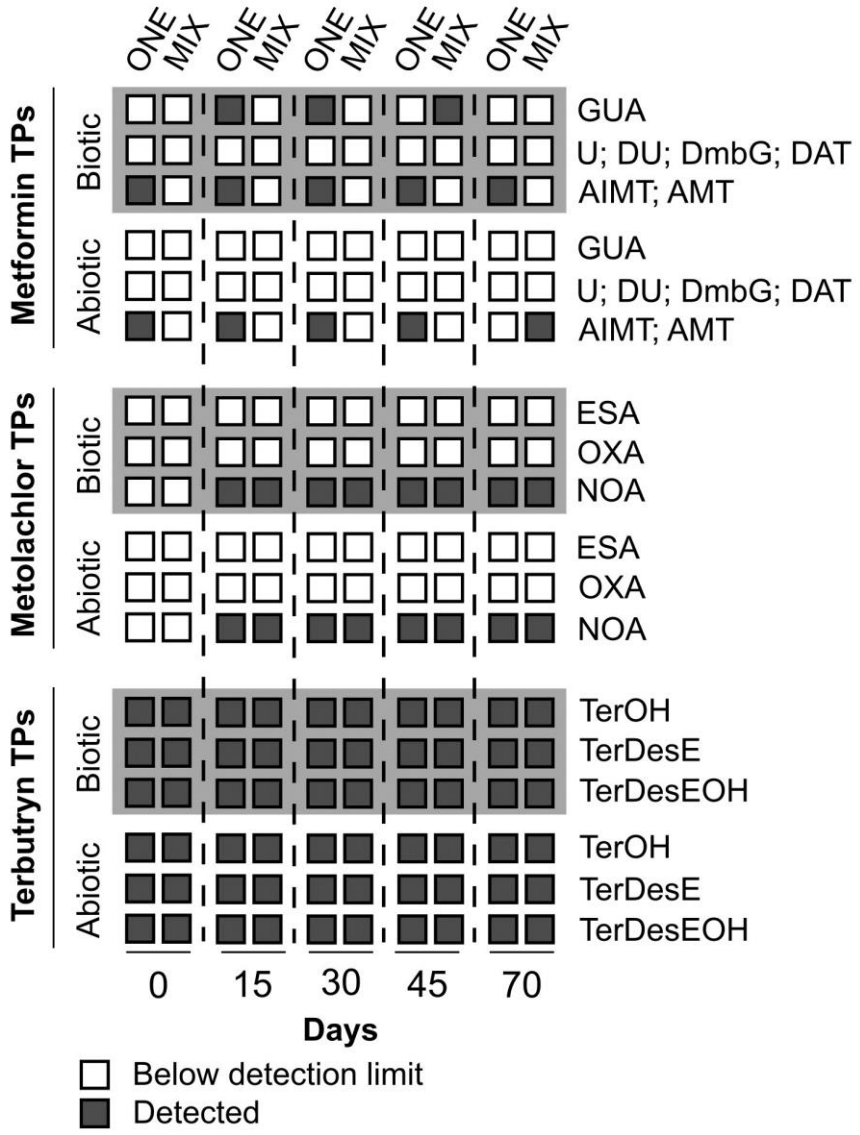

Figure 4.5*. Transformation products (TPs) detected over time in biotic and abiotic experiments: guanylurea (GUA); urea (U); dimethylurea (DU); dimethylbiguanide (DMbG); 2,4-diamino-1,3,5-triazine (DAT); 4-amino-2-imino-1-methyl-1,2-dihydro-1,3,5-triazine (AIMT); 2-amino-4-methylamino-1,3,5-triazine (AMT); metolachlor ethanesulfonic acid (ESA); metolachlor oxanilic acid (OXA); metolachlor N-oxa-ethanesulfonic acid (NOA); 2-hydroxy-terbutryn (TerOH); desethyl-terbutryn (TerDesE); desethyl-2-hydroxy-terbutryn (TerDesOH).*

4.3.2. Factors affecting prokaryotic communities in sediment-water microcosms

Prokaryotic diversity in microcosms was assessed by sequencing PCR amplicons of the 16S ribosomal gene V3-V4 variable region at initial and final time points. Diversity metrics in sediment and water phases remained very similar over time. Overall, the sediment showed markedly higher prokaryotic richness, evenness, and diversity indices than the water phase

(Table A4.2). Previous studies also documented higher diversity in the sediment than in the water phase in the same environmental context[195].

In contrast to what would be expected for acute pollution, e.g., by compounds in heavy industrial use such as organic solvents and hydrocarbons, diffuse environmental contamination by biocides and pharmaceuticals at low concentrations is not expected to yield readily discernible changes in specific taxa featuring strains utilizing these micropollutants as nutrients for growth. Nevertheless, micropollutants may significantly impact the composition of prokaryotic communities through their toxic effects[127,200–202]. Prokaryotic communities at the sediment-water interface are subject to chronic exposure to hydrophobic biocides in particular, primarily because of the persistence of such compounds in the sediment and associated exchanges with the water phase[203,204]. However, the complexity of natural environments and exposure scenarios usually represents a challenge to identify the primary determinants of changes in prokaryotic community composition[205]. Here, we were able to analyse observed differences in amplicon sequence variant (ASV) data in laboratory microcosm samples. Using distance matrices (Fig. 4.6) and statistical analysis (Table 4.4), the factors affecting prokaryotic community composition could be ranked in order of importance, with matrix ranking first, followed by time and then contamination type.

Overall, phase, timepoint and contamination type as well as interactions between these three factors (Table 4.4) accounted for over 67% of the observed variability in prokaryotic community composition, leaving a residual R^2 of 33%. This residual variation presumably represents unidentified experimental biases during set-up and sampling despite rigorous initial sediment homogenization. The observed clustering (Fig. 4.6) reveals substantial disparities in prokaryotic composition between sediment and water phases (NPMANOVA: R^2=0.13; F=15.56; p=0.0001). Indeed, 32 of the 47 prokaryotic phyla common to water and sediment samples showed significant differences in relative abundance between the two compartments (Wilcoxon; $p<0.05$; Table A4.3). For instance, the water phase showed higher relative abundance of Proteobacteria and Patescibacteria, and the sediment displayed significantly lower levels of Firmicutes, Chloroflexi, Actinobacteriota, and Desulfobacterota. Such differences between sediment and water were already documented previously[206], and likely find their origin in qualitative and quantitative differences in nutrient availability and organic substrates in the two environments.

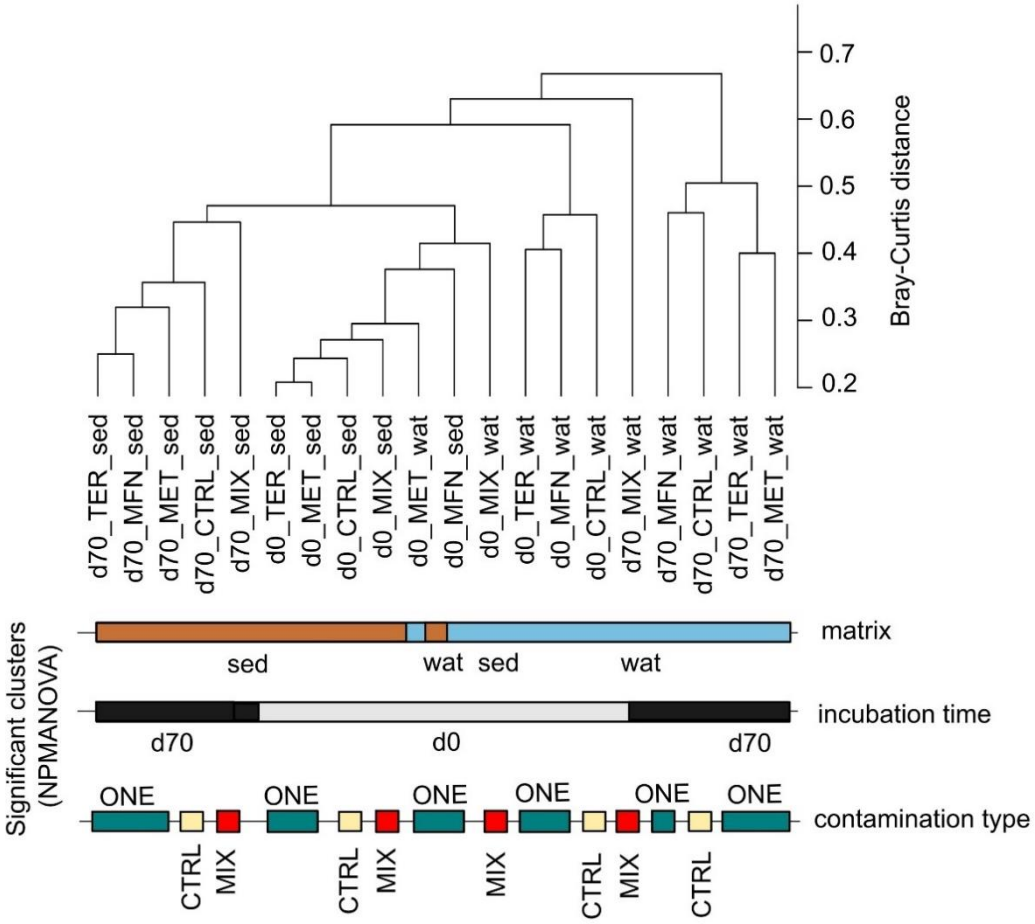

***Figure 4.6**. Dendrogram (mean Bray-Curtis distances) with clustering according to matrix (sediment (sed) or water (wat)), timepoint (d0/d70), and contamination type (ONE/MIX/CTRL).*

***Table 4.4**. Non-parametric multivariate analysis of variance (NPMANOVA) of prokaryotic communities in water-sediment microcosms. Analysis was performed for the main experimental factors time, matrix, and contamination (i.e., CTRL, MFN, MET, TER, and MIX).*

NPMANOVA

	Factors	Degree of freedom	Sum of Squares	R^2	F-statistic	p-value
	Time (1)	1	1.8525	0.13323	15.7432	0.0001
	Matrix (2)	1	1.8307	0.13166	15.5574	0.0001
	Contamination (3)	4	1.6538	0.11894	3.5136	0.0001
Interactions	(1) : (2)	1	0.6107	0.04392	5.1898	0.0001
	(1) : (3)	4	1.2585	0.09051	2.6737	0.0002
	(2) : (3)	4	1.1737	0.08441	2.4935	0.0002
	(1) : (2) : (3)	4	0.9354	0.06728	1.9874	0.0008
	Residual	39	4.5892	0.3305		
	Total	58	13.9045	1		

Incubation time was another important factor affecting prokaryotic community composition (NPMANOVA: R^2=0.13; F=15.74; p=0.0001, Table 4.4 and Table A4.4). As expected and also observed previously[207], prokaryotic community composition adjusted to laboratory conditions and also led to the development of initially undetected taxa during incubation, e.g., here for Iainarchaeota in the water phase and WS4 in the sediment. A trend towards increase in the proportion of Archaea across all microcosms was also observed (data not shown), i.e., from 3.4 ± 3.4% to 6.7 ± 5.9% in the sediment and from 1.3 ± 1.1% to 6.2 ± 5.0% in the water phase over the 70-day incubation period.

The composition of prokaryotic communities was also affected by the type of contamination as evidenced by significant difference observed across experiments (CTRL, MFN, MET, TER, and MIX) (NPMANOVA: R^2=0.12; F=3.51; p=0.0001, Table 4.4). We examined the effect of contamination in conjunction with time (day 0 or day 70) (Table 4.5). In order to prevent a confounding impact of phase (sediment or water), separate analyses were conducted for sediment and water samples at day 0 and day 70. No significant differences were observed between the different conditions in contamination (CTRL, MFN, MET, TER, and MIX) (Table 4.5).

We also evaluate whether observed changes in prokaryotic communities in the MIX experiment differed from the cumulative changes observed in MFN, MET, and TER experiments in sediment, water or the entire dataset at day 0 and day 70 (Table 4.6). The MIX experiment showed a significantly distinct community composition at the ASV level compared to the combined ONE experiments. However, there was no significant difference (p=0.10) between MIX and CTRL experiments, likely because of the limited sample size of each CTRL and MIX subgroup (n=3, Table 4.6).

Table 4.5. *Non-parametric multivariate analysis of variance (NPMANOVA) for prokaryotic communities in water-sediment microcosms. Pairwise comparisons were performed to assess differences in prokaryotic communities. Analysis included all combinations of contamination types such as CTRL, MFN, MET, TER, and MIX. Benjamini-Hochberg correction was applied to account for multiple comparisons. Permutations were constrained based on confounding factors matrix and time for the total dataset. Analyses were conducted without constraining permutations for four distinct subgroups: sediment and water samples collected at days 0 and day 70. * One water sample failed to be sequenced at day 0.*

	Pairwise NPMANOVA					
	Dataset	*Total dataset*	*Sediment d0*	*Water d0*	*Sediment d70*	*Water d70*
	Confounding factors	*matrix:time*	-	-	-	-
Tested hypotheses	CTRL : MFN	**0.019**	0.100	0.100	0.100	0.375
	CTRL : MET	**0.001**	0.100	0.100	0.100	0.333
	CTRL : TER	**0.001**	0.100	0.100	0.100	0.333
	CTRL : MIX	**0.001**	0.100	0.100	0.100	0.250
	MFN : MET	**0.001**	0.100	0.100	0.100	0.444
	MFN : TER	**0.008**	0.100	0.100	0.100	0.375
	MFN : MIX	**0.001**	0.100	0.100	0.100	0.250
	MET : TER	**0.008**	0.100	0.100	0.100	0.500
	MET : MIX	**0.001**	0.100	0.100	0.100	0.250
	TER : MIX	**0.001**	0.100	0.100	0.100	0.250
	Samples in dataset (n)	59	15	14	15	15
	Samples per hypothesis (h)	24 or 23*	6	6 or 5*	6	6
	Samples per factor (f)	12 or 11*	3	3 or 2*	3	3

Table 4.6. *Non-parametric multivariate analysis of variance (NPMANOVA) for prokaryotic communities in water-sediment microcosms. Pairwise comparisons were performed to assess differences in prokaryotic communities within water-sediment microcosms. The analysis included an aggregated subgroup of contamination types ONE referring to the pool of samples under individual contamination (with a sized-up sample size, combining MFN, MET, and TER samples), then the MIX and the CTRL samples. Benjamini-Hochberg correction was applied to account for multiple comparisons. Permutations were constrained based on confounding factors, specifically matrix and time, for the entire dataset (total dataset). Additionally, analyses were conducted without constraining permutations for four distinct subgroups: sediment samples collected at days 0 (sediment d0) or day 70 (sediment d70) and water samples collected at days 0 (water d0) or day 70 (water d70).*

		Pairwise NPMANOVA p-values, using Benjamini-Hochberg correction for multiplicity				
	Dataset	*Total dataset*	*Sediment d0*	*Water d0*	*Sediment d70*	*Water d70*
	Confounding factors	*matrix:time*	-	-	-	-
Tested hypothses	CTRL : MIX	0.002	0.100	0.100	0.100	0.150
	CTRL : ONE (**size up**)	0.002	0.009	0.042	0.006	0.208
	MIX : ONE (**size up**)	0.002	0.009	0.042	0.006	0.039
	Samples in dataset (n)	59	15	14	15	15
	Samples per hypothesis (h)	24 or *47 (ONE)*	6 or *12 (ONE)*	6 or *11 (ONE)*	6 or *12 (ONE)*	6 or *12 (ONE)*
	Samples per factor (f)	12 or *36 (ONE)*	3 or *9 (ONE)*	3 or *8 (ONE)*	3 or *9 (ONE)*	3 or *9 (ONE)*

Finally, in an attempt to identify any specific changes in prokaryotic communities associated with the nature of micropollutant exposure, we compared changes in relative abundances in MFN, MET, TER, and MIX experiments with those of control experiments without contamination (CTRL). A large proportion of taxa varied in relative abundance across all taxonomic levels from ASVs to phylum (Fig. 4.7, and data not shown). It is well-documented that contamination can have either positive or negative impacts on the relative abundance of different taxa[153]. Accounting for all taxonomic levels, 63 ± 2% of phyla showed an increase in relative abundance (FC>1), and 37 ± 2% a decrease in relative abundance (FC<1) at the end of the experiment compared to the corresponding control (CTRL) (Table A4.5).

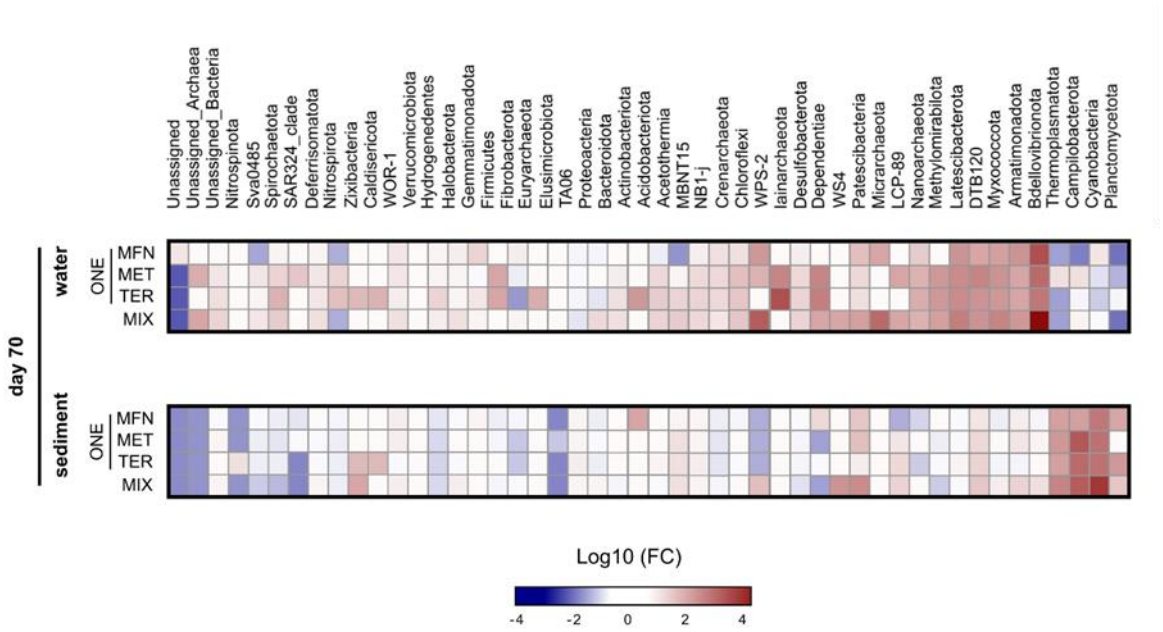

***Figure 4.7**. Heatmap of $log_{10}FC$ in relative abundance of phyla in ONE and MIX experiment compared to CTRL experiments for sediment and water phases at the end of microcosm incubations (day 70). Phyla showing an increase in relative abundance (positive $log_{10}FC$) compared to CTRL experiments are shown in red, and phyla showing a decrease (negative $log_{10}FC$) in blue.*

Some taxa showed clear responses to different micropollutants for a given phase. For example, in the water phase, the response of certain phyla such as Nanoarchaeota, Latescibacteria, and Bdellovibrionata was similar in ONE and MIX experiments (Fig. 4.7). Interestingly, Bdellovibrionota showed a strong increase in relative abundance in the MIX experiment compared to that observed in ONE experiments (average FC in ONE experiments = 262 ± 183, FC in MIX = 6253; Fig. 4.7). Previous research already demonstrated that mixtures of micropollutants may significantly amplify the effects of individual micropollutants[97]. This suggests that the effects of micropollutant mixtures on prokaryotic communities may be difficult to extrapolate from the effects of individual micropollutants. This encouraged us to explore the occurrence of three possible types of micropollutant interactions: additivity, when the observed effect on a given taxon in the MIX experiment corresponds to the total individual effects in ONE experiments; antagonism, when it is less than the total of individual micropollutant effects; and synergism, when it exceeds the sum of individual micropollutant effects.

4.3.3. Evidence for non-additive effects of micropollutants on prokaryotic communities

Non-additive effects of micropollutants on prokaryotic communities may arise for several reasons. For example, increased proliferation of pollutant-tolerant strains producing key nutrients or factors may promote growth of specific taxa[208]. Conversely, production of antibiotics or toxic compounds by pollutant-tolerant taxa may have inhibitory effects on other taxa[209,210]. Here, we introduce a new metric to perform the analysis of the effects of contaminant mixtures on prokaryotic communities in a robust and reliable way. Obtained

values of fold change (FC) were adjusted to facilitate comparative analysis of data obtained for exposure to individual contaminants or their mixture, and the resulting numbers termed interaction coefficient (IC) (see Section 2.4). This allowed us to assess potential non-additive effects for specific taxa at different taxonomic levels of interest.

Worthy of note, identified interactions across various matrices were largely consistent at different taxonomic levels (Fig. 4.8A). As expected, additivity emerged as prevalent (33-57% of cases) in line with the conservative criterium chosen our study, i.e., differences within 64% relative error were considered non-significant. Antagonistic interactions involving either repressing or opposing effects (see Materials and Methods) also accounted for a substantial proportion (34-52%) of the total identified interactions. Synergistic interactions in the effects of micropollutants were noted for only a minor proportion of taxa, in the range of 5% to 15% of the total across all taxonomic levels from ASV to Phylum. The proportion of additive outcomes decreased at more precise taxonomic levels (Fig. 4.8A), with the Phylum level demonstrating the highest degree of additivity (57%), and the ASV level exhibiting the lowest (33%). This trend presumably originates in the larger number of taxa detected in the MIX experiment at the ASV level (Fig. 4.8A and Table A4.2).

To illustrate the proposed approach, Phylum LCP-89 is an example of a Phylum-level taxon responding to micropollutants in an additive way in the sediment (Fig. 4.5B). The sum of individual IC values of MFN, MET and TER (IC_{ADD} = 1.5 ± 1) did not differ significantly from that observed in the corresponding MIX experiment (IC_{MIX} 2.4 ± 1.5). It is worth noting that an IC_{ADD} value can be computed from the sum of positive and negative individual IC values as for Phylum LCP-89, or from the sum of IC values sharing the same sign, as exemplified by Patescibacteria in the water phase (Fig. 4.8B).

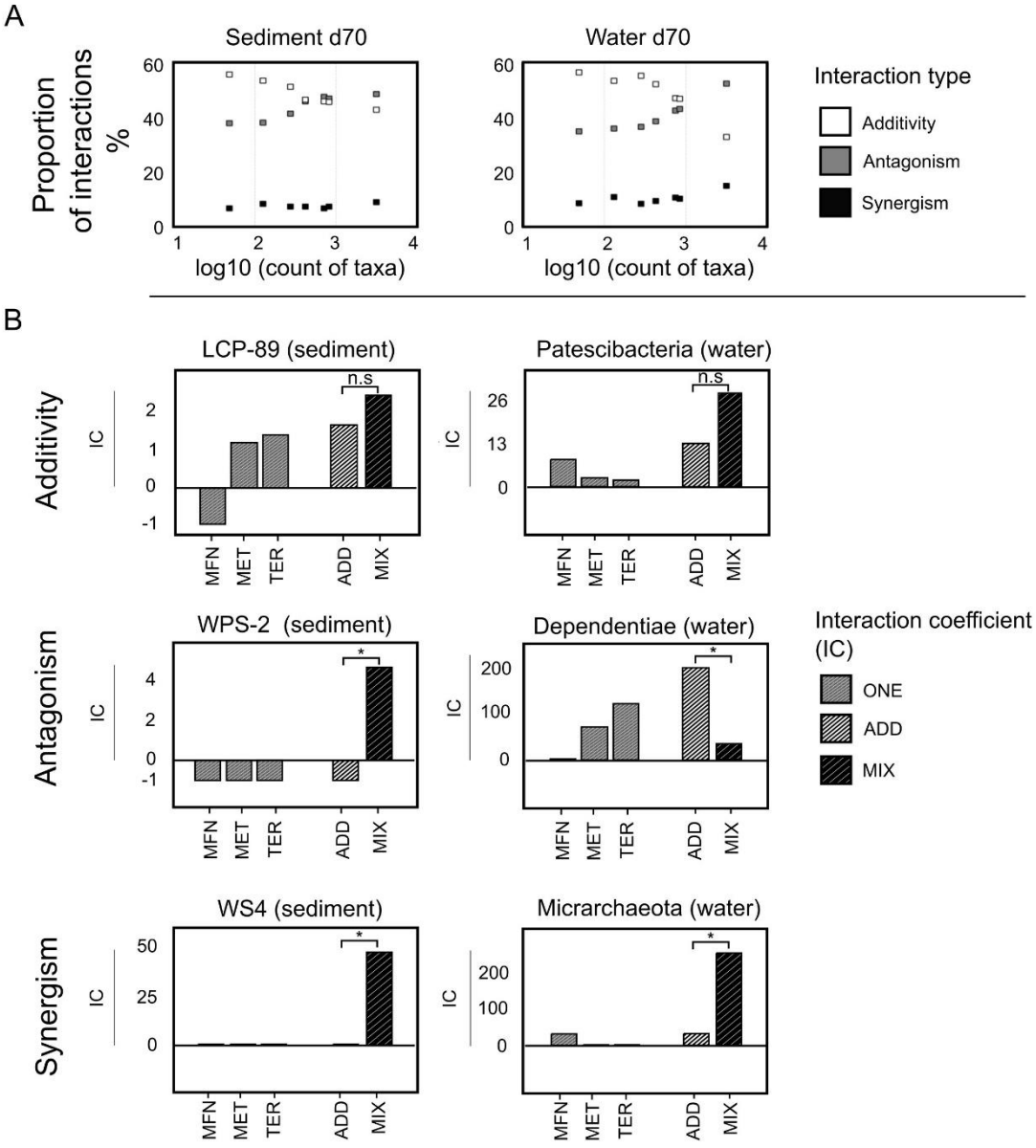

***Figure 4.8**. Interactions (additivity, antagonism, synergism) among micropollutant effects across taxonomic levels for sediment and water phases. (A) Proportion (percentage) of interactions as a function of number of taxa at different taxonomic levels (x-axis, from left to right: Phylum, Class, Order, Family, Genus, Species, ASV). (B) Examples of different interaction types at the Phylum level in sediment (left) and water (right). The relative error (RE) threshold for significance of differences in interaction coefficient (IC) values was set at ±64%. (*) denotes statistically significant differences between IC scores predicted for the ADD model and observed in the MIX experiment (n.s., not significant).*

Potential antagonistic interactions for the effects of the micropollutant mixture were also identified. In such cases, IC values for the micropollutant mixture differed from the IC_{ADD} value computed from the added effects of the three individual micropollutants in two different ways, termed 'antagonism (opposing)' and 'antagonism (repressing)' (Fig. 4.8B, middle row). The WPS-2 phylum in the sediment phase is an example of 'antagonism (opposing),' with a negative calculated IC_{ADD} value (−1.0 ± 0.6) and a positive observed IC_{MIX} (4.6 ± 2.9) (Fig. 4.5B). In contrast, Dependentiae in the water phase showed a lower IC_{MIX} value (35 ± 22) than the computed IC_{ADD} (193 ± 124), categorized as 'antagonism (repressing)'.

Examples of synergistic effects between pollutants, i.e., when IC values for the MIX experiment exceeded the summation of computed IC values in ONE experiments, include the case of Phyla WS4 in the sediment (IC_{ADD} = 0, IC_{MIC} = 47 ± 30) and Micrarchaeota in the water phase (IC_{ADD} = 30 ± 19, IC_{MIX} = 255 ± 163) (Fig. 4.8B).

Given the notable prevalence of additivity interactions, we conducted a ranking of individual micropollutant contributions to additivity. Micropollutants were assessed based on their FC scores in ONE experiments, comparing them to the FC scores of the MIX experiment (Fig. 4.9). MET and TER consistently emerged as the most frequent first and second contributors across the entire range of taxonomic levels (Fig. 4.9). MFN typically represented the smallest contributor, although differences were less pronounced in the sediment at the ASV level. These findings align with the fact that MET and TER are biocides designed to inhibit central metabolic pathways. In contrast, MFN primarily affects signal transduction in multicellular eukaryotic organisms[211]. Also, MFN is the least recalcitrant of these three compounds, and its relative effect compared to MET and TER may have decreased over time as its concentration diminished. This phenomenon warrants further investigation.

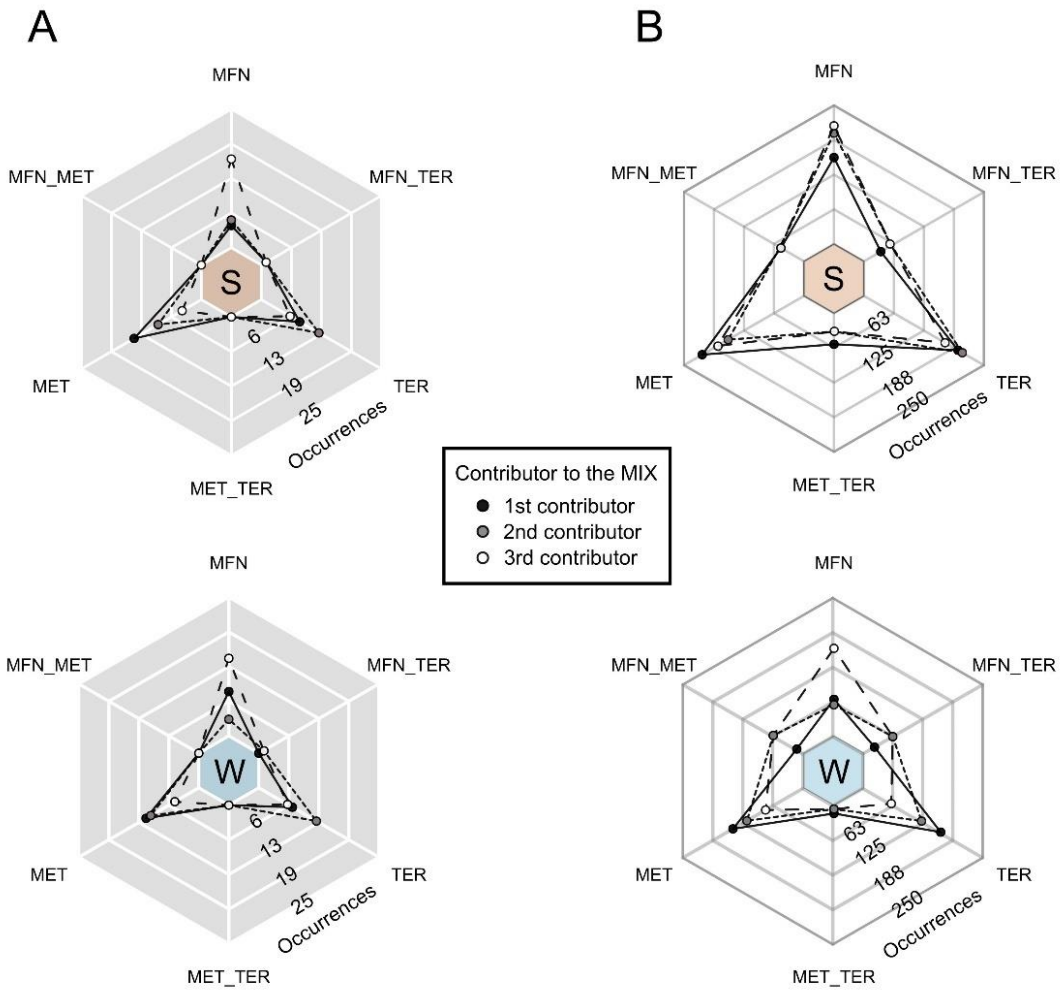

***Figure 4.9**. Contribution of micropollutants to the additive model at the Phylum (part A) and ASV (part B) levels in sediment (S) and water (W) compartments. Micropollutants contributed individually (MFN, MET, TER) or in binary combination to equal degrees (MFN_MET, MFN_TER, and MET_TER, see Materials and Methods) to the observed effects in the MIX experiment.*

4.4. Conclusion

Understanding the complex interplay of micropollutant dissipation, interactions between multiple micropollutants and prokaryotic community dynamics at the sediment-water interface represents a multifaceted challenge that requires consideration of micropollutant bioavailability, toxicity, and transformation. In our study, laboratory microcosms were used to mimic the sediment-water interface under controlled conditions and spiked with three prominent micropollutants, either individually or as a mixture. Degradation kinetics and formation of transformation products did not provide evidence for significant effects of mixtures of contaminants on the dissipation of individual micropollutants. Similarly, the nature of contamination did not markedly affect overall richness, evenness, or diversity of prokaryotic communities (Table A4.2). However, it had a discernible effect on their composition. Specific taxa were affected to varying degrees by micropollutants depending on the matrix and contamination type, and this was observed at different taxonomic levels. Furthermore, significant deviations from the sum of individual micropollutant effects were detected when micropollutants were provided at the same concentration in a mixture.

We anticipate that the analytical framework developed in this study may prove valuable for testing and prioritizing the biological effects of a specific compound in a complex micropollutant mixture. Such an approach may contribute to a more realistic assessment of the risks associated with multi-contamination in aquatic ecosystems.

Acknowledgements

This research and the fellowship of Adrien Borreca were funded by the CNRS 80|Prime program (2020-2023) and by the EU within the European Regional Development Fund (ERDF), support measure INTERREG VI in the Upper Rhine as part of the Reactive City project (Towards a Reactive City without Biocides). Chemical analyses were performed at the Pacite platform, ITES, University of Strasbourg. We acknowledge Arriheura Tiatia for help with DNA extraction, and Emilie Muller, Jérémy Masbou and Tetyana Gilevska for fruitful discussions.

4.5. Appendix

Table A4.1. *Studied micropollutants and their putative transformation products.*

Name	Abbreviation	Nomenclature	Potential precursor	Purity	Provider	Comment
metformin	MFN	$C_4H_{11}N_5$	-	≥ 97%	Acros organics	-
metolachlor	MET	$C_{15}H_{22}ClNO_2$	-	≥ 98%	Sigma-Aldrich	-
terbutryn	TER	$C_{10}H_{19}N_5S$	-	≥ 98%	Sigma-Aldrich	-
guanylurea	GUA	$C_2H_6N_4O$	MFN	≥ 99%	Sigma-Aldrich	-
dimethylguanidine	DMG	$C_3H_9N_3$	MFN	≥ 99.5%	Acros organics	-
dimethylbiguanide	DMbG	$C_4H_{12}ClN_5$	MFN	≥ 98%	Acros organics	-
dimethylurea	DU	$C_3H_8N_2O$	MFN	≥ 98%	Acros organics	-
urea	U	CH_4N_2O	MFN	≥ 99%	Acros organics	-
2,4-diamino-1,3,5-triazine	DAT	$C_3H_5N_5$	MFN	≥ 99%	Sigma-Aldrich	No available standard, use of melamine (MAM) as proxy [212]
2-amino-4-methylamino-1,3,5-triazine	AMT	$C_4H_7N_5$	MFN			
4-amino-2-imino-1-methyl-1,2-dihydro-1,3,5-triazine	AIMT	$C_4H_6N_4O$	MFN			
metolachlor ethanesulfonic acid	ESA	$C_{15}H_{23}NO_5S$	MET	≥ 95.0 %	Sigma-Aldrich	-
metolachlor oxanilic acid	OXA	$C_{15}H_{21}NO_4$	MET	≥ 98.0 %	Sigma-Aldrich	-
metolachlor N-oxa-ethanosulfonic acid	NOA	$C_{14}H_{17}NNa_2O_6$	MET	≥ 98.0 %	TechLab	-
terbutryn-2-hydroxy	TerOH	$C_9H_{17}N_5O$	TER	≥ 98%	HPC Standards GmbH	-
desethyl-terbutryn	TerDesE	$C_8H_{15}N_5S$		≥ 98%	HPC Standards GmbH	-
desethyl-2-hydroxy-terbutryn	TerDesEOH	$C_7H_{13}N_5O$		≥ 98%	HPC Standards GmbH	-
metformin-d6	MFNd6	$C_4H_5d_6N_5$	-	≥ 95%	Sigma-Aldrich	LC/MS-MS internal standard
metolachlor-d11	METd11	$C_{15}H_{11}d_{11}ClNO_2$	-	≥ 97%	Sigma-Aldrich	GC/MS internal standard

Table A4.2. *Sample size (i.e., number of samples in subgroups), richness, evenness, diversity indices and count of taxa at different taxonomic level across sediment and water samples, and subsequent subgroups of contaminants (CTRL, MFN, MET, TER, MIX) in sediment and water phases at day 70.*

				sediment day 70					water day 70				
		sediment	**water**	CTRL	MFN	MET	TER	MIX	CTRL	MFN	MET	TER	MIX
	sample size	29	30	3	3	3	3	3	3	3	3	3	3
Richness	Observed	1812 ± 293	1428 ± 421.51	1644 ± 76	1756 ± 329	1597 ± 127	1777 ± 453	1511 ± 46	965 ± 459	982 ± 193	1597 ± 127	1529 ± 325	1474 ± 440
	Chao1	1861 ± 321	1480 ± 443	1672 ± 63	1796 ± 368	1616 ± 134	1834 ± 502	1556 ± 59	1002 ± 459	991 ± 194	1616 ± 134	1607 ± 331	1512.49± 438
	ACE	1865 ± 324	1485 ± 444	1675 ± 66	1804 ± 374	1623 ± 139	1837 ± 506	1545 ± 49	1005 ± 449	995 ± 194	1623 ± 138	1617 ± 322	1525.38± 442
Evenness	camargo	0.44 ± 0.02	0.37 ± 0.11	0.46 ± 0.03	0.45 ± 0.01	0.45 ± 0.03	0.43 ± 0.01	0.44 ± 0.01	0.29 ± 0.17	0.5 ± 0.21	0.3 ± 0.13	0.32 ± 0.09	0.34 ± 0.15
	pielou	0.93 ± 0.01	0.78 ± 0.14	0.91 ± 0.03	0.93 ± 0.01	0.93 ± 0.01	0.92 ± 0.01	0.91 ± 0.01	0.61 ± 0.22	0.77 ± 0.13	0.68 ± 0.2	0.74 ± 0.19	0.71 ± 0.25
	simpson	0.29 ± 0.09	0.1 ± 0.11	0.25 ± 0.14	0.35 ± 0.04	0.27 ± 0.05	0.22 ± 0.06	0.24 ± 0.05	0.03 ± 0.04	0.06 ± 0.06	0.07 ± 0.11	0.04 ± 0.05	0.11 ± 0.14
Diversity	Shannon	6.93 ± 0.21	5.69 ± 1.21	6.78± 0.25	6.84± 0.21	6.87± 0.09	6.91± 0.22	6.68± 0.1	4.18± 1.8	5.27± 0.96	6.87± 0.09	5.41± 1.54	6.01± 0.88
	Simpson	1 ± 0	0.94 ± 0.09	1± 0	1± 0	1± 0	1± 0	1± 0	0.81± 0.16	0.94± 0.07	1± 0	0.9± 0.15	0.98± 0.02
	Non-null ASV count	2773	2426	897	1023	973	1082	892	300	309	710	800	690
	Phyla count	49											
	Family count	128											
	Order count	276											
	Class count	422											
	Genus count	727											
	Species count	832											
	ASV count	3146											

Table A4.3. *Relative abundance (%) of phyla in sediment compared to water phases at days 0 and 70, with statistical significance determined by Wilcoxon tests. n.s: non-significant.*

Phylum	Sediment (mean ± SD%)	Water (mean ± SD%)	Significance (p≤0.05)
Unassigned	0.01 ± 0.03	0.14 ± 0.5	n.s
Unassigned Archaea	0 ± 0.02	0 ± 0.01	n.s
Unassigned Bacteria	0.65 ± 0.29	0.36 ± 0.25	*
Acetothermia	0 ± 0.01	0 ± 0.01	n.s
Acidobacteriota	4.28 ± 1.13	1.77 ± 1.64	*
Actinobacteriota	12.86 ± 3.46	5.27 ± 3.07	*
Armatimonadota	0.06 ± 0.05	0.02 ± 0.02	*
Bacteroidota	9.24 ± 3.56	8.2 ± 6.81	*
Bdellovibrionota	0.17 ± 0.19	0.8 ± 3.21	n.s
Caldisericota	0.01 ± 0.02	0.01 ± 0.01	n.s
Campilobacterota	0.48 ± 0.6	1.27 ± 1.69	
Chloroflexi	7.91 ± 2.66	2.46 ± 1.81	*
Crenarchaeota	2.03 ± 1.45	1.21 ± 1.15	*
Cyanobacteria	0.18 ± 0.33	0.2 ± 0.46	n.s
DTB120	0.13 ± 0.15	0.03 ± 0.04	*
Deferrisomatota	0.02 ± 0.03	0.01 ± 0.02	n.s
Dependentiae	0.02 ± 0.05	0.02 ± 0.05	n.s
Desulfobacterota	7.62 ± 2.46	3.5 ± 2.28	*
Elusimicrobiota	0.04 ± 0.04	0.07 ± 0.09	n.s
Euryarchaeota	0.1 ± 0.14	0.02 ± 0.03	*
Fibrobacterota	0.03 ± 0.02	0.01 ± 0.03	n.s
Firmicutes	7.34 ± 2.01	5.65 ± 5.42	*
Gemmatimonadota	1.55 ± 0.44	0.9 ± 0.54	*
Halobacterota	3.25 ± 4.1	1.45 ± 2.56	*
Hydrogenedentes	0 ± 0.01	0 ± 0.01	n.s
Iainarchaeota	0 ± 0	0.06 ± 0.19	*
LCP-89	0.02 ± 0.03	0.01 ± 0.01	*
Latescibacterota	0.21 ± 0.11	0.07 ± 0.07	*
MBNT15	0.32 ± 0.17	0.09 ± 0.09	*
Methylomirabilota	0.08 ± 0.07	0.02 ± 0.02	*
Micrarchaeota	0 ± 0	0.02 ± 0.08	*
Myxococcota	1.46 ± 0.81	0.55 ± 0.37	*
NB1-j	0.77 ± 0.27	0.33 ± 0.23	*
Nanoarchaeota	0.12 ± 0.14	1.07 ± 1.92	*
Nitrospinota	0.07 ± 0.07	0 ± 0.02	*
Nitrospirota	2.27 ± 0.82	1.34 ± 0.88	*
Patescibacteria	0.35 ± 0.75	1.24 ± 3.12	*
Planctomycetota	0.01 ± 0.01	0.11 ± 0.22	*
Proteobacteria	34.4 ± 5.46	59.92 ± 17.18	*
SAR324_clade (Marine_group_B)	0.01 ± 0.02	0.03 ± 0.12	n.s
Spirochaetota	0.37 ± 0.35	0.19 ± 0.23	*
Sva0485	0.09 ± 0.11	0.02 ± 0.03	*
TA06	0.01 ± 0.02	0 ± 0	*
Thermoplasmatota	0.02 ± 0.03	0.01 ± 0.03	n.s
Verrucomicrobiota	1.33 ± 0.74	1.51 ± 1.11	*
WOR-1	0 ± 0	0 ± 0.01	n.s
WPS-2	0.02 ± 0.05	0.04 ± 0.12	n.s
WS4	0 ± 0.02	0 ± 0.01	n.s
Zixibacteria	0.19 ± 0.14	0.06 ± 0.07	*

Table A4.4 *Relative abundance (%) of phyla on day 70 compared to day 0, in sediment and water phases, with statistical significance determined by the Wilcoxon test. n.s: non-significant.*

Phylum	Day 70 (mean ± SD%)	Day 0 (mean ± SD%)	Significance (p≤0.05)
Unassigned	0.13 ± 0.5	0.01 ± 0.03	n.s
Unassigned Archaea	0.01 ± 0.02	0 ± 0	n.s
Unassigned Bacteria	0.62 ± 0.37	0.39 ± 0.14	*
Acetothermia	0.01 ± 0.02	0 ± 0	n.s
Acidobacteriota	2.29 ± 1.54	3.74 ± 1.95	*
Actinobacteriota	8.02 ± 4.52	10.01 ± 5.37	*
Armatimonadota	0.05 ± 0.06	0.03 ± 0.02	*
Bacteroidota	6.74 ± 6.5	10.76 ± 3.01	*
Bdellovibrionota	0.84 ± 3.21	0.13 ± 0.18	n.s
Caldisericota	0 ± 0.01	0.02 ± 0.02	n.s
Campilobacterota	0.14 ± 0.15	1.65 ± 1.56	n.s
Chloroflexi	5.85 ± 4.28	4.4 ± 2.45	*
Crenarchaeota	2.02 ± 1.38	1.19 ± 1.21	*
Cyanobacteria	0.32 ± 0.52	0.06 ± 0.07	n.s
DTB120	0.12 ± 0.15	0.04 ± 0.03	*
Deferrisomatota	0.02 ± 0.03	0.02 ± 0.02	n.s
Dependentiae	0.03 ± 0.07	0 ± 0.01	n.s
Desulfobacterota	5.41 ± 4.03	5.64 ± 1.87	*
Elusimicrobiota	0 ± 0.01	0.11 ± 0.07	n.s
Euryarchaeota	0.11 ± 0.13	0.01 ± 0.04	*
Fibrobacterota	0.02 ± 0.02	0.02 ± 0.03	n.s
Firmicutes	7.5 ± 5.38	5.42 ± 1.91	*
Gemmatimonadota	1.23 ± 0.69	1.22 ± 0.48	*
Halobacterota	3.51 ± 4.4	1.12 ± 1.5	*
Hydrogenedentes	0 ± 0	0 ± 0.01	n.s
Iainarchaeota	0.06 ± 0.19	0 ± 0	*
LCP-89	0.02 ± 0.03	0 ± 0.01	*
Latescibacterota	0.16 ± 0.13	0.12 ± 0.1	*
MBNT15	0.25 ± 0.22	0.15 ± 0.1	*
Methylomirabilota	0.06 ± 0.07	0.04 ± 0.04	*
Micrarchaeota	0.02 ± 0.08	0 ± 0	*
Myxococcota	1.16 ± 0.97	0.82 ± 0.44	*
NB1-j	0.62 ± 0.4	0.47 ± 0.22	*
Nanoarchaeota	1.15 ± 1.87	0.03 ± 0.04	*
Nitrospinota	0.02 ± 0.04	0.05 ± 0.07	*
Nitrospirota	2 ± 1.16	1.58 ± 0.66	*
Patescibacteria	1.35 ± 3.16	0.24 ± 0.27	*
Planctomycetota	0.03 ± 0.09	0.09 ± 0.22	*
Proteobacteria	46.2 ± 21.44	48.59 ± 14.12	*
SAR324_clade (Marine_group_B)	0.01 ± 0.02	0.04 ± 0.12	n.s
Spirochaetota	0.37 ± 0.39	0.18 ± 0.15	*
Sva0485	0.1 ± 0.1	0.01 ± 0.01	*
TA06	0.01 ± 0.02	0 ± 0	*
Thermoplasmatota	0.03 ± 0.04	0.01 ± 0.02	n.s
Verrucomicrobiota	1.19 ± 0.76	1.66 ± 1.07	*
WOR-1	0 ± 0.01	0 ± 0.01	n.s
WPS-2	0.05 ± 0.12	0 ± 0	n.s
WS4	0.01 ± 0.02	0 ± 0	n.s
Zixibacteria	0.18 ± 0.16	0.07 ± 0.05	*

Table A4.5. *Proportion of fold changes (FC) observed from CTRL to MFN, MET, TER, and MIX contamination types at different taxonomic levels. Fold changes with an exact value of 1, indicating the absence of taxa in both contaminant types and CTRL experiments, were excluded from the analysis. Proportions were adjusted by eliminating absent taxa.*

	Proportion (%) FC>1	Proportion (%) FC<1
Kingdom	38	63
Phylum	63	37
Class	63	37
Order	65	35
Family	65	35
Genus	63	38
Species	62	38
ASVs	61	39

Chapter 5.
Oxygen-dependent dynamics of metformin dissipation at the sediment-water interface and their effects on prokaryotic communities

The study presented in Chapter 4 examined the dissipation of three micropollutants, chemicals selected for study because of their varied uses and diverse physicochemical properties. This highlighted that the antidiabetic drug metformin was extensively biodegraded and did not accumulate at the sediment-water interface (SWI). Metformin thus emerges as a model compound of choice for comprehensive investigations into micropollutant biodegradation at the SWI and examination of combined chemical and physicochemical stresses relevant to aquatic ecosystems.

Given the widespread presence of metformin in rivers worldwide[46], continuous, chronic contamination by this pharmaceutical is likely to occur as a consequence of WWTP discharge. River ecosystems experience fluctuations in fluxes and nutrient inputs, which often result in significant variation of dissolved oxygen[213]. Previous studies emphasized metformin biodegradation under anoxic conditions[152,192,214], but corresponding studies remain limited. Rivers present large variations in oxygen concentrations, with potential impact on metformin transformation rates and pathways. Studies on other micropollutants, such as simazine[215], demonstrated increased dissipation upon changes between anoxic and oxic conditions. Examining the transformation of metformin under various oxygen regimes, e.g. constant oxic, anoxic, and alternating conditions, may thus improve our understanding of metformin transformation in aquatic ecosystems.

The response of SWI prokaryotic communities at the SWI to metformin demonstrated in Chapter 4 is likely to be modulated by changes in oxygen conditions. Indeed, literature on the effects of oxygen conditions on prokaryotic communities is extensive[216–218]. Nevertheless, little is yet known on the interactions between oxygen conditions and exposure to micropollutant and the combined effects of these factors on microbial communities in aquatic ecosystems. Using the model developed in Chapter 4, the study presented in Chapter 5 addresses the combined effects of metformin and oxygen conditions on the responses of prokaryotic communities at the SWI. The laboratory microcosm setup established in Chapter 4 was adapted for anoxic conditions, and metformin dissipation was monitored under both biotic and abiotic conditions and for different oxygen conditions following two successive events of metformin contamination. A thorough statistical analysis of 16S rRNA amplicon sequences was used to uncover the main factors responsible for the observed response of prokaryotic communities.

Our findings showed persistence of metformin under abiotic conditions. Under biotic conditions, metformin biodegradation occurred after a lag phase, with faster degradation under anoxic conditions. Guanylurea, the product of the recently reported metformin hydrolase-dependent bacterial pathway[92,219], was the dominant transformation product. Metformin and

oxygen conditions both affected prokaryotic communities, with their interaction yielding a predominantly additive effect. Observed changes in relative abundance of specific prokaryotic taxa allowed to tentatively identify potential taxonomic bioindicators of metformin exposure. Taken together, these results underscore the relevance of considering both environmental factors and prokaryotic communities in the evaluation of micropollutant transformation in aquatic settings. More generally, the approach presented in this study paves the way for more systematic studies of the combined effects of micropollutants and environmental factors, and in particular anoxia, on prokaryotic communities in various compartments of aquatic ecosystems including the sediment-water interface.

Chapter 5 presents an edited version of a manuscript to be submitted for publication to the journal Environmental Pollution.

Abstract

The major antidiabetic drug metformin is frequently detected in aquatic environments due to anthropic contamination by unmetabolized metformin and only partial subsequent removal by wastewater treatment. Here we examined the degradation and impact of metformin (17.6 µM) on prokaryotic communities in laboratory microcosms mimicking the sediment-water interface under different oxygen conditions, including alternance between oxic and anoxic conditions. Slow metformin dissipation and limited formation of transformation products were observed in abiotic experiments irrespectively of oxygen status. However, oxygenation and incubation time significantly affected the composition of prokaryotic communities under biotic conditions, with increasing effect of metformin upon repeated exposure. Metformin degradation was complete within less than 13 days after an initial lag up to 28 days. Guanylurea was detected transiently as the unique transformation product. This suggests that metformin was degraded through pathways involving metformin hydrolase yielding guanylurea and dimethylamine as a potential carbon source for microbial growth. Changes in procaryotic communities indicated that the combined effects of metformin exposure and oxygen levels were mainly additive. However, synergistic or antagonistic effects were also observed for some taxa, enabling the identification of potential bioindicators of metformin exposure under alternating oxygen conditions. Overall, this study underscores the importance of considering environmental factors, prokaryotic communities, and their interplay when evaluating pharmaceutical contamination and its effects at the sediment-water interface.

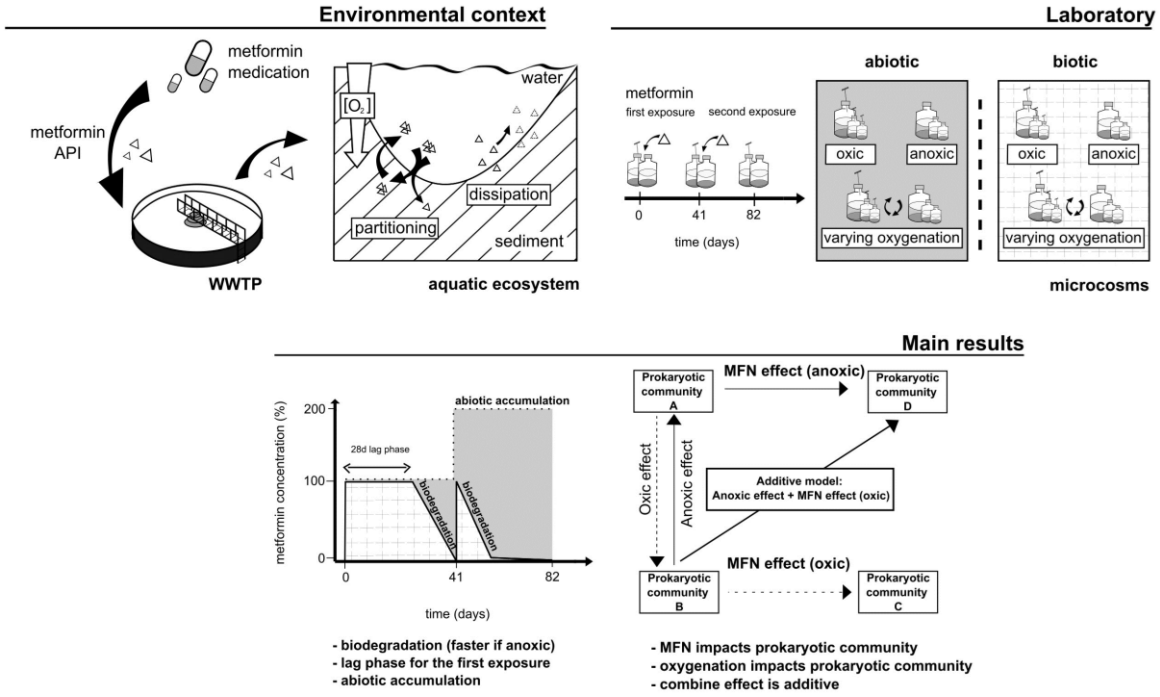

Keywords: Pharmaceuticals, metformin, sediment-water interface, oxygen conditions, microcosms, prokaryotic communities

5.1. Introduction

The commonly prescribed antidiabetic drug metformin is used as the mainstay treatment for type II diabetes[62]. Over 150 million people worldwide take metformin[220], with a minimal dose of 500 mg per day[221]. This represents a staggering consumption of over 27 million tons of metformin per year. Metformin shows promise in various therapeutic contexts beyond its established role in diabetes management, including for Parkinson, Alzheimer, and Huntington diseases, as well as for multiple sclerosis. This versatility suggests increased utilization in the future[62]. With only 55 ± 16% of ingested metformin undergoing metabolic transformation within the human body[222], a significant fraction of metformin is excreted in urine[223]. As a result, environmental contamination occurs due to unmetabolized metformin in human waste[224] and the low metformin removal efficiency of most wastewater treatment plants[224]. Globally, metformin already stands as the second most frequently detected and the third most concentrated active pharmaceutical ingredient in environmental compartments[46].

The ubiquity of metformin in surface water raises concerns as a potential endocrine disruptor[225], impacting fish at environmental concentrations[26], and modulating gene expression in aquatic organisms[226]. Metformin contamination of aquatic ecosystems will also impact the sediment-water interface (SWI), a biogeochemical hotspot crucial for the dissipation of micropollutants including pharmaceuticals[74,185]. The sediment-water interface is marked by redox variations, including at anoxic depths and oxic subsurface layers[152], which may affect the kinetics and pathways of metformin degradation. Metformin can be transformed by some bacteria[92,191,192,219], resulting in the formation of guanylurea and other degradation products[25]. However, knowledge on the transformation of metformin in aquatic ecosystems and its potential effect on organisms and biogeochemical functions remains limited.

In previous investigations with laboratory microcosms simulating sediment-water conditions, we observed that metformin affect prokaryotic community composition (Borreca *et al.*, under revision). However, the effect of oxygen conditions on metformin transformation at the SWI and associated prokaryotic communities remains unexplored. Various studies have established that prokaryotic communities can acclimate to environmental contamination[153] and that this response may depend on oxygen conditions[216–218]. Changes in oxygen levels have been shown to alter the biodegradation of organic micropollutants in different ways[215,227].

We hypothesized that metformin exposure and oxygen conditions affect the modes and kinetics of metformin dissipation and the composition of prokaryotic communities at the sediment-water interface. To investigate this hypothesis, we designed laboratory microcosms mimicking this key compartment of aquatic ecosystems to investigate exposure to metformin and its transformation in both water and sediment under different regimes of oxygenation, and associated changes in prokaryotic community composition using 16S rRNA metabarcoding analysis.

5.2. Materials and methods

5.2.1. Experimental sediments and laboratory microcosms

To assess the impact on microbial communities, microcosms were established employing the Souffel sediment (Chapter 3, Section 4.1). The establishment of microcosms adhered to the protocols detailed in Chapter 3, Section 1.

A total of 252 microcosms containing metformin (MFN) were established under oxic and anoxic conditions (Table 5.1). All conditions were investigated with triplicate microcosms. Half of the microcosms represented biotic conditions. The other half represented abiotic (autoclaved) conditions to examine abiotic metformin dissipation. Water and sediment phases of abiotic microcosms were independently sterilized by autoclaving three times at 24 h intervals. Control (CTRL) microcosms were also set up under biotic conditions but without metformin to assess the effect of metformin on prokaryotic communities (Table 5.1).

An initial one-week pre-incubation phase was implemented to ensure stable partitioning of ions, nutrients, and particles in the microcosms[161]. Following pre-incubation, microcosms underwent two successive spiking events, defining two successive experimental phases. On day 0, microcosms were spiked with either sterile milliQ water (CTRL) or metformin (MFN) at a concentration of 17.6 µM in the aqueous phase. Microcosms were then incubated for 41 days. Subsequently, microcosms previously spiked with metformin were spiked a second time with metformin to simulate successive events of metformin exposure in the environment and incubated for an additional 41 days. After the first metformin pulse, microcosms were incubated under oxic (O) or anoxic (A) conditions. After the second metformin pulse, microcosms were transitioned from oxic to anoxic (OA) or from anoxic to oxic (AO) status, or maintained in their original oxygenation status, i.e. oxic (OO) or anoxic (AA) (Table 5.1). Sampling was conducted by a sacrificial approach on days 0, 7, 15, 21, 28, 35, and 41 during both phases for analysis of metformin and its transformation products (TPs).

Table 5.1. *Microcosm experiment setup. The experiments included the spiking of either metformin (MFN) or water (CTRL), exposing them to oxic and anoxic conditions, under both abiotic and biotic conditions. The number of microcosms for each condition is specified in parentheses (biotic/abiotic).*

Phase	Spiking	Initial oxygen condition	Final oxygen condition	Sterility
1	MFN	Anoxic (21/21)	-	Abiotic and Biotic
		Oxic (21/21)	-	
	CTRL	Anoxic (21)	-	Biotic only
		Oxic (21)	-	
2	MFN	Anoxic	Anoxic (21/21)	Abiotic and Biotic
		Anoxic	Oxic (21/21)	
		Oxic	Oxic (21/21)	
		Oxic	Anoxic (21/21)	
	CTRL	Anoxic	Anoxic (21)	Biotic only
		Anoxic	Oxic (21)	
		Oxic	Oxic (21)	
		Oxic	Anoxic (21)	

5.2.2. Chemical analysis

5.2.2.1. Biogeochemistry

Dissolved dioxygen concentration was monitored *in situ* with non-invasive sensor spots (PreSens, Unisense) in all experiments. Total organic carbon (TOC) and dissolved organic carbon (DOC) were analyzed using a TOC analyzer (TOC-V-CPH Shimadzu, NF EN 1484). Major ions (NH_4^+, Na^+, K^+, Mg^{2+}, Ca^{2+}, Cl^-, NO_3^-, SO_4^{2-}, PO_4^{3-}) were quantified by ion chromatography (Dionex ICS-5000, Thermo Scientific). Water pH was also monitored routinely (Table A5.1).

5.2.2.2. Extraction and quantification of micropollutants

Metformin and its transformation products (TPs, Table 3.4) were directly analysed from the water phase. Previous laboratory experiments had shown negligible (<1%) partitioning of metformin in the sediment (Table 3.3). Quantification methods and limits of detection and quantification are provided in Chapter 3, part 5.2 and Table 3.4. Evaluation of micropollutant dissipation is conducted following procedures described in Chapter 3, Section 8.1.

5.2.3. Prokaryotic composition analysis

5.2.3.1. DNA extraction and sequencing

Environmental DNA was extracted from sediment and water using the DNeasy PowerSoil kit (Qiagen) according to the manufacturer's instructions. DNA extraction was performed on day 0 and day 41 during the initial experimental phase. In the second experimental phase, sampling collection was adapted since the residual concentration of metformin felt below 10% at different rates in different microcosms. Specifically, samples were collected on day 15 in anoxic experiments, on day 21 in experiments transitioning from anoxic to oxic, and on day 28 for experiments under steady oxic conditions and those shifting from oxic to anoxic conditions. DNA concentrations (average 19 ng μL^{-1}, maximum 360 ng μL^{-1}) were determined by fluorometry using Qubit® dsDNA HS and BR kits (Thermofisher Scientific). DNA preparations were stored at −20°C. Amplicon sequencing and processing.

Amplicon sequencing follow procedures described in Chapter 3, part 6.1. Obtained sequences were clustered at 100% identity, yielding a total of 39,542 Amplicon Sequence Variants (ASVs). Each ASV was annotated by applying QIIME2's classify-sklearn algorithm on the Silva database (version 138, December 2019). Good's coverage values indicated that sequencing depth exceeded 97.7% (average 97.8. ± 0.3 %). Sequencing data were obtained predominantly in triplicate and duplicate for water samples, and in unicate for sediment samples (Table A5.2). Amplicon sequence variants absent in at least two of triplicate samples within a given condition were excluded from the analysis. After filtering, the sediment and water datasets retained 12,106 and 4,643 ASVs, respectively. Combining these datasets resulted in a total of 13,739 ASVs, with 1,633 ASVs shared between sediment and water samples. Unassigned ASVs were grouped by affiliation to the most precise taxonomic level available. Sample rarefaction curves for Chao1 and Simpson indices (data not shown) suggested that sequencing depth was sufficient to capture prokaryotic diversity in all samples.

5.2.3.2. Data analysis

The obtained sequence dataset (Table A5.2) was analysed in R (version 4.3.1). Richness metrics (observed, Chao1, ACE), evenness indices (Camargo, Pielou, Simpson), and diversity measures (Shannon and Simpson) were computed. Bray-Curtis matrices and dendrograms were generated employing the 'phyloseq' package. Analyses of similarities (NPMANOVA) were conducted with the 'adonis2' package. Linear discriminant analysis Effect Size (LEfSe) was conducted with the 'lefser' package[179].

The presence of genes encoding enzymes putatively involved in the degradation of metformin, guanylurea, and caffeine as an N-methylated compound like metformin[228] was assessed with BLAST[229], using the megablast algortithm with gene sequences of identified biomarkers, using filtering on specific taxa of interest if and as required. Targeted reference gene sequences included: i) metformin hydrolase genes: *mfmA* and *mfmB* from *Pseudomonas mendocina* sp. MET-2 (NCBI, accession no. WP_254300333.1 and WP_254300332.1)[219], as well as the gene encoding metformin hydrolase in *Aminobacter niigataensis* MD1 (WP_318762986.1)[92]; ii) guanylurea hydrolase gene, *GuuH,* from *Pseudomonas mendocina* GU (MBF8163004.1)[25]; iii) *NdmA* gene encoding the methylxanthine N1-demethylase from *Pseudomonas putida* CBB5 (H9N289)[228].

Taxon-level mean fold change (FC) in relative abundance were calculated for each sample spiked with metformin relative to its corresponding control (CTRL), i.e., the non-spiked sample for the same matrix and timepoint as the sample of interest at all taxonomic levels according to eq. (4). A correction was applied, involving the addition of 0.001 to both the numerator (n) and denominator (d) (eq. (4)), to prevent division by zero. If a taxon showed one null abundance measurement in the three replicates of a given sample, the sample was treated as a duplicate for that taxon.

$$FC_{taxon,sample} = \left(\frac{mean_{(taxon,sample)}+0.001}{mean_{(taxon,control)}+0.001}\right) = \frac{n}{d} \; ; n = d * FC_{taxon,sample} \quad \text{Eq. 1}$$

A positive FC indicates an increase in relative abundance of a particular taxon when compared to the control condition. Log_{10} FC heatmaps were obtained after logarithmic transformation of FC values using “dplyr”, “tidyr”, “phyloseq”, “tibble”, and “heatmapply” packages.

The effect of different stressors on prokaryotic communities was assessed by comparison to corresponding control (CTRL) experiments. For example, the effect of metformin exposure (*MFN effect*) under oxic conditions was determined by the fold change observed relative to the CTRL experiment under oxic conditions (equation (2a)). The effect of anoxia (*Anoxic effect*) was determined by the FC observed from oxic to anoxic communities in CTRL experiments (equation (2b)). We assumed that the observed effect on the prokaryotic community exposed to metformin (MFN) under anoxic conditions relative to the non-spiked (CTRL) under oxic conditions (2c) results from the combined effects of MFN exposure and anoxia (equation (2d)).

$$MFN\ effect = \left(\frac{mean_{(taxon,Oxic_{MFN})}+0.001}{mean_{(taxon,Oxic_{CTRL})}+0.001}\right) \quad \text{Eq. 2a}$$

$$Anoxic\ effect = \left(\frac{mean_{(taxon,Anoxic_{CTRL})}+0.001}{mean_{(taxon,Oxic_{CTRL})}+0.001}\right) \quad \text{Eq. 2b}$$

$$Effect\ of\ MFN\ and\ anoxia_{observed} = \left(\frac{mean_{(taxon,Anoxic_{MFN})}+0.001}{mean_{(taxon,Oxic_{CTRL})}+0.001}\right) \quad \text{Eq. 2b}$$

$$Effect\ of\ MFN\ and\ anoxia_{theoretical} = MFN\ effect + Anoxic\ effect$$

$$= \left(\frac{mean(_{taxon,Oxic_{MFN}}) + 0.001}{mean(_{taxon,Oxic_{CTRL}}) + 0.001}\right) + \left(\frac{mean(_{taxon,Anoxic_{CTRL}}) + 0.001}{mean(_{taxon,Oxic_{CTRL}}) + 0.001}\right)$$

Eq. 2d

The potential occurrence of different types of interactions between stressors, i.e., additivity, antagonism, and synergism, was also examined. Fold Change (FC) values were converted according to equation (3) into *Interaction Coefficient* (IC) values to assess the change in relative abundance of a taxon from the control to the sample:

$$IC_{taxon,sample} = \left(\frac{n-d}{d}\right) = \left(\frac{d*FC_{taxon,sample}-d}{d}\right) = FC_{taxon,sample} - 1$$ Eq. 3

To evaluate the sum of stressors effects, the sum of IC values obtained for individual stressors was defined as $IC_{taxon,ADD}$, Eq. (4).

$$IC_{taxon,ADD} = IC_{taxon,sample_{MFN\ effect}} + IC_{taxon,sample_{Anoxic\ effect}}$$

Eq. 4

$IC_{taxon,ADD}$ values were constrained to a minimum value of -1, denoting the absence of the considered taxon in samples associated with MFN and anoxia effects, namely $Oxic_{MFN}$ and $Anoxic_{CTRL}$ (i.e., numerator in Eq. (2d)) Eq. (5).

$$If\ IC_{taxon,ADD} = \sum_{k=1}^{2}\left(IC_{taxon,sample_k}\right) = IC_{taxon,ADD} < (-1);\ IC_{taxon,ADD} = (-1)$$

Eq. 5

$IC_{taxon,ADD}$ values were then compared for each taxon with IC values of the corresponding experiment with metformin under anoxic conditions (IC_{OBS}). A conservative uncertainty of ±80 on IC values was set basing on the third quartile (Q3) of ASV relative abundances from replicate experiments. Thus, when IC_{OBS} ± 80 for a given taxon overlapped with IC_{ADD} ± 80, the interaction effect between MFN and anoxia stressors was considered additive. However, when IC_{OBS} ± 80 exceeded IC_{ADD} ± 80, interaction was considered synergistic. In contrast, when IC_{MIX} ± 80 was smaller than IC_{ADD} ± 80, interaction was classified as antagonistic. Two aggregated cases were distinguished in the antagonistic category, "repressing" when $IC_{OBS} < IC_{ADD}$, and "opposing" when IC_{OBS} and IC_{ADD} were of opposite sign, i.e., positive in IC_{ADD} and negative in IC_{OBS}, or the reverse.

The contribution of individual stressors to the additive model at the Phylum and ASV levels was evaluated based on the proportion of taxa exhibiting the least difference between the observed FC scores of the two stressors, *MFN exposure* (2.a) and *anoxia* (2.b) with the *MFN and anoxia* (2.c).

Statistical tests for significance ($p \leq 0.05$), including NPMANOVA, Wilcoxon, Dunn with Benjamini-Hochberg adjustment, Kruskal-Wallis, and the computation of confidence intervals, were conducted as required. For multiple comparisons, clusters were defined as samples sharing a specific set of variables. Application of the Benjamini-Hochberg correction and setting the significance level to 0.05 or lower allowed to maintain a controlled type I error rate, α, i.e., the probability of mistaken rejection of a null hypothesis that is actually true.

5.3. Results and discussion

Our laboratory microcosm study was designed to investigate metformin dissipation and the response of prokaryotic communities under varying oxic and anoxic conditions at the sediment-water interface, under otherwise controlled conditions. Initially, microcosms spiked with metformin were maintained under either oxic or anoxic conditions for 41 days. Subsequently, a second metformin spike was performed, and oxygenation conditions were kept constant or modified, i.e., from oxic to anoxic, and from anoxic to oxic.

Targeted oxygen conditions, i.e., oxic (>8 ppm of O_2), and anoxic (< 0.1 ppm of O_2) conditions were maintained in all microcosms as required over the entire duration of the experiment. Physicochemical parameters including pH, conductivity, and the concentration of major elements (NH_4^+; Na^+; K^+; Mg^{2+}; Ca^{2+}; Cl^-; NO_3^-; SO_4^{2-}; PO_4^{3-}), remained stable over the 82 days of the experiments (Table A5.2).

5.3.1. Metformin degradation under abiotic and biotic conditions

Metformin degradation kinetics varied widely across abiotic and biotic conditions, as well as under oxic and anoxic conditions. Metformin persisted under abiotic conditions regardless of oxygen levels. Metformin biodegradation, however, started after a lag period of variable duration, and was faster under most anoxic conditions. Guanylurea was identified as the main transformation product and detected only under biotic conditions.

Metformin may accumulate in environments characterised by low microbial activity, such as aquifers, regardless of oxygenation conditions[43]. Under abiotic conditions, metformin demonstrated persistence following the initial contamination event, and accumulation after repeated contamination, irrespective of oxygenation conditions (Fig. 5.1A). Following the first contamination, metformin exhibited moderate dissipation, compared to 90% dissipation after 41 days under biotic conditions (see Fig. 5.1B), resulting in its accumulation in the sediment. This indicates the potential formation of less-extractable metformin residues within the sediment under abiotic conditions[189], in agreement with prior research documenting metformin sorption to solid media in wastewater treatment plant (WWTP) sludge[152].

In contrast, metformin dissipation was readily observed under biotic conditions regardless of oxygenation levels. DT_{50} values ranged from 2 to 7 days under biotic conditions, with slightly but significant higher dissipation rates observed under anoxic conditions (Fig. 5.1C). This rapid dissipation followed an initial lag phase of 28 days (Table 5.2). This suggests microbial

acclimation to metformin as a novel carbon and energy source[230], as a prerequisite for efficient metformin removal[214]. Metformin is likely a secondary carbon and energy source in our experiments, used when other carbon sources become scarce or less available. Supporting this idea, a latency phase was not observed after a second contamination event.

***Table 5.2**. Identification of a lag-phase before metformin degradation. Identification is based on the mean biotic degradation (Dbiotic) and its standard error (SD), the statistical analysis through Dunn test and the significance of successive linear regression models for different subset periods.*

Oxygenation type	Dbiotic system (%) ± SD	Time (days)	Dunn Test	linear regression model on subset periods (days)	linear regression model significance	Phases of dissipation
Oxic	0 ± 21	1	a	-	-	Lag-phase
	-17 ± 18	7	a	[1-7]	n.s	
	21 ± 21	15	a	[1-15]	n.s	
	31 ± 56	21	a	[1-21]	n.s	
	61 ± 0 (n=1)	28	ab	[1-28]	n.s	
	64 ± 22	34	bc	[1-34]	0.02	Dissipation
	94 ± 0	41	c	[1-41]	0.01	
Anoxic	0 ± 28	1	a	-	-	Lag-phase
	31 ± 12	7	a	[1-7]	n.s	
	41 ± 4	15	a	[1-15]	n.s	
	47 ± 13	21	a	[1-21]	0.03	
	31 ± 6	28	a	[1-28]	n.s	
	78 ± 24	34	b	[1-34]	< 0.01	Dissipation
	97 ± 0	41	b	[1-41]	< 0.01	

Metformin dissipation at the sediment-water interface is known to result from a combination of non-degradative processes such as sorption[189], as well as abiotic and biotic degradative processes[193] leading to the formation of various metformin transformation products (TPs) (Fig. 5.1D). Guanylurea has long been identified as the major microbial TP of metformin, as confirmed by recent studies of metformin-degrading strains[92]. Metformin transformation to guanylurea may also be indirect, as observed for *Pseudomonas medocina* MET, which first degrades metformin to 1-N-methylbiguanide[191]. In our experiments, guanylurea was consistently and temporarily identified under biotic conditions across all experiments. The temporary detection of guanylurea indicates microbial degradation of guanylurea involving the reported guanylurea hydrolase pathway[25]. In contrast, no TPs were observed in our abiotic experiments, suggesting non-degradative processes predominantly involving sorption under these conditions (Fig. 5.1C).

Evidence for metformin degradation under anoxic conditions was already reported[152,190,191]. In our experiments, metformin biodegradation was significantly faster under anoxic conditions (Fig 5.1). The DT_{50} values of metformin across conditions followed from anoxic to oxic conditions as follows: Anoxic (first event) and Anoxic (second event) > Oxic (first

event) and Anoxic (second event) > Oxic or Anoxic (first event) and Oxic (second event) (Fig. 1C). Previous investigations documented metformin biodegradation under both oxic conditions[152,192,214] and anoxic conditions [190,191,214]. Our results diverge from those of two prior investigations, which suggested that MFN degradation under anoxic conditions was up to 50% slower compared to oxic conditions[190,212]. However, these previous studies documented oxygen concentrations in excess of 0.5 mg L^{-1} in the condition with limited oxygen[152], or low oxygen levels monitored solely through resazurin[190], suggesting that conditions may actually have been oxic/micro-oxic in these experiments. In contrast, our experimental set-up consistently maintained oxygen concentrations exceeding 8 mg L^{-1} and below 0.5 mg L^{-1} under aerobic and anaerobic conditions, respectively. Faster biodegradation of metformin under anoxic conditions may be due to efficient energy metabolism potentially enhancing cometabolic metformin biodegradation. Consistent with this hypothesis, earlier investigations demonstrated that anaerobic metformin degradation was enhanced in the presence of readily degradable organic compounds[214].

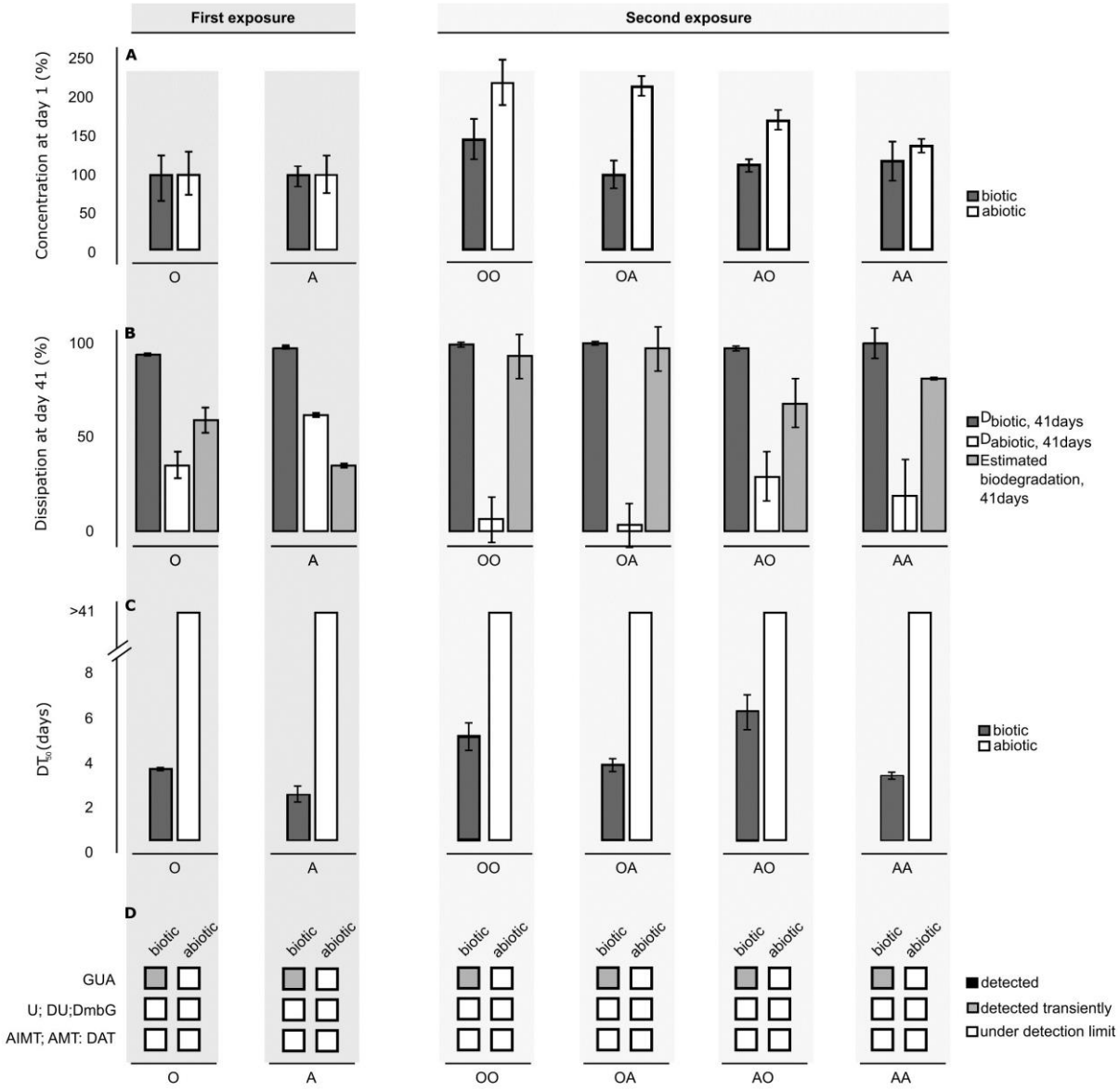

Figure 5.1. *Metformin dissipation in SWI microcosms. Data obtained 41 days after two successive metformin contamination events are shown. (Panel A) Oxygen regimes were oxic (O), and anoxic (A) in the first experimental phase; and oxic to anoxic shift (OA), from anoxic to oxic (AO), and steady state oxic (OO) and anoxic (AA) in the second experimental phase. (Panel B) Biotic and abiotic dissipation (%) of metformin and biodegradation estimates (Eq. 1 of section 3.8.1). (Panel C) Metformin half-life (DT_{50}) and associated confidence interval (CI 95%). DT_{50} values exceeding the duration of the experiment were set at >41 days. (Panel D) Formation of metformin transformation products guanylurea (GUA), urea (U), dimethylurea (DU), dimethylbiguanide (DmbG), 2-amino-4-methylamino-1,3,5-triazine (AMT), and 4-amino-2-imino-1-methyl-1,2-dihydro-1,3,5-triazine (AIMT).*

5.3.2. Determinants of prokaryotic communities at the sediment- water interface

Both successive spikes of metformin and variations in oxygen conditions influenced the kinetics of metformin degradation. Hence, the response of prokaryotic communities across these conditions and their potential role in metformin degradation was of interest. Matrix composition (i.e., sediment and water), experiment duration, and oxygen conditions were primary determinants of prokaryotic community change, as highlighted by multidimensional scaling (NMDS) (Fig. 5.2), and non-parametric multivariate analysis of variance (NPMANOVA). Metformin exposure was identified as a secondary determinant and led to significant changes in prokaryotic communities at the end of the experiment. Notably, the effect of metformin was dependent on oxygen conditions, as the effects of oxic and anoxic conditions on prokaryotic communities significantly diverged over time (Fig. 2).

Significant differences in prokaryotic community between sediment and water phases were also noted (NPMANOVA, $R^2 = 0.25$, $p < 0.0001$). Sediment samples displayed higher richness, evenness, and diversity metrics in comparison to water samples ($p < 0.001$; data not shown). These findings are consistent with previous observations of distinct structural and diversity patterns between sedimentary and planktonic bacterial communities[218,231]. Such disparities may reflect variations in nutrient availability, organic substrates, and metformin concentrations within sediment and water phases at the interface[218,231]. Considering NPMANOVA analysis revealed distinct communities between sediment and water phases, we examine the prokaryotic communities in the sediment and water compartments separately.

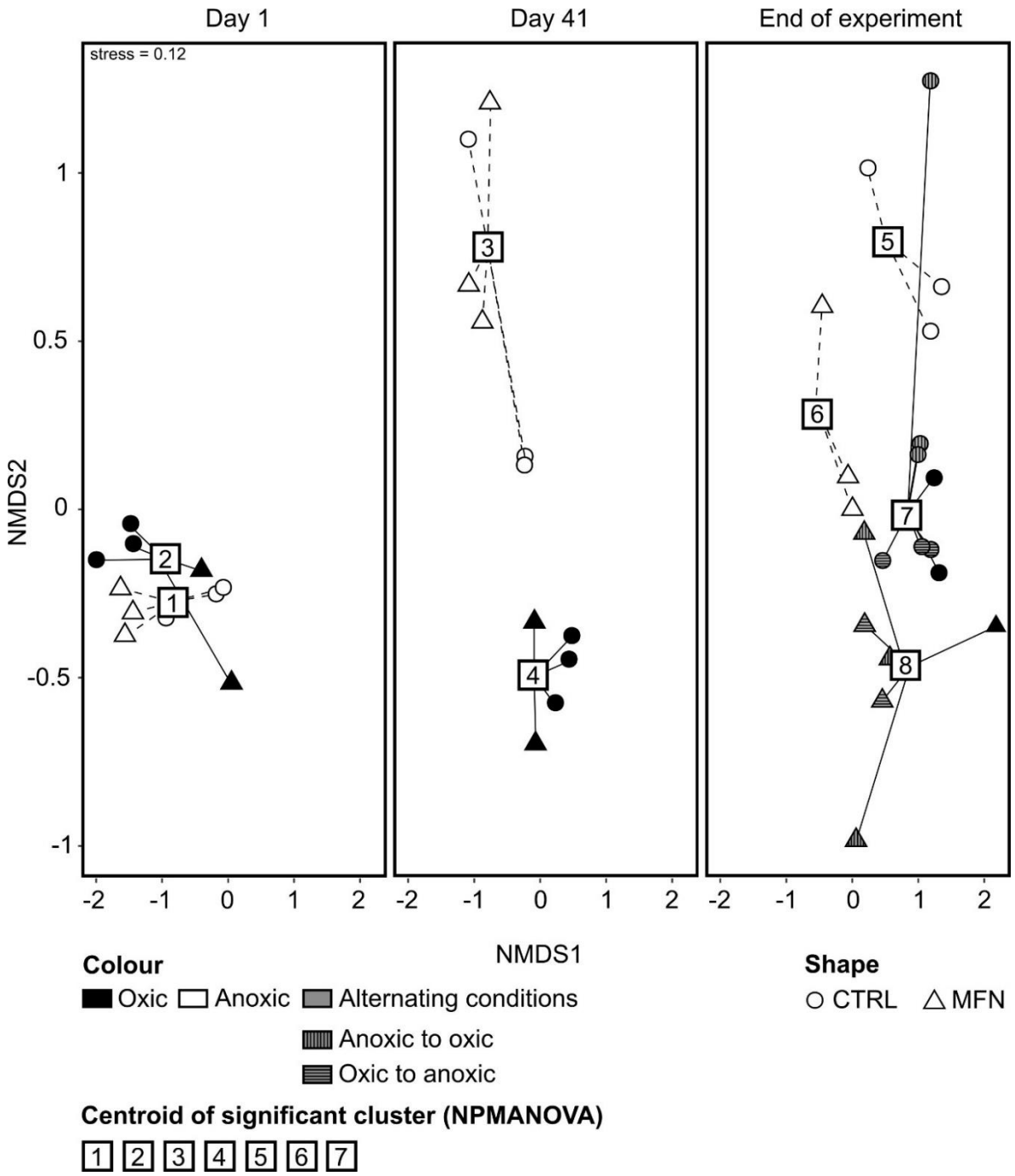

Figure 5.2. *Non-metric multidimensional scaling (NMDS) ordination of prokaryotic communities based on Bray-Curtis dissimilarity distances. NMDS is partitioned into three panels: day 1, day 41 of the first experimental phase, and at the end of the second period of the experiment. Stress was 0.12. Shapes indicate the following conditions: metformin-exposed MFN (triangles) and not exposed CTRL (circles) under anoxic (white), oxic (black), anoxic to oxic (grey horizontal cross-hatching) and oxic to anoxic (grey vertical cross-hatching). Numbered squares indicate centroids of significant NPMANOVA clusters: anoxic experiments (1), oxic experiments (2), anoxic experiments (3), oxic experiments (4), steady anoxic in CTRL experiments (5), steady anoxic in MFN experiments (6), 'subjected to oxygen once' in CTRL experiments (7), 'subjected to oxygen once' in MFN experiments (8).*

Analysis of sediment samples showed significant effects of incubation time (R^2 = 0.128; p = 0.0496) and oxygenation (R^2 = 0.112; p = 0.0276) on prokaryotic communities, with no discernible effect of metformin contamination (R^2 = 0.045; p = 0.3844). Richness, evenness, and diversity metrics indicated non-significant changes in response to variations in incubation time, oxygenation, and metformin exposure (data not shown). Although the lack of significant effect of metformin could indicate a genuine absence of effect, it could also be related to size heterogeneity in sediment samples predominantly consisting of singleton and duplicate samples (Table A5.2). Moreover, the complexity of the sediment matrix may confound the effect of other variables such as time, oxygen conditions, and metformin exposure.

In contrast, prokaryotic communities in the water phase showed significant sensitivity to incubation time, oxygen conditions, and metformin exposure (Table 5.3). Additional analyses (Table 5.4) indicated that the oxygenation level significantly altered prokaryotic communities in the water phase. The effect of metformin exposure on prokaryotic communities, however, was discernible only at the end of the experiment (Fig. 5.2 and Table 5.4). This suggests that the water prokaryotic community may not be significantly affected by a single/unique event of metformin exposure. Alternatively, changes induced by metformin exposure may remain below the threshold of statistical significance. This would be in line with previous studies demonstrating that successive contamination events first alter prokaryotic communities through a stochastic process, followed by subsequent events leading to community adaptation to the contaminant[232].

Table 5.3. *Non-parametric multivariate analysis of variance (NPMANOVA) of prokaryotic communities in water microcosms. The analysis accounted for the main experimental factors: time (t1/t2/t3), MFN contamination (CTRL vs MFN) and oxygenation (O. A. AO. OA. OO. AA). and their interaction in the model. Accounting for all samples. Time points indicate the start of the experiment (t1). the beginning of the second round of contamination (t2). or when metformin was fully dissipated after a second round (t3).*

NPMANOVA

	Factors	Degree of freedom	Sum of Squares	R^2	F-statistic	p-value	Significance
	Time (1)	2	2.5783	0.17854	5.6742	0.0001	***
	MFN (2)	1	0.6161	0.04266	2.7119	0.0009	***
	Oxygenation (3)	4	1.7891	0.12389	1.9687	0.0001	***
Interactions	(1) : (2)	2	1.0071	0.06974	2.2164	0.0001	***
	(1) : (3)	1	0.4271	0.02958	1.8800	0.0129	*
	(2) : (3)	4	1.7068	0.11819	1.8781	0.0001	***
	(1) : (2) : (3)	1	0.4095	0.02835	1.8023	0.0137	*
	Residual	26	5.9071	0.40905			
	Total	41	14.4412	1.0000			

Table 5.4. *Non-parametric multivariate analysis of variance (NPMANOVA) of prokaryotic communities in water microcosms. Comparison of the effect of effect of metformin contamination (1), oxygenation (2), and their interaction (1) : (2) at each time point in water samples (t1, t2, t3). P-value ≤ 0.05 (*); ≤ 0.01(**); ≤ 0.001(***). Time points indicate the start of the experiment (t1), the beginning of the second round of contamination (t2), or when metformin was fully dissipated after a second round (t3).*

	Factors	Degree of freedom	Sum of Squares	R^2	F-statistic	p-value	Significance
Day 1	MFN (1)	1	0.313	0.1336	1.9304	0.0515	n.s
	Oxygenation (2)	1	0.3236	0.1381	1.9958	0.0425	*
	(1) : (2)	1	0.5715	0.2439	3.5245	0.0001	***
Day 41	MFN (1)	1	0.4469	0.1414	1.6907	0.0724	n.s
	Oxygenation (2)	1	0.573	0.1813	2.1675	0.0347	*
	(1) : (2)	1	0.2895	0.0916	1.0952	0.3059	n.s
End of experiment	MFN (1)	1	0.8816	0.1386	3.621	0.0001	***
	Oxygenation (2)	3	1.3013	0.2046	1.7817	0.0012	**
	(1) : (2)	3	1.2552	0.1974	1.7185	0.0016	**

Overall, however, prokaryotic communities in the water phase at the end of the experiment did not significantly change (Table A5.3, *p* corrected by fdr > 0.5). Again, this may be attributed to limited statistical power resulting from duplicate and singleton samples (Table A5.2). To further explore the response of prokaryotic communities to different oxygen conditions, we assessed whether community alterations were primarily affected by (i) initial oxygen condition, (ii) final oxygen conditions, or (iii) exposure to oxygen at least once. Considering metformin exposure, the NPMANOVA model highlighted that community changes following at least one exposure to oxic conditions had the highest explanatory power (R^2= 0.080; p=0.034). In contrast, the other two hypotheses showed lower explanatory power and non-significant results ((i): R^2=0.062; p=0.150; (ii): R^2=0.067; p=0.096). This suggests a persistent effect of oxygen on prokaryotic communities in the water phase, wherein community alterations occur in response to the oxygen conditions encountered, in agreement with previous studies (e.g., Aldunate et al., 2018). The observed changes in prokaryotic community composition may predominantly correspond to shifts in terminal electron acceptor utilisation[233].

We further investigated the main factors affecting alpha-diversity of prokaryotic communities in the water phase employing measures of richness (ACE, Observed, Chao1) and evenness (Pielou's evenness, Simpson's evenness, Camargo's evenness) alongside diversity indices (Simpson, Shannon). Overall, richness, evenness, and diversity indices increased significantly over time ($p < 0.05$; data not shown). This increase was associated with a notable decline (from 71 ± 9% at day 1 to 46 ± 16% at the end of the experiment; Kruskal-Wallis, $p < 0.05$) in the relative abundance of Proteobacteria. In contrast, changes in oxygen availability or exposure to metformin did not affect alpha-diversity (n.s; data not shown).

5.3.3. Interplay between oxygen and metformin exposure on prokaryotic communities

We investigated the potential interplay between oxygen regime and metformin exposure in the observed impact on prokaryotic communities (Fig. 5.3A) in more detail. In order to do this, observed fold change (FC) values were converted to *Interaction Coefficient* (IC) (see Section 2.5.3) to evaluate the potential additivity of metformin and oxygen effects on prokaryotic communities. Specifically, we compared the steady-state anoxic experiment ('AA') with the experiment involving a transition from anoxic to oxic conditions ('AO'), which included triplicates under both metformin (MFN) and control (CTRL) conditions, at the final timepoint (Table A5.2). The theoretical model presented in figure 5.3.A allowed for various comparisons. However, only the mentioned conditions presented triplicates, which ensured a statistically more robust analysis.

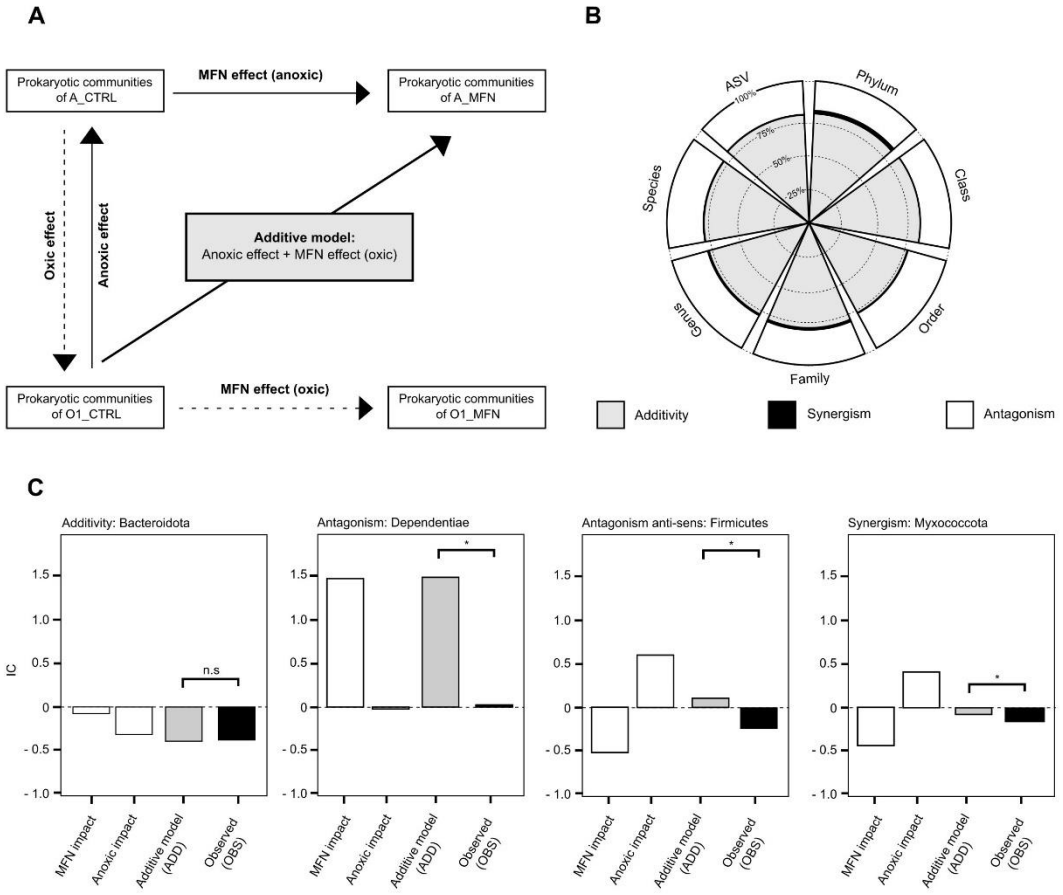

Figure 5.3. *Analysis of the potential interplay between oxygen and metformin exposure on prokaryotic communities. A. Model of interactions between effects of anoxia and metformin exposure in the water phase of microcosms experiments. B. Distribution of interaction types (Additivity, Synergism, Antagonism) from Phylum to ASV levels. C. Example of interactions at the Phylum level. The Additive model (ADD) represents the sum of Interaction Coefficient (ICs) which was compared with the observed IC (OBS) of metformin-contaminated experiments under anoxic conditions.*

Analysis of potential interaction effects indicated that additivity prevailed, representing 72-78% of the observed cases depending on the taxonomic level (Fig. 3B). Antagonism also seemed to play a significant role and predicted to account for 22-28% of interactions. Synergism, on the other hand, was the least frequently predicted interaction type, observed in only 0-2% of cases. This pattern of interaction effects remained consistent across taxonomic levels (Fig. 5.3B). Interactive effects were analysed for four phyla (Fig. 5.3C and Table A5.4), as representative examples of the different types of interaction. Notably, the interaction between metformin and anoxia exhibited an additive effect on Bacteroidota. Specifically, the sum of individual Interaction Coefficient (IC) values for anoxia and metformin exposure (IC_{ADD} = −0.41 ± 0.32) did not significantly differ from that observed in metformin experiments under anoxic conditions (IC_{OBS} = −0.38 ± 0.30). In contrast, IC values revealed antagonistic interactions, either repressive or opposition, in the case of Dependentiae (IC_{OBS} = 2.67 ± 2.13 and IC_{ADD} = 83.7 ± 66.2) and Firmicutes (IC_{ADD} = 0.06 ± 0.05 and IC_{OBS} = −0.26 ± 0.20). The interaction for Myxococcota featured synergism, with a significantly higher observed IC (IC_{OBS} = −0.19 ± 0.15) than the additive model (IC_{ADD} = −0.02 ± 0.01).

Worthy of note, metformin exposure contributed the most (54% to 62% of cases) to the additive model across all taxonomic levels (data not shown). This suggests that even though oxygen levels might interact with how metformin affects microbes, the presence of metformin itself has a more substantial and possibly direct effect. Indeed, its presence introduces a novel carbon source and potential stressor that prokaryotic communities need to adapt to, possibly affecting their growth and survival. In contrast, river sediments frequently experience hypoxic and sub-oxic conditions[234,235]. Prokaryotic communities might thus be accustomed to such fluctuations and developed mechanisms to cope with them. In contrast, metformin exposure represents a new and potentially acute stressor[236].

Dual stressors such as here oxygenation and contaminant exposure have received substantial attention. Yet specific studies on aquatic microbial ecosystems are still rare, preventing extensive comparisons with our study. Variations in interactive effects of dual stressors depend on multiple factors including the taxa and variables such as life stage, genotype, duration, frequency, and level of exposure, as well as the number of successively exposed generations of aquatic organisms[237]. Investigations of interactive effects of abiotic stressors on prokaryotic communities, e.g. heatwaves and micropollutants[238], or salinity and micropollutants[239], have reported inconclusive global trends including antagonistic, additive[240–242], or synergistic effects [241,243]. Models of the interactive effects of multiple stressors have emphasized the prevalence of antagonistic and additive interactions[244], with synergies emerging particularly under higher stress conditions. In the present study, however, metformin clearly exerted a low-magnitude stress. Consequently, synergistic effects of metformin with other factors may require more sustained and elevated levels of metformin exposure than those commonly observed in environmental settings.

5.3.4. Bioindicators of metformin exposure at the sediment-water interface

Building on our analysis of community composition dynamics, we endeavoured to identify taxonomic bioindicators for metformin exposure which would take the confounding factor of alternating oxygenation levels into account. A bioindicator may be defined as a species or group of species that readily indicates environmental changes[245]. Monitoring their presence in the environment allows for quantitative and qualitative assessment of the ecosystem's health[246]. In this way, 24 candidates for microbial bioindicators of metformin exposure were initially identified across various oxygen conditions through LEfSe analysis of metformin-spiked versus control samples (1, 1, 3, 5, 6, and 8 in descending taxonomic order of Phylum, Class, Order, Family, Genus, Species, respectively; Table A5.5). These potential bioindicators were distributed across 10 taxonomically related groups, so that some were taxonomically related, e.g. Solibacterales (Table A5.5). The increase in relative abundance in the presence of metformin was examined based on the log10 fold change (FC) values of 'O1' and 'AA' groups (Fig. 5.4B). Treatments with individual stressors (i.e., OO, OA, and AO) alone are present as triplicates and duplicates, result of further Wilcoxon test could suffer from its associated loss in power. Hence aggregation was considered. Although the log10 FC values of the 24 candidate bioindicators were higher in the metformin than in the control experiment (Fig. 5.4C), the increase was significant ($p < 0.1$) for only 17 taxa. These taxa were consequently regarded as relevant indicators of metformin exposure.

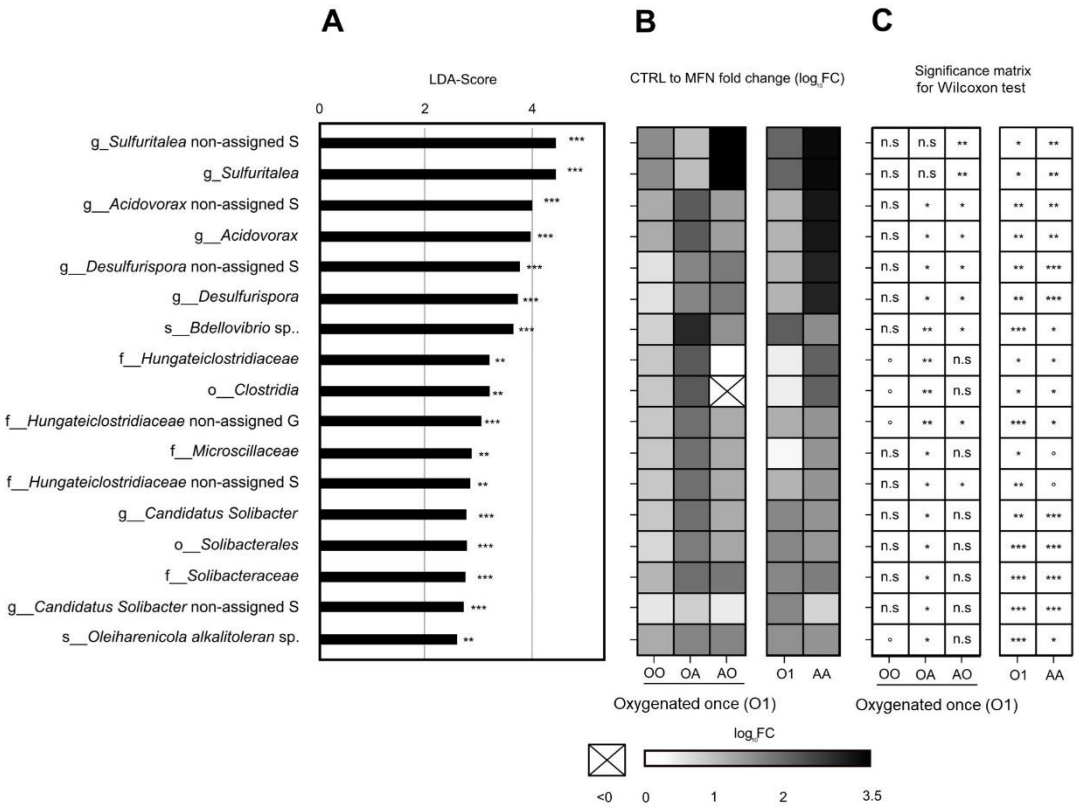

Figure 5.4. *Putative prokaryotic bioindicators of metformin exposure at the sediment-water interface and associated metrics, comprising (A) LDA-score, (B) p-value, (C) $log_{10}FC$, and Wilcoxon test comparing MFN with CTRL abundance across oxygen conditions (OO, AO, OA, O1, AA). Significance levels are defined as follows: ° p ∈]0.05; 0.10 (tendency); *: p<0.05; **: p<0.01; ***: p<0.001; ****: p<0.0001; non-significant results (n.s) for p>0.10. The prefix o, f, g, s_ designates the initial of the taxonomic level associated with the bioindicative taxa (Order, Family, Genus, Species). For taxa presenting the suffix non-assigned S (Species) or G (Genus), the prefix and name of the indicative match the closest taxonomic affiliation available.*

In contrast to control experiments, where they were present at low and decreasing abundance over time (Fig. 5.5), the 17 putative bioindicator taxa exhibited a concurrent increase in abundance in metformin treatments. This suggests that an increase in relative abundance of the selected metformin bioindicators over time may be useful for evaluating metformin exposure. The observed and significant increase in abundance of bioindicator taxa at days 1 and 41 suggests a potential impact of metformin contamination on prokaryotic communities despite the lack of statistically significant results (NPMANOVA). An additional analysis examining sensitive taxa, i.e., taxa that disappear after a metformin contamination event, could be valuable. Hence, the disappearance of such taxa could serve as an indicator of metformin contamination.

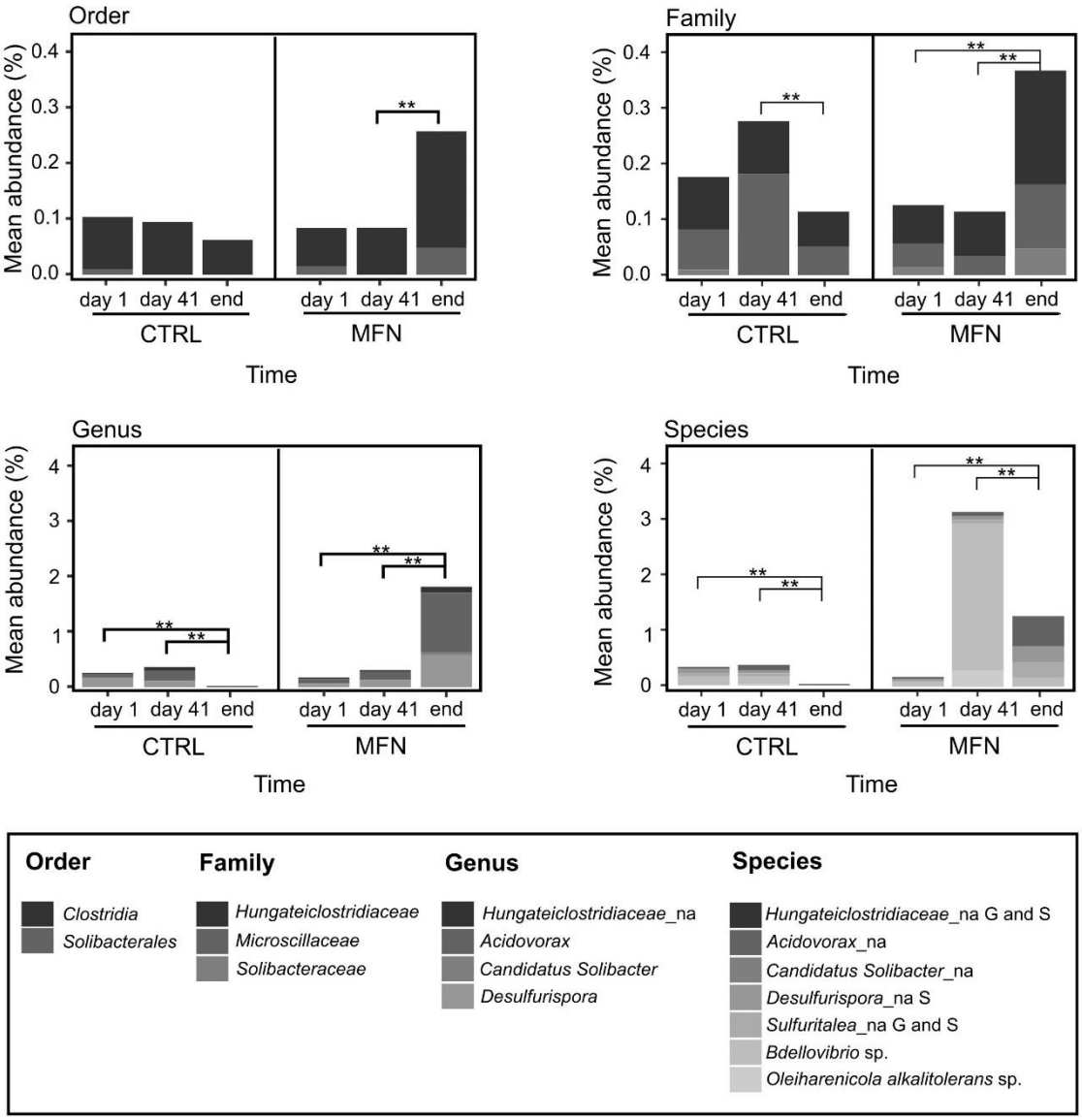

Figure 5.5. *Mean abundance (%) of putative metformin bioindicators over time in control (CTRL) and metformin (MFN) experiments across different taxonomic levels. Time points are indicated at day 1, day 41 and at the end of experiment (end). Significant results from Dunn test pairwise comparisons, corrected for alpha-inflation using the Benjamini-Hochberg method, are indicated (** $p < 0.01$). Non-assigned taxa (na) at the level of the Genus (G) or Species (S) are labelled with the closest taxonomic affiliation available.*

The identified potential bioindicators represent taxa that were significantly more abundant under metformin exposure. This overrepresentation may stem from their capability to utilise metformin as a carbon source, thereby conferring them a competitive advantage. To assess their potential role in metformin biodegradation, we further explored whether genes potentially associated with metformin degradation pathways were known for representatives of the biomarker taxa. However, this analysis remained inconclusive, possibly because of the still small numbers of complete genomes for the identified taxa. Alternatively, putative bioindicators might also harbour genes encoding enzymes involved in metformin degradation that have not yet been identified. For instance, the microbial P450 cytochrome family has been involved in

pharmaceutical biodegradation[138]. However, no microbial P450 cytochrome enzymes or associated genes have been identified in the process of metformin degradation so far. In the future, coupling metagenomic approaches with Stable Isotope Probing (SIP) could enhance the identification of genes overrepresented in organisms utilising metformin as a source of carbon and/or nitrogen, as previously shown with phenanthrene[180]. The isolation of new strains involved in metformin biodegradation could also lead to the identification of new genetic tools based on genome sequencing and mini-transposon mutagenesis[92].

5.4. Conclusion

Understanding the intricate relationships between the process of metformin dissipation and transformation and oxygen conditions, coupled with cumulative metformin exposure, presents a multifaceted challenge, further compounded by the necessity to consider the response and the roles of prokaryotic communities at the sediment-water interface in this process. In our study, laboratory microcosms mimicking the sediment-water interface under controlled conditions were spiked with metformin, one of the most common pharmaceutical contaminants found in the environment, under different oxygen regimes. Degradation kinetics and transformation products revealed faster biodegradation under anoxic environments. Metformin accumulated under abiotic conditions irrespectively of oxygen conditions, and this raises concerns about the risks associated with metformin exposure in ecosystems with limited microbial activity such as aquifers. Significant effects of both metformin exposure and oxygen regimes on prokaryotic community composition were observed. A model was developed to characterise the combined effects of contaminants and environmental conditions on procaryotic communities at the SWI. Here, co-occurrence of metformin exposure and anoxia had essentially additive effects. The performed analysis also allowed to identify certain taxa as potential bioindicators of metformin exposure that are independent of oxygen conditions. We anticipate that the analytical framework developed in this study could prove valuable in assessing and prioritising the specific biological effects of micropollutants in environments subject to physicochemical variations. This could contribute to a more robust and realistic evaluation of the risks associated with micropollutant-contaminated aquatic ecosystems.

Acknowledgements

This research and the fellowship of Adrien Borreca were funded by the CNRS 80|Prime program (2020-2023) and by the EU within the European Regional Development Fund (ERDF), support measure INTERREG VI in the Upper Rhine as part of the Reactive City project (Towards a Reactive City without Biocides). Chemical analyses were performed at the Pacite platform, ITES, University of Strasbourg. We acknowledge Emilie Muller, Jérémy Masbou and Tetyana Gilevska for fruitful discussions.

.

5.5. Appendix

Table A5.1. *Hydrochemistry of the microcosm water phase at incubation time t1. t2. t3 for pristine microcosms (CTRL). biotic and abiotic contaminated samples (MFN). Time points indicate the start of the experiment (t1). the beginning of the second round of contamination (t2). or when metformin was fully dissipated after a second round (t3).*

	t1			**t2**			**t3**		
	abiotic	**biotic**	**pristine**	**abiotic**	**biotic**	**pristine**	**abiotic**	**biotic**	**pristine**
NH_4^+ (mmol L^{-1})	0.07 ± 0.08	0.07 ± 0.11	0.01 ± 0.03	0.19 ± 0.21	0.28 ± 0.44	0.09 ± 0.16	0.47 ± 0.27	0.2 ± 0.35	0.2 ± 0.26
Na^+ (mmol L^{-1})	0.18 ± 0.03	0.17 ± 0.01	0.17 ± 0.02	0.31 ± 0.07	0.28 ± 0.02	0.26 ± 0.02	0.26 ± 0.05	0.28 ± 0.04	0.28 ± 0.02
K^+ (mmol L^{-1})	0.14 ± 0.02	0.15 ± 0.03	0.15 ± 0	0.19 ± 0.02	0.21 ± 0.04	0.2 ± 0.04	0.17 ± 0.02	0.17 ± 0.05	0.17 ± 0.02
Mg^{2+} (mmol L^{-1})	0.66 ± 0.03	0.78 ± 0.11	0.75 ± 0.05	0.91 ± 0.21	1.03 ± 0.13	1.11 ± 0.25	0.8 ± 0.1	1.05 ± 0.27	1.05 ± 0.18
Ca^{2+} (mmol L^{-1})	1.86 ± 0.05	1.7 ± 0.24	1.62 ± 0.11	2.27 ± 0.4	1.75 ± 0.61	1.46 ± 0.59	2.24 ± 0.26	2.22 ± 0.52	2.22 ± 0.44
Cl^- (mmol L^{-1})	0.18 ± 0.03	0.18 ± 0.02	0.17 ± 0.01	0.17 ± 0.02	0.19 ± 0.01	0.17 ± 0.01	0.17 ± 0.02	0.21 ± 0.01	0.21 ± 0.01
NO_3^- (mmol L^{-1})	0 ± 0	0 ± 0.01	0.01 ± 0.02	0.01 ± 0.01	0.01 ± 0.02	0.01 ± 0.01	0.01 ± 0	0.01 ± 0.01	0.01 ± 0
SO_4^{2-} (mmol L^{-1})	**0.98 ± 0.09**	0.06 ± 0.04	0.07 ± 0.02	0.06 ± 0.05	0.04 ± 0.02	0.15 ± 0.22	0.25 ± 0.2	0.22 ± 0.31	0.22 ± 0.3
PO_4^{3-} (mmol L^{-1})	0 ± 0	0 ± 0	0 ± 0	0.02 ± 0.02	0 ± 0	0 ± 0	0.02 ± 0.01	0.01 ± 0.01	0.01 ± 0
TOC (ppm)	**80.51 ± 6.23**	11.15 ± 1.89	10.11 ± 1.75	**109.64 ± 13.81**	26.34 ± 15.91	32.45 ± 14.33	**74.64 ± 8.32**	12.44 ± 2.95	12.44 ± 1.59
pH (-)	8.00	8.00	8.00	8.00	8.00	8.00	8.00	8.00	8.00
Conductivity (S m^{-1})	7.59 ± 0.35	5.64 ± 0.92	5.39 ± 0.35	7.41 ± 1.37	6.61 ± 1.7	6.19 ± 1.19	7.71 ± 0.82	7.86 ± 2.15	7.86 ± 1.72
Dissolved oxygen concentration. oxic (mg L^{-1})	>8.00	>8.00	>8.00	>8.00	>8.00	>8.00	>8.00	>8.00	>8.00
Dissolved oxygen concentration. anoxic (mg L^{-1})	<0.1 ppm	<0.1 ppm	<0.1 ppm	<0.1 ppm	<0.1 ppm	<0.1 ppm	<0.1 ppm	<0.1 ppm	<0.1 ppm

1

Table A5.2. *List of samples Passing or Failing sequencing in Sediment or Water matrices. The table illustrates the nature of samples subjected to metformin (MFN) or not (CTRL). indicating whether the samples were monitored at the start of the experiment (t1). the beginning of the second round of contamination (t2). or when metformin was fully dissipated after a second round (t3). Additionally. sequencing depth is displayed in the number of reads.*

Matrice	Contamination	Incubation time	Oxygenation	Oxygenation subgroup	Replicate	Sample	Sequencing	Sequencing depht
sediment	CTRL	t1	A	A1	a	sedimentCTRLt1Aa	PASS	34530
	CTRL	t1	A	A1	b	sedimentCTRLt1Ab	PASS	51877
	CTRL	t1	A	A1	c	sedimentCTRLt1Ac	FAIL	0
	CTRL	t2	A	A1	a	sedimentCTRLt2Aa	PASS	86593
	CTRL	t2	A	A1	b	sedimentCTRLt2Ab	FAIL	0
	CTRL	t2	A	A1	c	sedimentCTRLt2Ac	FAIL	0
	CTRL	t3	AA	A1	a	sedimentCTRLt3AAa	PASS	61198
	CTRL	t3	AA	A1	b	sedimentCTRLt3AAb	PASS	57660
	CTRL	t3	AA	A1	c	sedimentCTRLt3AAc	FAIL	0
	CTRL	t3	AO	O1	a	sedimentCTRLt3AOa	PASS	95700
	CTRL	t3	AO	O1	b	sedimentCTRLt3AOb	FAIL	0
	CTRL	t3	AO	O1	c	sedimentCTRLt3AOc	FAIL	0
	CTRL	t1	O	O1	a	sedimentCTRLt1Oa	FAIL	0
	CTRL	t1	O	O1	b	sedimentCTRLt1Ob	FAIL	0
	CTRL	t1	O	O1	c	sedimentCTRLt1Oc	FAIL	0
	CTRL	t2	O	O1	a	sedimentCTRLt2Oa	FAIL	0
	CTRL	t2	O	O1	b	sedimentCTRLt2Ob	PASS	56378
	CTRL	t2	O	O1	c	sedimentCTRLt2Oc	FAIL	0
	CTRL	t3	OO	O1	a	sedimentCTRLt3OOa	FAIL	0
	CTRL	t3	OO	O1	b	sedimentCTRLt3OOb	PASS	93461
	CTRL	t3	OO	O1	c	sedimentCTRLt3OOc	FAIL	0
	CTRL	t3	OA	O1	a	sedimentCTRLt3OAa	FAIL	0
	CTRL	t3	OA	O1	b	sedimentCTRLt3OAb	FAIL	0
	CTRL	t3	OA	O1	c	sedimentCTRLt3OAc	FAIL	0
	MFN	t1	A	A1	a	sedimentMFNt1Aa	FAIL	0
	MFN	t1	A	A1	b	sedimentMFNt1Ab	FAIL	0
	MFN	t1	A	A1	c	sedimentMFNt1Ac	PASS	86437
	MFN	t2	A	A1	a	sedimentMFNt2Aa	PASS	43663
	MFN	t2	A	A1	b	sedimentMFNt2Ab	PASS	42278
	MFN	t2	A	A1	c	sedimentMFNt2Ac	PASS	89075
	MFN	t3	AA	A1	a	sedimentMFNt3AAa	FAIL	0
	MFN	t3	AA	A1	b	sedimentMFNt3AAb	PASS	54005
	MFN	t3	AA	A1	c	sedimentMFNt3AAc	FAIL	0
	MFN	t3	AO	O1	a	sedimentMFNt3AOa	FAIL	0
	MFN	t3	AO	O1	b	sedimentMFNt3AOb	PASS	55734
	MFN	t3	AO	O1	c	sedimentMFNt3AOc	FAIL	0
	MFN	t1	O	O1	a	sedimentMFNt1Oa	FAIL	0
	MFN	t1	O	O1	b	sedimentMFNt1Ob	PASS	88599
	MFN	t1	O	O1	c	sedimentMFNt1Oc	FAIL	0
	MFN	t2	O	O1	a	sedimentMFNt2Oa	PASS	78639
	MFN	t2	O	O1	b	sedimentMFNt2Ob	FAIL	0
	MFN	t2	O	O1	c	sedimentMFNt2Oc	FAIL	0
	MFN	t3	OO	O1	a	sedimentMFNt3OOa	FAIL	0
	MFN	t3	OO	O1	b	sedimentMFNt3OOb	FAIL	0
	MFN	t3	OO	O1	c	sedimentMFNt3OOc	FAIL	0
	MFN	t3	OA	O1	a	sedimentMFNt3OAa	FAIL	0
	MFN	t3	OA	O1	b	sedimentMFNt3OAb	FAIL	0
	MFN	t3	OA	O1	c	sedimentMFNt3OAc	FAIL	0

*Table continues on next page

Matrice	Contamination	Incubation time	Oxygenation	Oxygenation subgroup	Replicate	Sample	Sequencing	Sequencing depht
water	CTRL	t1	A	A1	a	waterCTRLt1Aa	PASS	88262
	CTRL	t1	A	A1	b	waterCTRLt1Ab	PASS	52182
	CTRL	t1	A	A1	c	waterCTRLt1Ac	PASS	53011
	CTRL	t2	A	A1	a	waterCTRLt2Aa	PASS	88730
	CTRL	t2	A	A1	b	waterCTRLt2Ab	PASS	50939
	CTRL	t2	A	A1	c	waterCTRLt2Ac	PASS	82480
	CTRL	t3	AA	A1	a	waterCTRLt3AAa	PASS	90721
	CTRL	t3	AA	A1	b	waterCTRLt3AAb	PASS	92733
	CTRL	t3	AA	A1	c	waterCTRLt3AAc	PASS	33303
	CTRL	t3	AO	O1	a	waterCTRLt3OAa	PASS	94422
	CTRL	t3	AO	O1	b	waterCTRLt3OAb	PASS	95862
	CTRL	t3	AO	O1	c	waterCTRLt3OAc	PASS	87773
	CTRL	t1	O	O1	a	waterCTRLt1Oa	PASS	57161
	CTRL	t1	O	O1	b	waterCTRLt1Ob	PASS	67662
	CTRL	t1	O	O1	c	waterCTRLt1Oc	PASS	66933
	CTRL	t2	O	O1	a	waterCTRLt2Oa	PASS	76714
	CTRL	t2	O	O1	b	waterCTRLt2Ob	PASS	92922
	CTRL	t2	O	O1	c	waterCTRLt2Oc	PASS	97503
	CTRL	t3	OO	O1	a	waterCTRLt3OOa	PASS	85227
	CTRL	t3	OO	O1	b	waterCTRLt3OOb	FAIL	0
	CTRL	t3	OO	O1	c	waterCTRLt3OOc	PASS	85667
	CTRL	t3	OA	O1	a	waterCTRLt3AOa	PASS	81583
	CTRL	t3	OA	O1	b	waterCTRLt3AOb	PASS	82205
	CTRL	t3	OA	O1	c	waterCTRLt3AOc	PASS	96753
	MFN	t1	A	A1	a	waterMFNt1Aa	PASS	21958
	MFN	t1	A	A1	b	waterMFNt1Ab	PASS	46829
	MFN	t1	A	A1	c	waterMFNt1Ac	PASS	41691
	MFN	t2	A	A1	a	waterMFNt2Aa	PASS	99991
	MFN	t2	A	A1	b	waterMFNt2Ab	PASS	38532
	MFN	t2	A	A1	c	waterMFNt2Ac	PASS	93707
	MFN	t3	AA	A1	a	waterMFNt3AAa	PASS	86964
	MFN	t3	AA	A1	b	waterMFNt3AAb	PASS	50515
	MFN	t3	AA	A1	c	waterMFNt3AAc	PASS	69824
	MFN	t3	AO	O1	a	waterMFNt3OAa	PASS	80034
	MFN	t3	AO	O1	b	waterMFNt3OAb	FAIL	0
	MFN	t3	AO	O1	c	waterMFNt3OAc	PASS	86877
	MFN	t1	O	O1	a	waterMFNt1Oa	PASS	36493
	MFN	t1	O	O1	b	waterMFNt1Ob	PASS	89143
	MFN	t1	O	O1	c	waterMFNt1Oc	FAIL	0
	MFN	t2	O	O1	a	waterMFNt2Oa	FAIL	0
	MFN	t2	O	O1	b	waterMFNt2Ob	PASS	36745
	MFN	t2	O	O1	c	waterMFNt2Oc	PASS	33377
	MFN	t3	OA	O1	a	waterMFNt3AOa	PASS	44569
	MFN	t3	OA	O1	b	waterMFNt3AOb	PASS	74948
	MFN	t3	OA	O1	c	waterMFNt3AOc	PASS	75492
	MFN	t3	OO	O1	a	waterMFNt3OOa	FAIL	0
	MFN	t3	OO	O1	b	waterMFNt3OOb	PASS	96747
	MFN	t3	OO	O1	c	waterMFNt3OOc	FAIL	0

Table A5.3. *Pairwise-NPMANOVA for samples under contamination (MFN) or not (CTRL) at incubation time t3. under various oxygen levels. P-values are presented non corrected and corrected for alpha inflation by Benjami-Hochberg (FDR) and Bonferroni corrections.*

		Correction	
Pairwise comparisons	p-value	FDR	Bonferroni
non-spiked.AA_vs_non-spiked.AO.group	0.06	0.16	1
non-spiked.AA_vs_non-spiked.OA.group	0.43	0.16	1
non-spiked.AA_vs_non-spiked.OO.group	0.56	0.5	1
non-spiked.AA_vs_spiked.AA.group	0.01	0.16	1
non-spiked.AA_vs_spiked.AO.group	0.03	0.16	1
non-spiked.AA_vs_spiked.OA.group	0.02	0.16	1
non-spiked.AA_vs_spiked.OO.group	0.33	0.5	1
non-spiked.AO_vs_non-spiked.OA.group	0.14	0.16	1
non-spiked.AO_vs_non-spiked.OO.group	0.53	0.16	1
non-spiked.AO_vs_spiked.AA.group	0.06	0.16	1
non-spiked.AO_vs_spiked.AO.group	0.08	0.31	1
non-spiked.AO_vs_spiked.OA.group	0.07	0.16	1
non-spiked.AO_vs_spiked.OO.group	0.4	0.33	1
non-spiked.OA_vs_non-spiked.OO.group	0.5	0.37	1
non-spiked.OA_vs_spiked.AA.group	0.03	0.16	1
non-spiked.OA_vs_spiked.AO.group	0.04	0.16	1
non-spiked.OA_vs_spiked.OA.group	0.1	0.16	1
non-spiked.OA_vs_spiked.OO.group	0.5	0.5	1
non-spiked.OO_vs_spiked.AA.group	0.13	0.16	1
non-spiked.OO_vs_spiked.AO.group	0.14	0.37	1
non-spiked.OO_vs_spiked.OA.group	0.1	0.16	1
non-spiked.OO_vs_spiked.OO.group	0.33	0.37	1
spiked.AA_vs_spiked.AO.group	0.17	0.16	1
spiked.AA_vs_spiked.OA.group	0.06	0.16	1
spiked.AA_vs_spiked.OO.group	0.2	0.33	1
spiked.AO_vs_spiked.OA.group	0.12	0.16	1
spiked.AO_vs_spiked.OO.group	0.17	0.37	1
spiked.OA_vs_spiked.OO.group	0.25	0.33	1

Table A5.4. *Results from additive model at the Phylum level. Values presented are interaction relative changes (IC)*

Phylum	OBS	ADD	MFN impact	Anoxic impact
k__Archaea_NA	8.21 ± 6.57	4.1 ± 3.28	2.34	1.76
k__Bacteria_NA	0.52 ± 0.42	2.86 ± 2.29	3.52	-0.66
p__Acidobacteriota	-0.86 ± -0.69	-1.25 ± -1	-0.65	-0.6
p__Actinobacteriota	-0.67 ± -0.54	-0.64 ± -0.51	-0.69	0.05
p__Aenigmarchaeota	36.72 ± 29.38	36.72 ± 29.38	36.72	0
p__Altiarchaeota	64.91 ± 51.93	64.91 ± 51.93	64.91	0
p__Armatimonadota	-0.94 ± -0.75	-0.94 ± -0.75	0	-0.94
p__Bacteroidota	-0.38 ± -0.3	-0.41 ± -0.33	-0.09	-0.32
p__Bdellovibrionota	15.75 ± 12.6	33.02 ± 26.42	-0.52	33.54
p__Caldisericota	-0.93 ± -0.74	-0.93 ± -0.74	0	-0.93
p__Campilobacterota	-0.98 ± -0.78	-1.46 ± -1.17	-0.5	-0.96
p__Chloroflexi	-0.74 ± -0.59	-0.85 ± -0.68	-0.68	-0.17
p__Cloacimonadota	23.65 ± 18.92	23.65 ± 18.92	23.65	0
p__Crenarchaeota	-0.93 ± -0.74	-0.14 ± -0.11	0.82	-0.96
p__Cyanobacteria	-0.99 ± -0.79	-0.18 ± -0.14	-1	0.82
p__Dependentiae	2.67 ± 2.14	82.75 ± 66.2	83.71	-0.96
p__Desulfobacterota	8.56 ± 6.85	18.7 ± 14.96	19.23	-0.53
p__DTB120	0.33 ± 0.26	28.78 ± 23.02	29.74	-0.96
p__Elusimicrobiota	-0.97 ± -0.78	-1.53 ± -1.22	-0.91	-0.62
p__Euryarchaeota	9.57 ± 7.66	9.57 ± 7.66	9.57	0
p__FCPU426	-0.89 ± -0.71	-0.89 ± -0.71	0	-0.89
p__Fibrobacterota	18.75 ± 15	18.75 ± 15	18.75	0
p__Firmicutes	-0.26 ± -0.21	0.06 ± 0.05	0.59	-0.53
p__Fusobacteriota	-1 ± -0.8	-1.54 ± -1.23	-1	-0.54
p__Gemmatimonadota	0.12 ± 0.1	0.32 ± 0.26	0.64	-0.32
p__Halobacterota	46.01 ± 36.81	112.16 ± 89.73	112.75	-0.59
p__Hydrogenedentes	-0.97 ± -0.78	-0.97 ± -0.78	0	-0.97
p__Iainarchaeota	-0.69 ± -0.55	5.34 ± 4.27	-0.96	6.3
p__Latescibacterota	-0.95 ± -0.76	-0.95 ± -0.76	0	-0.95
p__LCP-89	20.16 ± 16.13	20.16 ± 16.13	20.16	0
p__MBNT15	3.91 ± 3.13	33.46 ± 26.77	34.32	-0.86
p__Methylomirabilota	25.71 ± 20.57	18.01 ± 14.41	0.44	17.57
p__Micrarchaeota	25.7 ± 20.56	10.8 ± 8.64	9.17	1.63
p__Myxococcota	-0.19 ± -0.15	-0.02 ± -0.02	-0.42	0.4
p__Nanoarchaeota	3.17 ± 2.54	3.9 ± 3.12	4.08	-0.18
p__NB1-j	0.24 ± 0.19	2.37 ± 1.9	3.06	-0.69
p__Nitrospirota	-0.22 ± -0.18	-0.21 ± -0.17	-0.25	0.04
p__Patescibacteria	-0.98 ± -0.78	-1.61 ± -1.29	-0.93	-0.68
p__Planctomycetota	-0.96 ± -0.77	1.71 ± 1.37	-0.99	2.7
p__Proteobacteria	1.1 ± 0.88	0.99 ± 0.79	0.12	0.87
p__SAR324_clade	-0.97 ± -0.78	-0.97 ± -0.78	0	-0.97
p__Spirochaetota	4.8 ± 3.84	287.43 ± 229.94	288.41	-0.98
p__Sva0485	-0.19 ± -0.15	25.74 ± 20.59	26.71	-0.97
p__TA06	-0.94 ± -0.75	-0.94 ± -0.75	0	-0.94
p__Thermoplasmatota	12.91 ± 10.33	12.91 ± 10.33	12.91	0
p__Verrucomicrobiota	-0.93 ± -0.74	-1.04 ± -0.83	-0.93	-0.11
p__WOR-1	-0.04 ± -0.03	6.01 ± 4.81	6.89	-0.88
p__Zixibacteria	-0.74 ± -0.59	19.88 ± 15.9	20.87	-0.99

Table A5.5. *Bioindicative taxa (24) of metformin contamination irrelevant of oxygen levels. across taxonomic range from Phylum to Species level. grouped based on their logical taxonomy.*

Taxonomic Related Groups	Phylum	Class	Order	Family	Genus	Species
1	k_*Bacteria*_naP	k_*Bacteria*_naP.C	k_*Bacteria*_ naP.C.O	k_*Bacteria*_naP.C.O. F	k_*Bacteria*_naP.C.O.F.G	k_*Bacteria*_naP.C.O.F.G.S
2			*Clostridia*	*Microscillaceae*		
3			*Solibacterales*	*Solibacteraceae*	*Candidatus Solibacter*	*Candidatus Solibacter*_naS
4				*Xanthobacteraceae*		
5			*Clostridia*	*Hungateiclostridaceae*	*Hungateiclostridaceae*_naG	*Hungateiclostridaceae*_naG.S
6					*Sulfuritalea*	*Sulfuritalea*_naS
7					*Acidovorax*	*Acidovorax*_naS
8					*Desulfurispora*	*Desulfurispora*_naS
9						*Oleiharenicola alkalitoleran* sp.

Chapter 6.
Impact of micropollutants on microbial activity and identification biodegradation players

The 16S amplicon sequencing strategy described in Chapters 4 and 5 proved valuable in evaluating the community-level response to micropollutant exposure and environmental factors. This approach effectively assesses changes in the presence, absence, and abundance of taxa within the prokaryotic community. However, it is crucial to acknowledge the limitations of this method, particularly when interpreting the absence of observed effects on day 0. The lack of observed effects on day 0 could reflect two potential scenarios: I) The microbial community may not have been immediately impacted by the micropollutant exposure. II) The 16S amplicon sequencing method and the subsequent analysis may lack the sensitivity to detect subtle and immediate changes in the microbial community. Additionally, 16S amplicon sequencing primarily focuses on taxonomic shifts, providing limited insights into the actual functional activities of the prokaryotes within the community and the identification of specific microorganisms involved in the degradation of the target micropollutant.

By combining 16S amplicon sequencing with the technique of Stable Isotope Probing (SIP), we can gain a more comprehensive understanding of the impact of micropollutants on microbial communities, targeting active prokaryotes potentially involved in biodegradation. Thus, the 16S amplicon sequencing can provide a broad overview of community-level changes, while SIP delves into the functional roles of specific microorganisms and their involvement in pollutant degradation. This integrated approach is essential for a holistic understanding of microbial responses to micropollutant exposure.

The microcosm experiments in previous Chapters explored the impact of metformin on sediment-water prokaryotes under various conditions, including co-contaminants, contrasting environments, and oxic/anoxic conditions. Despite metformin degradation occurring, the responsible and active microbes remain unidentified. Chapter 6 focuses on identifying the microbes accountable for metformin biodegradation. This is realised by using the SIP technique and facilitated by isotopically labelled metformin obtained through collaboration with UMR 7177 CNRS. Unlike most SIP studies that concentrate on legacy pollutants like polycyclic aromatic hydrocarbons (PAHs), this experiment targets a micropollutant recently introduced in the environment.

The acquisition of isotopically labelled compounds remains the most critical bottleneck in SIP applications. To optimise the SIP procedure for identifying potential degraders, a pilot experiment was first performed with readily available and relatively cheap ^{13}C-glucose. This not only benchmarked the SIP method but also allowed to assess its effectiveness in detecting the immediate effects (day 0) of single or mixed micropollutants on functional microbial communities. The pilot study indicated that micropollutants may impact functional prokaryotic communities specialised in glucose uptake upon acute exposure. Subsequently, the study identified potential players involved in metformin biodegradation. This pilot study served as a valuable starting point for further experiments employing isotopically labelled metformin in the

SIP technique to identify bacteria using metformin as a carbon source in environmental compartment, such as aquatic sediment.

6.1. Toward identification of acute micropollutant effects and associated bacteria

6.1.1. Stable isotope probing as a suitable and flexible tool

While 16S amplicon sequencing is a powerful tool for assessing changes in community composition, its reliance on relative abundance data has limitations. Changes in the abundance of specific microbial taxa do not always translate directly to changes in their activity. For example, an increase in a particular organism might not necessarily indicate increased activity. Conversely, a decrease might not reflect a decline in function. Several factors contribute to this disconnect between abundance and activity as residual DNA from dead or inactive cells persists in the environment, impacting relative abundance data[247] Microbial communities harbour dormant or inactive cells that contribute to the total abundance measured by 16S rRNA gene amplicon sequencing, even if they do not actively participate in biogeochemical processes or biodegradation[247]. Another bias of the 16S rRNA gene approach lies in the lack of statistical power of ecological studies. Detection of an effect is often linked to sample size and statistical power[248]. Also, the absence of a change in abundance does not necessarily indicate a lack of effects on microbial communities because such effects might be undetectable using current methods.

SIP provides a valuable approach to address limitations of 16S rRNA gene amplicon sequencing, but its applicability depends on the availability of a labelled compound. Unlike 16S rRNA gene sequencing which focuses on community composition, SIP directly links the identity of active microorganisms to their putative metabolic processes by tracking taxa that assimilated the labelled compound. To track active microbial communities, cDNA-based sequencing (derived from RNA) and stable isotope probing (SIP) methods emerge as the most suitable options. However, the cDNA approach is challenging to put into practice due to the difficulty to reliably extract representative RNA from environmental samples, high variability in rRNA stability and its inability to differentiate between biodegradation activity and other microbial activities such as necromass degradation[247]. Our initial efforts to extract RNA resulted in poor yields.

In contrast, DNA-SIP provides a more robust alternative. This method hinges on the assimilation of stable isotopes into newly synthesised DNA of microorganisms incubated with specific isotope-labelled substrates. Heavy isotope-labelled DNA is separated from unlabelled DNA by isopycnic centrifugation, followed by sequencing of the DNA isolated from individual fractions with distinct densities[163,247]. While SIP also does have some limitations, it offers several key advantages. Two of its primary strengths are its focus on active microorganisms and its reliance on readily available DNA extracted from environmental samples. SIP specifically targets and identifies active microorganisms involved in the assimilation of the labelled compound. This provides insights into which microorganisms are potentially responsible for pollutant breakdown. This focus is particularly valuable compared to traditional methods that rely on total community composition (cDNA approach). SIP narrows the spectrum down to microorganisms directly or indirectly (i.e., through cross-feeding) assimilating the

labelled compound. Extracted DNA serves as the foundation for SIP analysis. This reliance on readily available DNA simplifies the process compared to methods requiring RNA.

However, a significant limitation of SIP is the limited availability and cost of labelled forms of the compounds of interest. Consequently, we chose to initially calibrate the experiments using a readily available ^{13}C-labelled molecule, uniformly labelled $^{13}C_6$-glucose, before experiments with custom-synthesized $^{13}C_2$-labelled metformin provided by our collaborator.

6.1.2. Detection of micropollutant acute effects at the SWI

In aquatic environments, microbes rapidly utilize glucose released from the breakdown of leaf litter, plant exudates, and other polysaccharides[249,250]. Due to its rapid turnover by active prokaryotic communities[249,250], glucose SIP represents a tool of choice to identify glucose-assimilating prokaryotes, hereafter referred to as GAP for short substantial portion of prokaryotic diversity in soils, and assess how micropollutants affect their activity through inhibition or promotion. GAPs likely represent a substantial portion of prokaryotic diversity in soils.

A novel and cost-effective laboratory microcosm experiment design employing river sediment is introduced in this study. The aim is to investigate the effect of individual and combined exposures to pharmaceutical and biocide micropollutants (metformin, *(S)*-metolachlor, and terbutryn) on GAPs within the pristine river sediment community. We hypothesised that micropollutant exposure may impact GAPs differentially: i) Some GAPs may be adversely impacted by micropollutants. ii) Certain GAPs may benefit from the removal of competitors reliant on glucose, potentially enhancing their activity. iii) Some GAPs may show activity only in the presence of these micropollutants, and thus may be assimilated to potential degraders. iv) Some GAPs may demonstrate tolerance to micropollutants and persist in both contaminated and uncontaminated environments. This study used SIP with $^{13}C_6$-glucose (referred to as 13C-GLUCOSE in the following) to elucidate specific responses of GAPs at the sediment-water interface following single (SIN) or combined (DUO) micropollutant exposure.

This experiment also established the foundations for future in-lab methodology to identify potential micropollutant degraders. This methodology was then applied using SIP to identify potential metformin degraders, specifically metformin-dimethylamine assimilating prokaryotes (DAPs), using metformin ^{13}C-labelled on the two methyl carbon atoms of its dimethylamine functional group.

6.1.3. Detection of metformin degrading bacteria at the SWI

Research efforts aiming to understand metformin biodegradation have mainly focussed on WWTPs. Studies have utilized activated sludge rich in organic matter and diverse microbial communities under both oxic and anoxic conditions to isolate metformin-degrading bacteria[152,214]. This approach enabled the isolation and characterisation of strains growing with metformin[92,191,219], such as *Aminobacter* sp. MD1 in the team[92], and provided insights into the genes and enzymes involved in metformin biodegradation[92,191,219]. Strain MD1 utilises the dimethylamine portion of metformin as a carbon and nitrogen source. However, there is a significant knowledge gap in the assessment of metformin biodegradation potential in natural aquatic environments such as rivers, streams, and lakes. Microbial communities at the

sediment-water interface play a pivotal role in natural degradation processes. This makes this compartment ideal to investigate metformin biotransformation in rivers, streams, and lakes.

We designed a laboratory microcosm study using river sediment on the basis of our SIP experiments with ^{13}C-glucose (Section 2) to elucidate the involvement of prokaryotes in dimethylamine assimilation from metformin, employing methyl-labelled $^{13}C_2$-metformin (referred to as ^{13}C-metformin from now on for short). We were well aware that using this approach, it would be difficult to distinguish between prokaryotes that mineralize metformin, those which solely assimilate dimethylamine produced by metformin degradation. Indeed, the literature suggests that strains involved in metformin biodegradation and presenting metformin hydrolase utilise dimethylamine directly as a carbon and nitrogen source[92,191,219]. This possibility will be further discussed in Section 3.

6.2. Characterisation of micropollutant acute impact on the prokaryotic compartment

6.2.1. Experiment with labelled glucose

This experiment aimed to investigate the feasibility of using readily degradable substrates, rather than RNA, as an alternative for assessing the acute impact of micropollutants, either alone or in mixtures, on the activity of prokaryotic communities. Additionally, it established a foundational methodology for future SIP studies with metformin. The detailed protocol for this experiment is provided in Chapter 3, Section 4.2.1 (Fig. 3.4). In this experiment, sediment-water microcosms were subjected to various conditions: single contamination with either metformin (MFN) or terbutryn (TER), both (DUO), or no contamination (CTRL), in the presence of labelled 13C-glucose or 12C-glucose. A final control group, designated as pristine microcosms (PRIS), was established without the addition of any micropollutant or glucose.

6.2.2. Effect of micropollutant on microbial activity

Glucose was rapidly depleted, within two days (initial exposure) and one day (second exposure). This is faster than reported in similar studies, where glucose persisted in sediment-water systems for 2 to 7 days[164,251]. The higher temperature of the set-up, 30°C, likely accounts for the accelerated dissipation observed. Microbial activity, as assessed by FDA and ATP-metric assays (detailed in Chapter 3, Section 7), was significantly affected only in the water phase (Kruskal-Wallis, $p = 0.04$). This observation is consistent with our previous hypotheses outlined in Chapter 4, i.e., micropollutants tend to be more bioavailable in water and may interact more readily with microbial communities, thus enhancing their overall exposure to micropollutants. Additionally, microbial activity tended to increase in the presence of micropollutants alone, although this relationship was not statistically significant according to Dunn's test (Fig. 6.1). This suggests a combined impact of micropollutants on the microbial community.

Micropollutant dissipation was not monitored as our focus was on acute exposure impact and significant changes in concentration within 2 days were unlikely. Previously observed lag phases for metformin (28 days - Chapter 5) and terbutryn persistence (no change after 71 days - Chapter 4) support this assumption.

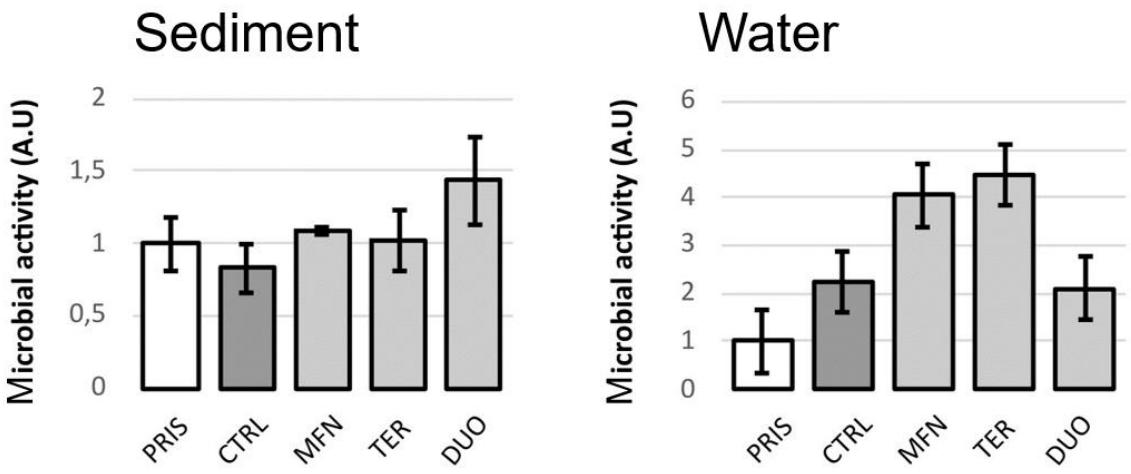

Figure 6.1. *Microbial activity from sediment assayed by the FDA method, (Section 3.7.1) and water phase assayed by the ATP-method (Section 3.7.2). Values were normalized to the reference level of microbial activity from pristine microcosms (PRIS).*

6.2.3. Approach of fraction sequencing

The remainder of the study depends on the success of 16S rRNA gene sequencing. The overall approach was outlined in Chapter 3, Section 6.3. Raw samples that did not undergo isopycnic fractionation were successfully sequenced. However, due to constraints in our experimental design, replicates or triplicates could not be obtained for most treatments, thus limiting the inclusion of robust control groups. Each light fraction was sequenced once for each contamination type (CTRL, MFN, TER, and DUO), and for both 12C and 13C experiments. Intermediate fractions, a mixture of labelled and unlabelled DNA at the interface between light and heavy fractions (as defined in Chapter 3, Section 6.1), were successfully sequenced for CTRL, MFN, and TER samples in the 13C experiment. Heavy fractions were successfully sequenced only for CTRL and DUO samples spiked with 12C-glucose, and MFN and TER samples spiked with 13C-glucose. Hence, controls are lacking for the heavy fractions (Table 6.1).

Although all raw samples were successfully sequenced and conducted in triplicates (a, b, and c), likely due to their high DNA concentration (157 ± 55 ng µL-1), some fractions encountered sequencing failures. The primary difference between raw samples and failed fractions lies in the DNA concentration. The findings suggest a potential threshold of at least 4 ng μL^{-1} for DNA concentration for successful amplicon sequencing. All sequenced fractions showed concentrations exceeding or meeting this threshold, except for three unlabelled heavy fractions. The DUO, CTRL, and pooled samples of heavy fractions fell below the limit of detection (b.d.l), consequently failing to sequence (refer to Table 6.1).

While all raw samples sequenced successfully (Table 6.2) and were analysed using the established pipeline (Chapter 3, Section 8.2) the absence of control fractions (Tables 6.1 and 6.2) precludes the use of classical identification methods for labelled prokaryotes (Chapter 3, Section 8.3).

Table 6.1. *Amplicon sequencing and diversity analysis in the glucose SIP experiment after fractionation. The term "Pooled" denotes combined samples from identical glucose experiments and fractions but from different contaminant conditions (CTRL, MFN, TER, DUO, see Materials and Methods, Section 3.6.3). Samples shaded in grey could not be sequenced.*

Fraction type	Glucose	Contaminant	DNA (ng μL^{-1})	Number of reads	Chao1	Shannon	Simpson's evenness
Light	12C-glucose	MFN	12	36991	2115	6.7	0.13
		TER	20	31030	1827	6.6	0.11
		DUO	19	38435	2044	6.8	0.16
		CTRL	10	50466	2535	7	0.16
		Pooled	15	42450	2273	7	0.18
	13C-glucose	MFN	15	41910	2415	7.1	0.3
		TER	19	40449	2283	7	0.21
		DUO	8	49582	2943	7.3	0.3
		CTRL	45	21705	1765	6.8	0.33
		Pooled	22	18383	1673	6.7	0.19
Intermediate	12C-glucose	MFN	2	-	-	-	-
		TER	2	-	-	-	-
		DUO	b.d.l	-	-	-	-
		CTRL	b.d.l	-	-	-	-
		Pooled	1	-	-	-	-
	13C-glucose	MFN	8	35413	719	4.9	0.05
		TER	12	36804	885	5	0.04
		DUO	b.d.l	-	-	-	-
		CTRL	4	39874	988	5.3	0.06
		pooled	6	47959	1030	5.1	0.04
Heavy	12C-glucose	MFN	b.d.l	-	-	-	-
		TER	b.d.l	-	-	-	-
		DUO	b.d.l	48473	2256	7.1	0.24
		CTRL	b.d.l	57568	2392	6.9	0.18
		Pooled	b.d.l	45635	2364	6.9	0.15
	13C-glucose	MFN	b.d.l	46643	267	2.3	0.02
		TER	b.d.l	45424	191	2.1	0.02
		DUO	b.d.l	-	-	-	-
		CTRL	5	-	-	-	-
		Pooled	1	-	-	-	-

Table 6.2. *Amplicon sequencing and diversity analysis from stable isotope probing experiment for glucose before fractionation. "Pooled" samples result from combination of equal DNA amounts of samples from the same glucose injection and fraction but from different contaminant conditions (CTRL, MFN, TER, DUO).*

Glucose	Contaminant	Replicate	DNA (ng/µL)	Number of reads	Chao1	Shannon	Simpson's evenness
None		a	186	13446	1360	6.5	0.24
None	PRIS	b	158	12277	1462	6.6	0.27
None		c	157	42053	2293	7.0	0.22
12C-glucose		a	297	15752	1622	6.6	0.19
12C-glucose	CTRL	b	88	38319	2161	6.9	0.16
12C-glucose		c	125	37593	1804	6.5	0.08
12C-glucose		a	190	37278	1033	4.3	0.02
12C-glucose	MFN	b	165	36614	1948	6.7	0.09
12C-glucose		c	165	33455	2021	6.9	0.22
12C-glucose		a	114	31863	1662	6.5	0.10
12C-glucose	TER	b	226	36294	1791	6.6	0.12
12C-glucose		c	110	47455	2112	6.7	0.09
12C-glucose		a	219	34824	1728	6.4	0.11
12C-glucose	DUO	b	133	38869	2080	6.8	0.16
12C-glucose		c	159	39058	1976	6.5	0.08
13C-glucose	CTRL	-	175	32497	1720	6.6	0.11
13C-glucose	MFN	-	62	29579	1896	6.6	0.10
13C-glucose	TER	-	85	26030	1777	6.6	0.11
13C-glucose	DUO	-	164	37135	2065	6.8	0.18

6.2.4. Effect of micropollutant and glucose on prokaryotic communities

The effect of three factors on the overall structure of prokaryotic communities (β-diversity) in raw samples was examined: glucose injection, glucose isotopologues, and type of contamination. An ordination analysis (Figure 3) coupled with statistical NPMANOVA analysis was conducted. The analysis revealed a significant difference (NPMANOVA, $p = 0.01$) between communities exposed to glucose (GLUC) or not (PRIS). However, no significant differences were observed for communities exposed to different glucose isotopologues (12C-glucose vs. 13C-glucose; NPMANOVA, $p = 0.49$) or for communities subjected to different contaminant types (CTRL, MFN, TER, DUO; pw-NPMANOVA, p ranging from 0.6 to 1).

The lack of observed impact by micropollutants on prokaryotic communities are consistent with the findings of Chapters 4 and 5. The absence of significant impact of the glucose isotopologues is encouraging, as this tracer molecule ideally should not alter the microbial communities. The observed impact of glucose exposure was expected, as prior research[252] established that aquatic prokaryotic communities are highly responsive to the organic substrates they encounter.

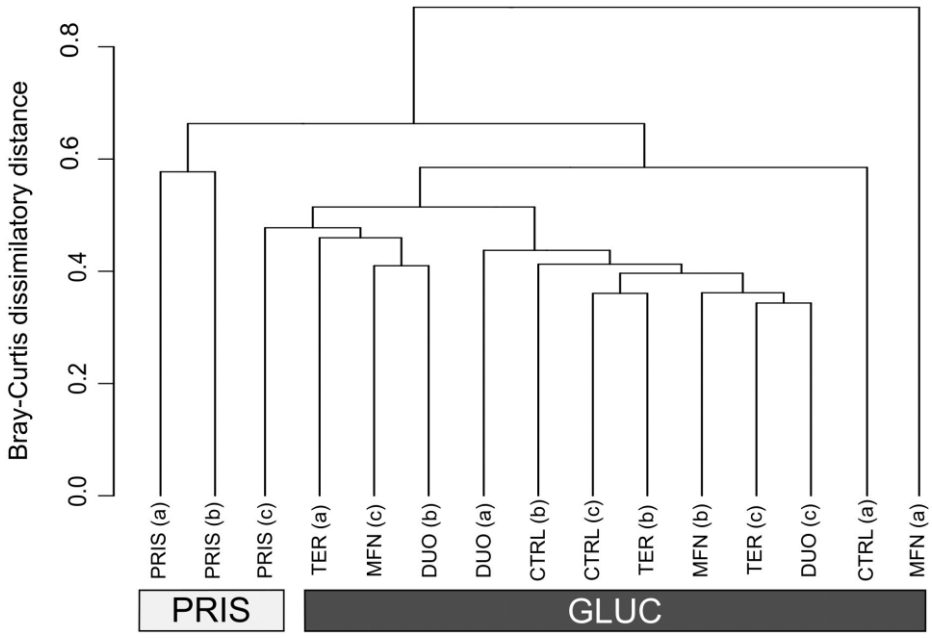

Figure 6.2. *Ordination by Bray-Curtis dissimilatory distances. Significant clusters defined by NPMANOVA include pristine prokaryotic communities not exposed to glucose and contaminants (PRIS), and communities exposed to glucose (GLUC) with (TER, MFN, DUO) or without (CTRL) micropollutant amendment. Letters (a), (b), and (c) denote replicate microcosms.*

Glucose emerges as the primary driver of alterations within the prokaryotic communities (Figure 6.2). Following exposure, a significant rise in the relative abundance of Proteobacteria and Bacteroidota was observed. Proteobacteria increased from 30 ± 5% to 45 ± 7% (fold change, FC = 1.52 ± 0.48), while Bacteroidota rose from 1.5 ± 0.6% to 2.3 ± 0.5% (FC = 1.53 ± 0.95). Conversely, several taxa, including unassigned bacteria, Deferrisomatota, Gemmatimonadota, Halobacterota, and Latescibacterota, displayed a notable decrease in relative abundance (FC < 1) (refer to Table 6.3). Analysis of alpha diversity (within-sample diversity) revealed no significant impact of contaminants, isotopologues, or glucose injections on richness, evenness, or overall diversity. Indices for Chao1, Shannon, and Simpson's evenness are provided for each sample in Tables 6.1 and 6.2.

Although the analysis of microbial communities in raw samples did not yield significant insights, we speculated that differences might become more apparent when considering fractions both within and between conditions. Initially, we anticipated distinctions among light, intermediate, and heavy fractions as their composition depends on GC content and density equilibrium, potentially leading to the selection of microorganisms across the gradient.

Table 6.3. *Differences between Phyla from pristine (PRIS) and glucose (GLUC) microcosms, and their associated mean ± standard deviation. Statistics were obtained through Wilcoxson test comparing Phylum abundance between PRIS and GLUC groups. Fold change from GLUC to PRIS was associated with an error calculated following. Standard deviation of the fold change was obtained using* $SD(C) = C\sqrt{\frac{SD(A)}{A} + \frac{SD(B)}{B}}$

Phylum	*p*-value	PRIS abundance (%)	GLUC abundance (%)	Fold change in abundance
k__Bacteria	0.03	1.7 ± 0.9	0.6 ± 0.6	0.4 ± 0.5
p__Bacteroidota	0.05	1.5 ± 0.6	2.3 ± 0.5	1.5 ± 1.0
p__Deferrisomatota	0.04	< 0.1	< 0.1	0.1 ± 0.9
p__Gemmatimonadota	0.02	2.8 ± 1.1	1.3 ± 0.4	0.5 ± 0.3
p__Halobacterota	0.05	7.6 ± 1.5	5.3 ± 2.1	0.7 ± 0.4
p__Latescibacterota	0.05	0.9 ± 0.3	0.5 ± 0.2	0.6 ± 0.4
p__MBNT15	0.01	0.3 ± 0.0	0.2 ± 0.1	0.8 ± 0.5
p__Myxococcota	0.01	5.6 ± 0.8	3.7 ± 1	0.7 ± 0.3
p__NB1-j	0.00	1.2 ± 0.2	0.8 ± 0.2	0.7 ± 0.3
p__Nitrospirota	0.03	1.3 ± 0.3	0.7 ± 0.2	0.6 ± 0.3
p__Proteobacteria	0.02	29.6 ± 5	45.1 ± 6.6	1.5 ± 0.5
p__Thermoplasmatota	0.02	< 0.1	< 0.1	6.4 ± 13.4

6.2.5. Changes of prokaryotic communities across fractions

Statistical evaluation of differences at fraction level presents challenges due to the limited number of samples available. Visually, however, microbial communities show variations across fractions (Figure 6.3). Thus, the SIP potentially and successfully selected the glucose-assimilating prokaryotes (GAPs) within the heavy fractions of 13C-glucose.

If SIP is associated with changes in prokaryotic communities as the density of the gradient increases, it may potentially alter richness and evenness. However, we lack sufficient data to apply statistical tests with adequate power. Therefore, we cannot draw conclusions regarding changes in α-diversity, and overall α-diversity remains consistent across fractions (Table 6.1).

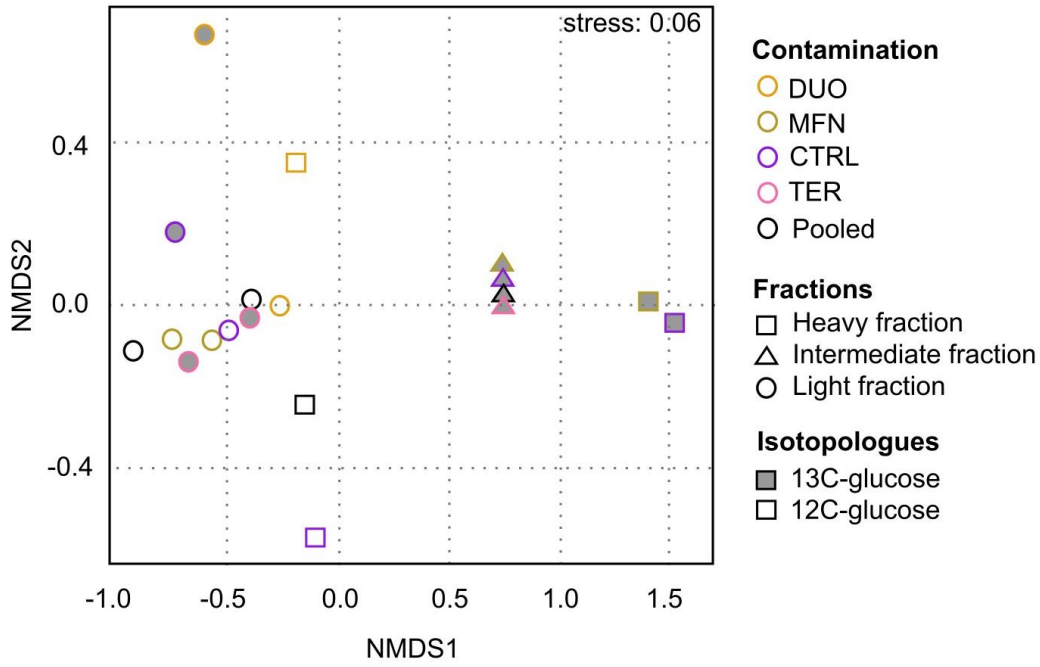

***Figure 6.3**. NMDS ordination for light (circle), intermediate (triangle), and heavy (square) fractions from GLU-SIP experiment. Contamination applied to microcosms is referred to as metformin (MFN), terbutryn (TER), both (DUO), or none (CTRL). Pooled contamination refers to an average sample obtained from evenly pooled fractions from microcosms MFN, TER, DUO, and CTRL. Fractions from labelled microcosms (13C-glucose) are shown with grey shading. Stress = 0.06*

6.2.6. Identification of glucose degrading bacteria across conditions

The inadequate sample size prevented the utilization of data analysis methodologies A, B, and C outlined in Chapter 3, Section 8.3 (Table 6.4). Consequently, an alternative approach, referred to as method D, was employed. This method was implemented using three distinct filters: 0, 0.05%, and 1%. Application of this method facilitated the identification of glucose-assimilating prokaryotes (GAPs) for MFN, TER, and CTRL conditions under each respective filter. However, due to data scarcity, no GAPs could be clearly discerned for the DUO condition (Table 6.4).

Table 6.4. *Feasibility of comparison among 12C and 13C experiments and among fractions. Unavailable samples are shown with grey shading.*

Fractions	12C-glucose	13C-glucose	Possibility for 12C/13C-glucose comparison	Possibility for comparison with light fractions
Light	CTRL	CTRL	yes	-
Light	MFN	MFN	yes	-
Light	TER	TER	yes	-
Light	DUO	DUO	yes	-
Int	CTRL	CTRL	no	yes
Int	MFN	MFN	no	yes
Int	TER	TER	no	yes
Int	DUO	DUO	no	no
Heavy	CTRL	CTRL	no	no
Heavy	MFN	MFN	no	yes
Heavy	TER	TER	no	yes
Heavy	DUO	DUO	no	no

Table 6.5. *Number of GAPs identified at different relative abundance thresholds for CTRL, MFN, and TER microcosms using method D.*

Threshold	GAPs-CTRL	GAPs-MFN	GAPs-TER
>0%	153	124	167
>0.05%	69	69	71
>1%	16	15	16
Relative count GAPs/total ASVs (%)	~0.01	~0.01	~0.01

Filters were applied to a total of 11,773 ASVs.

6.2.7. Variability in GAP numbers

Regardless of the filter applied, the quantity of glucose-assimilating prokaryotes (GAPs) remained consistent across conditions (Table 6.5). However, there is no indication that GAPs were the same across all conditions. Applying a filter set to a threshold of 1% abundance yields 20 unique GAPs, while a 0.05% filter results in 89 GAPs, and without any filter, 241 GAPs were identified (Fig. 6.5). A closer examination of GAP co-occurrence with a Venn diagram (see Fig. 6.4) reveals that many GAPs do not co-occur across CTRL, MFN, and TER conditions when no filter was applied. Out of 241 GAPs, 148 were exclusively present in one of these conditions. Table 6.5 demonstrates a clear impact of filter selection on the number of detected GAPs. A 1% filter results in the fewest GAPs, removing the filter entirely leads to a tenfold increase. A 0.05% filter appears to strike a balance, offering a good compromise between data

completeness and minimizing GAP detection in very low abundant taxa. Sequencing depth limitations in these cases could lead to errors.

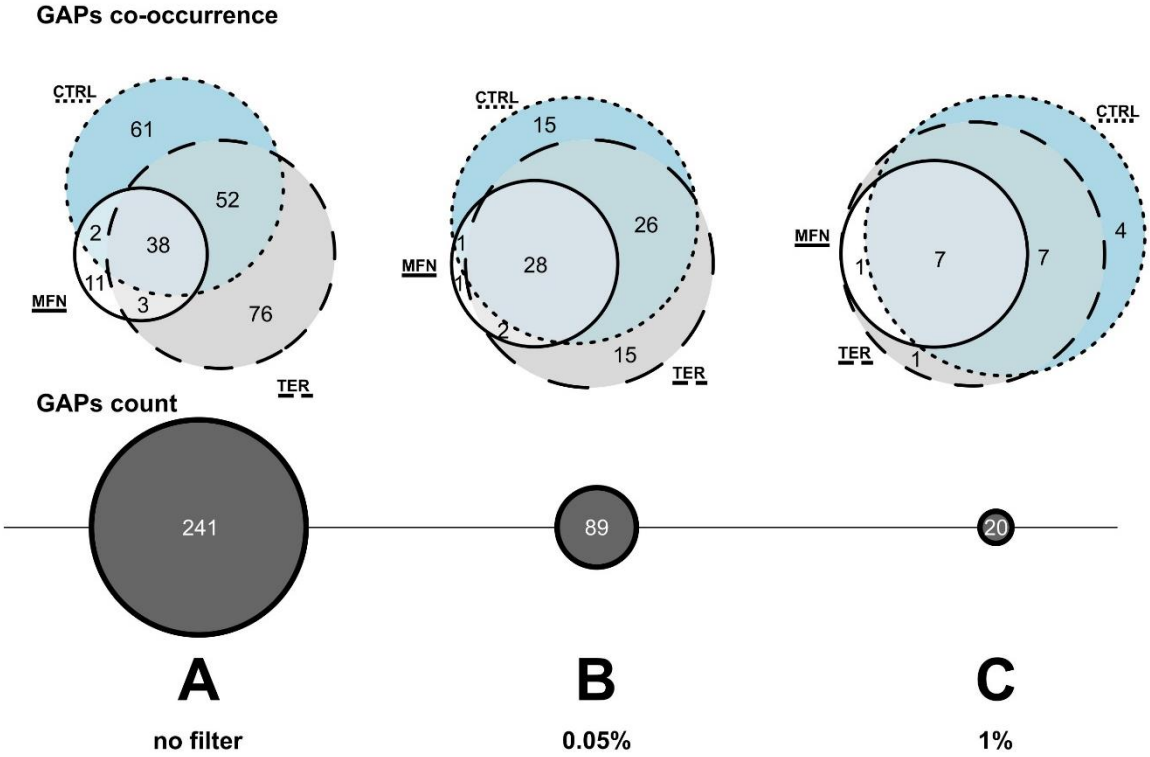

Figure 6.4. *Venn diagram for intersections of GAPs from CTRL, MFN, and TER microcosms, with A, B, and C as filter modalities.*

6.2.8. Do micropollutants select bacteria associated with glucose biodegradation?

This section examines the composition of GAPs at the phylum level, identified following analysis with a 0.05% filter. The analysis uncovers a 'core' set of GAPs, including Actinobacteriota and Proteobacteria, consistently present in control (CTRL) and contaminated samples MFN and TER (Fig. 6.5). I hypothesize that GAPs exclusively found in CTRL (e.g., *Fusobacteriota*, Gemmatimonadota, Bdellovibrionota, Cyanobacteria, Myxococcota) are inhibited by MFN or TER. Conversely, the presence of GAPs exclusively detected in contaminated samples, termed 'unique features,' suggests that contaminants may also stimulate glucose biodegradation in specific taxa. Analysis identified only one unique feature associated with MFN treatment. This feature was the presence of Firmicutes, accounting for 1 ASV. This suggests a high degree of overlap between GAPs found in the control and MFN groups. Approximately 87.5% of all GAPs were present in both groups, while less than 1% of GAPs appeared exclusively in the MFN treatment. For TER, 39% of the GAPs were shared with CTRL and MFN (core), and 21% were exclusively detected in the presence of TER. Hence, the impact of MFN appears less pronounced, with a higher proportion of its associated

GAPs representing core functionalities already present in the control. MFN and TER combined suppress the activity of 21% of the GAPs identified in the control samples (CTRL).

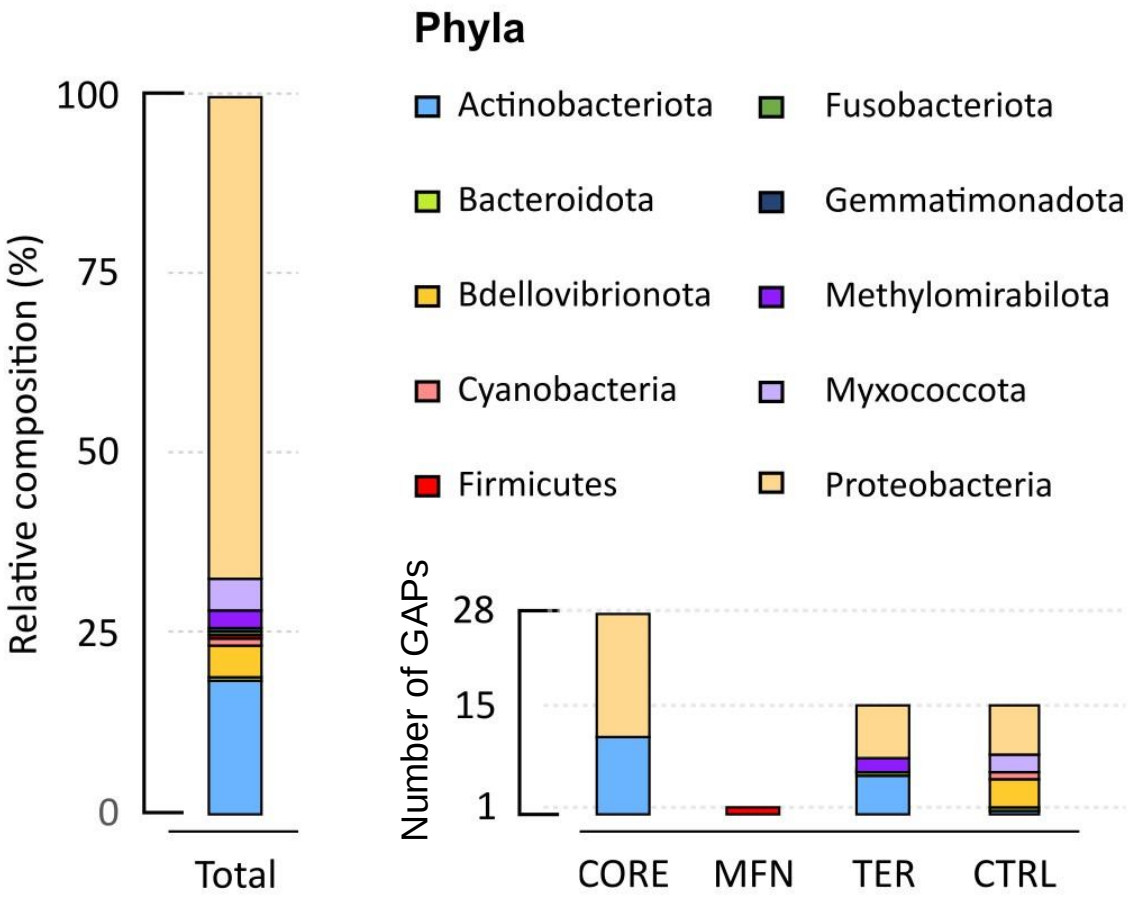

Figure 6.5. *Relative abundance of GAPs phyla, and their count when common (core) or specific (unique) to metformin and terbutryn. Data presented from 0.05% threshold.*

This experiment showcases the potential of SIP as a valuable tool for identifying activity changes within microbial communities exposed to environmental stressors. Due to the absence of technical replicates and control treatments, however, these observations should be viewed as preliminary trends and warrant further validation.

6.3. Toward identification of metformin biodegradation players

The second experiment capitalized on the technical knowledge obtained in the glucose-SIP experiment. Here, the focus shifted towards the identification of potential metformin-dimethylamine assimilating prokaryotes (DAPs). While the initial experiment provided valuable technical insights, limitations in the obtained data does not allow to draw definitive conclusions. Consequently, this second experiment implemented methods for identifying DAPs for the first time within this specific setup. The detailed protocol for this experiment can be found in Chapter 3 and Chapter 4.2.2. In essence, sediment-water microcosms were exposed to either unlabelled metformin (12C-metformin) or labelled metformin (13C-metformin). An autoclaved

setup was also employed to confirm that observed metformin dissipation was indeed biodegradation. Additionally, a final control group, designated as pristine microcosms (PRIS), was established without any addition of metformin (from Chapter 3, Fig. 3.5).

6.3.1. Effect of metformin on microbial activity

The complete dissipation of metformin took place in less than two weeks following the initial spike, and within less than three days after a second exposure under biotic conditions. Guanylurea was the sole transformation product detected (data not shown). In contrast, metformin concentration remained constant under abiotic conditions, indicating that biotic degradation prevailed. Comparable to the initial glucose experiment, microbial activity in sediments was unaffected by the presence of metformin ($p>0.10$, Wilcoxon). This was also observed in the water phase, with no significant changes in microbial activity ($p>0.10$, Wilcoxon).

6.3.2. Sequencing approach

In contrast to the amplicon sequencing of the previous experiment, replicates were available within the light, intermediate, and heavy fractions (Table 6.6). All raw samples were successfully sequenced and are represented in triplicates (Table 6.7). While the GC content was examined due to the expected impact of GC content on SIP, it was found to be largely irrelevant in the amplicons, which showed very low variability (GC content: 56.51 ± 0.65%).

Table 6.6. *Amplicon sequencing and diversity analysis from the stable isotope probing experiment for metformin after fractionation. "Pooled" samples result from the combination of equal amounts of DNA from replicates a,b,c of a sample. Amplicons from samples shaded in grey did not passed sequencing.*

Fraction type	Metformin	Replicate	DNA (ng μL^{-1})	Number of reads	Chao1	Shannon	Simpson's evenness
Light	12C-metformin	a	6	39239	1796	6.5	0.14
		b	7	42779	1836	6.4	0.12
		c	4	35643	1665	6.2	0.08
		Pooled	5	21331	1492	6.4	0.20
	13C-metformin	a	11	41468	1450	6.4	0.19
		b	19	22686	1931	6.7	0.19
		c	5	24342	1479	6.2	0.10
		Pooled	11	19522	1513	6.4	0.18
Intermediate	12C-metformin	a	b.d.l	-	-	-	-
		b	1	31115	946	3.9	0.01
		c	1	34189	966	4	0.01
		Pooled	1	-	-	-	-
	13C-metformin	a	1	-	-	-	-
		b	1	37542	1825	6.5	0.11
		c	1	40040	1786	6.3	0.09
		Pooled	1	-	-	-	-
Heavy	12C-metformin	a	b.d.l	-	-	-	-
		b	b.d.l	-	-	-	-
		c	1	50048	1355	4.4	0.01
		Pooled	1	-	-	-	-
	13C-metformin	a	1	-	-	-	-
		b	1	-	-	-	-
		c	b.d.l	-	-	-	-
		Pooled	b.d.l	-	-	-	-
	12C-metformin	c_fraction 39	b.d.l	51743	1532	5.2	0.02
	13C-metformin	b_fraction 39	b.d.l	49494	2058	6.3	0.06
	13C-metformin	c_fraction 43	b.d.l	54556	1394	5.1	0.02
	12/13C-metformin	Other individual fractions	b.d.l	-	-	-	-

Table 6.7. *Results of amplicon sequencing and diversity analysis from the stable isotope probing experiment for metformin before fractionation. Sample replicates are indicated as a, b, and c.*

Fraction type	Metformin	Replicate	DNA (ng μL^{-1})	number of reads	Chao1	Shannon	Simpson's evenness
Raw	Pristine	a	186	17386	1360	6.5	0.24
		b	158	16304	1462	6.6	0.27
		c	157	18314	2293	7.0	0.22
	12C-metformin	a	297	24361	1622	6.6	0.19
		b	88	16456	2161	6.9	0.16
		c	125	17876	1804	6.5	0.08
	13C-metformin	a	190	46164	1033	4.3	0.02
		b	165	36429	1948	6.7	0.09
		c	165	39188	2021	6.9	0.22

6.3.3. Effect of unlabelled and labelled metformin on prokaryotic communities

Amplicon sequencing data from raw samples provided valuable insights into the composition of microbial communities, enabling the exploration of two key questions. Firstly, whether the slight difference in mass between the ^{12}C and ^{13}C-metformin isotopologues affected microbial communities, and secondly, whether metformin exposure itself impacted these communities. Analysis revealed no significant differences in the prokaryotic communities exposed to either 12C-metformin or 13C-metformin (pw-NPMANOVA, corrected for FDR, $p_{corrected}$ = 0.2). Additionally, exposure to metformin (12C-metformin) compared to pristine conditions (PRIS) did not show any significant impact on the microbial communities (pw-NPMANOVA, corrected for FDR, $p_{corrected}$ = 0.8). 'Within sample' α-diversity was also investigated. No significant impact on richness, evenness, and global diversity were observed for metformin exposure and its isotopologues (Kruskal-Wallis and post-hoc Dunn test corrected for FDR). Chao1, Shannon, and Simpson's evenness indices are available for each sample in Tables 6.6 and 6.7.

6.3.4. Is fractionation associated with prokaryotic community shifts?

The composition of prokaryotic communities in isolated fractions showed variations depending on both the fraction type (light, intermediate, heavy) and the presence of 12C-metformin or 13C-metformin. These differences likely stem from successful labelling, which resulted in a shift in the molecular weight of labelled prokaryotic DNA thereby altering density and distribution across fractions. Notably, the prokaryotic communities of 12C-metformin and 13C-metformin microcosms were significantly different overall (NPMANOVA, p = 0.001). Within

12C-metformin samples, significant differences were observed among prokaryotic communities of the fractions (NPMANOVA, p = 0.004), as were those of 13C-metformin samples (NPMANOVA, p = 0.009). However, due to the lack of replicates for intermediate and heavy fractions, we could not rely on pw-NPMANOVA (non-significant results, possibly due to insufficient statistical power). Nonetheless, visual inspection (Fig. 6.6) suggest a noticeable divergence in prokaryotic communities of 12C-metformin and 13C-metformin as a function of the fraction type.

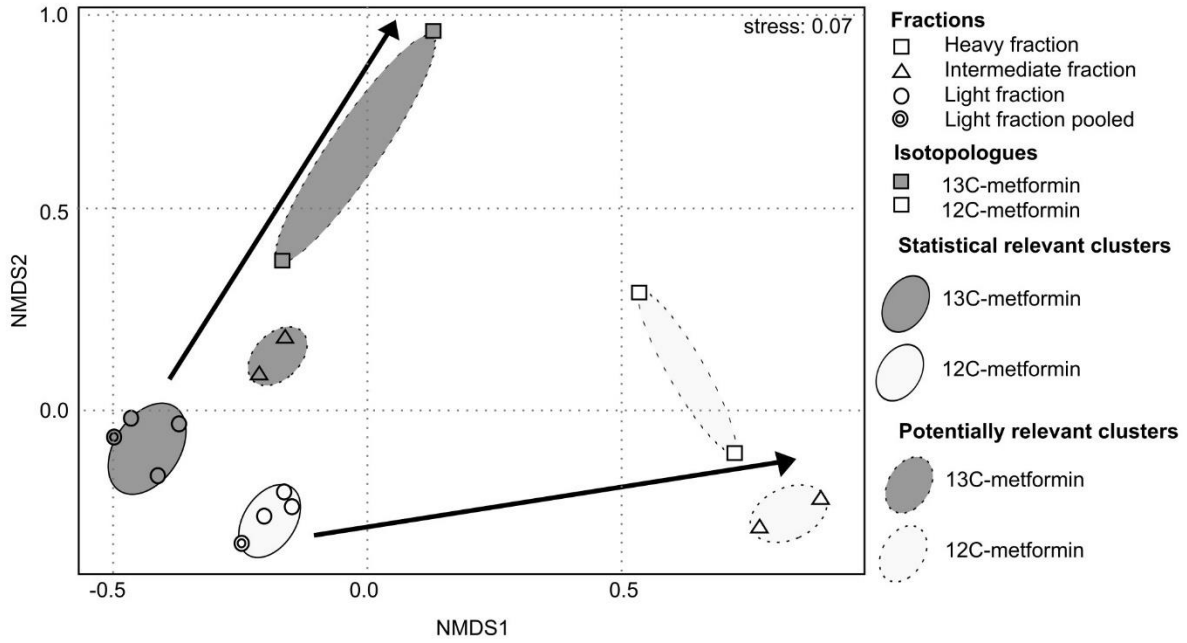

Figure 6.6. *NMDS ordination for light (circle), intermediate (triangle), and heavy (square) fractions from the MFN-SIP experiment. Dashed ellipses indicate significant cluster (NPMANOVA). Full line ellipses correspond to potential clusters (NPMANOVA significant, pw-NPMANOVA not significant). Arrows indicates the direction of shift in prokaryotic communities from light to heavy fractions. Fractions from labelled microcosms (13C-metformin) are shaded in grey. Stress = 0.06.*

Fractionation appeared to primarily affect Simpson's evenness (SE) (Kruskal-Wallis, p = 0.10), with other richness, evenness, and overall α-diversity indices remaining stable across fractions (Table 5 and Kruskal-Wallis, n.s). The decrease in evenness with higher density fractions suggests that certain prokaryotes may be overrepresented in heavy fractions compared to light fractions. However, a similar trend was also observed for both 12C-metformin and 13C-metformin, indicating that fractionation is potentially associated with a decrease in evenness of prokaryotic communities in individual fractions.

Comparison of SE scores across fractions reveals a low score (<0.05) for 12C-metformin in both intermediate and heavy fractions. Conversely, the 13C-metformin intermediate fraction shows a higher SE score (0.10). Similarly, the SE score for 13C-metformin in the heavy fraction (0.040 ± 0.028) is higher than that of 12C-metformin (0.015 ± 0.05) (Fig. 6.7). Higher SE scores are indicators of a more even distribution between taxa. In addition, changes in SE scores

reflect changes in proportion of these taxa. In contrast, no increase in richness (i.e., the number of different taxa) was observed. This suggests that taxa capable of utilizing metformin were already present in heavier fractions, and that their abundance increased due to 13C-metformin labelling.

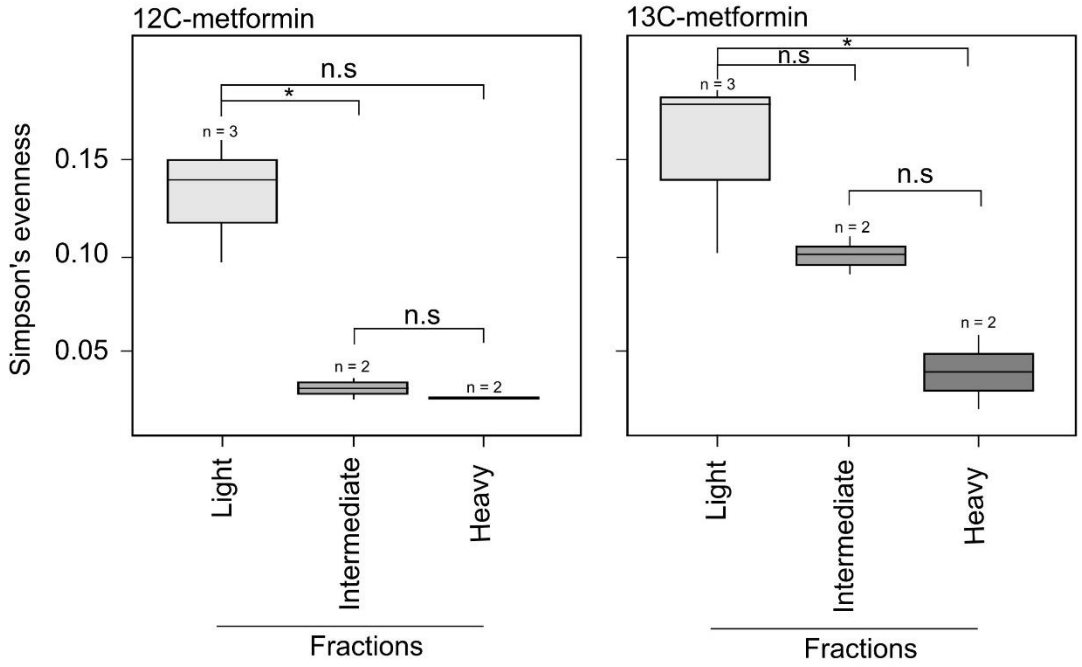

***Figure 6.7**. Simpson's evenness score across fractions from 12C-metformin and 13C-metformin. Sample size (n). Dunn's test significance: (*; p ≤ 0.05), (n.s; non-significant).*

6.3.5. Identification of metformin

Unlike in the initial glucose experiment, the data from this experiment met the criteria for analysis using methodologies A, B, and C. Method C was selected as an optimal compromise. Among the 2956 identified ASVs, 97 and 104 potential metformin degraders (DAPs) were identified in the intermediate and heavy fractions, respectively. This corresponds to less than 4% of the total ASVs. Low amounts of degraders can be observed, for example, 3 to 30 were found for phenanthrene-degrading bacteria in contaminated soils[253].

In the intermediate fractions, the abundance of previously identified DAPs increased 6.7-fold from the 12C-metformin experiment to the 13C-metformin experiment. This enrichment was not uniform across individual DAPs, with an average fold change (FC) of 11.1 ± 33.8. DAPs detected in the heavy fractions showed a lower fold change but greater uniformity, with an average FC of 5.9 ± 7.5. DAPs detected only in the 13C-metformin fractions were excluded from the average FC calculation. This is because since they were absent in the control (12C-metformin) group, their FC would be mathematically undefined, approaching positive infinity. These DAPs with undefined FC amounted to 41 DAPs in intermediate and 38 DAPs in heavy fractions (Table 6.8).

Analysis of these fractions revealed significant enrichment of certain prokaryotes in 13C-metformin compared to 12C-metformin, meeting the analysis criteria. By pooling the detected DAPs from both fractions, a final list of 109 unique DAPs identified at the species level was

obtained. This list constitutes the basis for future investigations into the identification and functional characterisation of these potential new metformin degraders.

Table 6.8. *Relative abundance of potential metformin degraders in intermediates and heavy fractions isotopologues 12C-metformin and 13C-metformin.*

Fractions	Isotopologues	Sum of relative abundance (%)	FC	Relative abundance (average ± SD)	FC (average ± SD)	Number of infinite FC
Intermediate	12C-metformin	3.50%	6.7	0.04 ± 0.08%	11.1 ± 33.8	41
	13C-metformin	23.70%		0.20 ± 0.60%		
Heavy	12C-metformin	8.90%	3.7	0.08± 0.32%	5.9 ± 7.5	38
	13C-metformin	33.20%		0.31 ± 0.95%		

6.3.6. Taxonomic diversity of potential metformin degraders

These 109 identified DAPs, despite representing only 6% of the total prokaryotic community, show a remarkable diversity, and are distributed across 21 different phyla (Table 6.9). This suggests that despite their low relative abundance, a wide range of microbes might play a role in metformin degradation within the microcosm. The majority of these MdAPs belong to Proteobacteria, Firmicutes, Actinobacteria, Bacteroidetes, and Acidobacteria, collectively representing 73% of all identified degraders (Table 6.9). The overrepresentation of DAPs among these phyla suggests a potential link to their known methylotrophic activity, which aligns with the expected dimethylamine assimilation pathway during metformin degradation. This finding suggests specific functional roles for these prokaryotic groups in the metformin biodegradation process.

Table 6.9. *Distribution of DAPs across the 21 Phyla.*

Phyla	Count	Relative count
Proteobacteria	**27**	**25%**
Firmicutes	**22**	**20%**
Actinobateriota	**13**	**12%**
Bacteroidota	**11**	**10%**
Acidobacteriota	**7**	**6%**
Chloroflexi	3	3%
Desulfobacterota	3	3%
Patescibacteria	3	3%
Spirochaetota	3	3%
Bdellovibrionota	2	2%
Crenarchaeota	2	2%
Dependentiae	2	2%
Nanoarchaeota	2	2%
Verrucomicrobiota	2	2%
Entotheonellaeta	1	1%
Fibrobacterota	1	1%
Gemmatimonadota	1	1%
Myxococcocota	1	1%
Sumerlaeota	1	1%
Thermoplasmatota	1	1%
WPS-2	1	1%
Total	**109**	**100%**

Methylotrophy is defined as the ability to utilize reduced single carbon (C1) substrates, such as methanol, methylamine and formaldehyde, as carbon and energy sources for growth[254]. The labelled metformin used in our experiments contains two labelled methyl groups on the dimethylamine-like moiety of the molecule. Therefore, DAPs could be methylotrophic prokaryotes, and the five phyla detected with significant labelling (Table 6.9) are indeed known to feature methylotrophic organisms. Proteobacteria appear to be the most dominant phylum when referring to the literature on methylotrophs[144,189,226,255–257]. The few recently isolated and described strains capable of degrading metformin are *Aminobacter* MD1[92], *Aminobacter* sp. strain NyZ550[192], *Aminobacter anthyllidis*[144], two *Pseudomonas* sp. strains[258], *Pseudomonas mendocina* MET, and *Aminobacter* sp. MET[259]. The common characteristic of these strains is that they all belong to the Phylum Proteobacteria. However, only one DAP matches the genus *Pseudomonas*, and no *Aminobacter* ASVs were found.

The metformin degradation pathway of *Aminobacter* strains involves hydrolytic cleavage of metformin to guanylurea and dimethylamine, which is then utilised for methylotrophic growth (Fig. 6.8). That of *Pseudomonas medocina* MET, in contrast involves the transformation of metformin into 1-N-methylbiguanide (Fig. 6.8). The methyl group could react with water molecule leading to the formation of formaldehyde, another C1 compound. The *Pseudomonas* genus is not recognized for methylotrophic capabilities. However, some species, like *Pseudomonas putida* and *aeruginosa*, show the ability to metabolize formaldehyde, a C1 compound, through pathways that are not strictly methylotrophic. One such pathway involves formaldehyde dissimilation mediated by the NAD^+-dependent enzyme Faldh[260]. The zinc-dependent pathway offers a plausible explanation for why *Pseudomonas* becomes labelled

with 13C despite not fitting the profile of a classic methylotroph. These organisms might indirectly metabolize the labelled methyl groups released during degradation of ^{13}C-metformin through this pathway.

Environmental studies have shown that some autotrophic archaea, such as *Metallosphaera yellowstonensis* MK1[261], can excrete formaldehyde which is then utilized by heterotrophic prokaryotes. This suggests that some prokaryotes might possess the ability to generate formaldehyde through metformin biodegradation and release it into the environment. Excreted formaldehyde could then be taken up by other prokaryotes capable of utilizing it as a carbon source through pathways like the serine cycle, the RUMP cycle, or even novel pathways[260]. This scenario implies potential cross-feeding interactions within the microbial community exposed to metformin. If *Pseudomonas medocina* MET and *Aminobacter* sp. MET or MD1 present the two most probable pathways for metformin biodegradation as suggested by Figure 6.8, then several scenarios warrant further exploration (Fig. 6.9).

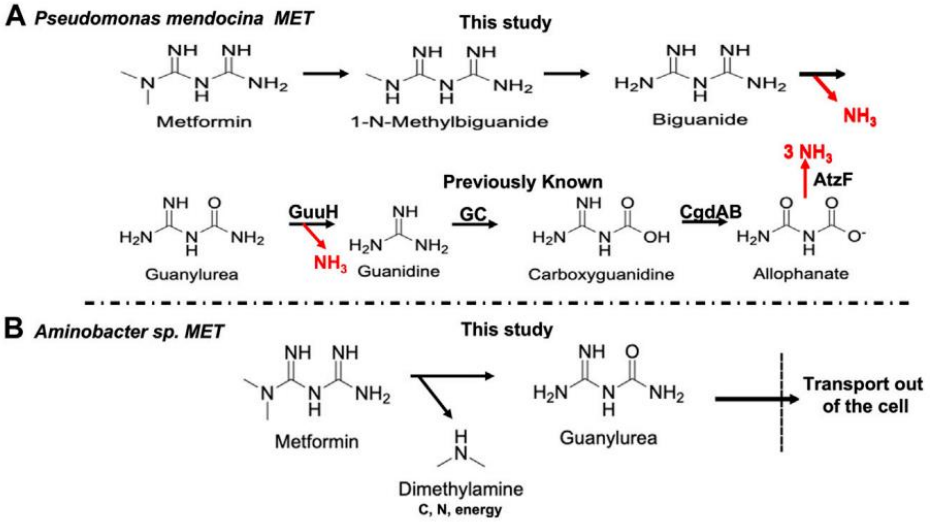

Figure 6.8. *Proposed biodegradation pathways for metformin by (A) Pseudomonas mendocina MET and (B) Aminobacter sp. MET. The known enzymes in the pathway are GuuH (guanylurea hydrolase), GC (guanidine carboxylase), CgdAB (carboxyguanidine deiminase) and AtzF (allophanate hydrolase). Taken from Martinez-Vaz et al. (2022)[259].*

On the one hand, metformin could be cleaved into labelled dimethylamine and guanylurea, or labelled formaldehyde produced during 1-N-methylbiguanide formation, and labelled carbon further assimilated in metabolism. Organisms with corresponding metabolism may be called 'first rank degraders'. On the other hand, dimethylamine or formaldehyde released from this metabolism could be excreted and used by other prokaryotes. In addition, labelled carbon dioxide, resulting from complete oxidation of metformin labelled carbon, could be used for growth by autotrophic prokaryotes. Corresponding organisms may be called 'second rank degraders', growing from labelled carbon by cross-feeding.Finally and less likely, DAPs could contribute to the formation of necromass. Subsequently, other prokaryotes may consume this necromass, potentially resulting in their indirect labelling. However, studies such as Dong *et al.* (2021) suggest slow degradation rates of necromass in soil (significant degradation observed after 30 days)[262], making necromass-based cross-feeding unlikely in our 2-day experiment (Fig. 6.9)

Figure 6.9. *Possible pathways for prokaryote labelling, including first rank and second-rank degraders and from indirect cross-feeding.*

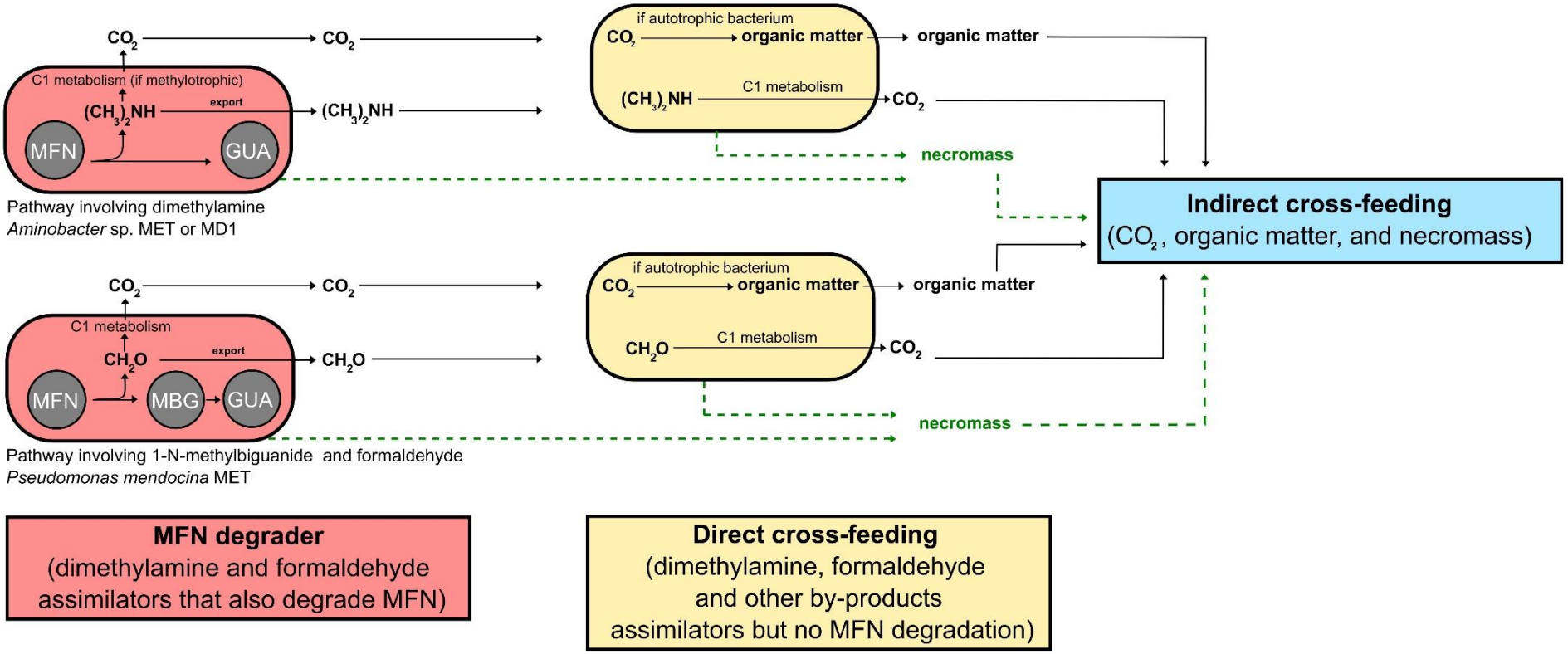

6.4. Discussion and perspectives for future work

Current literature suggests that most DAPs likely function as metformin degraders as well. Several experimental studies showed that strains involved in metformin biodegradation utilize potential metformin one-carbon transformation products such as dimethylamine or formaldehyde as carbon or nitrogen sources[92,259]. Thus, scenarios in which bacteria cleave metformin and discard C1 transformation products are rather unlikely at present.

Identification of microorganisms specifically benefiting from cross-feeding of metformin transformation products would be of interest. Multiple successive spikes of labelled metformin could help by amplifying the labelling[180,181]. Hence, the experiment could have been designed with a sacrificial approach, involving, for example, five successive spikes to observe the changes of prokaryotic communities over time. However, one concern is the potential bias introduced by the spiking process itself. The emergence of new populations of DAPs following each spike could arise from two sources: i) Cross-feeding where organisms benefit from byproducts generated by initial degraders. ii) Late degraders where prokaryotes with short generation times may not be readily detectable in earlier stages due to their slow generation time, as SIP relies on the requirement that cells must have undergone at least two cell divisions to incorporate ^{13}C into DNA[263].

To address the possibility of DAPs requiring metformin to initiate C1 metabolism, conducting a parallel experiment using labelled dimethylamine would thus be of interest. This would enable differentiation between DAPs directly assimilating dimethylamine and those relying on metformin for its utilization. The same rationale could be extended to formaldehyde. The presence of formaldehyde assimilators co-occurring as DAPs suggests potential labelling through formaldehyde, indicating direct cross-feeding. Similarly, observing labelled CO_2 would provide insights into indirect cross-feeding processes.

With regard to necromass derived cross-feeding, one could set up microcosms and repeatedly expose them to labelled metformin to label a significant portion of the prokaryotic community. The microcosm content could then be filtered through a 20 µm filter to concentrate the microorganisms, and sterilize this preparation using gamma irradiation[262]. The resulting "labelled necromass" could be introduced into new microcosms, and DNA extracted from spiked and control microcosms at different time points. By comparing DNA patterns in fractions from microcosms fed with "labelled necromass" and pristine ones, the minimum time required for necromass to contribute to cross-feeding could be identified. A significant increase in DNA concentration in the heaviest fractions would signify a shift indicative of the utilization of necromass by the prokaryotic community.

Labelling metformin on the two other carbons of the molecule associated with its guanylurea transformation product (Fig. 6.8A) could also be attempted. This approach would allow us to identify among the DAPs those that are also able to use the metformin transformation product guanylurea as a source of carbon[25].

Testing labelled versions of several potential transformation products of metformin, such as dimethylamine, guanylurea, dimethylurea, guanidine, dimethylguanidine and urea as growth substrates would present a further opportunity to identify organisms capable of utilizing

these compounds as energy sources. Comparing identified assimilators with the list of DAPs obtained in the metformin experiment could unveil the diversity of metabolic pathways and microorganisms potentially associated with metformin transformation. Additionally, recent studies suggest that metformin degradation can occur under anoxic conditions. Repeating the experiment under such conditions could yield valuable insights into potential differences in microbial community composition and degradation pathways in the absence of oxygen[152,214].

In summary, the exploratory work in this Chapter paves the way for future studies aiming the identification of potential metformin degraders. Such studies may employ more informative approaches such as metagenomics, in order to identify potential genes and functions involved in metformin biodegradation[180]. This avenue of analysis could offer a more comprehensive understanding of metabolic pathways involved in metformin degradation and provide deeper insights into the microbial response to environmental stressors. The envisaged approach would be similar to the SIP experiment conducted by Thomas *et al.* (2019)[180] for phenanthrene. Access to the metagenome would also allow for statistical comparison between genes and associated function between DAPs and non-DAPs. This first approach would enable a list of putative interest genes and functions paving the way for identification of potential genes and function involved in metformin biodegradation.

In the absence of metagenomic data, a predictive approach could have been utilized, by leveraging metagenome prediction and estimating associated functions using the PICRUST pipeline. By coupling these results with a statistical comparison tool such as LEfSe analysis, we could have predicted inhibited and overrepresented functions within DAPs compared to non-DAPs[179]. But this tool remained based on prediction and its use remains controversial because of its associated biases[264].

In conclusion, this study represents a first exploratory attempt at metformin-SIP. As detailed previously, many complementary experiments could be performed to characterise more deeply the pathways involved in metformin biodegradation *in situ*. Extending this approach to other interesting groups of microorganisms would also be of interest, such as Fungi, using 18S rRNA or internal transcribed spacer instead of 16S rRNA[265]. Also, testing the use of other experimental approaches, such as mRNA-based SIP to identify actively transcribed genes (transcriptome analysis)[266,267], would likely also provide valuable insights on the gene complement associated with metformin transformation. Nevertheless, the main and limitation of SIP-based approaches applied to micropollutants is the relatively high concentration of labelled compound required to obtain a labelling signal, which is difficult to reconcile with the low concentrations of micropollutants including metformin witnessed in the environment. Nevertheless and despite this intrinsic limitation, and provided labelled versions of compounds of interest can be made available, SIP approaches along the lines described in this chapter could be transposed to other API contaminants of current interest, such as carbamazepine, paracetamol, gabapentin, trimethoprim, and sulfatomethoxazole[46].

Chapter 7.
General discussion, conclusions, and perspectives

Aquatic ecosystems are especially vulnerable to micropollutants due to their susceptibility to contamination from various sources. These contaminants infiltrate surface and groundwater systems through multiple pathways. Herbicides used in agriculture[268] and building materials[61] can enter these aquatic ecosystems, along with pharmaceutical and personal care products (PPCPs). Incomplete transformation during wastewater treatment allows PPCPs to be released into surface waters[184]. In this context, the SWI plays a pivotal role in aquatic ecosystems, serving as a hub for biogeochemical reactions, including the recycling of organic matter and nitrogen cycling[65]. It also acts as a sink and a transformation hotspot[73,74] for micropollutants due to the constant exchange of water fluxes. The SWI is populated by prokaryotic organisms[83]. These microorganisms play a crucial role in aquatic ecosystems, acting as pillars of biogeochemical cycles[65]. Disturbances to the microbial communities can lead to potential changes and environmental risks. Conversely, microorganisms can also act as agents of biodegradation, detoxifying the environment, and sometimes using organic pollutants as a carbon source for growth[127].

In this context, my PhD thesis aimed to understand the dynamics and mechanisms underlying the dissipation of micropollutants at the SWI. Focusing primarily on micropollutant transformation and associated microbial communities, I worked to fill knowledge lacunae concerning the effect of micropollutants on biodegradation processes at the SWI and its prokaryotic compartment. In order to do this, I used laboratory experiments conducted in laboratory microcosms that simulate the SWI. This involved the use of high-throughput sequencing techniques to examine prokaryotic communities, and stable isotope probing (SIP) experiments to identify microorganisms involved in micropollutant biodegradation. My work can be summarized as follows.

In Chapter 4, I evaluated the impact of three selected micropollutants, individually and in mixtures, on the dissipation dynamics and responses of prokaryotic communities at the sediment-water interface. Here, I hypothesized that a mixture of micropollutants and their transformation products could exert cumulative and synergistic toxic effects on prokaryotic communities. Whether this led to a slowdown in the biodegradation of micropollutants when present as a cocktail was assessed. Chapter 5 investigated the effect of alternating oxic and anoxic conditions on the dissipation of sequential metformin pulses and the composition of prokaryotic communities. I hypothesized that metformin dissipation is dependent on oxygenation conditions, and that alternating oxic and anoxic conditions would lead to increased biodegradation as observed in previous experiments with simazine[269]. Chapter 6 explored whether specific prokaryotic taxa within the sediment-water interface associated with the use of metformin as a primary carbon source for growth could be identified using an isotopically labelled form of metformin.

In all experiments, laboratory microcosms were employed to mimic the sediment-water interface. This facilitated experimental implementation of micropollutant dissipation under diverse conditions, taking into account diverse biotic and abiotic factors, fluctuations in oxygen

levels, successive contamination events, and mixtures of micropollutants. The limitations and advantages of such experiments will be discussed in detail in Section 2.

These experiments shed light on micropollutant persistence, transport potential, and consequent environmental risks within aquatic ecosystems. Additionally, the thesis focused on the effects of micropollutants on prokaryotic communities under diverse environmental scenarios. Thereby, my thesis provided novel insights into ecosystem-level risks, considering potential interactive effects between micropollutants and environmental variables.

Taken together, the experiments carried out in my thesis contributed to assess how micropollutants modify prokaryotic community composition, which may in turn affect ecological processes within aquatic environments. My thesis also attempted to identify prokaryotic organisms involved in the biodegradation of metformin as an emblematic, ubiquitous pharmaceutical micropollutant. Obtaining such knowledge may be key in the design of micropollutant monitoring and bioremediation strategies in the future, as well as in risk assessment of micropollutants in the environment.

7.1. Summary of main results and implications

7.1.1. The fate of micropollutants depends on environmental factors

Micropollutants, including pesticides and pharmaceuticals and their transformation products, contaminate aquatic environments as complex mixtures. Some, like terbutryn, may persist in the environment, while others, like metformin, are expected to dissipate over time. In Chapters 4 and 5, we found that the dissipation of micropollutants, either individually or in mixtures, is affected not only by their inherent physicochemical properties but also by external factors such as microbial communities and environmental conditions including oxygen levels. Interestingly, micropollutants dissipated at comparable rates individually or as mixtures. This supports the idea that the micropollutants undergo degradation through separate and independent biotic and/or abiotic pathways. Hence, no competition in dissipation was observed for different micropollutants.

The dissipation rates of micropollutants, particularly pesticides, can decelerate or accelerate significantly under multi-contaminant scenarios. For instance, pesticide and micro-plastic result in an increase in the persistence of pesticides by sorbing to plastic particles[270]. However, details on dissipation rates under multi-contamination between pesticides and pharmaceuticals remains scarce. A study examined how various pesticides degrade under vine leaves. Some pesticides degraded faster in mixtures, while others degraded slower[271]. However, authors did not provide any insights on why it was the case. For biodegradation, we can posit that adverse impact of pesticide A on the degraders of pesticide B could lead to a slower dissipation rate for B. Conversely, these adverse effects might also reduce competition for some degraders, enhancing their potential of biodegradation.

7.1.2. Micropollutants and environmental factors alter prokaryotic communities

A general finding of the thesis is that micropollutants induce alterations in prokaryotic communities. This phenomenon was observed upon micropollutant spiking of microcosms, through SIP experiments using glucose, and further evidenced in Chapters 4 and 5 where variations in prokaryotic communities were observed over time in both water and sediment.

With regard to mixtures, micropollutant effects predominantly showed additive interactions, with synergistic or antagonistic effects for certain taxa. Additionally, environmental factors such as oxygenation also impacted prokaryotic communities. Specifically, the combined effect of oxygenation and metformin predominantly showed additive behaviour, although synergistic and antagonistic interactions were also observed for certain taxa. These findings show the importance of considering environmental variables, as their interactions with contaminant exposure may lead to non-additive effects.

We also observed that certain taxa emerged as potential bioindicators of micropollutant contamination and its degradation, particularly for metformin, due to their change in relative abundance in response to metformin contamination. Further research is required to validate their involvement in metformin degradation, and the enzymatic pathways involved. This finding is significant because the use of SIP for identifying micropollutant degraders (especially PPCPs) is still exploratory. At this stage, SIP represents a high potential approach alongside culturomics to identify micropollutant-degrading strains[25,92,272], since uncultivable prokaryotes represent a dominant portion of environmental microbial communities[135].

In summary, the results obtained in my PhD thesis by integration of analytical chemistry and high-throughput sequencing approaches emphasize the intricate interactions between micropollutants and prokaryotic communities in aquatic ecosystems, and the importance of the combined analysis of the effects of chemical and physical stressors on prokaryotic communities. Findings also confirm the recalcitrance of some micropollutants such as terbutryn[61], and even the potential accumulation and persistence of readily biodegradable micropollutants such as metformin in essentially abiotic aquifer environments[43]. Some critical points and additional perspectives are addressed in the subsequent sections. Indeed, a single study rarely tells the whole story, and a more accurate picture requires the integration of many different results[248]. Altogether, our results contribute to a better understanding of the interaction between micropollutant mixtures and prokaryotic communities at the SWI.

7.1.3. Positioning of this work within microbial ecotoxicology

Microbial ecotoxicology emerged recently (around 2014)[140], compared to the broader field of ecotoxicology, which dates back to 1977 [273]. Despite their small size, microorganisms play key roles in nutrient cycling within ecosystems[128]. Additionally, the ease of extracting DNA and RNA from sediment and water samples facilitates rapid community profiling and functional analysis using modern tools like metagenomics[128], allowing to assess the impact of contaminants at both taxonomic and functional levels on ecosystem function, stability, and recovery[8].

By incorporating both bacteria and usually overlooked archaea[141], this work offers a comprehensive evaluation of the prokaryotic response to environmental stressors. While fungi are increasingly recognized as valuable indicators for ecotoxicological studies[153,274–276], my PhD thesis focused on prokaryotic communities, which was driven by two main factors: cost limitations and the predominance of bacterial degraders for micropollutants, such as metformin. Archaea were also included in the analysis thanks to the primer pair used and did not add to the overall cost[169]. My work further aligns with the objectives of microbial ecotoxicology by the use of microcosms, a broad range of analytical tools from multidisciplinary fields (analytical chemistry and OMICs technology)[141], and a focus on the community level. Furthermore, previous research on the "cocktail effect" – the combined impact of multiple

contaminants –primarily focused on higher organisms such as crustaceans, macroinvertebrates, and amphibians[17,19,20], my thesis contributes to bring this concept to the microbial realm.

This work marks the first identification of putative metformin degraders using SIP. However, application of SIP to micropollutants is still limited, with studies e.g. on triclosan[277], pentachlorophenol[278,279], and glyphosate[280]. Several factors explain this. First, commercially available 13C-labelled compounds essential for SIP studies are often unavailable or prohibitively expensive. Second, knowledge of micropollutant degradation pathways is often limited, hindering the identification of genes responsible for degradation as well as of degrading organisms[281].

I also developed a computational model to evaluate the combined effects of multiple factors on prokaryotic communities. Unlike traditional models that rely on highly standardized data from model organisms, it utilizes data derived from laboratory microcosm experiments. While currently still a proposal, this model has potential for benchmarking and further refinement. It offers capabilities that broaden its applicability beyond aquatic ecosystems and expand its potential for ecotoxicological research. The proposed approach enables direct application to a wide range of ecosystems including terrestrial and soil environments, due to the model's ability to capture the response of microbial communities in microcosms which adequately reflect the conditions of natural environments. In contrast, traditional models such as Toxic Unit (TU)-based approaches often rely on data obtained from model organisms under highly controlled conditions to provide insights into the cumulative effects of contaminants[63,101]. This may lead to discrepancies in predicting real-world ecological responses. The proposed computational model overcomes this limitation by explicitly considering the interactions and dynamics within microbial communities, for a more comprehensive assessment of the combined effects of multiple stressors (contaminants and environmental factors).

I also wish to stress the care taken in statistical analysis in my work, as advocated e.g. by Kimmel *et al.* (2023)[248]. The applied statistical approaches thus pave the way to investigate in more details the effects of micropollutants and their interactions, whether compound-compound or compound-stressor, while being mindful of limitations of sampling size as warranted in environmental studies. First, statistical analysis increases the reliability of findings by differentiating between genuine micropollutant effects and random variations within the data. This distinction was essential to validate the observed relationships between micropollutants and prokaryotic communities. Second, the used statistical methods went beyond basic descriptive statistics often used in environmental research and facilitated a deeper exploration of patterns within the diverse data sets obtained (analytical chemistry data, ASV abundance data, and alpha and beta diversity metrics). This effectively made the used statistics a decision-making tool, guiding and supporting the conclusions that were made

7.1.4. A visual summary

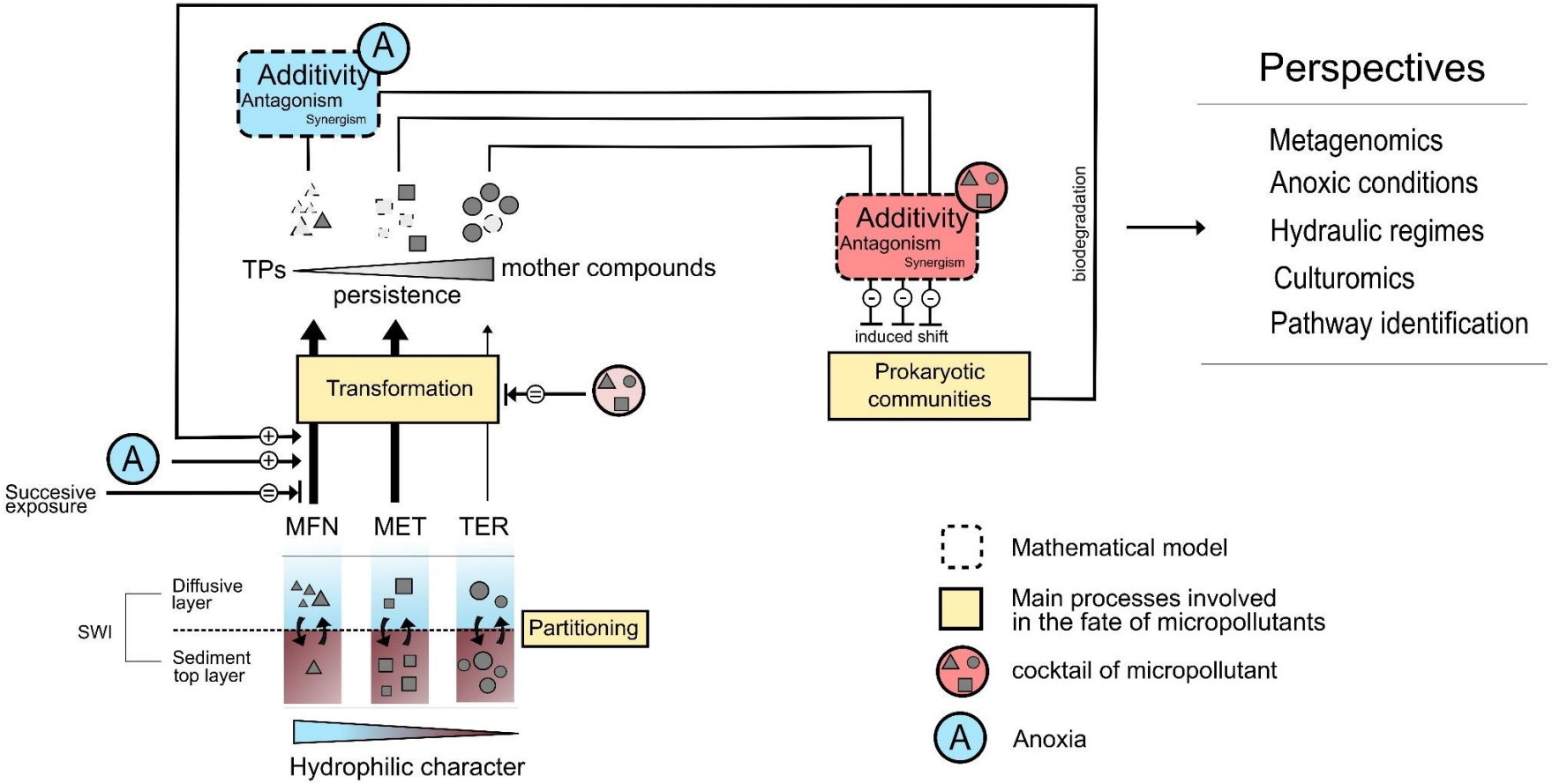

Figure 7.1. *Behaviour of micropollutants at the sediment-water interface under the effects of mutli-contamination and environmental factors. Metformin (dark triangles), (S)-metolachlor (dark squares), and terbutryn (dark circles) and their transformation products (open symbols) are shown. Enhanced effects are indicated by (+), negative effects by (-), and no effect by (=).*

7.2. Methodological improvements and limitations

A pivotal question often posed to a PhD candidate is, "In retrospect, what would you have done differently?". Reflecting on the experiments I conducted, it becomes evident that there were opportunities for alternative approaches and additional complementary analyses. In this section, I will critically assess areas for improvement and discuss alternative approaches to enhance the quality of future studies in our laboratory.

7.2.1. Suitability of microcosms and used sampling size for drawing strong conclusions

Microcosm experimental setups afford a high degree of control over variables such as temperature, reaction homogeneity, and exposition conditions, thereby facilitating experimental reproducibility in environmental studies. This level of control and replication is nearly impossible to achieve in most mesocosms studies and in field studies, rendering microcosms ideal for establishing fundamental mechanistic understanding. However, microcosms are not without drawbacks. They can be space-consuming and generate a substantial amount of data that necessitates extensive processing[139,143]. Their potential lack of perfect representativeness for natural ecosystems is a recognized limitation. To address this, we prioritize reproducibility in our microcosm design. One strategy is to use a one-week pre-incubation period. This allows ions and nutrients to reach equilibrium between water and sediment phases, mimicking a more established environment. Previous research highlights the importance of this step[160,161,282]. We also use triplicates for each treatment and include abiotic controls to minimize bias in data interpretation, allow for statistical analysis and thereby enhance reliability of findings. Abiotic controls provided a baseline for non-biological dissipation processes, and enabled to differentiate between biodegradation and simple abiotic loss of the target compound. Together, these strategies helped to generate a more accurate picture of the dynamic interplay between biodegradation and abiotic loss in microcosm experiments.

In microbial ecology, the use of triplicates has become a standard, although several publications still have an insufficient number of replicate experiments to guarantee satisfactory statistical power ($1-\beta \geq 0.6$)[248], where β is the probability of failing to reject the null hypothesis when it is actually false[283]. The direct drawback to insufficient statistical power is the high chance of missing an effect. For instance, in Chapters 4 and 5, when comparing prokaryotic communities between conditions with triplicates, Non-Parametric Multivariate Analysis of Variance (NPMANOVA) consistently failed to reject the null hypothesis, with p-values of at least 0.1. However, comparisons involving larger sample sets (matrices, time, oxygenation) showed p-values ranging from 0.001 to 1, suggesting a potential lack of power to detect significant changes with triplicates. In Chapter 5, we established significant differences in prokaryotic communities between sediment and water phases, consistent with the literature. We conducted NPMANOVA on 100 randomized datasets with fixed numbers of replicates (3, 4, 5, 6, 7, 8, 9, 10, 15, and 20) per condition, and monitored the resulting p-values (see Table 7.1). These results demonstrate that the statistical power would be sufficient with 4 replicates ($1-\beta = 0.59$) and very satisfactory with 5 replicates ($1-\beta = 0.77$). As the number of replicates decreases, the p-value tends to increase, making it increasingly challenging to detect significant differences between conditions. The statistical power of NPMANOVA is evidently insufficient when analysing triplicates. Therefore, when comparing two conditions with only three samples each, even if the null hypothesis should be rejected, the minimum observable

p-value would be p = 0.1 (as observed in Chapters 4 and 5, see Table 7.1). One potential solution would be to increase the threshold for the opposite error, Type I error (also known as α error). This error occurs when a true null hypothesis is rejected, mistakenly concluding there is an effect when actually there is none.

To address this issue, a preliminary experiment could have been designed to evaluate the variability of microbial communities. This could have involved sequencing a realistic maximum number of replicates, such as six, which could realistically be set up and utilized in the experiment. However, when a large number of experimental variables is investigated, the number of microcosms can then become an issue. When constraints such as costs, material availability or required time are of concern such as in the experiments reported in Chapter 4, an alternative approach could have been to reduce the number of micropollutant treatments while concurrently increasing the number of replicates.

Table 7.1. *Statistical power estimation performed on the NPMANOVA test for comparing prokaryotic communities between sediment and water conditions. The dataset underwent rarefaction and randomization to yield 3, 4, 5, 6, 7, 8, 9, 10, 15, and 20 samples (X) per condition, repeated 100 times. The results indicate the frequency of outcomes from the NPMANOVA test, categorized as non-significant (n.s), showing a tendency (°), or being significant (*; **; ***).*

	Number of replicates (X) per condition									
	3X	**4X**	**5X**	**6X**	**7X**	**8X**	**9X**	**10X**	**15X**	**20X**
(n.s) p > 0.10	31	19	15	2	3	1	0	0	0	0
(°) p ∈]0.05, 0.10]	69	22	8	5	3	0	0	0	0	0
(*) p ∈]0.01, 0.05]	0	59	23	15	17	19	5	2	0	0
(**) p ∈]0.001, 0.01]	0	0	54	78	41	33	28	19	0	0
(***) p ≤ 0.001	0	0	0	0	36	47	67	79	100	100
Associated power (1-B) (*i.e.,* relative count of significant tests)	0	0.59	0.77	0.93	0.94	0.99	1.00	1.00	1.00	1.00
Probability to obtain a false negative (B)	1	0.41	0.23	0.07	0.06	0.01	0	0	0	0.

7.2.2. Unassigned sequence data and functional prediction: a case for full-length 16S rRNA and whole metagenomic sequencing

Metabarcoding analysis allowed to compare the impact of microcosm conditions on the composition of prokaryotic communities. It also enabled the search for potential bioindicators of micropollutant degradation in SIP experiments. However, the Silva database used for taxonomic assignment is not up to date with the ongoing strong increase in taxonomic information in the microbial world, and its limited resolution, particularly at the genus and species levels, leads to a notable proportion of unassigned taxa, as observed in our study. In the experiments described in Chapter 4 and 5, over 90% of taxa were unassigned, a strong drawback limiting data analysis to very broad taxonomic levels (Phylum and Family).

Metabarcoding analysis also has limited power in describing the functional potential of a microbial community. Some tools such as PICRUST[284] attempt to predict an inventory of genes and functions from 16S rRNA data, , but their use remains controversial. For more precise taxonomic affiliation and for prediction of microbial functions, full-length 16S rRNA sequencing (FL-16S) and whole metagenome sequencing (WMS) or should be used. Overall, FL-16S rRNA sequencing shows promise as a less expensive and more practical tool than WMS for taxonomic profiling[285] and future microbiota analysis[286]. Compared to 16S rRNA metabarcoding, it enables finer differentiation between closely related organisms at the species level or even at the strain level[287]. This approach has now been utilised in several environmental studies, e.g. on the bacterial community structure in heavily polluted estuaries in China[288]. However, a serious drawback of the FL-16S technique currently is that is relatively new, so databases are not yet well-established. For example, Matsuo et al. (2021) reported that their analysis was limited due to a lack of sufficiently curated databases[289]. Therefore, at present, short length 16S rRNA metabarcoding may remain the best compromise in terms of efficiency and cost.

However, WMS remains necessary for direct functional prediction basing on genes associated with enzymatic reactions. Annotation data on functional genes potentially associated with the degradation of organic contaminants will provide useful information on the response of microbial communities to pollution. In addition, they may provide complementary predictions on the impact of contamination on microbial functions in biogeochemical cycles. For example, an observed decline in the abundance of denitrification genes could serve as an indicator of potential disruption of the nitrogen cycle. In my work, WMS could have been coupled with metformin SIP to identify genes and functions overrepresented in labelled organisms. A similar methodology was successfully employed in a previous study, where functional gene annotation was used to reconstruct complete pathways for the degradation of phenanthrene[180]. This approach could have been effectively applied to metformin biodegradation (Chapter 6 experiments), by identifying over-represented functions in labelled total DNA compared to unlabelled DNA. Following the identification of over-represented functions, we could have examined potential specific roles in either dimethylamine assimilation or metformin biodegradation. In particular, detection of the well-characterized metformin hydrolase gene[92,219] could have confirmed the effectiveness of SIP labelling.

While metagenomic assembled genomes (MAGs) are essential for linking taxonomic affiliation with function in microbial communities, they also have limitations. These limitations include accurately representing non-dominant taxa[290] and assembling plasmids[291]. This could lead to a gap in our understanding of key functions, particularly for less abundant organisms that might be relevant. For example, in Chapter 6, we observed that potential metformin degraders accounted for less than 10% of the total community. However, encouraging new techniques are emerging to improve the accuracy of MAG assembly for these less abundant taxa[290,292,293].

7.2.3. Representativeness of the experimental setup for aquatic ecosystems

Two key points on the performed experiments warrant attention, the concentrations of micropollutants that were used, and the temperature. In these experiments, microcosms were

maintained at 30°C and spiked with doses in milligrams per litre, rather than the naturally encountered micrograms per litre.

In terms of concentration, our aim was to mimic environmental conditions while ensuring compatibility with analytical instruments for monitoring micropollutant dissipation and the formation of transformation products (TPs). Resulting potential biases in prokaryotic responses compared to the situation prevailing *in situ* thus have to be accepted. The choice of a temperature of 30°C for our experiments was dictated by the limited time available enhances biodegradation of micropollutants[294]. We acknowledge that this may have skewed results against psychrophilic organisms, even if psychrotrophic microorganisms with a maximum growth temperature above 20°C are commonly found in natural environments[294]. Temperature will also impact partitioning of pollutants between the investigated water and sediment phases, with sorption decreasing with increasing temperature[295]. In our experiments, however, hydrophobic contaminants (MET and TER) were mainly found in the sediment as expected, and conversely, hydrophilic MFN was mostly found in the water phase. The observed distribution is thus as expected and suggests that temperature may not have severely impacted the representativeness of our experiments.

Other potential biases are possible with regard to toxicological assessment. The commonly accepted concept "the dose makes the poison" would suggest a direct relationship between toxic dose and its detrimental biological effect, and the assumption of a linear dose-effect relationship is the foundation of modern risk assessment. Hence and as done in my work, effects observed at high doses are used to predict lower dose effects (or absence of effect) [296]. However, recent research has shown that non-monotonous dose-effect relationships exist. For example, numerical simulations of the effects of antibiotics on the gut microbiota reveal non-monotonous patterns of effects on microbial communities, since richness and evenness metrics were not affected by an increase in antibiotic concentration[297]. Similarly, pesticide exposure (e.g. to captan, glyphosate, isoproturon, pirimicarb) caused concentration-dependent shifts in microbial communities compared to controls, suggesting adverse effects at both environmentally relevant and high concentrations[150]. Hence, decreasing concentrations of a contaminant over time, due e.g. to sorption or degradation, may be associated with multiple and complex shifts in microbial community composition and such shifts could be both concentration-dependent or concentration-independent.

Finally, our experiments could have benefitted from testing a wider range of contaminant exposures, and assessing alpha and beta diversity, as well as enzymatic activity (e.g., FDA/ATP), at low (environmentally most relevant), intermediate, and high concentrations in preliminary trials. However, a clear impact on prokaryotic community composition was only observed after 70 days (Chapter 4). Thus, the chosen setup ultimately fulfilled our goals of exploring the cocktail effect and its documentation, and captured the core aspects of multi-contamination on prokaryotic communities.

7.3. Outlook, future work

Building on this thesis and as an immediate first objective, a master's project could explore metformin degradation using a culturomics approach. As the thesis was already heavy in laboratory experiments, we did not try to select degraders based on our microcosms presenting biodegradation. Obtaining new strains from SWI experiments, as done from WWTP sludge by Chaignaud et al. (2022)[92], would be of great interest. I propose to use our existing microcosm

setup under both oxic and anoxic conditions to identify metformin-degrading microorganisms with a particular focus on potentially novel pathways, especially in anoxic environments. Corresponding microcosms could also be used to explore how oxygen availability impacts the degradation process. Such a project would involve a series of steps. First, oxic and anoxic microcosms would be subjected to successive spikes of metformin to assess the degradation capabilities of resident microbial communities under different oxygen conditions, and samples would be collected. Next, the method described by Martinez-Vaz et al. (2022)[259] would be adapted to isolate and select microorganisms capable of degrading metformin. This isolation process may require modifications to ensure successful selection under anoxic growth conditions. Obtained pure cultures would be characterised with regard to use of metformin as carbon and nitrogen source. Building upon the HPLC expertise gained during this thesis, the project would monitor metformin dissipation and the formation of transformation products. Additionally, the ability of newly isolated strains to transform metformin by replacing it with its own transformation products in the media would be investigated. Complete genome sequencing and functional annotation would be performed, and random transposon mutagenesis[92] to identify the specific genes essential for metformin degradation, would be employed. The project could potentially lead to the identification of novel pathways involved in metformin degradation, especially under anoxic conditions. Indeed, anoxic metformin degradation remains poorly explored and this would warrant a future doctoral thesis, since Chapter 5 demonstrated the occurrence of metformin biodegradation under anoxic conditions, while Chapter 6 focused on identifying the responsible microorganisms under oxic conditions only.

More generally, it would be worthwhile to better address the dynamic nature of flowing surface waters and its role in micropollutant dissipation than is possible with microcosm experiments. Indeed, microcosms offer only a simplified representation of the SWI and typically depict a steady state situation. Hydraulic regime and sorption are two parameters intimately linked with transport of dissolved contaminants at the SWI[44], with hydraulic regime significantly impacting residence time and reactivity of micropollutants. Therefore, an experiment could now be designed to explore the interplay between hydraulic regime, micropollutant dissipation, and their impact on prokaryotic communities. Given the widespread occurrence of metformin in rivers and its hydrophilic nature, it could serve as the focal point of this experiment. Previous research by the ITES team in a proof of concept laboratory river channel experiment allowed to develop a flow-reactive transport model (FRT) to better understand corresponding processes[44], by following the fate of caffeine under various hydraulic regimes at the SWI. The setup comprises a bench-scale river channel with recirculating water and is still available for experimentation. Thus, the envisaged study could examine metformin dissipation rates and the formation of potential transformation products over time and at different sediment depths within the river channel. This evaluation would be conducted under three distinct hydrological regimes: steady flow, low flow (e.g., 1.5 m/s), and high flow (e.g., 5.0 m/s). By examining these variations, how flow conditions affect both the dissipation rate of metformin, and the composition of the resident prokaryotic communities at the SWI could be determined. Furthermore, the experiment could investigate how combined exposure to metformin and different flow regimes affect prokaryotic communities in water and sediment. A complementary setup involving a mixture of micropollutants could be established to broaden the scope of investigation and address river pollution by multiple contaminants as is typically the case in natural rivers. Development of a numerical model could also be considered to further enhance the research. This model could be used to evaluate metformin dissipation and degradation under different river conditions, incorporating factors such as flow regime, microbial community composition, and the presence of other contaminants. By integrating experimental data with

modelling, a more robust understanding of the complex dynamics governing metformin fate in aquatic ecosystems could be gained.

In this context, sediment depth profiling of both micropollutants and prokaryotic communities and activity should prove interesting. For example, Cébron et al. (2020)[153] observed a shift in prokaryotic communities along longitudinal and vertical gradients, particularly under PAH contamination. Combining hydraulic regime experiments with sediment depth analysis could provide valuable insights into the capacity of micropollutant to penetrate vertically into deeper strata. Given the potentially lower activity levels in these deeper layers compared to the sediment-water interface (SWI), micropollutants may persist for longer periods and community changes may differ from top sediment in direct contact with the water. Moreover, this research could shed light on the possibility of micropollutants infiltrating underground water sources, and the associated risk of drinking water contamination.

To further enhance the investigation, the use of labelled metformin could be considered within this river channel microcosm. After successive pre-exposure to unlabelled metformin to ensure metformin biodegradation, labelled metformin would be introduced under different conditions, e.g. under oxic and anoxic conditions (potentially using a glove box) and at different flow rates. After a defined exposure period, sediment samples would be collected, and DNA would be extracted from the sediment and further processed following a SIP protocol. This analysis would offer valuable insights into the impact of hydraulic flow and oxygen availability on metformin degraders within a river aquatic ecosystem.

7.4. Conclusions

In my thesis, I initially focused on the investigation of the transformation and effect of three commonly used model micropollutants with distinct physical properties. These investigations, coupled with potential future experiments employing the Flow-Reactive Transport (FRT) model[44], may help to predict the fate of micropollutants, individual or in mixtures, and their effect on prokaryotic communities. My findings underscore the importance of considering hitherto overlooked variables in laboratory experiments, and the occurrence of non-additive effects. Failure to account for such variable may result in the underestimation of environmental risks associated with micropollutants.

My research has also yielded valuable insights into micropollutant dissipation at the sediment-water interface. The mathematical method I proposed to analyse the obtained data enabled to quantify and compare the combined effects of different factors, including contaminant-contaminant or contaminant-variable interactions, on prokaryotic community composition. The identification of potential metformin biodegraders using SIP also paves the way for further investigations in metformin degradation pathways and relevant bioindicators of exposure. Overall, this study establishes a foundation for future investigations into the fate of micropollutants at the SWI, and the response of the biotic compartment to micropollutant exposure. Such experiments will clearly need to include considerations of reactive transport and modelling under varying environmental conditions and types of contamination, and to examine the combination of physical and chemical stresses and their impact on microbial communities. Thus, the results obtained in this work underscore the importance of interactions between different scientific disciplines, and the merit of holistic approaches and of strong collaborations, such as those developed between BISE and AIME teams, to address the questions at the basis of this PhD thesis and to open new research perspectives.

References

1. Pesticide Atlas - Facts and Figures about Toxic Chemicals in Agriculture. (Heinrich-Böll-Stiftung, Berlin, p60, 2022).

2. World Food and Agriculture – Statistical Yearbook. (FAO, Rome, p380, 2022).

3. Dowler, C. Revealed: UK shipped more than 10,000 tonnes of banned pesticides overseas in 2020. (2022). https://unearthed.greenpeace.org/2022/02/22/bees-syngenta-paraquat-uk-exports/

4. Ministère de la Transition écologique et de la Cohésion des territoires (2022, 03, 24). Loi Egalim : un nouveau décret pour limiter l'exposition humaine, animale et environnementale aux produits phytopharmaceutiques. https://www.ecologie.gouv.fr/loi-egalim-nouveau-decret-limiter-lexposition-humaine-animale-et-environnementale-aux-produits (2022).

5. González Peña, O. I., López Zavala, M. Á. & Cabral Ruelas, H. Pharmaceuticals market, consumption trends and disease incidence are not driving the pharmaceutical research on water and wastewater. *Int. J. Environ. Res. Public Health.* **18**, 2532 (2021).

6. Beiras, R. Environmental Risk Assessment Of Pharmaceutical And Personal Care Products In Estuarine And Coastal Waters. In Pharmaceuticals in Marine and Coastal Environments 195–252 (Editors: Durán-Álvarez, J.C., Jiménez-Cisneros, B. Elsevier, 2021).

7. Piovani, D., Nikolopoulos, G. K. & Bonovas, S. Non-communicable diseases: the invisible epidemic. *J. Clin. Med.* **11**, 5939 (2022).

8. https://ourworldindata.org/grapher/pharmaceutical-personnel-per-1000.

9. Tansley, A. G. The use and abuse of vegetational concepts and terms. *Ecology* **16**, 284–307 (1935).

10. Grosberg, R. K., Vermeij, G. J. & Wainwright, P. C. Biodiversity in water and on land. *Curr. Biol.* **22**, R900–R903 (2012).

11. Mauser, K. M., Brühl, C. A. & Zaller, J. G. Herbicide Effects on Nontarget Organisms, Biodiversity and Ecosystem Functions. In Encyclopedia of Biodiversity 239–257 (Editors: Scheiner, S.M., Academic Press, Elsevier, 2024).

12. Bertini, S. C. B. & Azevedo, L. C. B. Soil Microbe Contributions in The Regulation Of The Global Carbon Cycle. In Microbiome Under Changing Climate 69–84 (Editors: Kumar, A., Singh, J., Fernando Romanholo Ferreira, L., Woodhead Publishing, Elsevier, 2022).

13. Dobretsov, G. E., Kharitonenkov, I. G., Mishiev, V. E. & Vladimirov, I. A. Relation between fluorescence and circular dichroism of the complex of the fluorescence

probe 4-dimethylaminochalcone with serum albumin. *Biofizika* **20**, 581–585 (1975).

14. Scherer-Lorenzen, M. et al. Pathways for cross-boundary effects of biodiversity on ecosystem functioning. *Trends Evol. Ecol.* **37**, 454–467 (2022).

15. Morin, P.J. & McGrady-Steed, J. Biodiversity and ecosystem functioning in aquatic microbial systems: a new analysis of temporal variation and species richness-predictability relations. *Oikos* **104**, 458–466 (2004).

16. Elsner, M. & Imfeld, G. Compound-specific isotope analysis (CSIA) of micropollutants in the environment — current developments and future challenges. *Curr. Opin. Biotechnol.* **41**, 60–72 (2016).

17. Gerbersdorf, S. U. et al. Anthropogenic trace compounds (ATCs) in aquatic habitats — Research needs on sources, fate, detection and toxicity to ensure timely elimination strategies and risk management. *Environ. Int.* **79**, 85–105 (2015).

18. Silva, L. L. S., Moreira, C. G., Curzio, B. A. & Da Fonseca, F. V. micropollutant removal from water by membrane and advanced oxidation processes—a review. *J. Water Resource Prot.* **9**, 411–431 (2017).

19. Carles, L. et al. Meta-analysis of glyphosate contamination in surface waters and dissipation by biofilms. *Environ. Int.* **124**, 284–293 (2019).

20. Arufe, M. I., Arellano, J., Moreno, M. J. & Sarasquete, C. Toxicity of a commercial herbicide containing terbutryn and triasulfuron to seabream (*Sparus aurata* L.) larvae: a comparison with the Microtox test. *Environ. Toxicol. Chem.* **59**, 209–216 (2004).

21. Guidelines for drinking-water quality. (World Health Organization, Geneva, 1993).

22. Agency for toxic substances and disease registry (ATSDR). 2003. Toxicological profile for atrazine. Atlanta, GA: U.S. Department of Health and Human Services, Public Health Services.

23. Seckar, J. A. et al. Environmental fate and effects of nicotine released during cigarette production. *Environ. Toxicol. Chem.* **27**, 1505–1514 (2008).

24. Hillebrand, O., Nödler, K., Licha, T., Sauter, M. & Geyer, T. Caffeine as an indicator for the quantification of untreated wastewater in karst systems. *Water Res.* **46**, 395–402 (2012).

25. Tassoulas, L. J., Robinson, A., Martinez-Vaz, B., Aukema, K. G. & Wackett, L. P. Filling in the gaps in metformin biodegradation: a new enzyme and a metabolic pathway for guanylurea. *Appl. Environ. Microbiol.* **87**, e03003-20 (2021).

26. Niemuth, N. J. & Klaper, R. D. Emerging wastewater contaminant metformin causes intersex and reduced fecundity in fish. *Chemosphere* **135**, 38–45 (2015).

27. Kummu, M. et al. The world's road to water scarcity: shortage and stress in the 20th century and pathways towards sustainability. *Sci. Rep.* **6**, 38495 (2016).

28. UNESCO global water assessment programme (2021). The United Nations world water development Report 2021. UNESCO. www.unesco.org/water/wwap.

29. Lin, L., Yang, H. & Xu, X. Effects of water pollution on human health and disease heterogeneity: a review. *Front. Environ. Sci*. **10**, 880246 (2022).

30. Wallet, F. Pesticides / Biocides. Environnement Risques Santé 19, 147–148 (Editor: John Libbey Eurotext, 2020).

31. Luft, A., Wagner, M. & Ternes, T. A. Transformation of biocides irgarol and terbutryn in the biological wastewater treatment. *Environ. Sci. Technol.* **48**, 244–254 (2014).

32. Cuñat, A., Álvarez-Ruiz, R., Morales Suarez-Varela, M. M. & Pico, Y. Suspected-screening assessment of the occurrence of organic compounds in sewage sludge. *J. Environ. Manage.* **308**, 114587 (2022).

33. Anses. Statut juridique des produits frontières : Relèvent-ils de la réglementation du médicament vétérinaire ? Ansm, 2019. https://www.anses.fr/fr/system/fi les/ ANMV-notedepositionqualifi cationdesproduitsfrontieres.pdf.

34. European directorate for the quality of medicines & healthcare. European Pharmacopoeia (11th ed.). Council of Europe. (2022).

35. Bouzas-Monroy, A., Wilkinson, J. L., Melling, M. & Boxall, A. B. A. Assessment of the potential ecotoxicological effects of pharmaceuticals in the world's rivers. *Environ. Toxicol. Chem.* **41**, 2008–2020 (2022).

36. Aus Der Beek, T. et al. Pharmaceuticals in the environment - global occurrences and perspectives. *Environ. Toxicol. Chem.* **35**, 823–835 (2016).

37. Delgado, N., Orozco, J., Zambrano, S., Casas-Zapata, J. C. & Marino, D. Veterinary pharmaceutical as emerging contaminants in wastewater and surface water: An overview. *J. Hazard Mater*. **460**, 132431 (2023).

38. Clara, M. et al. Occurrence of polycyclic musks in wastewater and receiving water bodies and fate during wastewater treatment. *Chemosphere* **82**, 1116–1123 (2011).

39. Montes-Grajales, D., Fennix-Agudelo, M. & Miranda-Castro, W. Occurrence of personal care products as emerging chemicals of concern in water resources: A review. *Sci. Total Environ.* **595**, 601–614 (2017).

40. Nørgaard, K. B. & Cedergreen, N. Pesticide cocktails can interact synergistically on aquatic crustaceans. *Environ. Sci. Pollut. Res.* **17**, 957–967 (2010).

41. Ruck, G. et al. Avoidance behaviour of aquatic macroinvertebrates for real-time detection of micropollutant surge in wastewater effluents. *Water Res*. **242**, 120228 (2023).

42. Van Meter, R. J., Glinski, D. A., Purucker, S. T. & Henderson, W. M. Influence of exposure to pesticide mixtures on the metabolomic profile in post-metamorphic green frogs (*Lithobates clamitans*). *Sci. Total Environ.* **624**, 1348–1359 (2018).

43. Prieto-Espinoza, M., Di Chiara Roupert, R., Belfort, B., Weill, S. & Imfeld, G. Reactive transport of micropollutants in laboratory aquifers undergoing transient exposure periods. *Sci. Total Environ.* **856**, 159170 (2023).

44. Drouin, G. et al. Pollutant dissipation at the sediment-water interface: a robust discrete continuum numerical model and recirculating laboratory experiments. *Water Resour. Res.* **57**, e2020wr028932 (2021).

45. Junginger, T. Transport and degradation of urban biocides from facades to groundwater. [Doctoral dissertation, Strasbourg University]. (2023). https://theses.fr/2023STRAH001.

46. Wilkinson, J. L. et al. Pharmaceutical pollution of the world's rivers. *Proc. Natl. Acad. Sci. U.S.A.* **119**, e2113947119 (2022).

47. Jesus, F. et al. Ozonation of selected pharmaceutical and personal care products in secondary effluent—Degradation kinetics and environmental assessment. *Toxics* **10**, 765 (2022).

48. Gouveia, T. I. A. et al. Nanofiltration combined with ozone-based processes for the removal of antineoplastic drugs from wastewater effluents. *J. Environ. Manage.* **348**, 119314 (2023).

49. Hey, G. et al. Removal of pharmaceuticals in WWTP effluents by ozone and hydrogen peroxide. *Water SA* **40**, 165 (2014).

50. OECD. Test No. 106: Adsorption -- desorption using a batch equilibrium method. (OECD, 2000).

51. PubChem database https://pubchem.ncbi.nlm.nih.gov.

52. Haenelt, S. et al. The fate of sulfonamide resistance genes and anthropogenic pollution marker *intI1* after discharge of wastewater into a pristine river stream. *Front. Microbiol.* **14**, 1058350 (2023).

53. Pérez-Lucas, G., Vela, N., El Aatik, A. & Navarro, S. Environmental Risk of Groundwater Pollution by Pesticide Leaching Through the Soil Profile. In Pesticides - use and misuse and their impact in the environment (Editors: Larramendy, M. & Soloneski, S., IntechOpen, 2019).

54. Gejlsbjerg, B., Klinge, C. & Madsen, T. Mineralization of organic contaminants in sludge-soil mixtures. *Environ. Toxicol. Chem.* **20**, 698 (2001).

55. Donner, E. et al. Ecotoxicity of carbamazepine and its UV photolysis transformation products. *Sci. Total Environ.* **443**, 870–876 (2013).

56. Moore, M. T., Greenway, S. L., Farris, J. L. & Guerra, B. Assessing caffeine as an emerging environmental concern using conventional approaches. *Arch. Environ. Contam. Toxicol.* **54**, 31–35 (2008).

57. Shen, C. et al. Predicting and assessing the toxicity and ecological risk of seven widely used neonicotinoid insecticides and their aerobic transformation products to aquatic organisms. *Sci. Total Environ.* **847**, 157670 (2022).

58. Boxall, A. B. A., Sinclair, C. J., Fenner, K., Kolpin, D. & Maund, S. J. Peer reviewed: When synthetic chemicals degrade in the environment. *Environ. Sci. Technol.* **38**, 368A-375A (2004).

59. Maggi, F & Tang, F. H. M. The global pesticide budget and river discharge to oceans. *Nature* **620**, 1013–1017 (2023).

60. État de la nappe phréatique d'Alsace et des aquifères du Sundgau : Premiers résultats sur les nitrates et les pesticides en 2016. Rapport APRONA (2016).

61. Junginger, T., Payraudeau, S. & Imfeld, G. Transformation and stable isotope fractionation of the urban biocide terbutryn during biodegradation, photodegradation and abiotic hydrolysis. *Chemosphere* **305**, 135329 (2022).

62. Isop, L. M. et al. Metformin: The winding path from understanding its molecular mechanisms to proving therapeutic benefits in neurodegenerative disorders. *Pharmaceuticals* **16**, 1714 (2023).

63. Pistocchi, A. et al. A screening study of the spatial distribution and cumulative toxicity of agricultural pesticides in the European Union's waters. *Front. Environ. Sci.* **11**, 1101316 (2023).

64. The Lakes Handbook: Limnology and Limnetic Ecology - Volume 1. (Editors: O'Sullivan, P.E., Reynolds, C.S., Blackwell Science Ltd, 2003).

65. Santschi, P., Höhener, P., Benoit, G. & Buchholtz-ten Brink, M. Chemical processes at the sediment-water interface. *Mar. Chem.* **30**, 269–315 (1990).

66. Herschy, R. W. et al. Paleolimnology. Encyclopedia of Lakes and Reservoirs 594–596. (Editors: Bengtsson, L., Herschy, R.W., Fairbridge, R.W., Springer, Dordrecht, 2012).

67. Bloesch, J. Sediments of aquatic ecosystems. in Encyclopedia of Inland Waters 479–490. (Editors: Likens, G.E., Academic Press, Elsevier, 2009).

68. Mugnai, R., Messana, G. & Di Lorenzo, T. The hyporheic zone and its functions: revision and research status in Neotropical regions. *Braz. J. Biol.* **75**, 524–534 (2015).

69. Peter, K. T. et al. Evaluating emerging organic contaminant removal in an engineered hyporheic zone using high resolution mass spectrometry. *Water Res*. **150**, 140–152 (2019).

70. White, D. S. Perspectives on defining and delineating hyporheic zones. *J. N. Am. Benthol. Soc*. **12**, 61–69 (1993).

71. Lorke, A. & MacIntyre, S. The Benthic Boundary Layer (in Rivers, Lakes, and Reservoirs). in Encyclopedia of Inland Waters 505–514. (Editors: Likens, G.E., Academic Press, Elsevier, 2009).

72. Hüneke, H. & Henrich, R. Pelagic sedimentation in modern and ancient oceans. in Developments in Sedimentology **63**, 215–351 (2011).

73. Datry, T., Dole-Olivier, M.J., Marmonier, P., Claret, C., Perrin, JF. et al. La zone hyporhéique, une composante à ne pas négliger dans l'état des lieux et la restauration des cours d'eau. Ingénieries - E A T, 2008, p. 3 - p. 18.

74. Golovko, O., Rehrl, A.-L., Köhler, S. & Ahrens, L. Organic micropollutants in water and sediment from Lake Mälaren, Sweden. *Chemosphere* **258**, 127293 (2020).

75. Gao, J. P., Maguhn, J., Spitzauer, P. & Kettrup, A. Sorption of pesticides in the sediment of the Teufelsweiher pond (Southern Germany). II: Competitive adsorption, desorption of aged residues and effect of dissolved organic carbon. *Water Res*. **32**, 2089–2094 (1998).

76. Huang, J. C. Effect of selected factors on pesticide sorption and desorption in the aquatic system. *J. Water Pollut. Control Fed.* **43**, 1739–1748 (1971).

77. Copaja, S. V. & Gatica-Jeria, P. Effects of clay content in soil on pesticides sorption process. *J. Chil. Chem. Soc.* **66**, 5086–5092 (2021).

78. Chaumet, B. et al. Role of pond sediments for trapping pesticides in an agricultural catchment (Auradé, SW France): distribution and controlling factors. *Water* **13**, 1734 (2021).

79. El-Aswad, A. F., Fouad, M. R., Badawy, M. E. I. & Aly, M. I. Effect of calcium carbonate content on potential pesticide adsorption and desorption in calcareous soil. *Commun. Soil. Sci. Plan.* **54**, 1379–1387 (2023).

80. He, W. et al. The partitioning behavior of persistent toxicant organic contaminants in eutrophic sediments: Coefficients and effects of fluorescent organic matter and particle size. *Environ. Pollut.* **219**, 724–734 (2016).

81. Wu, D., Yun, Y., Jiang, L. & Wu, C. Influence of dissolved organic matter on sorption and desorption of MCPA in ferralsol. *Sci. Total Environ.* **616–617**, 1449–1456 (2018).

82. Passeport, E., Benoit, P., Bergheaud, V., Coquet, Y. & Tournebize, J. Selected pesticides adsorption and desorption in substrates from artificial wetland and forest buffer. *Environ. Toxicol. Chem.* **30**, 1669–1676 (2011).

83. Imfeld, G. et al. The role of ponds in pesticide dissipation at the agricultural catchment scale: a critical review. *Water* **13**, 1202 (2021).

84. Valverde, A. et al. Pollution shapes the microbial communities in river water and sediments from the Olifants iver catchment, South Africa. *Arch. Microbiol.* **203**, 295–303 (2021).

85. European Food Safety Authority (EFSA) et al. Peer review of the pesticide risk assessment of the active substance S-metolachlor excluding the assessment of the endocrine disrupting properties. *European Food Safety Authority* **21**, (2023).

86. Lochte, K. & Pfannkuche, O. Processes Driven by The Small Sized Organisms at The Water-Sediment Interface. In Ocean Margin Systems 405–418 (Editors. Wefer, G., Billett, D., Hebbeln, D., Jørgensen, B.B., Schlüter, M., van Weering, T.C.E., Springer Berlin Heidelberg, Berlin, Heidelberg, 2002).

87. Katagi, T. Pesticide behavior in modified water-sediment systems. *Pestic. Sci.* **41**, 121–132 (2016).

88. Katagi, T. Direct photolysis mechanism of pesticides in water. *Pestic. Sci.* **43**, 57–72 (2018).

89. Masbou, J., Drouin, G., Payraudeau, S. & Imfeld, G. Carbon and nitrogen stable isotope fractionation during abiotic hydrolysis of pesticides. *Chemosphere* **213**, 368–376 (2018).

90. Tebes-Stevens, C., Patel, J. M., Jones, W. J. & Weber, E. J. Prediction of hydrolysis products of organic chemicals under environmental pH conditions. *Environ. Sci. Technol.* **51**, 5008–5016 (2017).

91. Fondriest Environmental, Inc. “pH of Water.” Fundamentals of environmental measurements. 19 Nov. 2013. Web. < https://www.fondriest.com/environmental-measurements/parameters/water-quality/ph/.

92. Chaignaud, P. et al. A methylotrophic bacterium growing with the antidiabetic drug metformin as its sole carbon, nitrogen and energy source. *Microorganisms* **10**, 2302 (2022).

93. Rice, P. J., Anderson, T. A. & Coats, J. R. Effect of sediment on the fate of metolachlor and atrazine in surface water. *Environ. Toxicol. Chem.* **23**, 1145–1155 (2004).

94. Drouin, G. et al. Direct and indirect photodegradation of atrazine and S -metolachlor in agriculturally impacted surface water and associated C and N isotope fractionation. *Environ. Sci. Process.* **23**, 1791–1802 (2021).

95. Metformin hydrochloride. Version 3 – November 2023 AstraZeneca report https://www.astrazeneca.com/content/dam/az/PDF/Sustainability/era/Metformin-hydrochloride.pdf.

96. Parkerton, T. F., French-McCay, D., De Jourdan, B., Lee, K. & Coelho, G. Adopting a toxic unit model paradigm in design, analysis and interpretation of oil toxicity testing. *Aquat. Toxicol.* **255**, 106392 (2023).

97. Joly, P. et al. Impact of maize formulated herbicides mesotrione and s-metolachlor, applied alone and in mixture, on soil microbial communities. *ISRN Ecol.* **2012**, 1–9 (2012).

98. Van Den Brink, P.J. et al. Effects of a herbicide–insecticide mixture in freshwater microcosms: Risk assessment and ecological effect chain. *Environ. Pollut.* **157**, 237–249 (2009).

99. Xiao, P., Liu, F., Liu, Y., Yao, S. & Zhu, G. Effects of pesticide mixtures on zooplankton assemblages in aquatic microcosms simulating rice paddy fields. *Bull. Environ. Contam. Toxicol.* **99**, 27–32 (2017).

100. Spilsbury, F., Kisielius, V., Bester, K. & Backhaus, T. Ecotoxicological mixture risk assessment of 35 pharmaceuticals in wastewater effluents following post-treatment with ozone and/or granulated activated carbon. *Sci. Total Environ.* **906**, 167440 (2024).

101. Inostroza, P. A., Elgueta, S., Krauss, M., Brack, W. & Backhaus, T. A multi-scenario risk assessment strategy applied to mixtures of chemicals of emerging concern in the river Aconcagua basin in Central Chile. *Sci. Total Environ.* **921**, 171054 (2024).

102. Wali, S. U. & Alias, N. Multi-pollutant approach to model contaminants flow in surface and groundwater: A review. *IOP Conf. Ser.: Mater. Sci. Eng*. **884**, 012030 (2020).

103. Xie, F. et al. A Prediction model of water in situ data change under the influence of environmental variables in remote sensing validation. *Remote Sens.* **13**, 70 (2020).

104. European Commission. Directorate general for health and consumers. toxicity and assessment of chemical mixtures. (Publications Office, LU, 2012).

105. Li, K.-B., Cheng, J.-T., Wang, X.-F., Zhou, Y. & Liu, W.-P. Degradation of herbicides atrazine and bentazone applied alone and in combination in soils. *Pedosphere* **18**, 265–272 (2008).

106. Fu, Q. et al. Comprehensive screening of polar emerging organic contaminants including PFASs and evaluation of the trophic transfer behavior in a freshwater food web. *Water Res*. **218**, 118514 (2022).

107. Tanvir, R. U., Hu, Z., Zhang, Y. & Lu, J. Cyanobacterial community succession and associated cyanotoxin production in hypereutrophic and eutrophic freshwaters. *Environ. Pollut.* **290**, 118056 (2021).

108. Xu, X., Wu, C., Xie, D. & Ma, J. Sources, migration, transformation, and environmental effects of organic carbon in eutrophic lakes: a critical review. *Int. J. Environ. Res. Public Health.* ***20***, 860 (2023).

109. Houghton, R. A. The contemporary carbon cycle. in Treatise on Geochemistry 399–435 (Elsevier, 2014).

110. The input and mineralization of organic carbon in anaerobic aquatic sediments. *Adv. Microb. Ecol.* **7**, 93-113 (1984).

111. Chen, Q. et al. Correspondence between DOM molecules and microbial community in a subtropical coastal estuary on a spatiotemporal scale. *Environ. Int.* **154**, 106558 (2021).

112. Isolda, A. & Hayasaka, S. S. Effect of herbicide residues on microbial processes in pond sediment. *Arch. Environ. Contam. Toxicol.* **20**, 81–86 (1991).

113. Kiene, R. P. & Capone, D. G. Stimulation of methanogenesis by aldicarb and several other n -methyl carbamate pesticides. *Appl. Environ. Microbiol.* **51**, 1247–1251 (1986).

114. Rumschlag, S. L. et al. Pesticides alter ecosystem respiration via phytoplankton abundance and community structure: Effects on the carbon cycle? *Glob. Change Biol.* **28**, 1091–1102 (2022).

115. Sim, J. X. F. et al. Impact of twenty pesticides on soil carbon microbial functions and community composition. *Chemosphere* **307**, 135820 (2022).

116. Ussiri, D. A. N. & Lal, R. Introduction to global carbon cycling: an overview of the global carbon cycle. in carbon sequestration for climate change mitigation and adaptation 61–76 (Springer International Publishing, Cham, 2017).

117. Fáberová, M., Ivanová, L., Szabová, P., Štolcová, M. & Bodík, I. The influence of selected pharmaceuticals on biogas production from laboratory and real anaerobic sludge. *Environ. Sci. Pollut. Res.* **26**, 31846–31855 (2019).

118. Appels, L., Baeyens, J., Degrève, J. & Dewil, R. Principles and potential of the anaerobic digestion of waste-activated sludge. *Prog. Energ. Combust.* **34**, 755–781 (2008).

119. Zehr, J. P. & Kudela, R. M. Nitrogen cycle of the open ocean: from genes to ecosystems. *Annu. Rev. Mar. Sci.* **3**, 197–225 (2011).

120. Pashaei, R., Zahedipour-Sheshglani, P., Dzingelevičienė, R., Abbasi, S. & Rees, R. M. Effects of pharmaceuticals on the nitrogen cycle in water and soil: a review. *Environ. Monit. Assess.* **194**, 105 (2022).

121. Wankel, S. D., Kendall, C. & Paytan, A. Using nitrate dual isotopic composition (δ 15 N and δ 18 O) as a tool for exploring sources and cycling of nitrate in an estuarine system: Elkhorn Slough, California. *J. Geophys. Res.* **114**, 2008JG000729 (2009).

122. Du, P. et al. Effects of trifluralin on the soil microbial community and functional groups involved in nitrogen cycling. *J. Hazard Mater*. **353**, 204–213 (2018).

123. Chen, Y., Su, X., Wang, Y., Zhao, S. & He, Q. Short-term responses of denitrification to chlorothalonil in riparian sediments: Process, mechanism and implication. *J. Chem. Eng.* **358**, 1390–1398 (2019).

124. Elias, D. & Bernot, M. J. Effects of atrazine, metolachlor, carbaryl and chlorothalonil on benthic microbes and their nutrient dynamics. *PLoS ONE* **9**, e109190 (2014).

125. Enrich-Prast, A. Effect of pesticides on nitrification in aquatic sediment. *Braz. J. Biol.* **66**, 405–412 (2006).

126. Feris, K. P. et al. Structure and seasonal dynamics of hyporheic zone microbial communities in free-stone rivers of the estern United States. *Microb. Ecol.* **46**, 200–215 (2003).

127. Imfeld, G. & Vuilleumier, S. Measuring the effects of pesticides on bacterial communities in soil: a critical review. *Eur. J. Soil Biol.* **49**, 22–30 (2012).

128. The University of Hong Kong & Gu, J.-D. Microbial ecotoxicology as an emerging research subject. *Appl. Env. Biotechnol*. **4**, 1–4 (2019).

129. Jessup, C. M. et al. Big questions, small worlds: microbial model systems in ecology. *Trends Evol. Ecol.* **19**, 189–197 (2004).

130. Coelho, F. J. R. C. et al. Interactive effects of global climate change and pollution on marine microbes: the way ahead. *Ecol. Evol.* **3**, 1808–1818 (2013).

131. Ivshina, I., Bazhutin, G. & Tyumina, E. *Rhodococcus* strains as a good biotool for neutralizing pharmaceutical pollutants and obtaining therapeutically valuable products: Through the past into the future. *Front. Microbiol.* **13**, 967127 (2022).

132. Zhu, J., Fu, L., Jin, C., Meng, Z. & Yang, N. Study on the isolation of two atrazine-degrading bacteria and the development of a microbial agent. *Microorganisms* **7**, 80 (2019).

133. Ma, L. et al. Rapid biodegradation of atrazine by *Ensifer* sp. strain and its degradation genes. *Int. Biodet. Biodeg.* **116**, 133–140 (2017).

134. Devers, M., Azhari, N. E., Kolic, N.-U. & Martin-Laurent, F. Detection and organization of atrazine-degrading genetic potential of seventeen bacterial isolates belonging to divergent taxa indicate a recent common origin of their catabolic functions. *FEMS Microbiol. Lett.* **273**, 78–86 (2007).

135. Wade, W. Unculturable bacteria--the uncharacterized organisms that cause oral infections. *J. Roy. Soc. Med.* **95**, 81–83 (2002).

136. Rastogi, G. & Sani, R. K. Molecular techniques to assess microbial community structure, function, and dynamics in the environment. in Microbes and Microbial Technology (eds. Ahmad, I., Ahmad, F. & Pichtel, J.) 29–57 (Springer New York, New York, NY, 2011).

137. Meroz, N., Tovi, N., Sorokin, Y. & Friedman, J. Community composition of microbial microcosms follows simple assembly rules at evolutionary timescales. *Nat. Commun.* **12**, 2891 (2021).

138. Bhattacharya, S., Vijayalakshmi, N. & Parija, S. C. Uncultivable bacteria: implications and recent trends towards identification. *Indian J. Med. Microbiol.* **20**, 174–177 (2002).

139. Benton, T. G., Solan, M., Travis, J. M. J. & Sait, S. M. Microcosm experiments can inform global ecological problems. *Trends Evol. Ecol.* **22**, 516–521 (2007).

140. Ghiglione, J.-F., Martin-Laurent, F., Stachowski-Haberkorn, S., Pesce, S. & Vuilleumier, S. The coming of age of microbial ecotoxicology: report on the first two meetings in France. *Environ. Sci. Pollut. Res.* **21**, 14241–14245 (2014).

141. Ghiglione, J.-F., Martin-Laurent, F. & Pesce, S. Microbial ecotoxicology: an emerging discipline facing contemporary environmental threats. *Environ. Sci. Pollut. Res.* **23**, 3981–3983 (2016).

142. Karpun, N. N. et al. Side effects of traditional pesticides on soil microbial respiration in orchards on the Russian Black Sea coast. *Chemosphere* **275**, 130040 (2021).

143. Albarano, L. et al. Marine sediment toxicity: A focus on micro- and mesocosms towards remediation. *Sci. Total Environ.* **708**, 134837 (2020).

144. Poursat, B. A. J. et al. Biodegradation of metformin and its transformation product, guanylurea, by natural and exposed microbial communities. *Environ. Toxicol. Chem.* **182**, 109414 (2019).

145. Aemig, Q. et al. Organic micropollutants' distribution within sludge organic matter fractions explains their dynamic during sewage sludge anaerobic digestion followed by composting. *Environ. Sci. Pollut. Res.* **26**, 5820–5830 (2019).

146. Achermann, S. et al. Trends in micropollutant biotransformation along a solids retention time gradient. *Environ. Sci. Technol.* **52**, 11601-11611 (2018)

147. Wang, W. et al. Impact of anthropogenic activities on the sediment microbial communities of Baiyangdian shallow lake. *Int. J. Sediment Res*. **35**, 180–192 (2020).

148. Powell, S. M., Bowman, J. P., Snape, I. & Stark, J. S. Microbial community variation in pristine and polluted nearshore Antarctic sediments. *FEMS Microbiol. Ecol.* **45**, 135–145 (2003).

149. Cao, Y. et al. Relationships between sediment microbial communities and pollutants in two California salt marshes. *Microb. Ecol.* **52**, 619–633 (2006).

150. Widenfalk, A., Bertilsson, S., Sundh, I. & Goedkoop, W. Effects of pesticides on community composition and activity of sediment microbes – responses at various levels of microbial community organization. *Environ. Pollut.* **152**, 576–584 (2008).

151. Droz, B. et al. Phase transfer and biodegradation of pesticides in water–sediment systems explored by compound-specific isotope analysis and conceptual modelling. *Environ. Sci. Technol.* **55**, 4720–4728 (2021).

152. Tisler, S. & Zwiener, C. Aerobic and anaerobic formation and biodegradation of guanyl urea and other transformation products of metformin. *Water Res*. **149**, 130–135 (2019).

153. Cébron, A., Borreca, A., Beguiristain, T., Biache, C. & Faure, P. Taxonomic and functional trait-based approaches suggest that aerobic and anaerobic soil microorganisms allow the natural attenuation of oil from natural seeps. *Sci. Rep.* **12**, 7245 (2022).

154. Alvarez-Zaldívar, P., Payraudeau, S., Meite, F., Masbou, J. & Imfeld, G. Pesticide degradation and export losses at the catchment scale: insights from compound-specific isotope analysis (CSIA). *Water Res*. **139**, 198–207 (2018).

155. Drouin, G. Micropollutant dissipation at the sediment-water interface by coupling modelling and compound-specific isotope analysis. [Doctoral dissertation, Strasbourg University]. (2020). http://www.theses.fr/2020STRAH018.

156. Droz-Dit-Busset, B. Pesticides dissipation at the sediment-water interface: insight from compound-specific isotope analysis (CSIA). [Doctoral dissertation, Strasbourg University]. (2020). http://www.theses.fr/2020STRAH015.

157. Barros, N., Feijoo, S., Pérez-Cruzado, C. & Hansen, L. D. Effect of soil storage at 4 °C on the calorespirometric measurements of soil microbial metabolism. *AIMS Microbiol.* **3**, 762–773 (2017).

158. Tennant, R. K. et al. In-situ sequencing reveals the effect of storage on lacustrine sediment microbiome demographics and functionality. *Environ. Microbiome* **17**, 5 (2022).

159. OECD. Test No. 309: Aerobic mineralisation in surface water – simulation biodegradation test. (OECD, 2004).

160. Torabi, E., Wiegert, C., Guyot, B., Vuilleumier, S. & Imfeld, G. Dissipation of S-metolachlor and butachlor in agricultural soils and responses of bacterial communities: Insights from compound-specific isotope and biomolecular analyses. *Environ. Sci.* **92**, 163–175 (2020).

161. Comeau, L.-P., Lai, D. Y. F., Cui, J. J. & Hartill, J. Soil heterotrophic respiration assessment using minimally disturbed soil microcosm cores. *MethodsX* **5**, 834–840 (2018).

162. Webster, G. et al. A comparison of stable-isotope probing of DNA and phospholipid fatty acids to study prokaryotic functional diversity in sulfate-reducing marine sediment enrichment slurries. *Environ. Microbiol.* **8**, 1575–1589 (2006).

163. Neufeld, J. D. et al. DNA stable-isotope probing. *Nat. Protoc.* **2**, 860–866 (2007).

164. Dunford, E. A. & Neufeld, J. D. DNA Stable-Isotope Probing (DNA-SIP). *JoVE* **42**, 2027 (2010)

165. Gilevska, T. et al. Simple extraction methods for pesticide compound-specific isotope analysis from environmental samples. *MethodsX* **9**, 101880 (2022).

166. Gilevska, T. et al. Do pesticides degrade in surface water receiving runoff from agricultural catchments? Combining passive samples (POCIS) and compound-specific isotope analysis. *Sci. Total Environ.* **842**, 156735 (2022).

167. B. Magnusson and U. Örnemark (eds.) Eurachem Guide: The fitness for purpose of analytical methods – A laboratory guide to method validation and related topics, (2nd ed. 2014). ISBN 978-91-87461-59-0. Available from www.eurachem.org.

168. Theodorsson, E. Limit of detection, limit of quantification and limit of blank. European Federation of Clinical Chemistry and Laboratory Medicine. Available at https://www.eflm.eu/files/efcc/Zagreb-Theodorsson_2.pdf.

169. Takahashi, S., Tomita, J., Nishioka, K., Hisada, T. & Nishijima, M. Development of a prokaryotic universal primer for simultaneous analysis of bacteria and archaea using next-generation sequencing. *PLoS ONE* **9**, e105592 (2014).

170. Callahan, B. J. et al. DADA2: High-resolution sample inference from Illumina amplicon data. *Nat. Methods* **13**, 581–583 (2016).

171. Adam, G. & Duncan, H. Development of a sensitive and rapid method for the measurement of total microbial activity using fluorescein diacetate (FDA) in a range of soils. *Soil Biol. Biochem.* **33**, 943–951 (2001).

172. Amalfitano, S. et al. Water quality and total microbial load: a double-threshold identification procedure intended for space applications. *Front. Microbiol.* **9**, 2903 (2018).

173. McMurdie, P. J. & Holmes, S. Waste not, want not: why rarefying microbiome data is inadmissible. *PLoS Comput. Biol*. **10**, e1003531 (2014).

174. Buttigieg, P. L. & Ramette, A. A guide to statistical analysis in microbial ecology: a community-focused, living review of multivariate data analyses. *FEMS Microbiol. Ecol.* **90**, 543–550 (2014).

175. Benjamini, Y. & Hochberg, Y. Controlling the false discovery rate: a practical and powerful approach to multiple testing. J. R. *Stat. Soc., Ser. B, Methodol.* **57**, 289-300. (1995).

176. García, L. V. Escaping the Bonferroni iron claw in ecological studies. *Oikos* **105**, 657–663 (2004).

177. Ricotta, C. & Podani, J. On some properties of the Bray-Curtis dissimilarity and their ecological meaning. *Ecol. Complex.* **31**, 201–205 (2017).

178. Anderson, M. J. A new method for non-parametric multivariate analysis of variance. *Austral Ecol.* **26**, 32–46 (2001).

179. Segata, N. et al. Metagenomic biomarker discovery and explanation. *Genome Biol.* **12**, R60 (2011).

180. Thomas, F., Corre, E. & Cébron, A. Stable isotope probing and metagenomics highlight the effect of plants on uncultured phenanthrene-degrading bacterial consortium in polluted soil. *ISME J.* **13**, 1814–1830 (2019).

181. Farhan Ul Haque, M., Hernández, M., Crombie, A. T. & Murrell, J. C. Identification of active gaseous-alkane degraders at natural gas seeps. *ISME J.* **16**, 1705–1716 (2022).

182. Wang, Z., Walker, G. W., Muir, D. C. G. & Nagatani-Yoshida, K. Toward a global understanding of chemical pollution: a first comprehensive analysis of national and regional chemical inventories. *Environ. Sci. Technol.* **54**, 2575–2584 (2020).

183. Filipova, M. Challenges and problems modern ecotoxicology faces. *Appl. Sci. Res*. **1**, 140–143 (2012).

184. Posselt, M. et al. Bacterial diversity controls transformation of wastewater-derived organic contaminants in river-simulating flumes. *Environ. Sci. Technol.* **54**, 5467–5479 (2020).

185. Gong, J., Ran, Y., Chen, D., Yang, Y. & Zeng, E. Y. Association of endocrine-disrupting chemicals with total organic carbon in riverine water and suspended particulate matter from the Pearl River, China. *Environ. Toxicol. Chem.* **31**, 2456–2464 (2012).

186. Schallenberg, M. & Kalff, J. The ecology of sediment bacteria in lakes and comparisons with other aquatic ecosystems. *Ecology* **74**, 919–934 (1993).

187. Wang, X. et al. Identification of microbial strategies for labile substrate utilization at phylogenetic classification using a microcosm approach. *Soil Biol. Biochem.* **153**, 107970 (2021).

188. Otte, J. M. et al. Sterilization impacts on marine sediment---Are we able to inactivate microorganisms in environmental samples? *FEMS Microbiol. Ecol*. **94**, (2018).

189. Straub, J. O. et al. Environmental risk assessment of metformin and its transformation product guanylurea. I. Environmental fate. *Chemosphere* **216**, 844–854 (2019).

190. Mrozik, W. & Stefańska, J. Adsorption and biodegradation of antidiabetic pharmaceuticals in soils. *Chemosphere* **95**, 281–288 (2014).

191. Martinez-Vaz, B. M. et al. Wastewater bacteria remediating the pharmaceutical metformin: Genomes, plasmids and products. *Front. Bioeng. Biotechnol*. **10**, 1086261 (2022).

192. Li, T., Xu, Z.-J. & Zhou, N.-Y. aerobic degradation of the antidiabetic drug metformin by *Aminobacter* sp. strain NyZ550. *Environ. Sci. Technol.* **57**, 1510–1519 (2023).

193. He, Y., Zhang, Y. & Ju, F. Metformin contamination in global waters: biotic and abiotic transformation, byproduct generation and toxicity, and evaluation as a pharmaceutical indicator. *Environ. Sci. Technol.* **56**, 13528–13545 (2022).

194. Tejada, M. Evolution of soil biological properties after addition of glyphosate, diflufenican and glyphosate+diflufenican herbicides. *Chemosphere* **76**, 365–373 (2009).

195. Ritter, S., Hauthal, W. H. & Maurer, G. Octanol/water partition coefficients for environmentally important organic compounds: test of three RP-HPLC-methods and new experimental results. *Environ. Sci. Pollut. Res*. **2**, 153–160 (1995).

196. Chefetz, B., Bilkis, Y. I. & Polubesova, T. Sorption–desorption behavior of triazine and phenylurea herbicides in Kishon river sediments. *Water Res*. **38**, 4383–4394 (2004).

197. Peng, K. Dong, Z., Di, Y-M.. & Guo, X. Contrasting analysis of microbial community composition in the water and sediments of the North Canal based on 16S rRNA high-throughput sequencing. *Huanjing Kexue* **42**, 5424-5432 (2021).

198. Muir, D. C. G. & Yarechewski, A. L. Degradation of terbutryn in sediments and water under various redox conditions. *J. Environ. Sci. Health B* **17**, 363–380 (1982).

199. Bollmann, U. E. et al. Biocide runoff from building facades: degradation kinetics in soil. *Environ. Sci. Technol.* **51**, 3694–3702 (2017).

200. Adyari, B. et al. Strong impact of micropollutants on prokaryotic communities at the horizontal but not vertical scales in a subtropical reservoir, China. *Sci. Total Environ.* **721**, 137767 (2020).

201. Coll, C. et al. Association between aquatic micropollutant dissipation and river sediment bacterial communities. *Environ. Sci. Technol.* **54**, 14380–14392 (2020).

202. Imfeld, G. et al. Toward integrative bacterial monitoring of metolachlor toxicity in groundwater. *Front. Microbiol.* **9**, 2053 (2018).

203. Droppo, I. G., Krishnappan, B. G. & Lawrence, J. R. Microbial interactions with naturally occurring hydrophobic sediments: Influence on sediment and associated contaminant mobility. *Water Res*. **92**, 121–130 (2016).

204. Aydin, M. E., Aydin, S., Beduk, F., Ulvi, A. & Bahadir, M. Accumulation of micropollutants in aqueous media and sediment, a risk assessment for Konya main drainage channel, Turkey. in Advances in Safety Management and Human Factors (ed. Arezes, P. M. F. M.) vol. 791 286–295 (Springer International Publishing, Cham, 2019).

205. Fent, K. Ecotoxicological problems associated with contaminated sites. *Toxicol. Lett.* **140–141**, 353–365 (2003).

206. Chao, C. et al. Response of sediment and water microbial communities to submerged vegetations restoration in a shallow eutrophic lake. *Sci. Total Environ.* **801**, 149701 (2021).

207. Compte-Port, S., Fillol, M., Gich, F. & Borrego, C. M. Metabolic versatility of freshwater sedimentary archaea feeding on different organic carbon sources. *PLoS ONE* **15**, e0231238 (2020).

208. Schink, B. Synergistic interactions in the microbial world. *Anton. van Leeuw.* **81**, 257–261 (2002).

209. Long, R. A. & Azam, F. Antagonistic interactions among marine pelagic bacteria. *Appl. Environ. Microbiol.* **67**, 4975–4983 (2001).

210. Wietz, M., Duncan, K., Patin, N. V. & Jensen, P. R. Antagonistic interactions mediated by marine bacteria: the role of small molecules. *J. Chem. Ecol.* **39**, 879–891 (2013).

211. Wasner, H. K. Metformin's mechanism of action is stimulation of the biosynthesis of the natural cyclic amp antagonist prostaglandylinositol cyclic phosphate (Cyclic PIP). *Int. J. Mol. Sci.* **23**, 2200 (2022).

212. Tisler, S. & Zwiener, C. Formation and occurrence of transformation products of metformin in wastewater and surface water. *Sci. Total Environ.* **628–629**, 1121–1129 (2018).

213. Nürnberg, G. K. Quantification of anoxia and hypoxia in water bodies. in Water Encyclopedia (eds. Lehr, J. H. & Keeley, J.) 64–69 (Wiley, 2004).

214. Janka, Carvajal, Wang, Bakke, & Dinamarca. Treatment of metformin-containing wastewater by a hybrid vertical anaerobic biofilm-reactor (HyVAB). *Int. J. Environ. Res. Public Health.* **16**, 4125 (2019).

215. Shareef, A. et al. Biodegradation of simazine and diuron herbicides under aerobic and anoxic conditions relevant to managed aquifer recharge of storm water. *Clean - Soil Air Water* **42**, 745–752 (2014).

216. Bryant, L. D., Little, J. C. & Bürgmann, H. Response of sediment microbial community structure in a freshwater reservoir to manipulations in oxygen availability. *FEMS Microbiol. Ecol.* **80**, 248–263 (2012).

217. Kiesel, B., Balcke, G. U., Dietrich, J., Vogt, C. & Geyer, R. Microbial community shifts as a response to efficient degradation of chlorobenzene under hypoxic conditions. *Biodegradation* **19**, 435–446 (2008).

218. Zhao, D. et al. Disproportionate responses between free-living and particle-attached bacteria during the transition to oxygen-deficient zones in the Bohai seawater. *Sci. Total Environ.* **791**, 148097 (2021).

219. Tassoulas, L. J., Rankin, J. A., Elias, M. H. & Wackett, L. P. Dinickel enzyme evolved to metabolize the pharmaceutical metformin and its implications for

wastewater and human microbiomes. *Proc. Natl. Acad. Sci. U.S.A.* **121**, e2312652121 (2024).

220. Drzewoski, J. & Hanefeld, M. The current and potential therapeutic use of metformin—the good old drug. *Pharmaceuticals* **14**, 122 (2021).

221. Sanchez-Rangel, E. & Inzucchi, S. E. Metformin: clinical use in type 2 diabetes. *Diabetologia* **60**, 1586–1593 (2017).

222. Graham, G. G. et al. Clinical pharmacokinetics of metformin. *Clin. Pharmacokinet.* **50**, 81–98 (2011).

223. Pentikäinen, P. J. Bioavailability of metformin. Comparison of solution, rapidly dissolving tablet, and three sustained release products. *Int. J. Clin. Pharmacol. Ther. Toxicol.* **24**, 213–220 (1986).

224. Elizalde-Velázquez, G. A. & Gómez-Oliván, L. M. Occurrence, toxic effects and removal of metformin in the aquatic environments in the world: recent trends and perspectives. *Sci. Total Environ.* **702**, 134924 (2020).

225. Ambrosio-Albuquerque, E. P. et al. Metformin environmental exposure: a systematic review. *Environ. Toxicol. Phar*. **83**, 103588 (2021).

226. Briones, R. M., Sarmah, A. K. & Padhye, L. P. A global perspective on the use, occurrence, fate and effects of anti-diabetic drug metformin in natural and engineered ecosystems. *Environ. Pollut*. **219**, 1007–1020 (2016).

227. Di Marcantonio, C., Chiavola, A., Bains, A. & Singhal, N. Effect of oxic/anoxic conditions on the removal of organic micropollutants in the activated sludge process. *Environ. Sci. Technol.* **20**, 101161 (2020).

228. Kim, J. H. et al. Structural and mechanistic insights into caffeine degradation by the bacterial N-demethylase complex. *J. Mol. Biol.* **431**, 3647–3661 (2019).

229. Zhang, Z., Schwartz, S., Wagner, L. & Miller, W. A Greedy algorithm for aligning DNA sequences. *Comput. Biol*. **7**, 203–214 (2000).

230. Foulk, J. A. & Bunn, J. M. Factors influencing the duration of lag phase during in vitro biodegradation of compression-molded, acetylated biodegradable soy protein films. *J. Food Eng.* **79**, 438–444 (2007).

231. Xia, M. et al. Different assembly patterns of planktonic and sedimentary bacterial community in a few connected eutrophic lakes. *Water* **14**, 723 (2022).

232. Izabel-Shen, D. et al. Repeated introduction of micropollutants enhances microbial succession despite stable degradation patterns. *ISME Commun.* **2**, 48 (2022).

233. Rojas, C. A., De Santiago Torio, A., Park, S., Bosak, T. & Klepac-Ceraj, V. Organic electron donors and terminal electron acceptors structure anaerobic microbial communities and interactions in a permanently stratified sulfidic lake. *Front. Microbiol.* **12**, 620424 (2021).

234. Friedrich, J. et al. Investigating hypoxia in aquatic environments: diverse approaches to addressing a complex phenomenon. *Biogeosciences* **11**, 1215–1259 (2014).

235. Tyson, R. V. & Pearson, T. H. Modern and ancient continental shelf anoxia: an overview. *Arct. Antarct. Alp. Res.* **58**, 1–24 (1991).

236. Tlili, A., Montuelle, B., Bérard, A. & Bouchez, A. Impact of chronic and acute pesticide exposures on periphyton communities. *Sci. Total Environ.* **409**, 2102–2113 (2011).

237. Dinh, K. V. et al. Interactive effects of warming and pollutants on marine and freshwater invertebrates. *Curr. Pollution. Rep.* **8**, 341–359 (2022).

238. Polazzo, F. et al. Combined effects of heatwaves and micropollutants on freshwater ecosystems: Towards an integrated assessment of extreme events in multiple stressors research. *Glob. Change Biol.* **28**, 1248–1267 (2022).

239. Velasco, J. et al. Effects of salinity changes on aquatic organisms in a multiple stressor context. *Phil. Trans. R. Soc. B* **374**, 20180011 (2019).

240. Elbrecht, V. et al. Multiple-stressor effects on stream invertebrates: a mesocosm experiment manipulating nutrients, fine sediment and flow velocity. *Freshw. Biol.* **61**, 362–375 (2016).

241. Romero, F., Acuña, V. & Sabater, S. Multiple stressors determine community structure and estimated function of river biofilm bacteria. *Appl. Environ. Microbiol.* **86**, e00291-20 (2020).

242. Stampfli, N. C. et al. Two stressors and a community – effects of hydrological disturbance and a toxicant on freshwater zooplankton. *Aquat. Toxicol.* **127**, 9–20 (2013).

243. Crain, C. M., Kroeker, K. & Halpern, B. S. Interactive and cumulative effects of multiple human stressors in marine systems. *Ecol. Lett.* **11**, 1304–1315 (2008).

244. Turschwell, M. P. et al. Interactive effects of multiple stressors vary with consumer interactions, stressor dynamics and magnitude. *Ecol. Lett.* **25**, 1483–1496 (2022).

245. Gerhardt, A. Biomonitoring of Polluted Water. (Trans Tech Publications, Zurich-Uetikon (CH), 2000).

246. Parmar, T. K., Rawtani, D. & Agrawal, Y. K. Bioindicators: the natural indicator of environmental pollution. *Front. Life Sci*. **9**, 110–118 (2016).

247. Alcolombri, U., Pioli, R., Stocker, R. & Berry, D. Single-cell stable isotope probing in microbial ecology. *ISME Commun.* **2**, 55 (2022).

248. Kimmel, K., Avolio, M. L. & Ferraro, P. J. Empirical evidence of widespread exaggeration bias and selective reporting in ecology. *Nat. Ecol. Evol.* **7**, 1525–1536 (2023).

249. Karhu, K. et al. Microbial carbon use efficiency and priming of soil organic matter mineralization by glucose additions in boreal forest soils with different C:N ratios. *Soil Biol. Biochem.* **167**, 108615 (2022).

250. Mganga, K. Z. et al. Microbial carbon use efficiency along an altitudinal gradient. *Soil Biol. Biochem.* **173**, 108799 (2022).

251. Graue, J., Kleindienst, S., Lueders, T., Cypionka, H. & Engelen, B. Identifying fermenting bacteria in anoxic tidal-flat sediments by a combination of microcalorimetry and ribosome-based stable-isotope probing. *FEMS Microbiol. Ecol.* **81**, 78–87 (2012).

252. Alonso-Saez, L. et al. Changes in marine prokaryotic community induced by varying types of dissolved organic matter and subsequent grazing pressure. *J. Plankton Res.* **31**, 1373–1383 (2009).

253. Lemmel, F., Maunoury-Danger, F., Leyval, C. & Cébron, A. DNA stable isotope probing reveals contrasted activity and phenanthrene-degrading bacteria identity in a gradient of anthropized soils. *FEMS Microbiol. Ecol*. **95**, fiz181 (2019).

254. Anthony, C. The Biochemistry of Methylotrophs. Academic Press, New York. (New York, 1982).

255. Ellenbogen, J. B. et al. Methylotrophy in the mire: direct and indirect routes for methane production in thawing permafrost. *mSystems* **9**, e00698-23 (2024).

256. Puri, A. W. Specialized metabolites from methylotrophic proteobacteria. *Curr. Issues Mol. Biol.* **33**, 211–224 (2019).

257. McGonigle, J. M., Lang, S. Q. & Brazelton, W. J. Genomic evidence for formate metabolism by chloroflexi as the key to unlocking deep carbon in lost city microbial ecosystems. *Appl. Environ. Microbiol.* **86**, e02583-19 (2020).

258. Hillmann, K. B. & Niehaus, T. D. Genome sequences of two *Pseudomonas* isolates that can use metformin as the sole nitrogen source. *Microbiol. Resour. Announc.* **11**, e00639-22 (2022).

259. Martinez-Vaz, B. M. et al. Wastewater bacteria remediating the pharmaceutical metformin: genomes, plasmids and products. *Front. Bioeng. Biotechnol*. **10**, 1086261 (2022).

260. Klein, V. J., Irla, M., Gil López, M., Brautaset, T. & Fernandes Brito, L. Unravelling formaldehyde metabolism in bacteria: road towards synthetic methylotrophy. *Microorganisms* **10**, 220 (2022).

261. Moran, J. J. et al. Formaldehyde as a carbon and electron shuttle between autotroph and heterotroph populations in acidic hydrothermal vents of Norris Geyser basin, Yellowstone National Park. *Extremophiles* **20**, 291–299 (2016).

262. Dong, W. et al. Decomposition of microbial necromass Is divergent at the individual taxonomic level in soil. *Front. Microbiol.* **12**, 679793 (2021).

263. Stable isotope probing and related technologies. (ASM Press, Washington, DC, 2010).

264. Hellal, J. et al. Unlocking secrets of microbial ecotoxicology: recent achievements and future challenges. *FEMS Microbiol. Ecol.* **99**, fiad102 (2023).

265. Liu, J., Yu, Y., Cai, Z., Bartlam, M. & Wang, Y. Comparison of ITS and 18S rDNA for estimating fungal diversity using PCR–DGGE. *World J. Microbiol. Biotechnol.* **31**, 1387–1395 (2015).

266. Ghori, N.-U.-H. et al. RNA Stable isotope probing (RNA-SIP). in Stable Isotope Probing (eds. Dumont, M. G. & Hernández García, M.) vol. 2046 31–44 (Springer New York, New York, NY, 2019).

267. Bradford, L. M. et al. transcriptome-stable isotope probing provides targeted functional and taxonomic insights into microaerobic pollutant-degrading aquifer microbiota. *Front. Microbiol.* **9**, 2696 (2018).

268. Gilevska, T. et al. Do pesticides degrade in surface water receiving runoff from agricultural catchments? Combining passive samplers (POCIS) and compound-specific isotope analysis. *Sci. Total Environ.* **842**, 156735 (2022).

269. Geed, S. R., Prasad, S., Kureel, M. K., Singh, R. S. & Rai, B. N. Biodegradation of wastewater in alternating aerobic-anoxic lab scale pilot plant by *Alcaligenes* sp. S3 isolated from agricultural field. *J. Environ. Manage.* **214**, 408–415 (2018).

270. Wang, F. et al. The influence of polyethylene microplastics on pesticide residue and degradation in the aquatic environment. *J. Hazard Mater*. **394**, 122517 (2020).

271. Balkan, T. & Kara, K. Dissipation kinetics of some pesticides applied singly or in mixtures in/on grape leaf. *Pest Manag. Sci.* **79**, 1234–1242 (2023).

272. Li, T., Xu, Z.-J. & Zhou, N.-Y. Aerobic degradation of the antidiabetic drug metformin by *Aminobacter* sp. strain NyZ550. *Environ. Sci. Technol.* **57**, 1510–1519 (2023).

273. Truhaut, R. Ecotoxicology: objectives, principles and perspectives. *Environ. Toxicol. Chem.* **1**, 151–173 (1977).

274. Lemmel, F., Maunoury-Danger, F., Leyval, C. & Cébron, A. Altered fungal communities in contaminated soils from French industrial brownfields. *J. Hazard Mater*. **406**, 124296 (2021).

275. Soares, D. M. M. et al. Fungal bioassays for environmental monitoring. *Front. Bioeng. Biotechnol.* **10**, 954579 (2022).

276. Spinelli, V., Ceci, A., Dal Bosco, C., Gentili, A. & Persiani, A. M. Glyphosate-eating fungi: study on fungal saprotrophic strains' ability to tolerate and utilise glyphosate as a nutritional source and on the ability of *Purpureocillium lilacinum* to degrade it. *Microorganisms* **9**, 2179 (2021).

277. Lolas, I. B., Chen, X., Bester, K. & Nielsen, J. L. Identification of triclosan-degrading bacteria using stable isotope probing, fluorescence in situ hybridization and microautoradiography. *Microbiology* **158**, 2796–2804 (2012).

278. Li, X. et al. Enhanced microbial degradation of pentachlorophenol from soil in the presence of earthworms: evidence of functional bacteria using DNA-stable isotope probing. *Soil Biol. Biochem.* **81**, 168–177 (2015).

279. Tong, H. et al. The key microorganisms for anaerobic degradation of pentachlorophenol in paddy soil as revealed by stable isotope probing. *J. Hazard Mater*. **298**, 252–260 (2015).

280. Wang, S. et al. (Bio)degradation of glyphosate in water-sediment microcosms – a stable isotope co-labeling approach. *Water Res*. **99**, 91–100 (2016).

281. Jiang, B., Jin, N., Xing, Y., Su, Y. & Zhang, D. Unraveling uncultivable pesticide degraders via stable isotope probing (SIP). *Crit. Rev. Biotechnol.* **38**, 1025–1048 (2018).

282. Wang, X. et al. Identification of microbial strategies for labile substrate utilization at phylogenetic classification using a microcosm approach. *Soil Biol. Biochem.* **153**, 107970 (2021).

283. Banerjee, A., Chitnis, U., Jadhav, S., Bhawalkar, J. & Chaudhury, S. Hypothesis testing, type I and type II errors. *Ind. Psychiatry. J.* **18**, 127 (2009).

284. Douglas, G. M. et al. PICRUSt2 for prediction of metagenome functions. *Nat. Biotechnol.* **38**, 685–688 (2020).

285. Rubiola, S. et al. Comparison between full-length 16S rRNA metabarcoding and whole metagenome sequencing suggests the use of either is suitable for large-scale microbiome studies. *Foodborne Pathog. Dis.* **19**, 495–504 (2022).

286. Buetas, E. et al. Full-length 16S rRNA gene sequencing by PacBio improves taxonomic resolution in human microbiome samples. *BMC Genomics* **25**, 310 (2024).

287. Johnson, J. S. et al. Evaluation of 16S rRNA gene sequencing for species and strain-level microbiome analysis. *Nat. Commun.* **10**, 5029 (2019).

288. Hongxia, M. et al. Full-length 16S rRNA gene sequencing reveals spatiotemporal dynamics of bacterial community in a heavily polluted estuary, China. *Environ. Pollut.* **275**, 116567 (2021).

289. Matsuo, Y. et al. Full-length 16S rRNA gene amplicon analysis of human gut microbiota using MinIONTM nanopore sequencing confers species-level resolution. *BMC Microbiol*. **21**, 35 (2021).

290. Vollmers, J., Correa Cassal, M. & Kaster, A.-K. “Midi-metagenomics”: A novel approach for cultivation independent microbial genome reconstruction from environmental samples. Preprint at https://doi.org/10.1101/2023.01.26.525644 (2023).

291. Maguire, F. et al. Metagenome-assembled genome binning methods with short reads disproportionately fail for plasmids and genomic islands. *Microbial Genomics* **6**, 436 (2020).

292. Abdulkadir, N. et al. Combining flow cytometry and metagenomics improves recovery of metagenome-assembled genomes in a cell culture from activated sludge. *Microorganisms* **11**, 175 (2023).

293. Goussarov, G. et al. Accurate prediction of metagenome-assembled genome completeness by MAGISTA, a random forest model built on alignment-free intra-bin statistics. *Environ. Microbiome* **17**, 9 (2022).

294. Gounot, A.-M. Psychrophilic and psychrotrophic microorganisms. *Experientia* **42**, 1192–1197 (1986).

295. Ten Hulscher, Th. E. M. & Cornelissen, G. Effect of temperature on sorption equilibrium and sorption kinetics of organic micropollutants - a review. *Chemosphere* **32**, 609–626 (1996).

296. Zoeller, R. T. & Vandenberg, L. N. Assessing dose–response relationships for endocrine disrupting chemicals (EDCs): a focus on non-monotonicity. *Environ. Health* **14**, 42 (2015).

297. Newton, D. P., Ho, P.-Y. & Huang, K. C. Modulation of antibiotic effects on microbial communities by resource competition. *Nat. Commun.* **14**, 2398 (2023).

Adrien Borreca

Biodégradation des micropolluants à l'interface sédiment-eau, approche biomoléculaire et géochimique

Résumé

Les micropolluants, dont les pesticides et les résidus pharmaceutiques, constituent une menace pour les écosystèmes aquatiques. Dans ces écosystèmes, les micropolluants rencontrent l'interface sédiment-eau (SWI), une zone biogéochimiquement active pour leur dissipation. Cette thèse examine les facteurs environnementaux impliqués dans la dégradation des micropolluants emblématiques, tels que le *(S)*-métolachlore (herbicide agricole), le terbutryn (biocide urbain) et la metformine (médicament antidiabétique), dans des microcosmes de laboratoire mimant l'interface eau-sédiment. Elle explore comment les communautés procaryotes répondent à l'exposition à des mélanges de micropolluants, à des événements de contamination successifs et à des conditions variables d'oxygène. La metformine et le métolachlore se sont dissipés, tandis que la terbutryne persiste. La metformine se dégrade aussi en anoxie. L'analyse de séquence des amplicons du gène 16S ARNr a mis en évidence des réponses distinctes des communautés microbiennes dans les expériences avec des micropolluants individuels ou en mélanges, ainsi qu'un effet combiné de l'exposition à la metformine et des alternances des conditions d'oxygène. Un nouveau modèle a mis en évidence des effets non additifs, antagonistes et synergiques des micropolluants sur des taxons spécifiques. Enfin, des expériences exploratoires de marquage isotopique stable avec du glucose ^{13}C et de la metformine $^{13}C_2$-méthylée permettent d'identifier les procaryotes assimilant potentiellement la metformine-diméthylamine. Cette thèse fournit un cadre pour l'étude des dynamiques régissant le comportement des micropolluants et souligne la diversité des interactions potentielles entre les micropolluants, les communautés procaryotes et les facteurs environnementaux dans l'étude de l'interface eau-sédiment multi-contaminée.

Mots clefs : Interface eau-sédiment, micropolluants, biodégradation, effets cocktails, écotoxicologie microbienne, marquage isotopique stable

Abstract

Micropollutants, including pesticides and pharmaceuticals, pose a growing threat to aquatic ecosystems. In aquatic ecosystems, micropollutants encounter the sediment-water interface (SWI), a crucial biogeochemical hotspot for their dissipation. This PhD thesis examines the effects of environmental factors on the degradation of emblematic micropollutants, such as *(S)*-metolachlor (agricultural herbicide), terbutryn (urban biocide) and metformin (antidiabetic drug) in laboratory microcosms mimicking the sediment-water interface. Additionally, it explores how prokaryotic communities respond to exposure to micropollutant mixtures, successive contamination events, and varying oxygen conditions. Dissipation of metformin and metolachlor occurred while terbutryn persisted. Metformin dissipation also occurred under anoxic conditions. Sequence analysis of 16S rRNA gene amplicons evidenced distinct responses of prokaryotic communities in experiments with individual micropollutant or mixtures thereof, and a combined effect of metformin exposure and alternances of oxygen conditions. A newly developed model highlighted non-additive antagonistic and synergistic effects of micropollutants on specific taxa across taxonomic levels. Finally, exploratory Stable Isotope Probing experiments with 13C-glucose and methyl-labelled 13C2-metformin were designed to identify potential metformin-dimethylamine assimilating prokaryotes. Altogether, this thesis provides a framework to investigate dynamics governing the behaviour of micropollutant mixtures and underscores the diversity of potential interactions between micropollutants, prokaryotic communities, and environmental factors in the study of multi-contaminated SWI.

Keywords: water-sediment interface, micropollutants, biodegradation, cocktail effects, microbial ecotoxicology, stable isotope probing